CYTOREMEDIATIVE POTENTIALS OF *Vitellaria paradoxa* (Gaertn. C.F) IN ARSENIC-INDUCED TOXICITY IN WISTAR RAT, HARWICH FRUIT FLY AND ITS ANTIPROLIFERATIVE ACTIVITY IN MCF-7 CELLS

BY

AGHOGHO OYIBO

Matric NO.: 172882

B. Sc. Biochemistry (Uniport), M.Sc. Biochemistry (Ibadan)

A Thesis in the Department of Biochemistry,
Submitted to the Faculty of Basic Medical Science
in partial fulfilment of the requirement of the Degree of

DOCTOR OF PHILOSOPHY

of the

UNIVERSITY OF IBADAN

NOVEMBER 2021

CERTIFICATION

I certify that this work was carried out by Miss. Aghogho Oyibo in Cancer Research and Molecular Biology Laboratories, Department of Biochemistry, University of Ibadan, Nigeria.

…….

Supervisor

Oyeronke A. Odunola

B.Sc., M. Sc., Ph.D. (Ibadan)

Cancer Research and Molecular Biology,

Professor, Department of Biochemistry,

University of Ibadan, Nigeria.

DEDICATION

This thesis is dedicated first to the Almighty God, the God who took me over my walls and the giver of all knowledge, insight and wisdom.

Secondly, to my parents Mr and Mrs Henry Oyibo, the ones who through the help of God gave all in their power for the completion of this prestigious degree.

ACKNOWLEDGEMENTS

Firstly, I acknowledge the El-shaddai, the Jehovah overdo God who is my all in all. Thank you for writing my script and taking me through, even when I never understood initially.

My deep and sincere heart-warm gratitude goes to my Mentor and academic mummy who is also the Head of Department of Biochemistry, Professor Oyeronke A. Odunola. She accepted me first as her student, then as a mentee and daughter. She has never stopped giving her guidance, support and prayers; indeed in the multitude of counsels there is safety. Thank you for imparting in me the attitude of good science. May God bless you mummy and much love from me. I sincerely appreciate my Host Professor Vikram Gota (HOD, Clinical Pharmacology, ACTREC), who accepted me as a TWAS-DBT research fellow and provided all necessary reiuitrements to achieve the research objectives.

I appreciate Professor O.O. Olunrosogo for his fatherly support and for acting as a referee for my TWAS-DBT fellowship application. Also I acknowledge Professor E.O. Farombi who was first my teacher and under whom I served as the departmental Post graduate School Scholar. I thank him for the support all through these years of scholarship and assistantship in the department. My sincere appreciation goes to Professor M.A Gbadegesin who has always stood in support of my research. I thank him so much for taking out time to read through my manuscripts and other works. My appreciation goes also to Professor C.O.O. Olaiya for his support and supervision during my M.Sc. research. I acknowledge all members of staff of the Department of Biochemistry.

In a special way, I appreciate Dr A.O. Abolaji, who with open hands accepted me into the *Drosophila* Laboratory and made sure I learnt the techniques involved in handling and working with this novel organism. I am grateful and thankful for the mentorship. I appreciate Dr S.E. Owumi for the support and most especially for coming early to my rescue when my laptop was stolen in the course of this Ph.D. research. Specially, I want to appreciate Dr J.O. Olugbami and Dr A.M. Adegoke for timely counsel and linkage with my host in India.

To my sweet parents, Mr and Mrs H. A. Oyibo, who gave the go ahead to undergo a doctorate degree and supported me till the end. I really love you both and my prayers for you is to live long in peace and health to eat the fruit of your labour.

I can't forget my wonderful siblings, Sister Akpevweoghene, Brother Ogheneakpobor Oghenetega Edewve nee Oyibo, Oghenetejiri Ebojoh nee Oyibo, Dr Okeoghenemeyoma Blessing Ojezuabi nee Oyibo, Oghenevwegba Favour Olaitan nee Oyibo, and Oghenerugba Prevail. I know your prayers and care have contributed to this success story. I pray that God will lift every one of us up beyond our imagination.

I appreciates my sister husband's (Edafe Edewve, Pius Ebojoh and Dr Miracle Ojezuabi) and my little nieces and nephew (Marvelous Edevwe, Excel Ebojoh, Golden Edevwe, Triumph Ojezuabi, Nora Edevwe and Perfect Ebojoh) for the care and concern all through this journey.

Sometimes, God orders your step to special people, and this is the case of my Ibadan parents, Rev and Dr (Mrs) Ademola Nike Falade, whose house have been a place of comfort for me throughout this journey. God bless you daddy and mummy.

I sincerely appreciate, Professor Olajire A. Adegoke (Department of Pharmaceutical Chemistry, UI) of blessed memory, for taking out time to encourage, read and correct my write up's. I pray God's hand will keep resting on his family. To Dr A.T. Jarikre, I am grateful for assisting with the histopathalogical analysis.

I cannot but acknowledge the support of past and present students of CRMB Laboratories and Drosophila laboratory, Department of Biochemistry, University of Ibadan from 2015/2016 session till date. I have found a golden heart in each of you Tomiwu, Eunice, Dr Agu, Nirane, Chisom, Noah, Tobi, Seun, Desmond, Bello, Mr Otituoluwa, Adeola Adedara, Bolaji, Onaara.

Indeed, God took me by His hand over to Clinical Pharmacology Laboratory, Actrec, India. I thank my guide Dr Kushboo Gandhi and Dievya Gohil, for teaching me the techniques of cell culturing. I appreciate members of Gota laboratory (Bharti, Sampati, Karpita, Muharisa)

and the family in Clinical Biology laboratory (Venkandish, Sister and Simter) for their act of kindness and love.

I specially want to appreciate Dr Goda Jayant Sastri, the collaborator of my host under whose laboratory all the cell lines studies were carried out.

I acknowledge the Post graduate College, University of Ibadan for the Postgraduate scholarship awarded to me for three sessions (2016/2017 session to 2019/2020 session) and for the teaching assistantship position. Indeed, this scholarship was a great financial relief to me.

It was only God who gave the TWAS-DBT fellowship as a consolation just after losing the opportunity of travelling to the USA for a conference presentation due to visa denial despite a Travel award from the Society of Toxicology to attend the 2019 Conference. Hence, I sincerely acknowledge The World Academy of Science (TWAS) and the Department of Biotechnology, Ministry of Science and Technology, India who awarded me the Postgraduate Sandwich Fellowship for twelve months. Indeed, this is one opportunity I will not forget in my life-time, because it afforded me the privilege of gathering experience in cell culturing thereby making me a better scientist.

The special friends from the Post Graduate Hall (Balewa) which I can't forget are Dr Lola, Mrs Ope, Miss Blessing, Dr Segun, Dr Tayo, Dr Muyin whose words of encouragement and prayers were timely. I appreciate all the ministers for their prayers through this journey. God bless you.

Finally, I return all glory to God, my father, my keeper, the lifter of my head. I thank Him for pouring His oil on me and causing it to run over. Indeed, He watches over His words to see to their fulfilment.

ABSTRACT

Arsenic, a class 1 carcinogen, is a major contaminant in drinking water globally. When ingested by humans and animals, it contributes to tissue damage through the mechanisms of oxidative stress and inflammation. Search is ongoing for plants with antioxidative and anti-inflammatory properties that might ameliorate toxic effects of arsenic. *Vitellaria paradoxa* (Vp) was reported to possess anti-oxidative and anti-inflammatory properties. Therefore, cytoremediative potentials of Vp against Sodium arsenite (SA)-induced toxicity in Wistar rats and fruit fly (*Drosophila melanogaster)*, as well as its anti-proliferative action on breast cancer cell line (MCF-7) were evaluated.

Leaves of Vp were obtained from Saki, Oyo State, authenticated at University of Ibadan Herbarium (UIH-22624), air-dried and pulverised. Hydroethanol leaf extract of Vp was obtained by maceration in 70% ethanol (ELVp), and fractionated by vacuum liquid chromatography to obtain four fractions including Ethyl acetate Fraction (EAcF). Forty male Wistar rats, divided into 8 groups (n=5), were administered distilled water 2mL/kg (Control), Vitamin E (100 mg/kg), ELVp (100, 200 mg/kg), SA (2.5 mg/kg), SA + Vitamin E, SA + ELVp (100, 200 mg/kg) orally for 14 days. Serum Alanine Aminotransferase (ALT), Alkaline Phosphatase (ALP), creatinine, urea and malondialdehyde were determined spectrophotometrically. Micronucleated Polychromatic Erythrocytes (mPCE), liver and kidney histology and immunohistochemistry of proteins [(Nuclear Factor kappa B (NF-κB), P53, B-Cell Lymphoma 2 (BCL-2)] were evaluated. Ameliorative role of EAcF in SA-induced toxicity in *D. melanogaster* was evaluated by measuring longevity rate, Nitric Oxide (NO), Hydrogen Peroxide (H_2O_2), Total Thiol (T-SH), reduced glutathione (GSH) levels, catalase and glutathione S-transferase (GST) activities. Anti-proliferative effects of EAcF on MCF-7 cells were determined by measuring viability, colony formation and Reactive Oxygen Species (ROS) generation. Also, cell cycle was determined using flow cytometer. Data were analysed using ANOVA at $\alpha_{0.05}$.

Co-treatment of SA with ELVp (100 mg/kg) significantly reduced serum ALT (68.73±0.50 vs 89.67±8.78U/L), ALP (174.80±1.84 vs 450.20±69.47U/L), creatinine (1.32±0.00 vs 1.93±0.15mg/dL), urea (33.72±9.07 vs 75.14±1.13mg/dL), malondialdehyde (0.049±0.005

vs 0.067±0.012µmol/gprotein) and mPCEs (10.00±2.83 vs 16.00±2.00mPES/1000PCEs) relative to SA. The ELVp (200 mg/kg) ameliorated SA-induced severe periportal and mild peritubular inflammation of the liver and kidney of rats, respectively. The ELVp ameliorated SA-induced increase in BCL-2 protein expression without significant effects on NF-κB and P53 expression in both organs. The EAcF increased longevity of *D. melanogaster* by 20.0% compared with control and ameliorated SA-induced elevation of NO and H_2O_2 levels by 24.0% and 19.0%, respectively. Also, it ameliorated SA-induced reduction of contents of T-SH by 88.0%, GSH by 253.0% and inhibition of catalase and GST activities by 57.8% and 156.0% respectively. The EAcf showed anti-proliferative activity, reduced ROS generation, induced Sub G0 cell death and arrest at G0/G1 phase in MCF-7 cells.

Hydroethanol leaf extract and ethyl acetate fraction of *Vitellaria paradoxa* demonstrated antihepatotoxic, antinephrotoxic and antioxidative properties against sodium arsenite-induced toxicity in rat and *Drosophila melanogaster*. The anti-proliferative activity in MCF-7 cells was via inhibition of reactive oxygen species accumulation and G0/G1 cell cycle arrest.

Keywords: Sodium arsenite, *Vitellaria paradoxa*, Antioxidant status, Oxidative stress.

Word Count: 481

TABLE OF CONTENTS

	Page
Certification	i
Dedication	ii
Acknowledgements	iii
Abstract	vi
Table of Contents	viii
List of Tables	xiii
List of Figures	xiv
List of Plates	xix
Abbreviation and Glossary	xx
CHAPTER ONE	1
INTRODUCTION	1
1.1 Background of the study	1
1.1.1 Statement of problem	3
1.2 Justification of study	4
1.3 Aim and objectives	5
CHAPTER TWO	6
LITERATURE REVIEW	6
2.1 Cancer	6
2.1.1 Cancer incidence in Nigeria	6

2.1.2 Carcinogenesis 7

2.1.3 Models of cancer research 10

2.1.4 Apoptosis 15

2.1.5 Cell cycle 21

2.1.6 Risk factors influencing cancer 21

2.2 Arsenic 22

2.2.1 Sources of arsenic 22

2.2.2 Absorption and metabolism of arsenic 23

2.2.3 Arsenic and toxicities 25

2.3 Medicinal plants 28

2.3.1 *Vitellaria paradoxa* 29

CHAPTER THREE 32

MATERIALS AND METHODS 32

3.1 Collection of *Vitellaria paradoxa* plants and certification 32

3.1.1 *V. paradoxa* leaf extract preparation 32

3.1.2 Preparation of seed for extraction 34

3.1.3 Cold hydroethanol extract 36

3.2 Fraction of leaf extract by Vacuum Liquid Chromatography (VLC) 36

3.3 Phytochemical screening method (qualitative) 36

3.4 Assessment of antioxidant activity (*In vitro*) 36

3.4.1 Total antioxidant capacity 36

3.4.2 Reducing power assay 37

3.4.3 2,2-diphenyl-1-picrylhydrazyl (DPPH) assays 37

3.4.4 Total phenol content 37

3.4.5 Total flavonoid content (TFC) 37

3.5 Bacterial strain and culture 38

3.6 *In vitro* assessment of genotoxicity of hydroethanol extracts of *V. paradoxa* 38

3.7 Lethal dose (LD50) determination of leaf extract of *V. paradoxa* 39

3.8 Animal experimental design and treatments 39

3.9 Serum collection 41

3.10 Assays of liver function enzymes 41

3.11 Kidney function test 41

3.12 Organ preparation for histological analysis 41

3.13 Determination of hematological parameters 42

3.14 Determination of micronuclei 42

3.15 Immunohistochemistry of NF-κB, P53, BCL-2 43

3.16 Culturing of *Drosophila melanogaster* 44

3.17 Experimental designs 44

3.18 Determination of survival rate of *D. melanogaster* orally exposed to Sodium arsenite 48

3.19 Anesthetizing of flies 48

3.20 Preparation of *D. melanogaste*r for biochemical assays after a five days treatment 48

3.21 Biochemical assays 48

3.21.1 Protein determination 49

3.21.2 Assay for catalase activity 49

3.21.3 Estimation of glutathione-S-transferase activity 49

3.21.4 Total thiol level estimation 49

3.21.5 Determination of reduced glutathione (GSH) level 50

3.21.6 Hydrogen peroxide generation 50

3.21.7 Determination of nitrite (nitric oxide) level 50

3.21.8 Assessment of acetylcholinesterase activity 50

3.22 Negative geotaxis 51

3.23 Determination of flies emergence 51

3.24 *D. melanogaster* fat bodies histology 51

3.25 Cell lines and culture 52

3.26 Trypan blue assay 52

3.27 MTT assay 52

3.28 Cell colony formation assay 53

3.29 ROS generation assay 54

3.30 Cell cycle analysis 54

3.31 Western blot analysis 55

3.31.1 Determination of protein 57

3.31.2 SDS PAGE gel preparation 57

3.31.3 Sample preparation 60

3.31.4 Electrophoresis 60

3.32 Determination of bioactive compounds in ethyl acetate fraction (EACF) Of *V. paradoxa* using Gas Chromatography-Mass Spectrometry (GC-MS) method 61

3.33 Research work flow 62

3.34 Statistical analysis 63

CHAPTER FOUR 64

RESULTS 64

4.1 Phytochemical screening of *Vitellaria paradoxa* extracts 64

4.2 Antioxidant contents of *V. paradoxa* extracts 68

4.3 Genotoxic effect of *V. paradoxa* extracts 72

4.4 Median lethal dose (LD50), percentage change in body weight and histological examination of female Wistar rats treated with ELVp 74

4.4.1 Acute toxicity analysis 74

4.4.2 Effects of ELVp on percentage change in body and relative liver weights 76

4.4.3 Histological examination of rats' liver treated with ELVp 79

4.5 Effect of *Vitellaria paradoxa* hydroethanol leaf extract on sodium arsenite-induced toxicity in male Wistar rats 81

4.5.1 Effects of ELVp on sodium arsenite-induced change on % body weight and relative organs weight 81

4.5.2 The hepato-remedative potential of ELVp on sodium arsenite-induced toxicity 84

4.5.3 Liver histological examination 87

4.5.4 The nephron-remediative potential of ELVp on sodium arsenite-induced toxicity 89

4.5.5 Kidney histological examination 92

4.5.6 Assessment of the remediative potential of ELVp on sodium arsenite-induced toxicity on haematological parameters 94

4.5.7 Effect of ELVp in sodium arsenite-induced lipid peroxidation 97

4.5.8 Effect of ELVp on SA-induced clastogenicity 100

4.5.9 Effect of ELVp on SA-induced inflammation 102

4.5.10 Effect of ELVp on SA-induced apoptotic markers 107

4.6.1 Qualitative phytochemicals, total flavonoid and phenol content of fractions of ELVp 117

4.6.2 *In vitro* antioxidant content of fractions of ELVp 121

4.7 Effect of sodium arsenite on survival rate and generation of reactive oxygens species of *Drosophila melanogaster* 124

4.7.1 Effects of SA on adult survival and offspring emergence of *D. melanogaster* 124

4.7.2 Elevation of NO and H_2O_2 levels by SA in *D. melanogaster* 128

4.7.3 Inhibition of catalase, GST activities and reduction of total thiol and GSH contents by SA in *D. melanogaster* 131

4.7.4 Effect of SA on locomotive performance of *D. melanogaster* 136

4.8 Effects of fractions of *Vitellaria paradoxa* leaf extract on longevity and generation of reactive oxygen species of *Drosophila melanogaster* 138

4.9 The cytoremediative potentials of ethyl acetate fraction of *Vitellaria paradoxa* Leaf extract on sodium arsenite-induced toxicity in *D. melanogaster* 143

4.9.1 EACF reduced the elevation of H_2O_2 and NO levels induced by SA in *D. melanogaster* 143

4.9.2 EACF elevated SA-induced reduction of total thiol and GSH levels in *D. melanogaster* 146

4.9.3 EACF elevated SA-induced reduction of catalase and GST activities in *D. melanogaster* 149

4.9.4 Effect of EACF and SA on offspring emergence, locomotive and acetylcholinesterase activities in *D. melanogaster* 152

4.9.5 Histological analysis of fat body cell of *D. melanogaster* 157

4.10 Evaluation of cytotoxicity of fractions of *Vitellaria paradoxa* on three cancer cell lines 159

4.10.1 Effect of fractions of ELVp on cytotoxicity of MCF-7 cells 159

4.10.2 Cytotoxic activity of EACF in MCF-&, Hep G2 and A549 cells 163

4.10.3 Anti-proliferative activities of EACF in MCF-7 cells 166

4.10.4 EACF reduced ROS production in MCF-7 cells 171

4.10.5 Effect of EACF on cell cycle phases of MCF-7 cells 173

4.10.6 Effects of EACF on protein expression of cleaved caspase 3 and pro-caspase 3 180

4.10.7 Analysis of active compounds present in EACF using GC-MS 184

CHAPTER FIVE 191

DISCUSSION 191

5.1 Phytochemical, and antioxidant profile of *Vitellaria paradoxa* 192

5.2 Safety assessment indices of *Vitellaria paradoxa* 193

5.3 Body weight, organo somatic and haematological indices 193

5.4 Modulation of liver and kidney biomarkers 195

5.5 Effect on ROS and antioxidant pathways 196

5.6 Survival and fat body histopathological indices 199

5.7 Effect on clastogenic and proliferative mechanism 200

5.8 Cell cycle and apoptotic pathway 202

CHAPTER SIX 203

SUMMARY AND CONCLUSION 203

6.1 Summary 203

6.2 Conclusion 204

6.3 Recommendation 204

6.4 Contribution to knowledge 205

REFERENCES 206

Appendices 235

LIST OF TABLES

		Page
Table 3.1	Experimental design	40
Table 3.2	Experimental design for sodium arsenite treated *Drosophila melanogaster*	45
Table 3.3	Experimental design for fractions of ELVp	46
Table 3.4	Experimental design for co-treatment of ethyl acetate fraction EACF and sodium arsenite	47
Table 3.5	Lysis buffer preparation	56
Table 3.6	Resolving gel preparation	58
Table 3.7	Stacking gel preparation	59
Table 4.1	Percentage yield of ethanol leaf and seed extracts of *Vitellaria paradoxa*	65
Table 4.2	LD_{50} study of hydroethanol leaf extract of *V. paradoxa* (ELVp) in Wistar rats	75
Table 4.3	Effect of ELVp on sodium arsenite-induced change on % body weight and relative organs weight	83
Table 4.4	Remediative potential of ELVp on sodium arsenite induced toxicity on haematological parameters	96
Table 4.5	The qualitative phytochemical of fractions of hydroethanol leaf extract of *Vitellaria paradoxa*	118

Table 4.6 Chemical compounds detected from GC/MS analysis of ethyl acetate fraction of *V. paradoxa* 186

LIST OF FIGURES

		Page
Figure 2.1	Carcinogenesis stages	9
Figure 2.2	Life cycle of D*rosophila*	12
Figure 2.3	The biochemical pathway of apoptosis	18
Figure 2.4	BCL-2 protein family a key player in apoptosis regulation	20
Figure 2.5	Mechanism of arsenic metabolism	24
Figure 4.1	Total flavonoid capacity of *Vitellaria paradoxa* extracts using quercetin as standard	66
Figure 4.2	Total phenol content of *Vitellaria paradoxa* using gallic acid as standard	67
Figure 4.3	*Vitellaria paradoxa* extracts DPPH scavenging activity	69
Figure 4.4	Reducing power scavenging activity of *V. paradoxa* extracts and positive control (ascorbic acid)	70
Figure 4.5	The total antioxidant capacity of *V. paradoxa* extracts	71
Figure 4.6	Genotoxic effect of *Vitellaria paradoxa* extracts and the positive control (4-nitroquinoline -1-oxide)	73
Figure 4.7	The effect of ELVp on percentage change in body weight of female Wistar rats	77
Figure 4.8	Effect of ELVp on relative liver weight of female Wistar rats	78
Figure 4.9	The results of the liver function markers in the treated and control	

	animals	86
Figure 4.10	Effect of ELVp on the urea concentration of sodium arsenite-induced nephrotoxicity	90
Figure 4.11	Effect of ELVp on creatinine concentration of sodium arsenite-induced nephrotoxicity	91
Figure 4.12	The remeiative potential of ELVp against sodium arsenite-Induced liver lipid peroxidation	98
Figure 4.13	The remediative potential of ELVp against sodium arsenite-induced kidney lipid peroxidation	99
Figure 4.14	Remediative potential of ELVp on clastogenicity induced by sodium arsenite	101
Figure 4.15	Effect of vitamin E, ELVp or SA on NF-κB expression in liver	104
Figure 4.16	Effect of vitamin E, ELVp or SA on NF-κB expression in kidney	106
Figure 4.17	Effect of vitamin E, ELVp or SA treatment on P53 expression in liver	109
Figure 4.18	Effect of vitamin E, ELVp or SA treatment on P53 expression in kidney	111
Figure 4.19	Effect of vitamin E, ELVp or SA treatment on BCL-2 expression in liver	114
Figure 4.20	Effect of vitamin E, ELVp or SA treatment on BCL-2 expression in kidney	116

Figure 4.21	Total flavonoid content of the fraction in relation to quercetin	119
Figure 4.22	Total phenol content of the fractions in relation to gallic acid	120
Figure 4.23	Antioxidant potential of ELVp fractions to reduce iron (iii) to iron (ii)	122
Figure 4.24	Total antioxidant capacity of the fractions	123
Figure 4.25	Effect of sodium arsenite (SA) on survival of *D. melanogaster* after 14 days	125
Figure 4.26	Dose effect of sodium arsenite on survival rate of *D. melanogaster*	126
Figure 4.27	Effect of sodium arsenite on *D. melanogaster* emergence rate	127
Figure 4.28	Effect of sodium arsenite (SA) on the levels of hydrogen peroxide generation of *D. melanogaster*	129
Figure 4.29	Effect of sodium arsenite on the level of nitric oxide generation using *D. melanogaster* model	130
Figure 4.30	Sodium arsenite inhibits catalase activity of *D. melanogaster*	132
Figure 4.31	Sodium arsenite inhibits glutathione-S-transferase (GST) activity in *Drosophila melanogaster* treated for five days	133
Figure 4.32	Sodium arsenite inhibit the level of total thiol level in *D. melanogaster*	134
Figure 4.33	Sodium arsenite deplete glutathione content in *D. melanogaster* after treatment for five days	135
Figure 4.34	Effect of sodium arsenite on locomotor performance of	

D. melanogaster after five days treatment 137

Figure 4.35 Longevity of *Drosophila melanogaster* treated with three concentration of *Vitellaria paradoxa* leaf fractions 139

Figure 4.36 Hydrogen peroxide level of *D. melanogaster* treated with *Vitellaria paradoxa* fractions for five days 140

Figure 4.37 Nitric oxide level of *D. melanogaster* treated with *Vitellaria paradoxa* Fractions for five days 141

Figure 4.38 Effect of *Vitellaria paradoxa* fraction on *D. melanogaster* total thiol content after five days treatment 142

Figure 4.39 Effect of ethyl acetate fraction on sodium arsenite induced hydrogen peroxide elevation in *D. melanogaster* 144

Figure 4.40 Ethyl acetate fraction of ELVp protected against sodium arsenite-induced elevation of nitric oxide in *D. melanogaster* 145

Figure 4.41 Effect of ethyl acetate fraction of *V. paradoxa* leaf on sodium arsenite-induced reduction in total thiol content 147

Figure 4.42 Effect of ethyl acetate fraction of *V. paradoxa* on sodium arsenite-induced reduction in reduced glutathione content 148

Figure 4.43 Effect of ethyl acetate fraction of *Vitellaria paradoxa* leaf on sodium arsenite reduced catalase activity in *D. melanogaster* 150

Figure 4.44 Ethyl acetate fraction of ELVp improves sodium arsenite-induced reduction in GST activity 151

Figure 4.45 Percentage of offspring's emergence from treated flies with sodium arsenite and ethyl acetate fraction of *V. paradoxa* leaf extract 154

Figure 4.46 Negative geotaxis of *D. melanogaster* treated with sodium arsenite and ethyl acetate fraction of *V. paradoxa* leaf extract 155

Figure 4.47 Effect of ethyl acetate fraction of *V. paradoxa* leaf on the activity of acetylcholinesterase activity on *D. melanogaster* induced with sodium arsenite 156

Figure 4.48 Effect of fraction of *V. paradoxa* on MCF-7 cell viability after 24 hrs treatment 160

Figure 4.49 Effect of *V. paradoxa* fraction on MCF-7 cell viability after 48 hrs of treatment 161

Figure 4.50 Effect of *V. paradoxa* fraction on MCF-7 cell viability after 72 hrs of treatment 162

Figure 4.51 Cell viability of Hep G2, MCF-7 and A549 cells exposed to ethyl acetate fraction for 24 hrs 164

Figure 4.52 Cell viability of Hep G2, MCF-7 and A549 cells exposed to ethyl acetate fraction for 72 hrs 165

Figure 4.53 Cell viability of MCF-7 cells after 24 hrs treatment with various IC_{50} range of doses 167

Figure 4.54 Cell viability of MCF-7 cells after 48 hrs treatment with various IC_{50} range of doses 168

Figure 4.55 Cytotoxic effect of ethyl acetate fraction of *V. paradoxa* on MCF-7 cells at 48 hrs 169

Figure 4.56 Effect of 24 hrs treatment with ethyl acetate fraction of *V. paradoxa* on MCF-7 colony formation 170

Figure 4.57 Effect of ethyl acetate fraction of *V. paradoxa* leaf on ROS generation after 6 hrs treatment 172

Figure 4.58A Flow cytometry analysis of MCF-7 cells after 24 hr treatment with EACF 174

Figure 4.58B Cell cycle phase after 24 hrs treatment with EACF of *V. paradoxa* 175

Figure 4.59A Flow cytometry analysis of MCF-7 cells after 48 hr treatment with EACF 176

Figure 4.59B Cell cycle phase after 48 hrs treatment with EACF of *V. paradoxa* 177

Figure 4.60A Flow cytometry analysis of MCF-7 cells after 72 hr treatment with EACF 178

Figure 4.60B Cell cycle phase after 72 hrs treatment with EACF of *V. paradoxa* 179

Figure 4.61 Cleaved caspase 3 and pro-caspase 3 protein expression after 24 hr treatment 181

Figure 4.62 Pro-caspase 3 protein activity in MCF-7 cells treated for 24 hrs 182

Figure 4.63 Cleaved caspase 3 protein activity in MCF-7 cells treated for 24 hrs 183

Figure 4.64 Analysis of ethyl acetate fraction of *V. paradoxa* ethanol leaves extract using GC/MS 185

Figure 4.65A Chemical structures of compounds present in ethyl acetate fraction of *Vitellaria paradoxa* leaf 187

Figure 4.65B Chemical structures of compounds present in ethyl acetate fraction of *Vitellaria paradoxa* leaf 188

Figure 4.65C Chemical structures of compounds present in ethyl acetate fraction of *Vitellaria paradoxa* leaf 189

Figure 4.65D Chemical structures of compounds present in ethyl acetate fraction of *Vitellaria paradoxa* leaf 190

LIST OF PLATES

		Page
Plate 3.1	Picture of leaves of *V. paradoxa*	33
Plate 3.2	Pictures of fruit, kernels and seeds of *V. paradoxa*	35
Plate 4.1	Photomicrograph of ELVp effect on the liver of Wistar rats	80
Plate 4.2	Liver photomicrographs of rats administered ELVp and sodium arsenite	88
Plate 4.3	Kidney photomicrograph of rats administered ELVp, vitamin E and sodium arsenite	93
Plate 4.4	Photomicrograph of liver showing the expression of NF-κB	103
Plate 4.5	Photomicrograph of kidney showing the expression of NF-κB	105
Plate 4.6	Photomicrograph of liver showing the expression of P53	108
Plate 4.7	Photomicrograph of kidney showing the expression of P53	110
Plate 4.8	Photomicrograph of liver showing the expression of BCL-2	113
Plate 4.9	Photomicrograph of kidney showing the expression of BCL-2	115
Plate 4.10	Pictomicrograph of *D. melanogaster* fat bodies following exposure to sodium arsenite and ethyl acetate fraction of *V.paradoxa* leaf extract	158

ABBREVATION AND GLOSSARY

AChE – Acetyl Choline Esterase

APAF-1 – Apoptosis Protease Activating Factor-1

As – Arsenic

BSA – Bovine Serum Albumin

CAT – Catalase

CDK – Cyclin Dependent Kinase

CDNB – 1-Chloro-2,4- dinitrobenzene

DCFDA – 2,7- dichloroflurosen diacetate

DD - Death Domain

DED – Death Effector Domain

DISC – Death Inducing Signal Complex

DMEM – Dulbecco's Modified Eagle's Medium

DPPH - 1,1-Diphenyl-2- picrylhydrazyl

DTNB- 5,5- dithiobis-2- nitrobenzoic acid

ELVp – Ethanol leaf extract of *Vitellaria paradoxa*

FBS -Foetal Bovine Serum

GC-MS – Gas Chromatography- Mass Spectrometry

GIT – Gastrointestinal Tract

GSH- Reduced Glutathione

GST – Glutathione –S- Transferase

HCT- Haematocrit

HGB – Haemoglobin

IAP – Inhibitors of Apoptotic Proteins

LD50 –Lethal Dose

MDA- Malondialdehyde

MMA- Monomethyl arsonous Acid

mPCEs – Micronucleated Polychromatic Erythrocytes

MTT – 3-(4,5-dimethylthiazol-2-yl) 2,5-diphenyltetrazolinediamide

NF-κB – Nuclear Factor kappa B

NO –Nitric oxide

4-NQO – 4- Nitroquinoline-1-oxide

PBS – Phosphate Buffer Saline

PCEs- Poly Chromatic Erythrocytes

PI – Propidium Iodide

RNS – Reactive Nitrogen Species

ROS – Reactive Oxygen Species

SAM – S-Adenosyl Methionine

SA – Sodium arsenite

SOD – Superoxide dismutase

SOSIF- SOS Inducing Factor

TAC – Total Antioxidant Content

TNF- Tumour Necrosis Factor

VCH- 4-Vinylcyclohexene

VLC – Vacuum Liquid Chromatography

WBC – White blood cell

CHAPTER ONE
INTRODUCTION

1.1 Background of the study

Cancer also called neoplasm and malignant tumour, is described by a non-stop growth and spread of strange cells (ACS, Cancer Facts and Figure, 2019). Second to heart diseases, it primarily causes death with an estimate of 19.3 million new cancer presentations and 10 million cancer deaths globally (Sung, 2021). Worldwide, about 27.5 million new cases of cancer is projected by 2040 (ACS, Global Cancer Fact and Figure, 2018). Furthermore, third world nations recorded above two- thirds of cancer death i.e. approximately 70 % of death resulting from cancer (WHO, 2018). In 2008, an estimate of 681,000 new cases of cancer was recorded in Africa, with 15 % of these cases from Nigeria (Sylla and Wild, 2012). High cases of mortality have been reported in Nigeria, due to increase in number of cancer incidence with over 100,000 fresh cases of cancer being presented yearly (Ferlay *et al*., 2010). In addition, Ibadan and Abuja cancer Registries reported that the incidence of invasive cancer is based on age with higher occurrence in women and breast cancer being the most prevalent (Jedy-Agba *et al*., 2012). The increased number of cancer cases in most African countries may be attributed mainly to lack of awareness and superstitious causes resulting in delayed presentation and diagnosis. Also, lack of access to health care, shortage of oncology specialist and indulgence in junk foods (Ogunbiyi *et al*., 2016). The predisposing factors leading to incidences of cancer can either be internal (genetic, age, hormonal status) or external (diet, alcohol, tobacco, lack of exercise, viruses, radiation, industrial and environmental chemicals) (Gutierrez and Salsamendi, 2001; Wu, *et al*., 2018). One of such environmental toxicant known to induce cancer is arsenic (Ganapathy *et al*., 2019; Oyibo *et al*., 2021).

Arsenic is a key environmental toxicant associated with carcinogenesis (Ganapathy *et al*., 2019; IARC, 2018). It is of paramount importance in public health globally because of its ubiquitous nature and deleterious effects to both man and livestock's (Chiochetti *et al*., 2019). Ultimately, sources of arsenic include water, air, food, drug, industrial and agricultural chemicals (Biswas *et al*., 2019). Natural phenomena and anthropogenic effects, contribute to arsenic release into waterbodies (Azam *et al*., 2016). This in turn affects seafoods and agricultural products which are used as food. Egbinola and Amanambu, (2014) examined ground water in both dry and wet season at Ibadan, Nigeria using 16 locations and discovered that the amount of arsenic in water below the earth surface exceeded WHO estimated range.

The chief route of absorption of arsenic is through inhalation (nostrils), oral and skin (Chen *et al*., 2013). When absorbed, it is evenly distributed among different organs of the body. Furthermore, it is transformed by the liver to monomethylarsonic and dimethylarsinic acid, a highly reactive product via methyl addition reaction twice (Hughes, 2002). A major mechanism by which this heavy metal (arsenic) acts is by inducing Reactive Oxygen Species (ROS). This effect, will result to increased hydrogen peroxide production, lipid peroxidation induction and enzymatic antioxidant inhibition. This consequently leads to oxidative stress-antioxidant imbalance (Shahid *et al*., 2014). Excessive stress from oxidation results in negative changes of deoxy-ribonucleic acid (DNA) and this is a key step in the induction of cancer. In a normal cell, such DNA damage initiates positive cell cycle regulation or apoptosis leading to repair or removal of such damaged DNA. However, in cancerous cells, these two key processes are escaped by down regulation of p53. Therefore, agents causing arrest or programed death of cancerous cells are strategic for anticancer therapy (Kamalabadi- Farahani *et al*., 2019).

The conventional cancer care includes; surgery, radiotherapy, chemotherapy and hormone therapy but the main opposing effect with some of these therapies is their inability to selectively target cancer cells, hence subjecting normal cells to danger (Mathew *et al*.,

2019). Thus, the need for the discovery of medicinal plant which possess natural phytochemicals with protective antioxidant properties that would inhibit cancer development yet protect normal cells (Kooti *et al*., 2017).

Even in recent times, traditional herbal medicine is still prominent in some countries' primary health care system because they are cheaper and easily accessible (Mahomoodally, 2013). One of such commonly used medicinal plants in Africa is *Vitellaria paradoxa (V. paradoxa).*

Vitellaria paradoxa usually called shea butter tree, has many uses in folkloric medicine. The mesocarp of the fruit is of high nutritional value (Ugese *et al*., 2008). Traditionally, the leaf is used for treating Burili ulcer (Yemoa *et al*., 2008), while the bark is used for treating malaria, dental pain and neuralgia (Serene *et al*., 2008), and to treat diabetes (Coulibaly *et al*., 2014). Studies have documented anti-inflammatory, anti-arthritis, antibacterial, and antiproliferative ability in extracts of *V. paradoxa* (Foyet *et al*., 2015; Fodouop *et al.*, 2017; Tagne *et al*., 2014).

Despite several reported pharmacological activities of *V. paradoxa,* there is dearth of information on the cytoremediative potentials of *V. paradoxa* leaf against arsenic-induced toxicity and its mechanism for antiproliferative activity. Hence, it was hypothesised that *V. paradoxa* could offer cytoremediative effects against carcinogen sodium arsenite-induced toxicity as well as therapeutic potentials on different human cancer cell lines.

1.1.1 Statement of problem

In 2020, 10 million deaths arose around the globe due to cancer (Sung, 2021). Also, cancer burden in Sub-Saharan Africa is growing significantly with about two-third of death arising from an estimated 626,400 new cases presented in 2012 (National Cancer Control Plan, 2018). In Nigeria out of 102,000 new cases of cancer presented yearly, 72,000 cancer patients die per year (NCCP, 2018). The increase in cases and deaths resulting is associated with lack of awareness, late diagnosis, increase in adoption of risk behaviour such as unhealthy diets, lack of physical exercise, harmful use of alcohols and tobacco, infections and exposures to environmental/ industrial toxicants such as arsenite from contaminated water and food, cosmetics, pesticides and mining activity etc. (Torre *et al*., 2016).

Amongst the various factors responsible for carcinogenesis, arsenic is one of the prevalent and extensively studied carcinogen. It is further categorised as a class 1 human carcinogen linked with skin, lungs, bladder, kidney, liver and prostate cancer (IARC, 2018; Steinmaus

et al., 2014). Its' ubiquitously spread in the natural environment enhances exposure via the intake of contaminated water or diet to human and animals (Chiocchetti *et al*., 2019). Aside carcinogenic effects, toxicological health implications of arsenite, have been documented in hepatic toxicity (Odunola *et al*., 2008, Adegoke *et al*., 2015), clastogenicity (Gbadegesin *et al*., 2009, 2014), hemato- biochemical and histology indices (Ola- Davis and Akinrinde, 2016). Furthermore, one key mechanism linked with the toxicity of arsenite is oxidative stress (Tokar *et al*., 2010). Arsenic exposure induces the generation of intracellular reactive oxygen species (ROS), which mediate multiple changes to cell behaviour by altering signalling pathways and epigenetic modifictions or cause direct oxidative damage to molecules (Yuxin *et al*., 2020)

1.2 Justification of study

Arsenic is an environmental carcinogen known to induce cancer via accumulation of ROS that triggers cell injury (Roy *et al*., 2018). Although, several treatments namely surgery, radiotherapy, immunotherapy, are used in cancer treatment, the use of conventional therapy in management of cancer induces death of normal cells along with cancerous cells, resulting in undesirable side effects (Phi *et al*.,2018).

As part of global research efforts in finding effective treatments for this deadly disease, phytochemicals are being considered for the treatment of cancer. Newman and Cragg latest study (2016) reported that a large number of new drugs approved by the FDA between early 1980's and 2014 came directly from natural products or their derivatives. Interestingly, it has been shown that a diverse range of bioactive molecules produced by plants have activities that work against excessive proliferation of cells (Neena *et al*., 2019). Cragg and Pezzuto. (2016), noted that 6 out of every 10 drugs used in cancer treatment comes from natural sources.

Vitellaria paradoxa (Von Gaertner, 1807) is one of such promising plants indigenous to Africa. Phytochemicals such as tannin, cardiac glycoside, phlobatanin, anthraquinone (Ojo *et al*., 2006) have been isolated in this plant. Apart from its nutritional properties, the leaf, root, seed, fruit and stem bark also possess many medicinal properties such as treatment of diverse skin and gastro intestinal tract infections (Soladoye *et al*., 1989; Ferry *et al*., 1974). Its protective activity against acetaminophen-induced hepato-toxicity (Ojo *et al*., 2006), and

anti-diabetic properties (Coulibaly *et al*., 2014) have been reported. Its stem bark have been shown to have antiproliferative (Tagne *et al*., 2014) properties. Despite these qualities/attributes, information about the cytoremediative potentials of *V. paradoxa* leaf against toxicity generated by sodium arsenite in Wistar rats and *D. melanogaster* and its antiproliferative action on MCF-7 cells have not further been documented. It can therefore be hypothesized that;

1. *Vitell*aria *padoxa* have cytoremediative potentials against arsenic induced toxicity in Wistar rats and *D. melanogaster*.
2. *Vitell*aria *paradoxa* will mitigate the proliferative activity of MCF-7 cells.

1.3 Aim and objectives

Considering the diverse effect of arsenic on human and animals, this study was aimed at evaluating the cytoremediative potentials of *Vitellaria paradoxa* against Sodium Arsenite (SA)-induced toxicity in Wistar rats and *Drosophila melanogaster* along with its anti-proliferative action on MCF-7 cells. The specific objectives of the study were to;

- carry out extraction of *V. paradoxa* leaf and seed samples and profile for the *in vitro* antioxidant and genotoxic potentials of the hydroethanol extracts of *Vitellaria paradoxa.*
- determine the median lethal dose of hydroethanol leaf extract of *V. paradoxa* (ELVp) using Wistar rats
- determine the effect of ELVp on the hepatotoxicity, renal toxicity and haematological indices of sodium arsenite – treated male Wistar rats.
- evaluate the effect of ELVp on clastogenicity, expression of inflammatory (NF-κB) and apoptotic (p53 and BCL-2) proteins in sodium arsenite-treated male Wistar rats.
- determine the effect of ethyl fraction of ELVp on life span elongation and oxidative status of sodium arsenite –treated *Drosophil*a *melanogaster*.
- determine the anti-proliferative mechanism of ethyl acetate fraction of *Vitellaria paradoxa* leaf in MCF-7 cell line using colony formation ability, ROS generation, cell cycle distribution and expression of apoptotic proteins (pro-caspase 3 and cleaved caspase 3).

CHAPTER TWO

LITERATURE REVIEW

2.1 Cancer

In 2020, cancer accounted for 10 million deaths around the globe. Lungs, breast, colorectal and prostate cancer were the most prevalent presentations while lungs, colorectal, stomach, liver and breast cancer were the predominate cause of death (WHO, 2018). It is a malignant disease identify by gene mutation, unrestrained growth, generation of new blood vessel and lymph node (angiogenesis). Additionally, it is characterised by insensitivity to antigrowth factors, invasion, metastasis, resistance to apoptosis, inflammation and genome instability (de Sá Junior *et al*., 2017). While cancer mortality rate in high income countries is declining because of timely screening, detection and better care, the incidence and morbidity rates are raising in economically developing countries (Torre *et al*., 2016).

2.1.1 Cancer Incidences in Nigeria

About 70% of cancer mortality occurred in middle and less developed nations (WHO, 2018). According to Sylla and Wild (2012), of the 681,000 new cancer cases presented in Africa in 2008, 15% were from Nigeria. In addition, an estimate of 4,521 cases were recorded in the Cancer Registry of Ibadan and Abuja in 2009-2010 with an estimate of 2,985 (66%) female and 1,536 (34%) male cases respectively. Furthermore, cancer of the breast was the most presented with an incidence of 54.3 per 100,000, while the second was cervical cancer among females and prostate cancer among males (Jedy-Agba *et al*., 2012). With respect to age groupings, there was 10 years difference between both registries with Ibadan having the highest grouping (45-54) and Abuja the least (35-44) for women. While for men it was 65 years and above in both registries (Jedy-Agba *et al*., 2012).

2.1.2 Carcinogenesis

Carcinogenesis, also known as tumorigenesis is a multifaceted process that leads to the production of cancer. It has three unique stages which are initiation, promotion and progression (Basu, 2018).

Initiation: Carcinogenesis begins with an initiator which is classified either as virus, chemical toxicant or irradiation (Basu, 2018). The covalent binding of the initiator with the DNA of a normal cell result in an irreversible change genetically which is called DNA adduct (Oliveira *et al*., 2007). This process may involve more than one stable spontaneous attack (exposure) by a carcinogen on the normal cell. In return, it results in cellular mutation of genes acting as vital controller of the cells. Subsequently, loss of functions of these genes aggravates proliferation of abnormal cell if there is no repair of DNA or death by apoptosis (Trosko, 2001).

Promotion: This stage stimulates the initiated cell into further proliferation. The transformed cell can remain harmless unless when awakened by a promoter. A promoter can be a chemical that do not alter directly DNA structure but contribute to further mutation of an initiated cell. Also via a series of epigenetic processes, the promoter induces key growth stimulating signals, enhance free radical production and inhibit innate immunity of cells. This generally is categorised as hyperplasia (Basu, 2018). In addition, because tumour cells still require oxygen yet have low supply, they make use of the process of angiogenesis by the production of growth factors which prompt the development of new blood vessels that supplies the abnormal cell with oxygen and nutrients (Ahluwalia *et al*., 2014). This process encourages cell proliferation leading to an excessive cellular multiplication and progressive genome damage (Ahluwalia *et al*., 2014).

Progression: It is a series of process through which neoplasm is acquired from pre-neoplastic cells. At this stage, the distinct feature include irreversible genetic instability, continuous growth leading to increase in size of tumour, biochemical, metabolic and morphological changes in cell, inversion and metastasis (Oliveira *et al*., 2007).

Invasion and Metastasis: These occurs only in malignant neoplasm. This stage includes the spread of neoplastic cell from one part of the body to another. It involves the primary tumour cell invading locally surrounding extracellular matrix and stromal cell layer. Also, intravasation into the luminal of blood vessel which requires survival through the rigor of

transportation through the vasculation and arrest at distant organ site. Lastly, extravasation into the parenchyma of the distant organ/ tumour and the survival in this foreign micro environment. This leads to re-initiation of proliferation and generation of detectable neoplastic growth (Cominetti *et al*., 2019). This cascade of invasion and metastasis involve the breakage of the basement membrane by the carcinoma secreted proteases (Moirangthem *et al*., 2016).

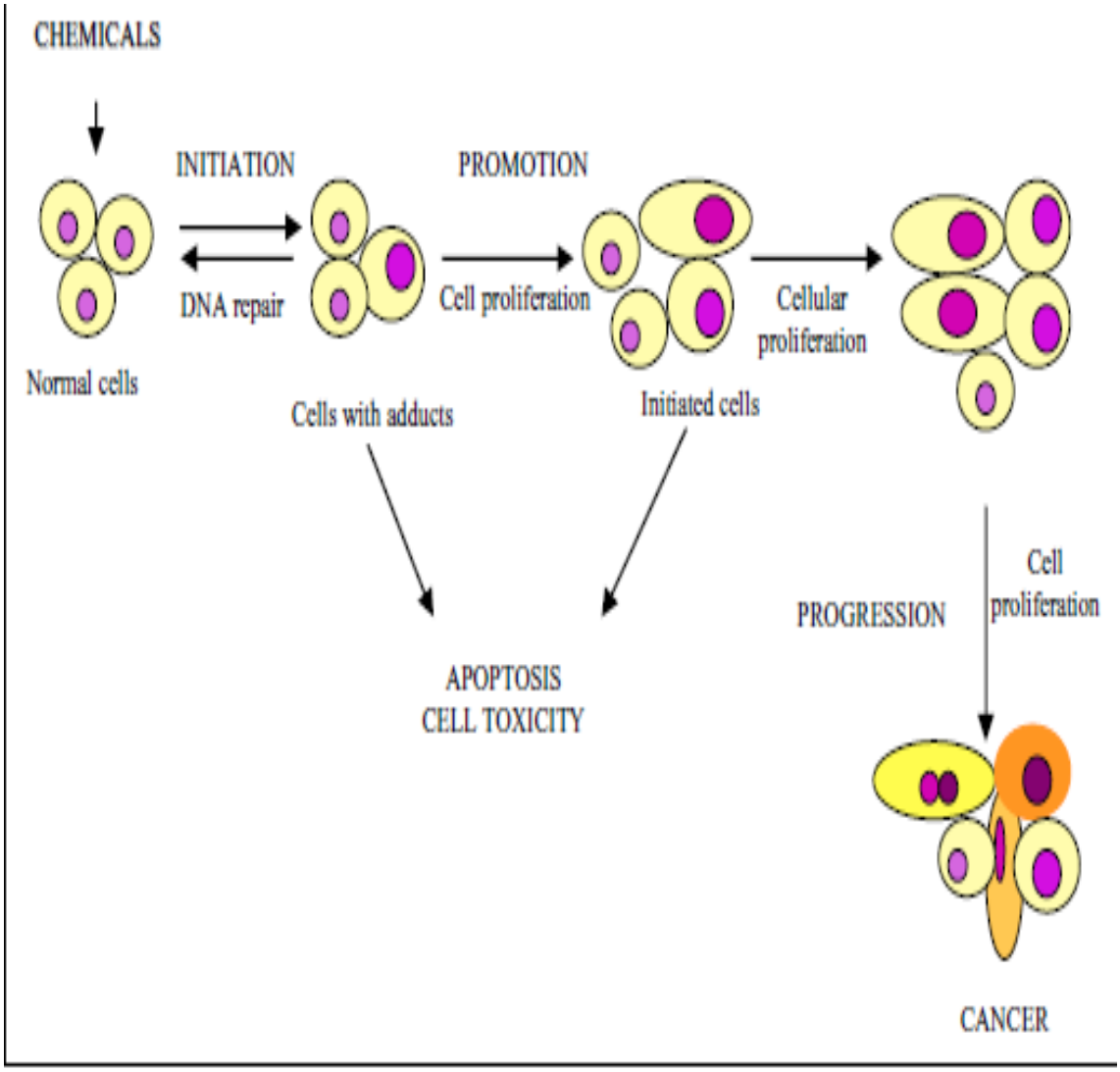

Figure 2.1: Carcinogenesis stages

(Oliveira *et al*., 2007).

2.1.3 Models for cancer research

Diverse model such as cancer cell lines, *Drosophila melanogaster* and animals have been used in the study of cancer.

2.1.3.1 Cancer cell lines

This are cells obtained from multiple sub - culture of primary cells obtained from the cancer patient tissue. In cancer studies, human derived cancer cell lines are one vital preliminary model used for cancer biology study and testing the effectiveness of cancer treatment (Gillet *et al*., 2013). These cell lines are use either as *in vitro* monolayer culture or as xenograft in mice, rats studies (Biau *et al*., 2016). In case of *in vitro* culture the advantages includes: not been costly, easy maintenance over a long time duration. However, some major disadvantages include the risk of contaminations of cell lines and alteration of cell morphology due to prolonged culture (Goodspeed *et al*., 2016). In addition, various mechanisms used by cancer cells can be understood better within a short period of time. Mechanism such as cell proliferation, colony formation, apoptosis, cell cycle evasion and invasion are been studied by scientists using this model (He *et al*., 2019). Using this model development of medications for cancer diagnosis and management have been encouraged (Katt *et al.,* 2016). Furthermore, many plant extracts and their bioactive compounds have been made known to have anti-carcinogenic properties via this model (Tagne *et al,* 2014).

2.1.3.2 *Drosophila melanogaster*

Drosophila melanogaster (Fruit fly) is a member of the Drosophilidae family. The merit of this model is ascribed to its short life cycle of about 12 days, production of large numbers of offspring, easy handling, simple food requirement, availability of large number of genetically defined mutant fly's (Tolwinski, 2017).

Although it has an impressive history as the genetic model for developmental studies (Ugur *et al*., 2016), it has been demonstrated to be an outstanding model for studying human diseases, because more than 70% genes associated with human ailments have orthologists within fruitfly genome (Chien *et al.,* 2002). Hence, it is being used as a prized model for gaining insight into non-communicable diseases for example cancer (Herranz and Cohen, 2017). Also, over the years, Drosophilists have built a strong database of mutants and

transgenic lines involving molecular techniques and tools which enhance detailed study of fruit fly (Vasudevan and Ryoo, 2016).

2.1.3.2.1 Life cycle

Drosophila melanogaster undergoes complete metamorphosis beginning from egg → larva → pupa → adult. However depending on the degree of temperature the length of complete cycle may varies from 10 to 15 days (Deepa *et al*., 2009).

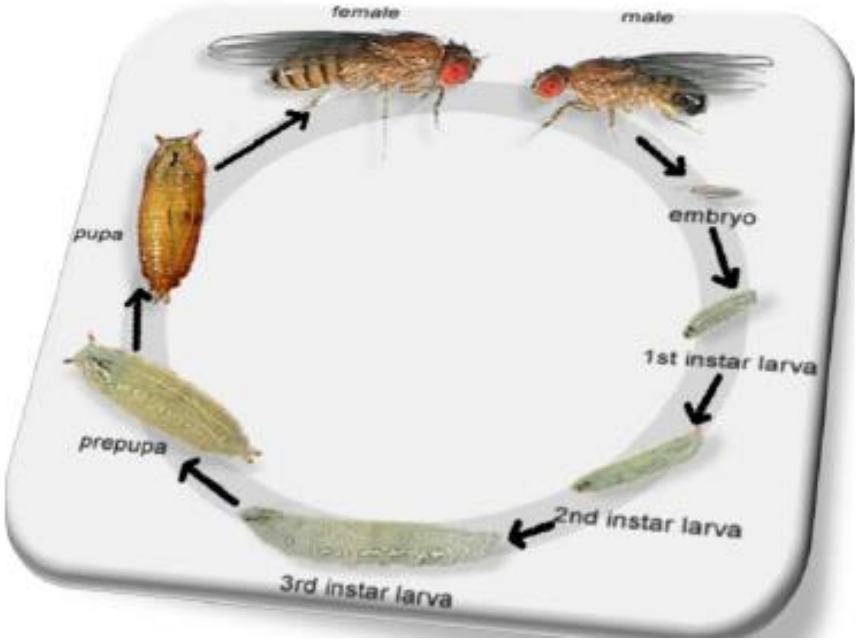

Figure 2.2: Life Stages of *Drosophila*

(Abolaji *et al*., 2013)

Egg stage

The female *Drosophila melanogaster* has the capacity to store the spermatozoa after mating with the male. Therefore, fertilization of eggs occurs when one spermatozoon passes through the opening (micropyle) at the anterior of the conical protrusion. Thereafter eggs are laid on the diet and within 12-15 hours it is hatched. Structurally, *D. melanogaster* egg is about 0.5 millimetre (mm) long, consisting of an opaque outer investing membrane (charion) with patterns of hexagonal mark (Demerec and Kaufman, 1996).

Larva stage

This is the active stage because the larva are voracious feeders. During this stage the larva undergoes two molting process consist of three instars in which the entire cuticle of the insect including the mouth armature and spiracle are shredded off and remodelled. Anatomically, it has a soft flexible body wall consisting of both outer noncellular cuticula and inner cellular epidermis. Also, well spread in the body are sense organs which includes fat bodies, the yellow malpighian tubules, the coiled intestine as well as the gonads. At the final instar stage they attain a length of about 4.5 mm (Demerec and Kaufman, 1996; Deepa *et al*., 2009).

Pupa stage

Shortly after the larva stage, it crawls into the side of the culture bottle and reduces its activity (Ong *et al*, 2015). Acquiring is pupa shape gradually the cuticle of the larva is shortened by muscular action. During the pupation stage there is differentiation of the un-differentiated cells like imaginal disc and histoblast. Pupation last for four to six days depending on the temperation before an adult fly is formed (Deepa *et al*., 2009).

Adult stage

This is the last stage of metamorphosis of the fly. A fragile, light coloured adult fly emerges from the pupa with not fully expanded wings. However, within few hours, the fly becomes dark with expanded wings. This dark colouration is used in differentiating a newly emerged fly and old ones present in same culture bottle. In addition, the female fly does not mate 10-12 hours after emergence, hence they are commonly called virgin flies. However, after this duration it can mate with a male, storing the sperm in the receptacles (Deepa *et al*., 2009).

Distinguishing features of an adult female fly from male are:

I. In general, the female *Drosophila* is bigger than the male
II. Female *Drosophila* has elongated abdomen while male has round abdomen
III. The alternate dark band on the female thorax is separate, hence they have seven segments while that of the male are fused at the last few segment hence the male has five segments.

2.1.3.2.2 *D. melanogaster:* A model for cancer

D. melanogaster has immensely revealed diverse aspect of human malignant tumours (Gonzalez, 2013). *Drosophila* embryo is an outstanding system for studying cell proliferation during development (Foe *et al*., 1993).The specialised epithelial cell sac of *D. melanogaster* known as imaginal disc is used to study the initial stage of cancer (Tamori, 2019). This disc has the capacity to proliferate during the larva stage of the flies producing matured disc with characteristic morphologies which differentiates into adult structure (Bryant and Schmidt, 1990). Also, it is fascinating that the cell cycle machinery/ regulators is highly conserved from fly to humans hence these homologs of *Drosophila* has facilitated the study of proliferation during malignancy (Potter *et al*., 2000). Furthermore, numerous fly genes have been spotted as homology of human oncogene and tumour suppressor (Miklos and Rubin, 1996). Using various advance techniques, tumours can be expressed in *Drosophila* flies using specific promoters which can be either ubiquitous or tissue specific. One of such advanced system used is the yeast UAS/GAL 4 system (Brand and Perrimon, 1993).

Notably, one mechanism that kick start the transformation of cells to cancerous cells is excessive production of free radical. Hence, it is worth noting *D. melanogaster* is used to study free radicals and antioxidant in balance arising from occupational and environmental toxicant exposure (Abolaji *et al*., 2014; Abolaji *et al*., 2015).

2.1.3.2.3 *Drosophila*: model for oxidative stress studies

Oxidative damage to tissues can occur due to imbalance between free radicals, commonly grouped as reactive oxygen or nitrogen species and antioxidants, which can either be intracellularly generated or from external source (Donnez *et al*., 2016). Various scientists

have employed the *D. melanogaster* model in elucidating biochemical and metabolic pathways resulting from environmental or occupational toxicants exposure. Abolaji *et al*., (2014), stated that the link of 4-vinylcyclohexene (VCH) - induced toxicity with oxidative damage, is via reduced survival and expression of key antioxidant enzymes. Further, using both metabolites of VCH, Abolaji *et al.,* (2015) envisaged the toxicity of VCH resulted from is downstream metabolite. In line with toxicity studies various compounds derive from plant have been shown to protect /attenuate the toxicity induced by toxicant exposure in *D. melanogaster* (Farombi *et al*., 2018).

Contrastingly, excessive/ continuous exposure to most environmental and occupational toxicants result in DNA damage leading to alteration of genes and proteins expressed if not checked by the control mechanism put in place by the body (Poirier, 2012). Hence, studies of the molecular interactions have proven that a prominent hallmark of cancer is escaping arrest of processes involve in cell growth/doubling and controlled death (Plati *et al*., 2011).

2.1.4 Apoptosis

In multicellular organism between development and maturation new cell are formed while some cell die creating a balance/ homeostasis (Goldar *et al*., 2015). Evasion of cell death is a key mechanism used by cancer cells in survival (Plati *et al*., 2011). Diverse cell death which includes apoptosis, necrosis, autophaphy, ferroptosis, necroptosis, pyroptosis have been established; however apoptosis is fundamental in maintenance of genome stability.

The term apoptosis (literally connoting “falling off”) was proposed foremost by Kerr *et al*., (1972). This cell death is distinct from other forms because it is programmed. Morphologically, its’ unique features shows shrinking of cells, condensation of chromatin, nuclear fragmentation resulting in membrane blebbing and formation of distinct apoptotic bodies (Xulu and Hosie, 2017). During these processes there is movement of phosphatidylserine a phospholipid from inside the cell to the membrane outer surface. Also, chromosome is cleaved into inter-nucleosomal fragments and caspases are turned on (Ouyang *et al*., 2012).

2.1.4.1 Mechanism of apoptosis

This unique programmed cell death is centred on two pathways: extrinsic and intrinsic (Hassen *et al*., 2012). However, cytotoxic T-cell have been found to induce an alternate mechanism involving the perforin. This third pathway is called perforin /granzyme (Jin and El-Deiry, 2005).

Extrinsic pathway (Death receptor pathway)

This pathway involves transmembrane receptors (death receptors); examples are FAS and TNF receptor. Upon specific ligand (Fas ligand for FAS receptor and TNF α for the TNF receptor) binding signal is translated resulting to trimerization and cross linking via disulphide formation leading to receptor stability and activity (Jin and El-Deiry, 2005; Goldar *et al*., 2015). Therefore, the corresponding adaptor protein (FADD & TRADD) is enlisted via the cytoplasmic death domain (DD) (Tomita, 2017). These adaptor proteins contain death effector domain (DED) whose dimerization recruit pro-caspase 8 resulting in death inducing signal complex (DISC) production. Moving further, formation of DISC enhance inactive-caspase 8 auto-proteolysis to is activated form (initiator caspase) which triggers the executional phase producing cell death (Pistritto *et al*., 2016).

Intrinsic pathway

This intracellular pathway occurs at the mitochondria. Diverse stress generated intracellularly activates p53 a transcription protein which up-regulate the pro-apoptotic Bcl-2 protein (Bax, Bak) ensuing permeabilization of the outer membrane of the mitochondria (Hata *et al*., 2015). Hence, there is loss of control of the power house transmembrane potential resulting in discharge of two basic group of pro-apoptotic proteins to the cytoplasmic matrix. Firstly, Cytochrome C and dATP release causes the apoptosis protease-activating factor 1 (Apaf-1) protein adopt a form in favour of the heptameric wheel structure (apoptosome) (Yuan and Akey, 2013) on which inactive-caspase 9 binds leading to caspase 9 activation and downstream activation of effector proteins (Acehan *et al*., 2002). The second group of proteins released are smac/Dablo and HtrA2/Omi, they act as apoptosis promoters by inhibiting IAP (inhibitor of apoptosis proteins) (Vande Walle *et al*., 2008).

Executional pathway

This is the last phase of apoptosis. It is at this point, the extrinsic and intrinsic pathway come to a termination. During this phase the effectors (caspase 3, 6 and 7) are activated leading

to mitochondria releasing Alf, endonuclease G and CAD proteins which induce DNA fragmentation, nucleus chromatin condensation, cleavage and degradation of cytoskeletal protein such as PARP and NUMA. These are the surface structure and biochemical events observe in apoptosis (Elmore, 2007).

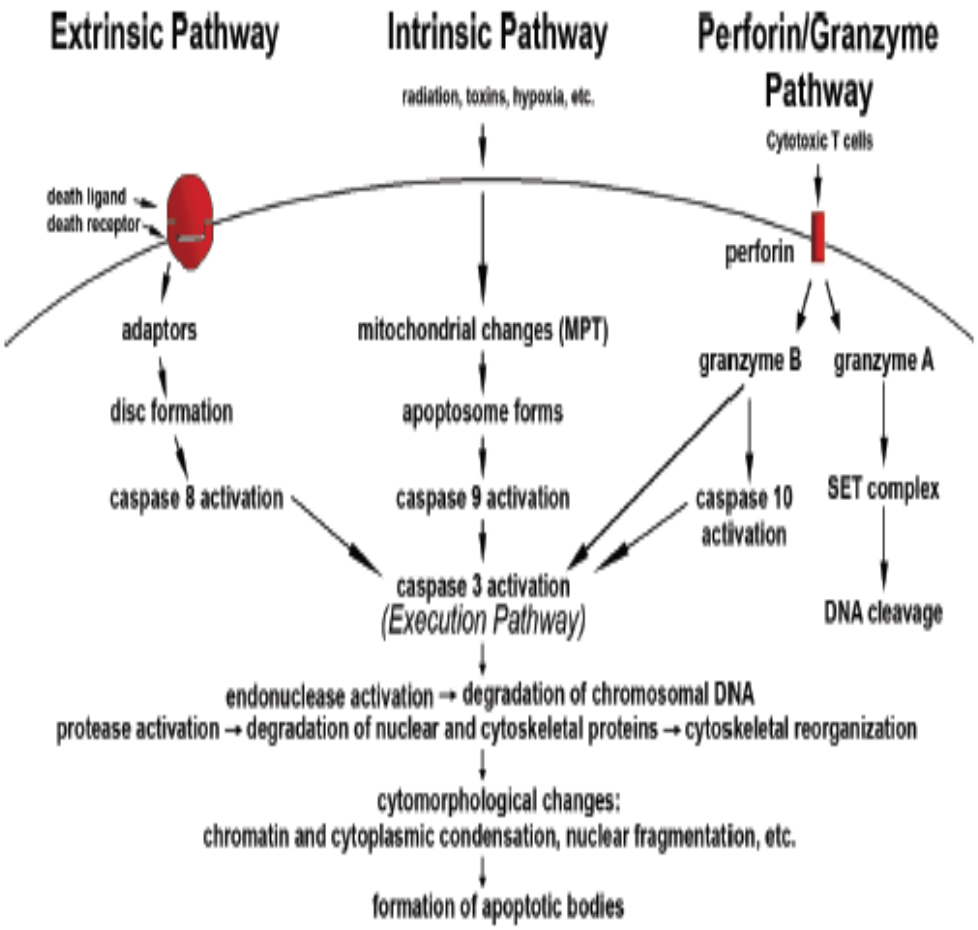

Figure 2.3: The biochemical pathways of apoptosis

(Elmore, 2007)

2.1.4.2 Regulation of apoptosis

Maintenance of homeostasis is required since the point of no return is reached when caspases become enzymatically active in cleaving target proteins hence it become necessary for apoptosis regulation (Pristritto *et al*., 2016). Two class of proteins are involved in this regulation (proapoptotic or an antiapoptotic proteins). Apart from the IAP (inhibitors of apoptotic proteins) grouped as antiapoptotic protein, the BCL-2 protein family have both positive and negative regulators of apoptosis (Pfeffer and Singh, 2018). The positive regulators includes Bax, Bak, Bik, Bad, Bim and Bid while the negative regulators embraces BCL-proteins (Borner, 2003).

Streamlining it down to the two protein of interest in my research, the binding of BCL-2 to the BH3 domain of Bax inhibits is upregulation. Hence preventing is oligomerization and protecting the mitochondrial from permeabilization consequently blocking cytochrome C release which is key for intrinsic pathway (Opferman and Kothari, 2018). However, upon cellular stress, BH3 only proteins binds to Bcl-2 hence preventing is inhibition on pro-apoptotic protein like Bax. This triggers other downstream proteins which lead to apoptosis (Ashkenazi *et al*., 2017)

Another key player of apoptosis regulation is p53 a transcription factor acting as the keeper of the genome (Hientz *et al*., 2017). Cellular stress triggers up-regulation of p53 leading to his release from MDM2 his potent inhibitor. This induced the transcription of pro-apoptotic protein like DR-5, Bax, Bak, PUMA and NOXA and reduction in the expression of proteins that inhibit apoptosis like BCL-2 and sulvivin (Goldar, *et al*., 2015). Thus, promoting permeabilization of the mitochondria resulting to cytochrome c release and APAF1, which trigger a downstream reaction that causes apoptosis (Pflaum *et al*., 2014).

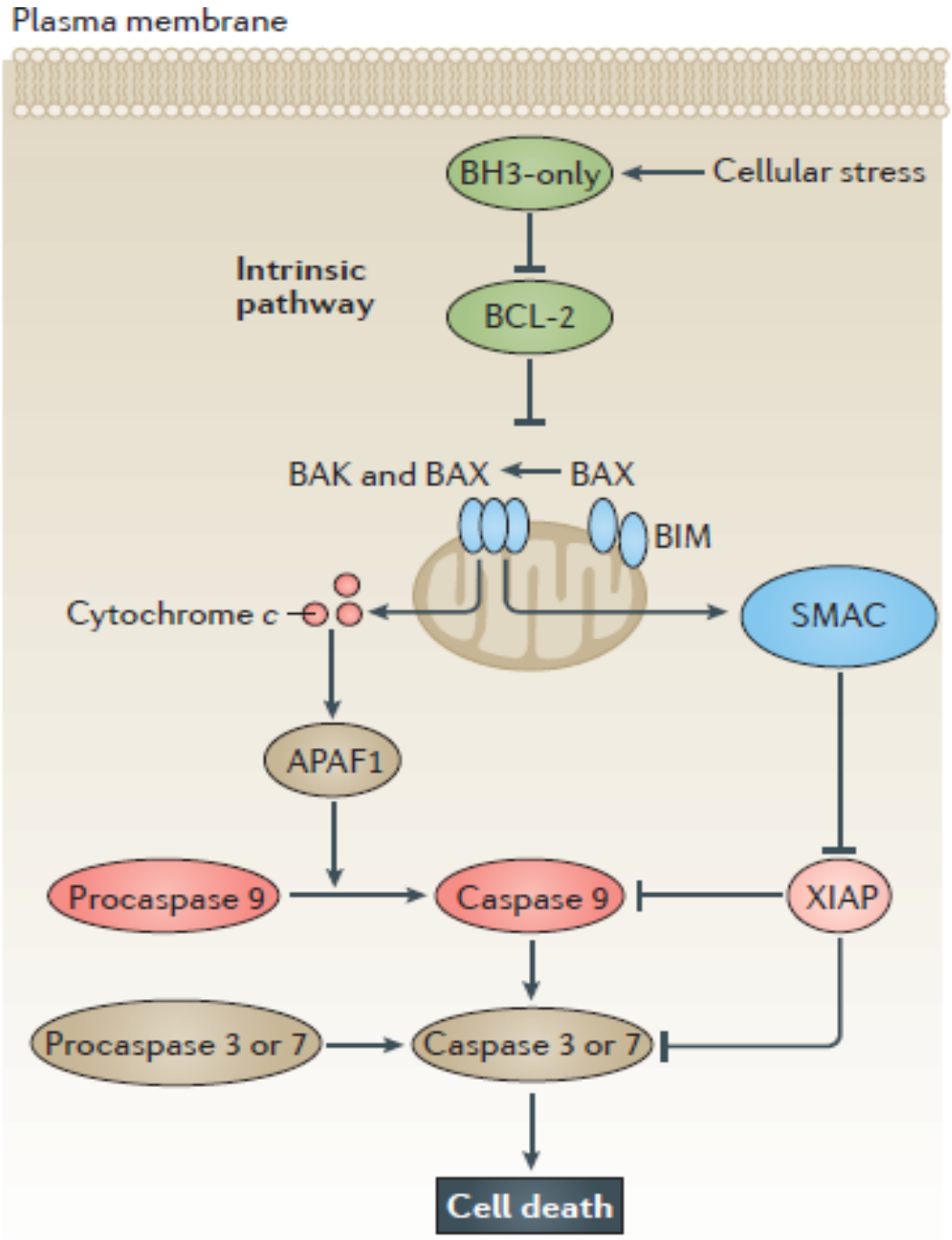

Fig 2.4: Bcl-2 protein family a key player in apoptosis regulation

(Ashkenazi *et al*., 2017)

2.1.5 Cell cycle

Another key regulating mechanism that can circumvent cells from cancer is cell cycle. It involves ordered sets of molecular events a cell undergoes in order to replicate its DNA and segregate (divide) into two daughter cells (Mills *et al*., 2017). It is majorly divided into four phase which are G1 (preparatory stage for DNA replication), S (DNA replication) G2 (mitosis preparatory stage) and M phase which is mitosis (Mills *et al*., 2017). These processes are controlled by a cascade of protein phosphorylation (cyclin/ cyclin dependent kinase) and the check points. Also, p53 play a vital role in enhancing cell cycle regulation (Engeland, 2018).

2.1.5.1 P53 and cell cycle regulation

P53 is also very relevant in regulating cell cycle. It act in both G1/S and G2/M check point (Agarwal *et al*., 1995). In G1/S check point, when a DNA damaged is observed the Ataxia Telangiectasia Mutated (ATM) kinase is activated, this induced phosphate group addition to p53, therefore decreasing is bond for Mdm2 is negative regulator leading to p53 stabilization (Visconti *et al*., 2016), and inducing is downstream protein which is p21. This p21 bind and further inhibit the cyclin A/CDK2 and cyclin E/CDK2 complex until DNA is repaired, on the other hand if not corrected apoptosis is induced (Chen *et al*., 2013).

2.1.6 Risk factors influencing cancer

From earlier research it is believed that environmental factors lead to approximately 80 % of cancer while genetic factor explain for 5% of all cancer (Sankpal *et al*., 2012).

The factors that influence cancer can be classify into intrinsic (non-modifiable, endogenous, biological) and extrinsic (modifiable, exogenous) (Gutierrez and Salsamendi, 2001).

Intrinsic (non-modifiable) Factor: These are factors that are inert; that is they are genetic and cannot be changed. They are age, sex, hormonal status of individual, family history, genetic predisposition (Wu, *et al*., 2018).

Extrinsic (Modifiable) Factor: These are factors that can be avoided or prevented by taken personal caution. They include environmental factors and carcinogens such as diet, tobacco, alcohol, viruses, irradiation and chemicals (Synthetic and natural) (Wu, *et al*., 2018).

2.1.6.1 Chemical Compounds

These compounds can either be natural or synthetic. Also, they can either be genotoxic or non-genotoxic. In addition exposure can be through occupational activities or environmental (which include exposure through water or diet). Some examples of this chemical carcinogens include poly aromatic hydrocarbon (benzo α pyrene, bisphenol A), nitrosamine, pesticide and heavy metals (arsenic, nickel, chromium) (Lagoa *et al*., 2020). One mechanism used by these chemicals is the generation of free radicals which have an inducing effect on DNA resulting in DNA adduct formation or covalent bonding with other biological molecules likes proteins, lipid and carbohydrate. This effect can lead to formation of cancer if the DNA is not repaired hence a transfer of damaged DNA to the daughter cell (Ohshima *et al*., 2005).

One environmental carcinogen that is grouped as a class 1 carcinogen is arsenic (Ganapathy *et al*., 2019; IARC, 2018)

2.2 Arsenic

Arsenic (As) is a toxic heavy mental and a class one chemical carcinogen which is abundant in nature. It has three allotropic form (α, β and γ) and more than two oxidation state (+5, +3, 0, -3) which enhance the easy formation of its organic and inorganic forms (Medina-Pizzali *et al*., 2018). This inorganic arsenite is found in the groundwater of a range of countries in Asia, Europe, North America and South America (Naujokas *et al*., 2013). Furthermore, Nigeria, South Africa and the Democratic Republic of Congo have been linked with adverse health conditions resulting from arsenic toxicity (Genthe *et al*., 2018; Nemery and Nkulu 2018; Anetor, 2016).

2.2.1 Sources of Arsenic

The main sources of arsenite are air, food, water, drug and industrial chemicals such as agricultural chemicals which include herbicides, insecticides, rodenticides, wood preservative, food preservatives and cosmetics (Adil *et al*., 2015). The release of arsenic into our environment can be either through unprecedented natural events such weathering of rocks and volcanic eruption or through man made activities i.e. (occupational, agricultural, pharmacological). These activities have enhanced the leaching of this

poisonous chemical into the water bodies which is absorbed by plants and in turn eaten by humans (Azam *et al*., 2016). Genthe *et al*., (2018) observed, that heavy metals including arsenic in river catchment of South Africa have exceeded the WHO safe level. According to the review of Nemery and Nkulu (2018) people living close to or working in the Katanga mining zone in the Democratic Republic of Congo were seen with high amount of arsenic when urine screening was carried out.

2.2.2 Absorption and metabolism of arsenic

The major route by which arsenite access the body is through the gastrointestinal tract (GIT), through inhalation (nostril) to the lungs and by the skin (Chen *et al*., 2006). Ingestion of arsenic contaminated water or diet is a wide road for access into the body. Depending on it's from it is absorbed through intestine via different transporters which include (sodium dependent glucose transporters, aquaporin 3 or 10, and organic anion polypeptide transporter for As (III) or phosphate transporter for As (V) (Mondal and Chattopadhyay, 2020). Furthermore, it is metabolised by the hepatocytes through a biomethylation process forming monomethylarsonic acid and dimethylarsinic acid by two major reaction which are reduction reaction involving arsenate reductase and oxidative methylation reaction involving S-adenosyl methionine (SAM) and Reduced Glutathione (GSH) (Jomova *et al*., 2011; Mondal and Chattopadhyay, 2020). In these forms it is excreted out by the kidney (Wang *et al*., 2018). Hence, studies have shown liver and kidney as the prime targets of arsenic toxicity.

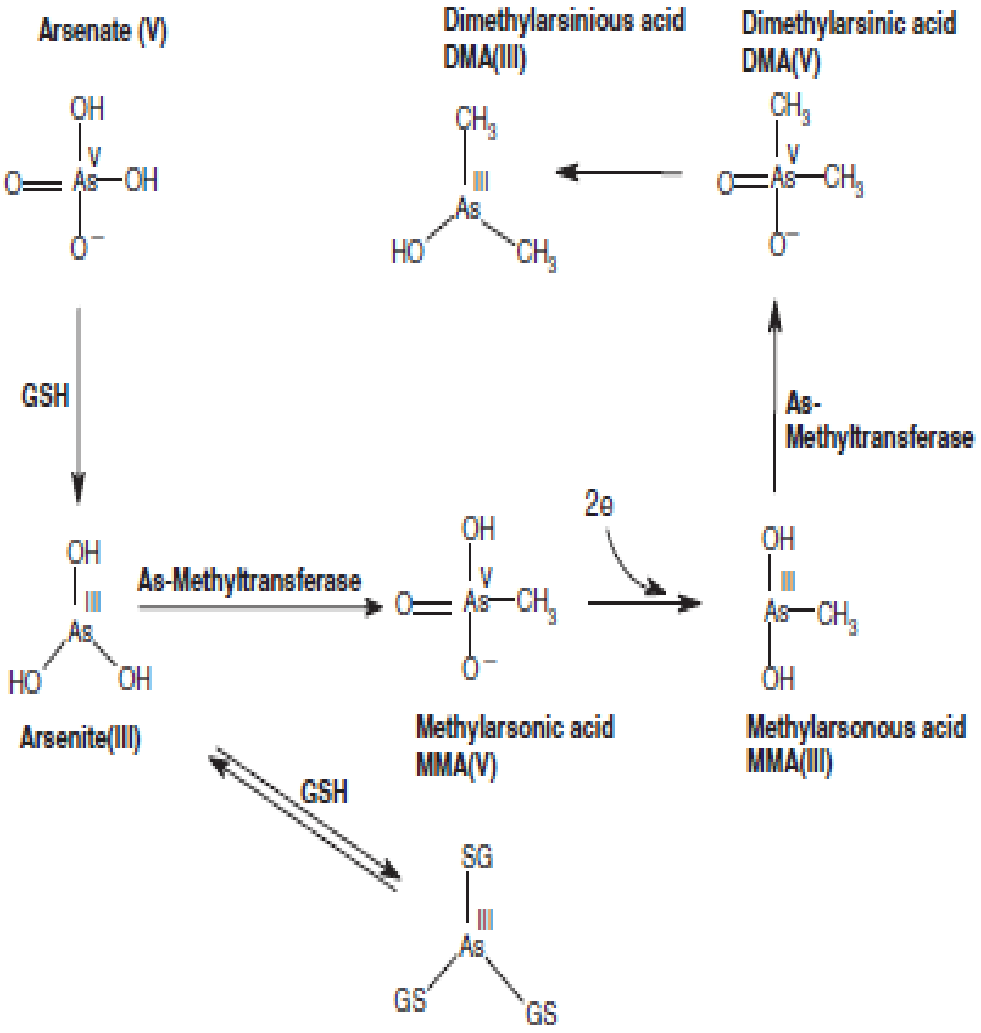

Fig 2.5: Mechanism of arsenic metabolism

(Jomova *et al*., 2011 citing Hughes, 2002)

2.2.3 Arsenic and toxicities

The toxicity of arsenic (As) is resting on is physical and chemical form. Generally, toxicity is attributed to the As form without carbon. In this form As (III) induces more toxicity than As (V) (Susan *et al*., 2019). Categorizing arsenic toxicity into two, Muscular pain, nausea, abdominal pain, vomiting and weakness are signs of acute arsenic toxicity while chronic toxicity is characterised by multiple organ failure, cancer, hyperpigmentation of skin, neurological disorders and behavioural abnormalities (Costa, 2019). Arsenic (As) have been shown to induce toxicity through various mechanism such as ROS generation (Susan *et al*., 2019) which in turn oxidize various biological molecules like lipid leading to lipid peroxidation production (Jomova *et al*., 2011). It is further associated with epigenetic alterations (Bjørklund *et al*., 2018) and DNA damage.

2.2.3.1 Arsenic, redox / antioxidant imbalance

Induction of ROS by arsenic involves oxidation reaction. It can either be through a direct oxidation of As(III) to As (V) under natural conditions in an organism system leading to production of hydrogen peroxide (H_2O_2) which can be catabolised by Fenton reaction producing the highly reactive hydroxyl radical (Jomova *et al*., 2011). Secondly, the secondary metabolite of As (dimethylarsine) through oxidation, forms dimethylarsenic radical and superoxide anion. In addition, further oxidation of dimethyl arsenic radical results in the formation of its peroxyl radical. The research of Mehrzadi *et al*. (2018) reported that sodium arsenite-induced elevation of nitric oxide in hepatic and renal tissues. Also, it has been reported that arsenic induces ROS lead to irregularities in mitochondrial membrane potential which may be key in apoptosis. According to Choudhury *et al*., (2016), ROS generation resulting from arsenic initiate nuclear factor erythroid 2 related factor (NRF-2) and nuclear factor kB (NF-kB), alongside increases phosphorylated Ik-B). Hence, arsenic damaged is involved in activating NF-kB signalling pathway and fundamental in inflammatory response (Liu *et al*., 2017). This increase in ROS result in depletion of reduced glutathione (GSH) / other biological catalyst involve in antioxidantive process. Turk *et al*. (2019) reported the reduction of catalase activity in rats administered sodium arsenite (10 mg/kg). While activation of nitric oxide synthase was observed by Costa, (2019), hence, the resultant oxidative stress. Therefore, oxidative stress results from an

altered Redox regulation which lead to an imbalance. The downstream effect of oxidative stress is lipid peroxidation, DNA damage, protein depletion and damage activation of p53 and Bax leading to apoptosis (Choudhury *et al*., 2016).

2.2.3.2 Arsenite and liver toxicity

The liver is a key organ where arsenic harmful nature is implicated (Li *et al*., 2013). The functions of the liver include: detoxification, synthesis of protein, regulation of glucose levels and key in maintaining and producing energy even during fast using is specialized hepatocytes (Kalra *et al*., 2021). In fruit fly, the homolog of liver is the fat bodies. It is in charge of energy storage and utilization in *D. melanogaster* (Chatterjee *et al*., 2014).

Liver toxicity can be seen in different forms such as hepatitis, cirrhosis, liver cancer. Liver toxicity is usually diagnosed through the determination of some liver enzymes in serum like aspartate aminotransferase (AST), alanine aminotransferase (ALT) and alkaline phosphatase (ALP). During arsenic toxicity, it induces a resultant increase of these enzymes due to leakage from hepatocyte to the serum (Gbadegesin *et al*., 2014; Gholamine et al., 2019). In extreme cases, liver histology picto-micrograph is use to confirm the result gotten from the serum assays. According to Gbadegesin *et al*. (2014), the histology of rat liver treated with sodium arsenite alone indicated widespread thinning of hepatic cords which is an indication of cell death by necrosis while Adegoke *et al.* (2017) showed cellular infiltration by mononuclear cells at the periportal region of the hepatocyte which indicate inflammation.

2.2.3.3 Arsenite and kidney toxicity

The kidneys are bean shape organ, weighing around 135-150g in humans, typically they are 10-12cm long, 5-7cm wide and 2-3 cm thick (Wein *et al*., 2007). Functionally they are involved in filtration, reabsorption of water, urea and ammonium excretion, electrolyte regulation hence maintaining fluid and acid base balance in addition to stimulation of red blood cell production. In order to monitor kidney toxicity key enzymes assayed for are creatinine and urea. Research from Adil *et al*., (2015) and Sarker *et al*., (2013) revealed a decrease in relative kidney weight upon treatment with sodium arsenite. At the same time, result from Adil *et al*., (2015) showed rise in serum creatinine, urea and blood uric nitrogen

from sodium arsenite which was further buttressed by the reduction observed from the oxidative stress markers of the kidney which are superoxide dismutase (SOD), GSH and increase lipid peroxidation. Das *et al*., (2016) observation was in agreement with Adil *et al* research. Also, Turk *et al*., (2019) indicated elevated serum Urea and creatinine by SA however a protective effect by hesperidin was noted.

2.2. 3.4 Arsenic role in genotoxicity

The genotoxic nature of arsenite have been linked up with ROS production (Roy *et al*., 2018). ROS production by arsenic is linked with chromosomal aberration, micronuclei formation and DNA damage. Studies of both outside and inside an organism have been employed in demonstrating genotoxic nature of arsenic (Faita *et al*., 2013; Cohen *et al*., 2007). Anwar and Qureshi (2019) reported a dose and time dependent trigger of oxidative and genotoxic stress in testes and epididymis organs of mice (*in vitro*). Furthermore, the genotoxic nature of arsenic could be attributed to is bio-transformed metabolite monomethylarsonous acid (MMA). Xu *et al*. (2018) recently reported DNA damage of mouse killer cells by MMA a major arsenic metabolite. In addition, it was demonstrated that As reduced DNA repair using comet assay both in an *in vitro* study involving cultured human cell model and exposed individual using their cryopreserved lymphocyte. It reported a decline in the expression of ERCC1 (excision repair cross – complement 1) at the transcription and translation levels (Anderw *et al*., 2006). Apart from the above, experiment involving micronucleus assay for animal model have also show case the genotoxic nature of arsenic - via the induction of micronuclei in the poly chromatic erythrocytes (PCEs) of cells involve in blood production (Odunola *et al*., 2007).

In line with this, the genotoxic effect of arsenic arising from ROS generation and depletion of antioxidant enzymes has been linked with initiation of cancer due to DNA damage. According to Steinmaus *et al*., (2014) cancer such as skin, lungs, bladder, liver and kidney is connected with environmental arsenic toxicity.

The primary option for the treatment of cancer remains surgery, radiotherapy and chemotherapy. However, the major draw backs limiting their use in the clinic include; drug resistance, tumour relapse and post-treatment toxicity (Phi *et al*., 2018).This has sparked a renewed interest and aggressive quest in natural sources for new agents that inhibits cancer

that are cost effective and efficient with minimal side effects (Desai *et al*., 2008). Plants are rich in natural compounds. They are used in ancient times in medicine, however, it was only suggested two decade back for treating and managing arsenic toxicity (Bhattacharya, 2017). In addition, Liskova *et al*., (2020) review on dietary phytochemicals further boosters the protective effect of plant-based products against carcinogen exposure and in turn cancer formation.

2.3 Medicinal plants

From ancient times plant have been of medicinal value to man. In the primary health care system of most Africa and Asians countries orthodox use of plants (herbs) for treatment and management of diseases is still in place (Famewo *et al*., 2016; Mahomoodally, 2013). Furthermore, about 80 % of conventional drugs are derived from plant and his product. This is because plant which are of medicinal values possess active biological compound (Mahomoodally, 2013). These active compounds are call phytochemicals. They are classified into various categories such as phenols, flavonoids, saponins, tanins, anthraquinones, terpenoids, alkaloids etc. (Barbieri *et al*., 2017)

A few decade ago, scientist based on cancer research have also focussed most of their research on the medicinal potentials of plants in treating cancer (Greenwell and Rahman, 2015; Abu-Darwish and Efferth, 2018). Specifically, plants such as Curcuma longa, Allium sativum, Ageratina have been studied using cancer cell lines in other to determine their mechanistic pathway against cancer (Kooti *et al*., 2017). Through this method, the most effective extracts or fractions are being showcased in some cases. Hence, drugs such as vincristine, vinblastine, paclitaxel, podophyllotoxin and camptothecin made from plants with ability to inhibit/prevent cancer, are used in the treatment of cancer patients (Lichota and Gwozdzinski, 2018).

One of Africa's main tree species is the shea butter tree, due to its high potential to contribute to reducing rural poverty, hunger, disease and enhance environmental sustainability.

2.3.1 *Vitellaria paradoxa*

Vitellaria paradoxa (formerly *Butryspermum paradoxum*) (Henry *et al*., 1983), belong to the Sapotaceae family. Paradoxa is known as the only specie of Vitellaria however it has two sub-species which are subsp. *paradoxa* commomly associated with West Africa (Nyarko *et al.*, 2012) and subsp. *nilotica* commonly associated with East Africa (Gwali *et al.*, 2011) which is consistent with his indigenous links to Africa (Okollu *et al.*, 2004). Also, in English it is called Shea-butter, Emi (Yoruba), Okwuma (Igbo, Nigeria), Kadanya (Hausa, Nigeria) (Hall *et al.*, 1996). Kareje (Fulfulde, Nigeria), Koita (Gbagi, Nigeria), Mmameng (Cham, Nigeria).

2.3.1.1 Plant description

Vitellaria paradoxa is a medium size tree having height of around 10-20 meters when fully matured (Von-Maydell, 1990). The trunk has a diameter of about 0.5-2.5 meters however this is relative to tree height. It is in fused with rough thick dark gray bark. Attached to this trunk are branches bearing the leaves. The leaves are borne in terminal whorls, they are long and have wavy margins. Also both ends of *V. paradoxa* leaf is rounded (Iwu, 1993). Below is the picture of *V. paradoxa* leaf as seen in Figure 6. According to (Jøker, 2000) *V. paradoxa* tree begins to produce flower when it is about 15 years old. The flowers are bisexual and are a greenish/yellow in colouration. Also, the fruit emerges after the flowering period. The fruit is made up of a thin, nutritious pulp that cover up the oil-rich oval shaped seed (Maranz and Wiseman, 2003).

2.3.1.2 Phytochemicals

Ndukwe *et al*., (2007) stated that extract of *V. paradoxa* stem bark has alkaloid, tannins, saponins, steroid and carbohydrate as phytochemicals. In addition to phytochemicals listed above El-Mahmood *et al*., (2008) also revealed cardiac glycosides. Researching on the methanol leaf extract Olaleye *et al*., (2015) qualitatively determined the phytochemical present to be tannins, flavonoids, phenolics, steroids, alkaloids and phlobatannins.

2.3.1.3 Acute toxicity of *Vitellaria paradoxa*

Acute toxicity is measured by determining the lethal dose (LD_{50}). This is a one-time dose which causes 50 % of death of the experimental model. Hence, it is used to assess plant extracts, drugs or chemicals toxic nature (OECD, 2008).

The LD_{50} of *Vitellaria paradoxa* stem bark methanol extract have been shown to be more than 5000 mg/kg after an oral administration to Wistar rats (Mainasara *et al*., 2016) because no mortality was recorded even at this dose which was the highest administered. Also, Fodouop *et al*., (2017) reported the acute dose of the aqueous leaf extracts as 12000 mg/kg using mice, they noticed no change in behaviour at doses less than 8000 mg/kg.

2.3.1.4 Uses of *Vitellaria paradoxa*

Primarily the use of *Vitellaria paradoxa*, is associated with the seed which contain about 50 % fat. This fat is used by many people locally as a cooking fat or oil, as well as making soap, ointment and cosmetic. Furthermore, the fat extract have been reported to possess great medicinal properties which is associated with the triterpenes ester a high UV absorbent (Brucken *et al*., 2008) hence is skin promoting and protecting properties. In addition, it has been shown to contain high phenolic content of which eight are catechins and they function as antioxidant (Akhter *et al*., 2008). Apart from the seed, the sweet pulp is nutritious with high source of energy and medicinal applications is associated with its roots, bark and leaf.

2.3.1.4.1 Antimicrobial activity of *Vitellaria paradoxa*

The bark of *vitellaria paradox* is found to be antifungal against *Aspergillus spp, E. floccosun, M. audouini*i and *T. mentagrophytes* of which the ethanolic extract was the most effective (Ahmed *et al*., 2009), Ei-mahmood *et al*., (2008) and Ayankunle *et al*., (2012) showed the antibacterial activity of the stem bark against Escherichin *coli, Kiebsiclla pneumoniac* and the ethanol extract was also more effective**.**

2.3.1.4.2 Medicinal Uses of *Vitellaria paradoxa*

Orthodox doctors apply the plant fat in treating various dermatitis such as rash, chap, inflammation, skin irritation, skin ulcer and rheumatism (Hong *et al*., 1996). Different parts

of *V. paradoxa* is associated with medicinal benefits. For example, decoctions of the leaf is used for stomach and head ache treatment while oral administration of the bark paste is used for treating jaundice, diarrhea, and chronic sore (Mallogo, 1989). Also using the stem bark, child birth and breast milk production is facilitated. In addition, it helps in treating leprosy and neutralises of snake bites (Vining, 1992). Various parts are used for enteric and gastro intestinal infections treatment (Soladoye *et al*., 1989). The plant have been found to be antidiabetic by (Coulibaly *et al*., 2014) who assessed the antidiabetic property of *Vitellaria paradoxa* bark extract using both crude aqueous extract and hydro- ethanolic extract in oryctolaguscuniculus rabbit. The hydro- ethanolic extract induced hypoglycemic and antihyperglycemic activity. The methanolic stem bark extract have ameliorated the scopolamic- induced memory disfunction in rat by reducing hippocampus oxidative stress (Harquin *et al*., 2015).

CHAPTER THREE
MATERIALS AND METHODS

3.1 Collection of *Vitellaria paradoxa* plant parts and certification

Leaves and kernels of *V. paradoxa* were procured from 'Alubarika' area along 'Ogboro' Road Saki, Oyo State, Nigeria between March to June 2016 at intervals. They were identified at the Department of Botany, University of Ibadan, Nigeria and given the authentication number: UIH-22624.

3.1.1 *V. paradoxa* leaf extract preparetion

The leaves of *V.paradoxa* were weighed using a table top scale, washed to remove all sand and air-dried at the drying room in the Department of Biochemistry, University of Ibadan. Thereafter, it was milled to a powdery form which was used for the leaf extracti

Plate 3.1: Leaves of *V. paradoxa*

Taken March 18, 2016 at 4.30pm by Oyibo, Aghogho

3.1.2 Preparation of Seed for extraction

The kernels were washed, air-dried and broken to obtain the seeds which were cut into bits and oven-dried at 60℃ to reduce the moisture content. They were milled and the fat content was extracted using petroleum ether as the solvent in a Soxhlet extractor. The resultant cake was used for the extraction of seed extract.

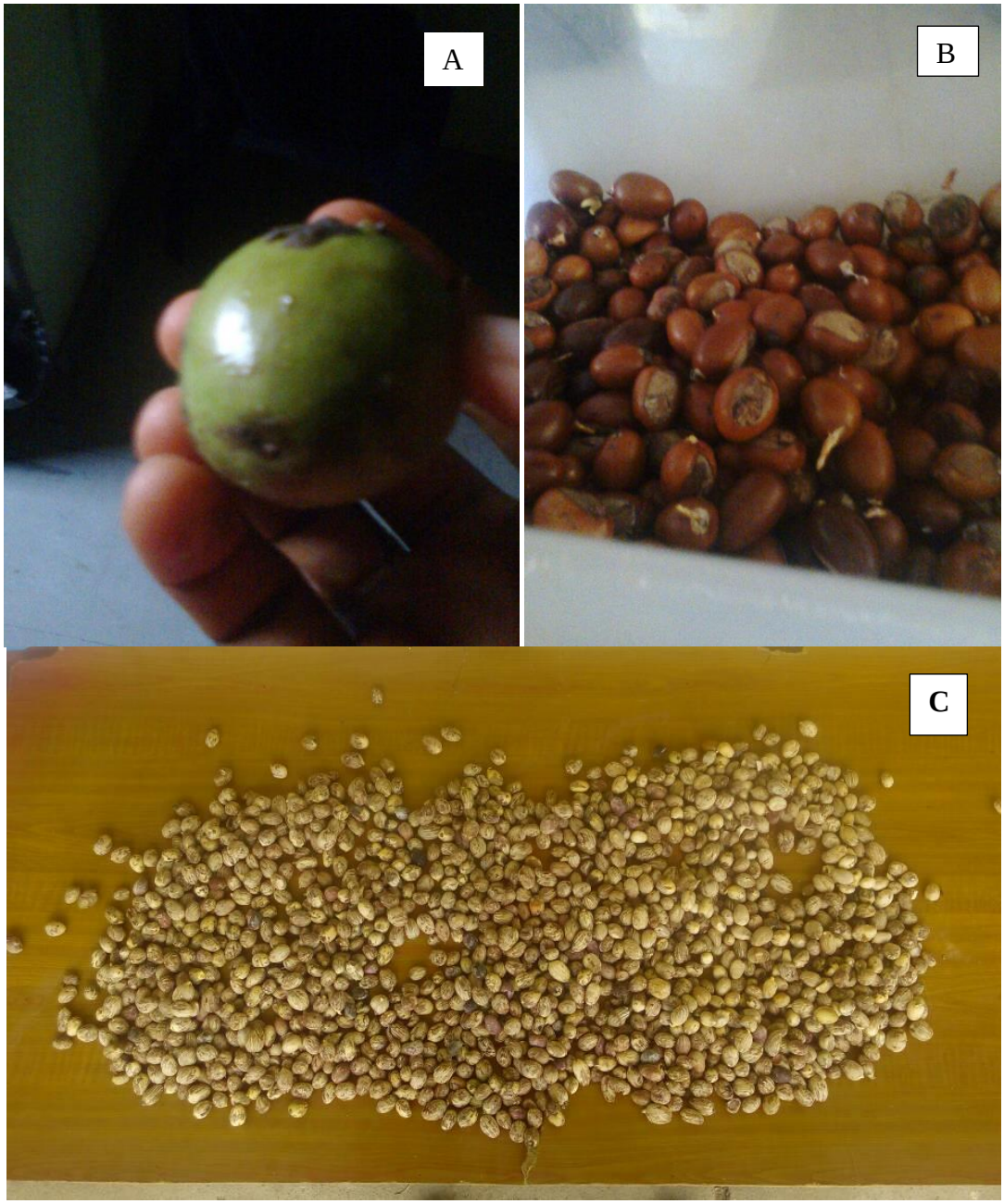

Plate 3.2: Fruit, kernels and seeds of *V. paradoxa*

(Taken June 18, 2016 at 10.am by Oyibo Aghogho).

3.1.3 Cold hydroethanol extract

Cold extractions were carried out on the powdery leaf sample and the resultant cake of the seed respectively. Then 500 g of the powdery leaf and seed respectively were soaked in 2500 mL in a ratio of 3:7 (water: ethanol) at room temperature for 72 hours. Thereafter, filtration and concentration of each filtrate at 40℃ by means of a rotary evaporator. The concentrates of both extract were kept in the refrigerator at 4℃ until when needed for administration to the experimental animals. The yield for hydroethanol leaf extract of *Vitellaria paradoxa* (ELVp) was 32.29 % while that of the hydroethanol seed extract of *Vitellaria paradoxa* (ESVp) was 23.8 %.

3.2 Fractionation of leaf extract by Vacuum Layer Chromatography (VLC)

Vitellaria paradoxa leaf extract (109 g) was brought to solution in 300 mL of ethanol and water (ratio of 2:1). Thereafter 109 g of silica gel was added and properly mixed and the extract air dried for two days, meshed and filtered to give a powdery sample.

Fractionation was carried out with the aid of sintered glass, vacuum pump and round bottom flask. The sintered glass was packed with silica gel first and thereafter, the powdery sample with the aid of the vacuum pump. This was partitioned with solvents starting with the least polar (n-hexane → chloroform → ethyl acetate → 70 % ethanol). The various fractions were concentrated using rotatory evaporator at 40℃. The percentage yield were n –hexane 0.11 %, chloroform 2.96 %, ethyl acetate 11.05 % and 70 % ethanol 3.1%.

3.3. Phytochemical screening method (qualitative)

According to Odebiyi and Sofowora (1978) fractions of *V.paradoxa* leaf extract were screened for saponin, alkaloids, phenolic, tannin, steroids, flavonoids, glycosides and anthraquinones in order to determine their phytochemical constituents.

3.4 Assessment of antioxidant activity (*In-vitro*)

3.4.1: Total antioxidant capacity

Total antioxidant capacity was determined according to Prieto *et al*., (1999) method. Aliquot of *V.paradoxa* extracts/fractions 0.3 mL + 3 mL of reagent mixture (0.6 M sulphuric acid, 28 mM sodium phosphate and 4 mM ammonium molybdate) was mixed in a test

tube.Thereafter, it was covered, subjected to heat for 90 mins in water bath at 95℃ after which it was left to drop down in temperature. At 696 nm optical density reading was read against blank. The blank was distilled water while standard was ascorbic acid (Appendix 1).

3.4.2: Reducing power assay

Following Oyaizu (1986) method the ability of both extracts / fractions of *V. paradoxa* to reduce iron (iii) to iron (ii) was determined. Briefly, 1mL of varying concentrations (25, 50, 100, 200, 400, 800 µg/mL respectively) of extracts was prepared to which phosphate buffer (pH 6.6) 2500 µL was added and 2500 µL of $K_3Fe(CN)_6$. This mixture was pre-heated for 10 mins at 50℃. Thereafter, 2500 µL of 10 % TCA (w/v) was put into it and spinned for 600 secs at 3000 rpm. Thereafter, 2500 µL supernatant was put into 2500 µL distilled water + 500 µL of $Fe(Cl)_3$ (0.1 %w/v). At 700 nm absorbance reading was read against blank.

3.4.3: 2,2-diphenyl-1-picrylhydrazyl (DPPH) assays

Both extracts scavenging power for DPPH was determined using Brand-williams *et al*., (1995). The extracts solution 1 mL of various concentrations was mixed with 1 mL DPPH (0.5 mM). This was kept in a dark cupboard to prevent light rays, after 30 minutes readings of absorbance was taken at 517 nm.

3.4.4: Total phenol content

Following Kim *et al*., (2003) method total phenol content was determined. Briefly, 500 µL of dissolved extracts/ fractions was mixed with 1000 µL of Folin-Ciocalteu phenol reagent and left standing for 5 mins. Thereafter, 7 % $NaCO_3$ solution (10 mL), distilled water (13 mL) was put into it. After proper mixing, it was kept in a dark cupboard at 25℃ for 90 mins and read at 750 nm using a UV/VIS spectrometer 725S.

3.4.5: Total flavonoid content (TFC)

The total flavonloid content was assessed using spectotometer following Zhishen *et al*., (1999) method. 500 µL of 2 % ethanol $AlCl_3$ solution was infused with 500 µL of dissolved extract/ fractions solution. Thereafter, it was kept for 45 mins at ambient temperature and at 420 nm absorbance was read. Standard curve was determined using quercetin.

3.5 Bacterial strain and culture

The SOS chromotest kit was purchased from Environmental Bio-detection Product Inc (ebpi). The bacterial strain used is *E. coli* PQ37. The content of the growth media was transferred into a vial containing the bacterial cell and was given a quick shake to ensure it is well mixed. It was incubated overnight for 16 hrs at 37℃ up to an absorbance of 0.3 at 600 nm.

3.6 *In vitro* assessment of genotoxicity of hydroethanol extracts of *V.paradoxa*

The genotoxic nature of both extracts of *V.paradoxa* was assessed using SOS chromotest following the protocol of Quillardet *et al*., (1982). Briefly, the bacterial cell (*E.coli* PQ37 strain) obtained from the exponential phase culture was diluted 1:9 into fresh medium. 10 µl of diluent (10 % DMSO) was placed in the wells of the microplate with the exception of column A. Thereafter, 20 µL of 4-Nitroquinoline-1- oxide (4-NQO) and test extracts respectively was placed in column A's and made down the column into six series of two fold dilutions. 100 µL of the prepared bacterial was added to each containing either 4-NQO or extracts (ELVp, ESVp). It was incubated for two hrs at 37℃. Using the simultaneous activity check of β-galacctosidase and alkaline phosphatase, 100 µL of a chromogenic substrate (gotten from the mixture of the blue chromogen and dry alkaline phosphate substrate) was inputted per well. It was there after heated for 90 mins at 37℃ until a green colour appeared. 50 µL of a solution that terminate the reaction was added to the individual well and with the aid of a microplate reader, it was read at 600 nm to determine β-galacctosidase production (genotoxicity) and 420 nm to determine viability of bacterial against negative control. The SOS inducing factor (SOSIF) was calculated.

$$SOSIF = \{(OD600i)/(OD420i)\}/\{(OD600, negative)/(OD420, negative)\}$$

Where OD600i and OD 420i, are the absorbance of sample (control and extracts) at a certain concentration at each indicated wavelength, and OD600, negative and OD420, negative are the absorbance of the negative control at each indicated wavelength.

3.7 Lethal dose (LD_{50}) determination of leaf extract of *Vitellaria paradoxa*.

Acute toxicity study was accessed following the Organization for Economic Co-operation and Development guidelines 420 (OECD, 2008).

Eighteen female Wistar rats were procurred from the animal house in Apata, Ibadan which weighed between 69-89 g. They were housed at the Department of Biochemistry, University of Ibadan animal house on plastic cages with a diameter of 45 cm length, 32 cm width and 26 cm height. They were kept at room temperature between 25℃ at 12 hrs light and dark phase. They were feed with Ladokun rat pellets and water liberally.

The first two weeks after purchased of the rats was used for acclimatization after which their weight was between 100 -110 g. Randomly dividing the rat into 6 groups comprising of 3 animals each, a single oral dose was administered using oral cannula. The grouping are control (distilled water), ELVp 5, 50, 300, 2000 and 5000 (mg/kg), respectively. Thereafter for the first four hrs after administration toxicity symptom was watch out for and subsequently for 24 hrs. Any mortality and weekly weight was also recorded.

3.8 Animal Experimental design and treatments

The proposal for the use of Wistar rats was endorsed by the Animal Care Use and Research Ethic Committee (ACUREC) University of Ibadan. The assigned number is UI-ACUREC 16/0019.

Forty male rats, weight range 80-100 g were procured and kept in the experimental animal facility as described in Section 3.7. Ladokun rat pellets was used as their feed and water was given *ad libitum*. An initial two week acclimatization of albino rats was done prior to the commencement of the study. Based on treatment doses, five rats per group were randomized into eight group as shown in Table 3.1. In addition, a 12 hrs light/dark phase was maintained at 29 ± 2℃ room temperature and treatments were administered for 14 days.

Table 3.1: Experimental design

GROUPS	TREATMENTS/ DOSES (mg/kg)
1	Control (distilled water)
2	Vitamin E 100
3	ELVp 100
4	ELVp 200
5	Sodium arsenite 2.5
6	Sodium arsenite 2.5 + Vitamin E 100
7	Sodium arsenite 2.5 + ELVp 100
8	Sodium arsenite 2.5 + ELVp 200

Food was withheld from the rats overnight and they were sacrificed by cervical dislocation.

3.9 Serum collection

Each rat blood was taken from the orbital sinus into properly labelled plain centrifuged bottle and left on bench at room temperature to enable clotting. Thereafter, centrifugation at 3000 g for 10 mins. Furthermore, proper collection of the supernatant (the serum) was done by the use of 100 µL micropipette and stored at -20℃.

3.10 Assays of liver function enzymes

Liver function markers: alanine aminotransferase (ALT), aspartate aminotransferase (AST) and alkaline phosphatase (ALP) activities were assessed on the serum samples using Randox kits purchased from Randox Laboratory Ltd, United Kingdom (UK), according to the manufacturer's protocol. Alanine aminotransferase (ALT) and aspartate aminotransferase (AST) were measured at 546 nm according to Reitman and Frankel (1957) while alkaline phosphatase (ALP) was measured at 405 nm according to (DGKC, 1972) using a UV/VIS spectrometer 725S. For standard plot of ALT and AST (see Appendix 2 and 3) and only the absorbance of the sample was used in the calculation of the enzyme activities.

3.11 Kidney function test

Serum sample collected from the blood of the rats were use in assessing the kindey function markers; creatinine and urea concentration by using Randox kits, according to the manufacturer's protocol. Creatinine was measured at 492 nm after 30 secs and 2 mins while urea was measured at 546 nm.

3.12 Organ preparation for histological analysis

Rat liver and kidney organs were harvested, rinsed with KCl, sections of both organs was cut, fixed in 10 % buffered formalin and fixed in phosphate buffer pH 7.4 at 40℃ for 12 hrs. The dehydrated tissue was inserted in paraffin wax, 5-µm of tissue was sectioned, placed on microscope slide, stained with Haematoxylin- Eosin dye and viewed with a light microscope (Winsor, 1994).

3.13 Determination of hematological parameters

Whole blood examination; differential white blood cell counts, estimation of red blood cells, haemoglobin / heamatocrit levels, lymphocyte and platelet was done using the blood collected on lithium heparinized sample bottle. The blood was analyzed using a 3- part differential haematology auto-analyzer, (Surgified, England).

3.14 Detection of micronuclei

This was achieved through micronucleus assay. Micronucleus assay is one of the set of tests use for toxicological screening of potential genotoxic agents. It is particularly one of the successful and reliable assay for genotoxic carcinogens. It is used to detect chromosome aberration indirectly through nucleus loss of chromatin resulting to micronuclei in the cell cytoplasm. Micronucleus assay is achieved through the method described by Heddle *et al*., (1981). It involves scoring the micronucleated polychromatic erythrocytes (mPCEs) frequency in 1000PCEs. The higher the frequency of mPCEs, the greater the clastogenic effect of the test substance.

Bone marrow smears preparation

Bone marrow smear was performed according to Schmid (1975) with slight modification. Both femurs of rat was harvested and cleaned by removing all muscle tissue. Using a pair of scissors the iliac region of the femur was cut, a 2 mL syringe needle was pushed through marrow carnal at the epiphyseal end and this help to exude the marrow on a fixed slide through the opening at the iliac end. A drop of fetal bovine serum was added, mixed and smear by using a clean slide. This was allowed to air dry.

Fixing and staining of smeared slides

The smeared slides were fixed in methanol for 5 mins and allowed to dry completely at room temperature. This was stained with 0.4 % May-Gruwald stain 1 for 3-4 mins and transferred immediately to May-Gruwaid stain 2 for another 3-4 mins. Slides were washed in distilled water, air dry and stained with 5% Giemsa for at least 30 mins. Furthermore, slides were rinsed with phosphate buffer for 30 secs, distilled water and air dry. The slides were fixed in xylene for 20 mins, air dry and mount using DPX.

Slide scoring

The mounted slides was viewed under a light microscope. Using a medium magnification first, suitable region for scoring was gotten after which magnification was changed and with the help of a tally counter polychromatic erythrocytes which contain micronuclear was counted.

3.15 Immunohistochemistry of NF-κB, P53, BCL-2

Using Ramos-Vara and Miller (2014) method markers of inflammation and apoptosis was determined using immunohistochemical techniques. Sections were cut from the tissue inserted in paraffin wax into charged slides. Its' deparaffinization was via 5 mins immersion in xylene (twice). While immersion in ethanol of 100 % 3 mins (twice), 95 % 3 mins (twice) and 70 % at 3 mins (once) resulted in rehydration. Thereafter using wash buffer it was rinsed for briefly (twice). To expose the antigen epitope, antigen retrieval was done by about 20 mins incubation in 10 mM citrate buffer pH 6.0. Thereafter, a brief wash with wash buffer was done (twice). Sections were blocked using 10 % FBS in PBS and subjected to15 mins incubation at room temperature in a humidified chamber. The slides were buffer washed, and 130 µL of primary antibody diluted appropriately was applied to the section. It was subjected to incubation for 1 hr at room temperature and a brief buffer wash (twice). 0.13 mL of diluted biotinylated + streptavide HRP secondary antibody was applied to sections, subjected to room temperature incubation for 30 mins in a humidified chamber and a 5 mins wash with washed buffer was given (twice). Next, slides were preheated with Sev-HRP conjugate for 15 mins and briefly given a wash with wash buffer (twice). 130 µL DAB substrate solution was applied to the sessions on the slide for 3 mins to reveal the colour of antibody staining. Slide were washed with running water 3 times (2 mins each) and were counter stained in hematoxylin for 10-20 secs. This was rinsed in running tap for 10 mins. After this, slide were dehydrated by transferring to alcohol (95 %, 95 %, 100 %, 100 %) 5 mins each. Lastly, pass slides through xylene for 5 mins (thrice), cover with a coverslip and view under the optical light microscope at X400.

3.16 Culturing of *Drosophila melanogaster*

D. melanogaster (Harwich strain & both gender) cultured over time at the *Drosophila* laboratory, Department of Biochemistry, University of Ibadan, Nigeria with fly diet consisting of 60 g of corn flour, 5 g yeast, 7.6 g agar and 0.6 g nipagin at room temperature and 60 % relative humidity, under a half day dark/ light cycle was used.

3.17 Experimental designs

The experimental design for involving *D. melanogaster* is divided into three as shown in Table 3.2-3.4

Table 3.2: Experimental design for sodium arsenite treated *Drosophila melanogaster*

GROUPS	TREATMENT/DOSES (mM)
1	Control (distilled water)
2	Sodium arsenite 0.0312
3	Sodium arsenite 0.0625
4	Sodium arsenite 0.125

Each group had 50 flies in five replicate

Table 3.3: Experimental design for fractions of ELVp

GROUPS	TREAMENTS (mg/10 g diet)
1	Control (2% ethanol)
2	Chloroform fraction (CHLF) 1
3	CHLF 2
4	CHLF 3
5	Ethyl acetate fraction (EACF) 1
6	EACF 2
7	EACF 3
8	Ethanol fraction (EOH) 1
9	EOH 2
10	EOH 3

Various biochemical assays and longevity assays was conducted during this experiment.

Table 3.4: Experimental design for co-treatment of ethyl acetate fraction (EACF) and sodium arsenite (SA)

GROUPS	TREAMENTS
1	Control (2% ethanol)
2	EACF (1 mg/10 g diet)
3	EACF (3 mg/10 g diet)
4	SA (0.0625 mM)
5	SA +EACF (1 mg/10 g diet)
6	SA +EACF (3 mg/10 g diet)

In this experiment, 1500 flies were divided into 6 groups of five vials of 50 flies each

All treatment was for five days after which the flies was homogenized and supernatant used for various biochemical assays.

3.18: Determination of survival rate of D. melanogaster orally exposed to sodium arsenite

A pilot study was first conducted using arsenite concentration 0.125 mM to 1.0 mM according to Polak *et al*., (2002). From this study the least dose was picked and scaled down.

Adult fruit flies (males and females, 24-72 hours old) were grouped into four of 30 flies per treatment vial. Treatment per group are as follows (distilled water (control), 0.0312 mM, 0.0625 mM, 0.125 mM of sodium arsenite respectively). This was done in triplicate, each day dead fruit flies was counted. Data were subjected to analysis and presented as percentage of live flies.

3.19 Anesthetizing of flies

Anesthetizing of flies was done in order to incapacitate the flies. This process is usually carried out when flies are being transferred from cultured vial so that they can be treated or when being transferred from treatment vials to eppendorf tube so they can be homogenized. Also flies are anesthetized before being viewed under the microscope. The process of anesthetizing of flies was done with either CO_2 or on ice.

3.20 Preparation of *D. melanogaster* for biochemical assays after treatments a five days

The treated flies were collected after anesthetizing, measured with weighing balance, blended in 100 mM phosphate buffer, pH 7.4 on iced and spinned in a Mikro 220R centrifuge (Germany) at 4000 g for 10 mins at 4℃. Supernatant from homogenate was gently pipetted into tubes labelled accordingly and storage was at -20℃. These samples was used for the evaluation of redox and antioxidant markers.

3.21. Biochemical assays

To understand the effect of sodium arsenite and extract / fraction of *Vitellaria paradoxa* on *D. melanogaster*, various biochemical parameters were assessed.

3.21.1 Protein determination

The samples protein concentration was ascertained following Lowry (1951) method with little modification. Briefly, 135 µL of distilled water was placed in an Eppendorf tube. Thereafter, 25 µL of your diluted sample (1:9), 400 µL of solution C (a reagent mixture of 0.1 M NaOH+ 2% Na2CO3 +1% CuSO4.5H2O + 2% Na-K tartarate) and 40 µL of (1:4) folin diluent was added. Absorbance was read at 650 nm against a blank. Extrapolation of protein concentration was done with the held of a standard curve (see Appendix 4)

3.21.2 Assay for catalase activity

Using Claiborne (1985) method catalase activity was determined based on the loss of splitting ability of hydrogen peroxide by catalase over time at 240 nm. Briefly, 590 µL of 19 mM solution of hydrogen peroxide was pipetted into quartz cuvette and 10 µL of sample was put into it. The mixture was quickly upturned and read in the spectrophotometer at 240 nm over a period of 2 mins.

Catalase activity was stated as µmol/min/mg protein using the extinction coefficient of hydrogen peroxide at 240 nm as 0.0436 $Mm^{-1}cm^{-1}$ (Noble and Gibson, 1970).

3.21.3 Estimation of glutathione-S-transferase activity

Using Habig and Jakoby (1981) method GST activity was determined. 170 µL of solution A (made with 20 mL of 250 mM phosphate buffer pH 7.0 + 10.5 mL of distilled water + 500 µL of 0.1 M GSH) was added to 20 µL of sample and 10 µL of 25 mM CDNB was then added. It was vortexed and readings taken every 10 second for 2 mins at 340 nm absorbance in spectrophotometer.Calculations: The extinction coefficient of CDNB = 9.6 $mM^{-1}cm^{-1}$

3.21.4 Total thiols level estimation

In line with Ellman (1959) method the level of total thiols was determined. Briefly, 510 µL of 0.1 M phosphate buffer pH 7.4 was added to 25 µL of sample. Thereafter, 35µL of H_2O and 30 µL of 10 mM DNTB was added. It was mixed and incubated at room temperature

for 30 mins. The absorbance was read at 412 nm using a spectrophotometer. Extrapolation of thiol levels was done with the held of a standard curve generated using 1 mM GSH (see Appendix 5)

3.21.5 Determination of reduced glutathione (GSH) level

Following Jollow *et al*., (1974) method GSH was determined. In a ratio of 1:1 the samples were precipitated with sulphosalicyclic acid (4%). It was kept at 4℃ for 1 hr and spin down at 5000 rpm for 10 mins at 4℃ . To 100 µL of the upper layer of the spinned sample, 550 µL of 0.1 M phosphate buffer pH 7.4 and 100 µL of 10 mM DTNB was added. The wavelength was read at 412 nm. Extrapolation of GSH levels was done with the held of a standard curve generated using 1 mM GSH (see Appendix 6)

3.21.6 Hydrogen peroxide generation

Following Wolff, (1994) method hydrogen peroxide generation was determined. 590 µL of FOX1 (a reagent mixture of 10 mL of 100 mol/L Xylenol orange + 10 mL of 100 mmol/L sorbitol + 50 mL of 250 mol/L ammonium ferrous sulphate + 30 mL of distilled water) was added to 10 µL of sample. The assay mixture was thoroughly mixed by vortexing. After 30 mins of preheating at ambient temperature, a pale pink colour complex is formed. At 560 nm, the optical density was read against a blank

3.21.7 Determination of nitrite (nitric oxide) level

Using Green *et al*., (1982) method nitrite level was determined. The mixture of equal volume (250 µL) of sample and Griess reagent 1:1 was incubated for 20 min at room temperature and spectrophotometrically at 550 nm absorbance was read.

Using sodium nitrite concentration as a standard, the concentration of nitrite was calculated (see Appendix 7).

3.21.8 Assessment of acetylcholinesterase activity

Acetylcholinesterase activity was assessed following Ellman *et al*., (1961) method. Acetylcholinesterase (EC 3.1.1.7, AChE), hydrolysis acetylcholine to acetate and choline,

resulting to the relaxation of cholinergic neuron. Simple direct and Ellman method, in which acetylcholineesterase react with with DTNB to form a thiocholine a yellow colour whose intensity is measured at 412 nm was used.

Briefly, 285 µL of distilled water was added to 180 µL of 0.1 M phosphate buffer (pH 7.4). Thereafter, 60 µL of DTNB , 15 µL of sample and 60 µL of 8 mM acetylthiocholine was added. It was mixed by inverting and read for 2 mins at 15 secs interval at 412 nm.

3.22 Negative geotaxis

Following Feany and Bender, (2000) method the climbing performance of the flies were investigated. In this study, 10 flies from each group was anaesthetised separately with CO_2 in a cylindercal tube (height 15 cm; diameter 1.5 cm). When the flies woke up, they were gently tapped to the tube base, and the number of flies that walked up to the 6 cm mark of the tube in 6 secs were written down. The procedure is repeated thrice at 1 min interval. This was expressed as percentage locomotive activity

3.23 Determination of flies emergence

The emergence of *D. melanogaster* treated flies from egg to adult was determined according to Farombi *et al*., (2018). 1-3 days old flies (10 males and 10 female) was placed in each vial in a replicate of 5 vial per group. They were exposed to the treatment through their diet for 24 hrs after which all the flies was removed from the vial. Thereafter, the complete life cycle was monitored. And the numbers of flies which emerged from the egg into adult flies was counted and expressed in relation to control group.

3.24 *D. melanogaster* fat bodies histology

1-3 days old flies (10 males and 10 female) was placed in each vial per group. They were exposed to the treatment through their diet for 5 days after which all the flies was removed from the vial into an Eppendorf tube. 150 µL of bouin solution was put in to each and it was left to fix the flies for 24 hrs. Thereafter, the bouin solution was removed and each tube containing the flies was rinsed properly with phosphate buffer until white. 10 % of phosphate buffer formalin was added to each tube in other to fix the flies. The dehydrated flies was sub-merged in a paraffinised wax, 5-µm sections was cut, placed on microscope slide, stained with haematoxylin- eosin dye and observed with a light microscope .

3.25 Cell lines and culture

Three different cell lines namely A549 (lung carcinoma), MCF-7 (breast carcinoma) and Hep G2 (hepatic carcinoma) were investigated at the screening stage of this study after which the cell line with the best cytotoxic effect was assessed for mechanistic studies. All cells were cultured with Dulbecco's Modified Eagle's Medium (DMEM) with 10 % foetal bovine serum (FBS), 1 % antibiotic (100 U/mL penicillin, 100 U/mL streptomycin) and maintained in the incubation chamber at 37°C in atmosphere with 5 % CO_2.

3.26 Trypan blue assay

This was applied to ascertain the number of active cells before seeding into well plates used for culturing the cells. Cells plated in flask was used for this assay. Previous culture media was taken away flask and cells was rinsed with PBS (×1) thereafter cells was trypsinized by inputting 1 ml of trypsin-EDTA (0.25 %). This was kept in the incubator for 2 min to enable detachment from flask. Thereafter, 4 mL of complete media (made up of DMEM + 10 % FBS + 1 % antibiotic) was inputted to terminate the effect of trypsin. By pipetting cells was completely detached and picked into centrifuge tube. It was spinned using a centrifugal force at 1200 rpm for 5 min. The upperlayer was discard and 1 mL of complete media was put to dissolve pellet by pipetting gently. In the ratio of 9:1, 90 µL of trypan blue (0.4 %) was put into 10 µL of the cells which was mixed properly. From this 10 µL was placed on the hemocytometer and cell was counted in all four square box.

3.27 MTT assay

The cytotoxic activity of fractions of ELVp was accessed by MTT assay on all cell lines fore mentioned according to Mosmann *et al*., (1983) based on active cells converts MTT a pale yellow salt into a purple coloured formazan product which is dissolved and measured at 570 nm.

Briefly, a total of 5000 cells per well were seeded in triplicates for each group in a 96 well plate and left to adhere on it for 24 hrs. Thereafter, varying concentration (50, 100, 250, 500 and 1000 µg/mL) of fractions of *V. paradoxa* were administered to cells for 24, 48 & 72 hrs while 0.1 % DMSO was the vehicle control. Treatment media was pipetted out and every well received 100 µL of 0.5 mg/mL MTT (3-(4,5-dimethylthiazol-2-yl)-2,5-diphenyltetrazolium bromide) solution, it was kept at 37°C in the incubator chamber for 4

hrs. This medium was taken out by the aid of a pipette and the formazan crystal was made to solution by applying 100 µL DMSO. After 30 mins of standing on bench, using a microplate reader (Bio Tek Instruments Inc, Highland Pack, USA, REF EPOCH2, SN 1603116) absorbance was read at 570 nm. The experiment was performed in duplicate for each cell lines. Results were expressed as a percentage of cell viability relative to media control using the equation below

% cell viability = Absorbance of sample @ 570 nm/ Absorbance of media control) × 100.

IC_{50} was calculated using the AAT Bioquest IC_{50} calculator.

In the further studies MCF-7 cell was used because it was the best of all three cell lines used for cytotoxicity. In addition, ethyl acetate fraction was used for these studies and all mechanism assays.

3.28 Cell colony formation assay

Colony formation assay is centered on the fact that single cells have the potential to grow into cell colony. Using Franken *et al*., (2006) protocol with slight modification the ability of cell treated with IC_{50} dose ethyl acetate (EACF) was determined as described below.

500 cells of MCF-7 were seeded per well of six (6) well plate in triplicate for each treatment group. Apart from the media control group, there was a DMSO 0.1 % group and EACF group. Also each group was treated for 24 hrs respectively. After attachment of cell, previous media was pipetted out and replaced with fresh media containing the treatment. This was removed after the 24 hrs and replaced with complete DMEM media (i.e DMEM containing 5 % FBS and 1 % antibiotic). This was replaced every four days and at the 13 day complete media was removed by pipetting, plates was washed with PBS ×1, and using absolute ethanol cell was fixed in the plate for 20 mins. Thereafter, 3 mL of crystal violet was added for 40 mins. This was discarded and plate was washed with tap water filled in a dish for 2-3 mins, plate were air dried and colonies was counted manually.

3.29 ROS generation assay

Using 2’ 7’-dichlorofluorescin diacetate (DCFDA) a flurogenic dye ROS generation after treatment with EACF was determined in comparison to medial control according to Anatole

et al., (2013). It is based on DCF-DA to diffuse into cells, get deacetylated by cellular esterase to a non-fluorescent compound which is rapidly oxidized into DFC (2'7-dichlorofluorescein) by ROS which can be detected by fluorescent spectroscopy at excitation/emission ray of 485/535 nm.

Briefly 5000 cells of MCF-7 was seeded into black 96 well plate per well. After the cells attached to the plate, it was treated for 6 hrs with EACF (at IC_{50} or double IC_{50}) respectively. Thereafter, media was pipetted out and cells washed with 200 µL of ×1 PBS. Lastly 5 µm of DCFDA was put into each well and was incubated for 30 mins in the dark (CO_2 incubator). Using a fluorescent spectrophotometer (Bio Tek Instruments Inc, USA, REF 8040579, SN 500593) at 485 nm excitation and 535 nm emission absorbance was measured. Percentage of ROS generation was expressed as ratio over control.

3.30 Cell cycle analysis

The cellular DNA content and analysis of cell cycle was assessed by means of a flow cytometer according to He *et al*., (2019). In this experiment, the cell were fluorescently labelled with propidium iodide (PI). It is centered on the ability of the DNA binding dye (propidium iodide) to enter cells whose membrane have been raptured.

Approximately 1×10^6 cells of MCF-7 were seeded into 6 well plates and left overnight to attach. Thereafter, cells were administered IC_{50} dose of EACF, 0.1 % DMSO and media alone respectively. The duration for treatment was 24, 48 and 72 hrs respectively. After the duration of treatment elapsed, media in the plate was collected into 15 mL centrifuge tubes, cells was washed with ×1 PBS and collected into same tube before harvesting of the adherent cells in the plate by adding 500 µL of trypsin-EDTA for 2 mins which enhanced the detachment of cells from plate. This was collected into same tube and centrifuged at 1000 rpm for 3 mins. The uppersurface liquid layer was thrown away, cells were washed with PBS, centrifuged and supernatant discarded. Thereafter, ice cold 70 % ethanol was used for fixation of the cells overnight. Using cold centrifuge (Thermo Fisher Scientific, made in Germany, Serial No 41616173 and Cat- No 75004380) cells were spun at 2500 rpm for 10 mins. The upper liquid layer was thrown off, cells were washed with PBS (×1), centrifuged and supernatant removed. 1mL of propidium iodide (PI) solution (gotten from

the stock made up of 50 mg of sodium citrate, 50 mL of PBS (×1), 2 mg of RNase, 50 µL of triton X-100 and 2.5 mg of PI) was put into each tube in the dark and incubated at 37℃ for more than 30 mins. This was centrifuged for 5 mins, 700 µL of the supernatant was discarded while the remaining was used to lyse the cell before passing it through syringe such that cell came out singling. This was subjected to analysis by flow cytometric using Attune NxT acoustic focusing cytometer (Life Technologies) and the cell cycle distribution including the apoptosis was analysed using Modfit LT for Mac v3.0 software.

3.31 Western blot analysis

Cells were seeded in 100 mm dimension plates and cultured to 60-70 % confluence. There after cells were treated according to these grouping (Medial control, DMSO 0.1 %, and EACF at IC_{50} dose) for 24 hrs. Preparation of lysis buffer is as shown in Table 3.5 below. All media was discarded, cells washed with PBS (×1) and 1 mL of trypsin-EDTA 0.5 % was used to detached cells after which complete media was added to stop the reaction. By pipetting cells was completely detached and collected into a 15 mL centrifuge tube placed in ice. This was spun at 1100 rpm for 3 mins, upper liquid layer thrown off and ice cold PBS was used to wash cell again and centrifuged. All tubes were placed on ice, 1mL of ice cold lysing buffer was applied/tube and using a 1 mL micropipette this was gently pipetted and picked into an Eppendorf tube all process in ice. Each tube was placed in an ice pack tube and using a Branson digital sonicator model 102c (CE) S/N OBU14049778G cell were sonicated at temperature 80 % and pulse 2 sec/mins 3 times. Thereafter, tubes were returned to the ice pack and tapped every 5 mins for 30 secs this process was for 30 mins. Thereafter cells were spun down at 13000 rpm for 20 mins using cold centrifuge (Themo Fisher Scientific, made in Germany, Serial No 41616173 and Cat- No 75004380). Supernatant was gently collected into an ice cold Eppendorf tube and sample was kept in – 20℃ refrigerator.

Table 3.5: Lysis buffer preparation

Reagent	Final concentration	Stock concentration	Volume
NaCl	125mM	1 M	625 µL
Tris-buffer pH 8	50mM	1 M	250 µL
Triton-X 100	0.5%	100%	25µL
Sodium orthovendate			500 µL
Protease inhibitor cortail			50 µL

Distilled water was used to make up to 5 mL.

3.31.1 Determination of Protein

The protein of the lysed smples was quantified using Braford method. The lysed cell sample was diluted 1:10. 5 µL of the serially diluted four lysed cell sample was picked into a 96 well plate in triplicate and 250 µL of barford reagent was added in the dark. It was cover with foil paper to prevent light penetration and kept standing for 30 mins after which it was read at 590 nm using a microplate reader (Bio Tek Instruments Inc, Highland Pack, USA, REF EPOCH2, SN 1603116). Extrapolation of protein concentration was done with the held of a standard curve generated using 1 mg Bovin Serum Albumin (see Appendix 8)

3.31.2 SDS PAGE gel preparation

The glass plates and spacer for gel casting unit was cleaned properly with distilled water and 70 % ethanol. Plates with the spacer was assembled on a stable even surface to prevent leakage. Leakage was tested for by putting in distilled water on the assembled plate and observed for 10 mins for leaking water. Thereafter, the water was moped out using tissue paper. Thereafter 10 mL of 10 % resolving gel was prepared as shown in Table 3.6 below. Using a 1 mL pipette the resolving gel solution was pipetted into the assembled plate with spacers up to the green mark. It was overlaid with isopropanol or water to maintain an even / horizontal surface. This was allowed to solidify for about 20-30 mins at room temperature. Thereafter, 6 % stacking gel solution for 5 mL was prepared as shown in the Table 3.7 below. The over laid isopropanol on the resolving gel was removed and replaced with stacking gel solution. The comb was inserted immediately gently ensuring no air bubble are trapped in the gel or near the wells. The gel was allowed to set for 20-30 mins at room temperature.

Table 3. 6: Resolving gel preparation

S/N	Reagent	volume
1	Distilled water	4.05 mL
2	Tris-HCL p^H 8.8	2.5 mL
3	30 % acrylamide	3.3 mL
4	10 % SDS	100 µL
5	APS	100 µL
6	TEMED	10 µL

Table 3.7: Stacking gel preparetion

GEL %	Water (mL)	30 % acrylamide (mL)	Tris-Hcl p^H 6.8 (mL)	10 % SDS (µL)	APS (µL)	TEMED (µL)
6%	2.7	1	1.25	50	50	5

3.31.3 Sample preparation

5 µL of distilled water was mixed with 5 µL of lyste sample and 5 µL of 3×loading dye. This was heated for 10 mins at 100℃ in a dry bath. This was centrifuge for 1 min in a microcentrifuge.

3.31.4 Electropherosis

Assembled plated which have been packed with the resolving and stacking gel is placed into the electrophoretic tank making sure red end is on red and black end is on black. The samples prepared were loaded gently into every empty comb space. Thereafter, running buffer was poured into the tank and covered with the tank cover making sure red is on red and black is on black and voltage is set at 100 v thereafter, it is increased to 120 v and it is run until bands move down below the green line. With this, tank was put off and the small plate was gently removed. The stacking gel was cut off gently and gel also at the side. Gel was put in the rinsing bowl and coomassie blue was added to it covering it and placed on a rocking shaker for 1 hr. Thereafter, the coomassia blue was removed and destaining solution was added and it was placed on the rocking table, this was taken out every 15 mins and it was replaced with destaining solution thrice. Thereafter, gel was kept in distilled water overnight.

The bands on the gel was transferred into a cellulose paper at 100 V for 1 hr 30 mins using a transfer buffer. The blot was briefly rainsed in water and stained with Ponceau S solution to check the transfer quality. The Ponceau S stain was rinsed off with TBST (thrice), thereafter, it was blocked using 5 % BSA in TBST at room temperature for 1 hour. It was incubated overnight with primary antiboby pro-caspase 3, Caspase 3 cleaved and β- tubulin at 4℃ . Blots was washed with fresh TBST (thrice) for 15 min each and once with TBS. 4-5 mL secondary antibody was applied to each blot and incubated at room temperature for 1 hr. It was given a TBST wash (thrice) and TBS was once before the bands were developed.

3.32 Determination of bioactive compound in ethyl acetate fraction (EACF) of *V. paradoxa* using Gas Chromatography-Mass Spectrometry (GC-MS) method

The bioactive compounds of EACF of V. paradoxa was performed using GC-MS (7890 A-5975C, Agilent Technologies Inc., Sata Rosa, CA, USA). Briefly, the sample extracted is put in a vial bottle which is placed in the sample compartment of the auto injector which injects the sample into the liner. The temperature of the injector port was 250℃ while the oven temperature was programmed to be 80℃ for 1 min as the initial temperature and a gradual increase of 10℃/min until it reaches 240℃ for 6 min. The mobile phase (helium gas) pushes the sample from the liner into the column, where separation at different retention time takes place into different component based on their volatility. The identification of the separated constituent were based on their mass spectra with those in NIST and by comparing their retention indices.

3.33 Research work flow

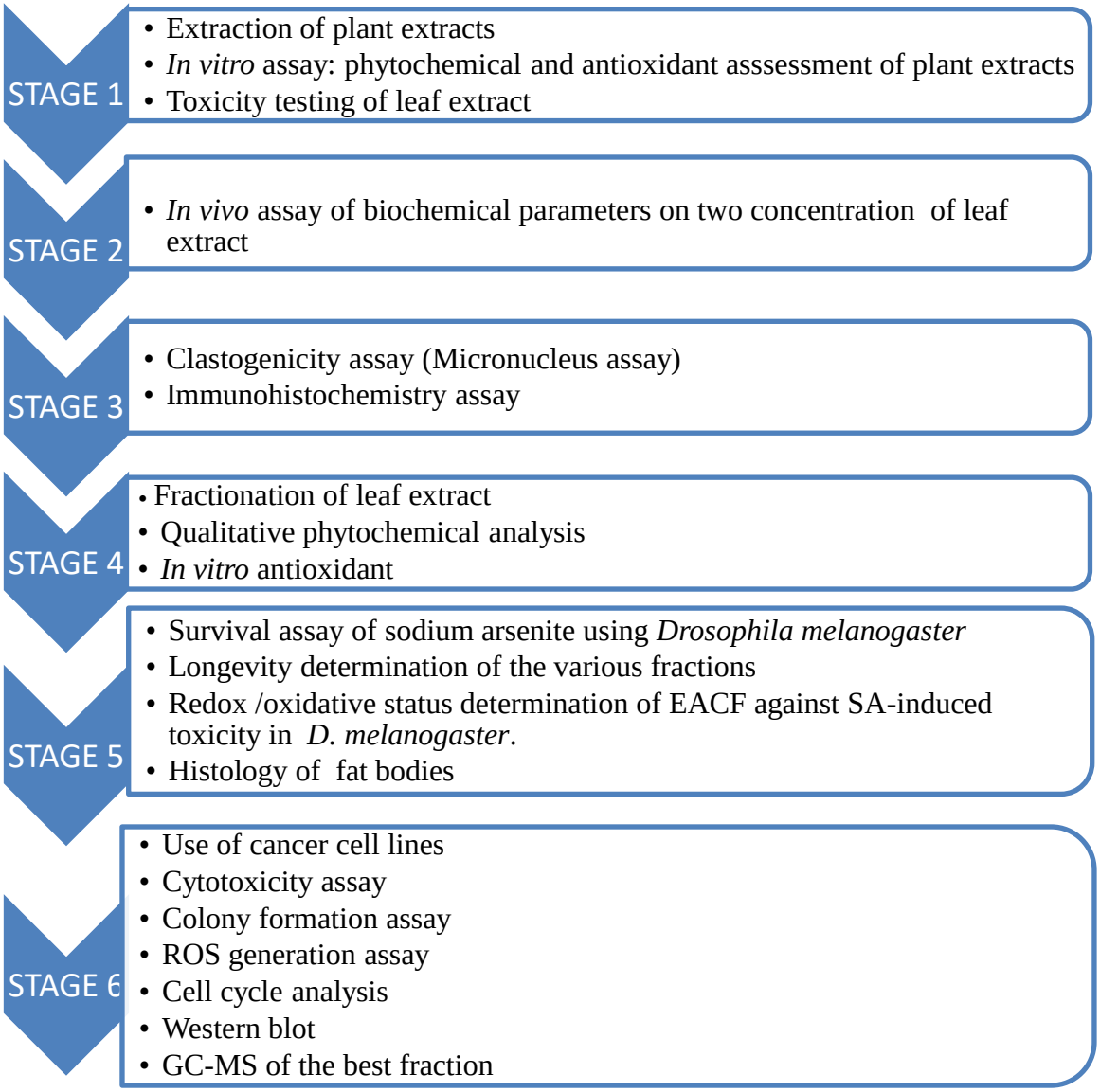

3.34 Statistical analysis

Differences in mean values of parameters across treatment groups were tested statistically using One Way Analysis of Variance (ANOVA). Significant differences between groups were detected using Post-hoc test Turkeys Sb. All differences were considered statistically significance at $p < 0.05$.

All analysis were carried out using Graph Pad Prism Version 6.0 software for Windows.

CHAPTER FOUR

RESULTS

4.1 Phytochemical screening of *Vitellaria paradoxa* extracts

The leaf and seed extracts of *V. paradoxa* were used in this study. Table 4.1 shows the percentage yield of leaf (ELVp) and seed (ESVp) extracts of *V. paradoxa*. The mean Percentage yield increased with 16 % from the seed extract to the leaf extract (23.99 ± 2.034) to (28.53 ± 2.171) although there was no significant difference.

The total flavonoid and phenol contents of both extracts are presented in Figure 4.1-4.2. The total flavonoid content (TFC) was 21.83 ± 0.7631 for ELVp and not detected for ESVp at 800 µg/ml. The higher TFC ($p<0.05$) was recorded in ELVp (21.83 ± 0.7631) while TFC was not detected in ESVp (Fig. 4.1).

Total phenol content (TPC): The TPC was 83.46 ± 0.4167 in ELVp and 68.88 ± 4.330 in ESVp. The higher TPC was recorded for ELVp (83.46 ±0.4167) although it was not significant when compared to ESVp (Fig. 4.2).

Table 4.1: Percentage yield of ethanol leaf and seed extracts of *Vitellaria paradoxa*

Extracts	Percentage yield
ELVp	28.53 ± 2.171
ESVp	23.99 ± 2.034

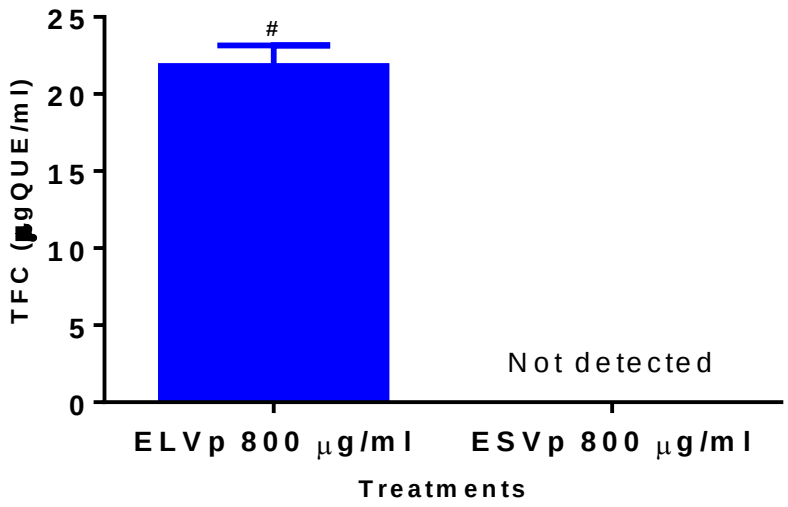

Figure 4.1: Total flavonoid capacity of *Vitellaria paradoxa* extracts using quecestin as standard.

Where # represents significant when compared to ESVp treatment.

ELVp represent the ethanol leaf extract of *Vitellaria paradoxa* while ESVp represent the ethanol seed extract of *Vitellaria paradoxa*

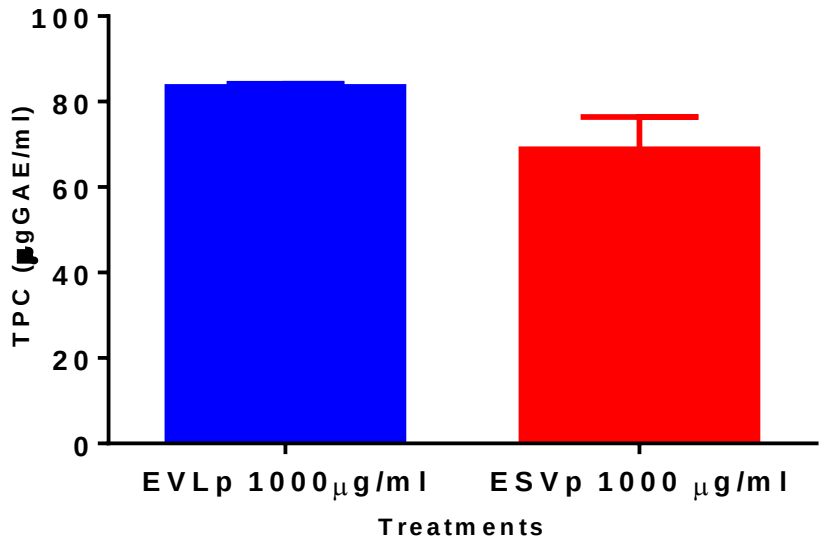

Figure 4.2: Total phenol content of *Vitellaria paradoxa* extracts using gallic acid as standard

ELVp represent the ethanol leaf extract of *Vitellaria paradoxa* while ESVp represent the ethanol seed extract of *Vitellaria paradoxa*.

4.2 Antioxidant contents of *V. paradoxa* extracts

The DPPH, reducing power and total antioxidant content of the extracts are presented in Figure 4.3-4.5.

DPPH: The percentage inhibition for DPPH of both ELVp and ESVp was lesser than ascorbic acid a known antioxidant (Fig. 4.3).

Reducing power: Both ELVP and ESVp showed a concentration dependent reducing ability for iron (III). Further more when compared to ascorbic acid there was significant ($p<0.05$) reduction from 50 µg/ml to 400 µg/ml of both ELVP and ESVp. However there was no significant difference in value recorded at 800 µg/ml for ascorbic acid and ELVp (1.410 ±0.06444 and 1.360 ±0.06444) respectively (Fig. 4.4).

Total antioxidant content (TAC): The TAC of *Vitellaria paradoxa* was 362.6 ± 31.76 µgAAE/mL in ELVp and 237.8 ± 4.174 µgAAE/mL in ESVp (Figure 4.5). Significant ($p<0.05$) increase in TAC activity was recorded in ELVp. This represent increase of 52.4 % over ESVp (Fig. 4.5).

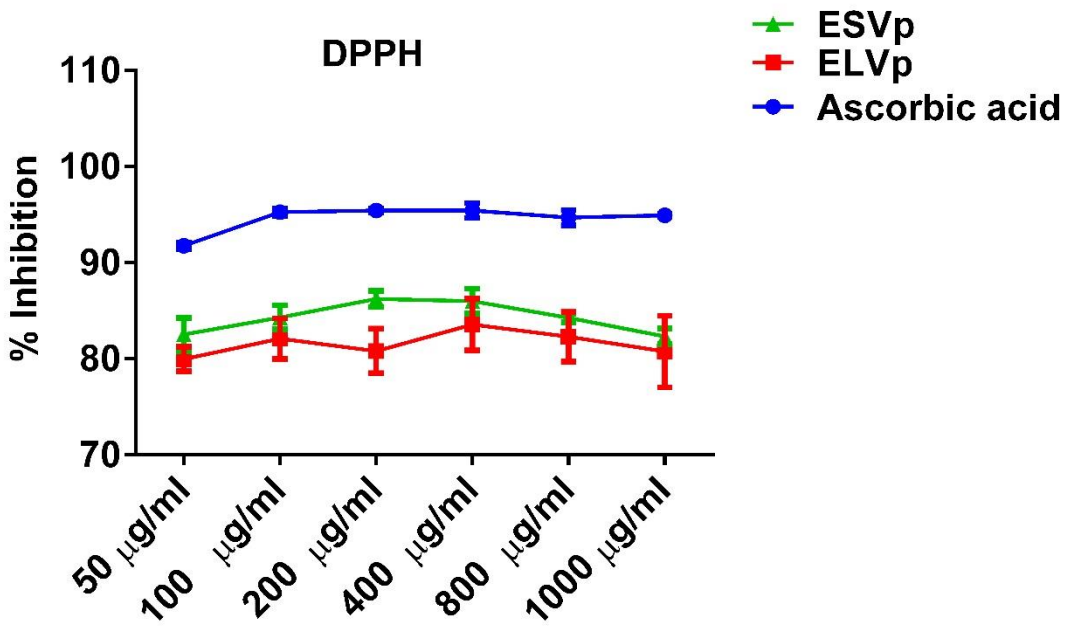

Figure 4.3: *Vitellaria paradoxa* extracts DPPH scavenging activity.

ELVp represent the ethanol leaf extract of *Vitellaria paradoxa* while ESVp represent the ethanol seed extract of *Vitellaria paradoxa*

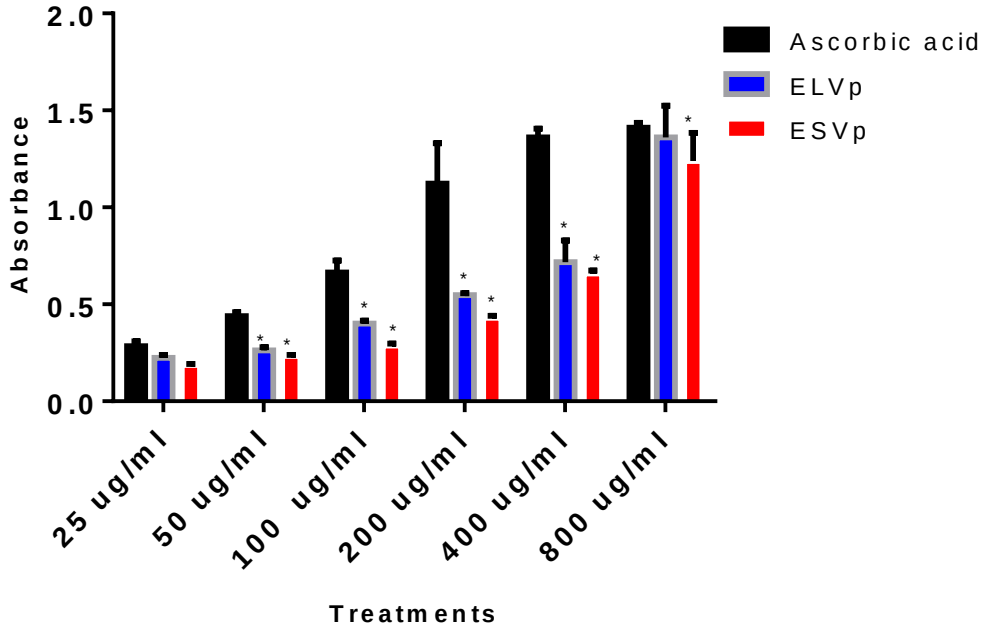

Figure 4.4: Reducing power scavenging activity of *V. paradoxa* extracts and positive control (ascorbic acid).

Where '*' represent significant when compared to ascorbic acid.

. ELVp represent the ethanol leaf extract of *Vitellaria paradoxa* while ESVp represent the ethanol seed extract of *Vitellaria paradoxa*

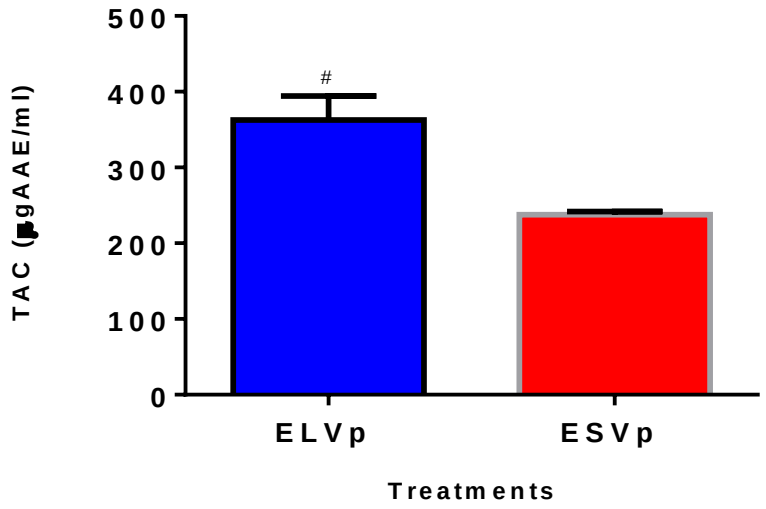

Figure 4.5: The total antioxidant capacity of *V. paradoxa* extracts

represent significant when compared to ESVp treatment.

ELVp represent ethanol leaf extract of *Vitellaria paradoxa* while ESVp represent the ethanol seed extract of *Vitellaria paradoxa*

4.3 Genotoxic effect of *V. paradoxa* extracts

In vitro genotoxicity assessment of the extracts showed that both ELVp and ESVp extracts was not genotoxic at dilution folds of 2 to 64 i.e 400 µg/mL to 5 µg/mL. However, the stock (800 µg/mL) showed marginal genotoxicity but significantly lower than the positive control (4-nitroquinoline-1-oxide).

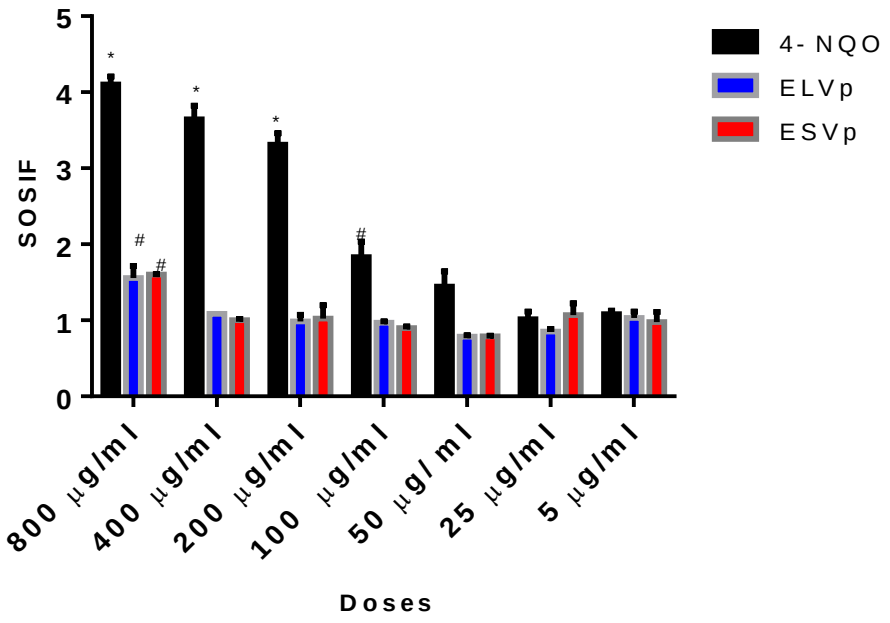

Figure 4.6: Genotoxic effect of *Vitellaria paradoxa* extracts and the positive control (4- nitroquinoline-1-oxide).

Where * represents genotoxic since SOS inducing factor is ≥ 2 and # represent marginal genotoxic (inconclusive).

4-NQO represent 4-nitroquinoline-1-oxide, ELVp represent ethanol leaf extract of *Vitellaria paradoxa* while ESVp represent the ethanol seed extract of *Vitellaria paradoxa*

4.4: Median lethal dose (LD50), percentage change in body weight and histological examination female Wistar rats treated with ELVp

The median lethal dose (LD50), percentage change in body weight, relative liver weight and histological examination of the liver are presented in Table 4.2, Figure 4.7-4.8 and Plate 4.1 respectively.

4.4.1 Acute toxicity analysis

The administration of ELVp from the least dose 5 mg/kg to the highest dose 5000 mg/kg did not induced mortality to the rats (Table 4.2).

Table 4.2: LD_{50} study of hydroethanol leaf extract of *V. paradoxa* (ELVp) in Wistar rats.

Group	Number of animals	Number of death
Control	3	0
ELVp 5 mg/kg	3	0
ELVp 50 mg/kg	3	0
ELVp 300 mg/kg	3	0
ELVp 2000 mg/kg	3	0
ELVp 5000 mg/kg	3	0

4.4.2 Effects of ELVp on percentage change in body and relative liver weights

Percentage change in body weight (BW): The percentage change in body weight was 34.96 ±1.37 in control, 22.52 ±1.49 in 5 mg/kg, 16.28 ±3.58 in 50 mg/kg, 20.34 ±2.52 in 300 mg/kg, 16.19 ±1.52 in 2000 mg/kg and 15.27 ±2.70 in 5000 mg/kg (Fig. 4.7). The lowest Percentage body weight ($p<0.05$) was recorded in 5000 mg/kg (15.27±2.70). Also, significant ($p<0.05$) reductions in percentage change in body weights was observed in all treatment groups (Fig. 4.7).

Relative liver weight (RLW): The relative liver weight (RLW) of female wistar rats treated with ELVp was 3.48 ± 0.26 in control, 3.31 ± 0.38 in 5 mg/kg, 3.62 ± 0.16 in 50 mg/kg, 3.41 ± 0.43 in 300 mg/kg, 3.30 ± 0.04 in 2000 mg/kg and 3.45 ± 0.30 in 5000 mg/kg. There were no significant differences in values recorded upon treatment with ELVp (Fig. 4.8).

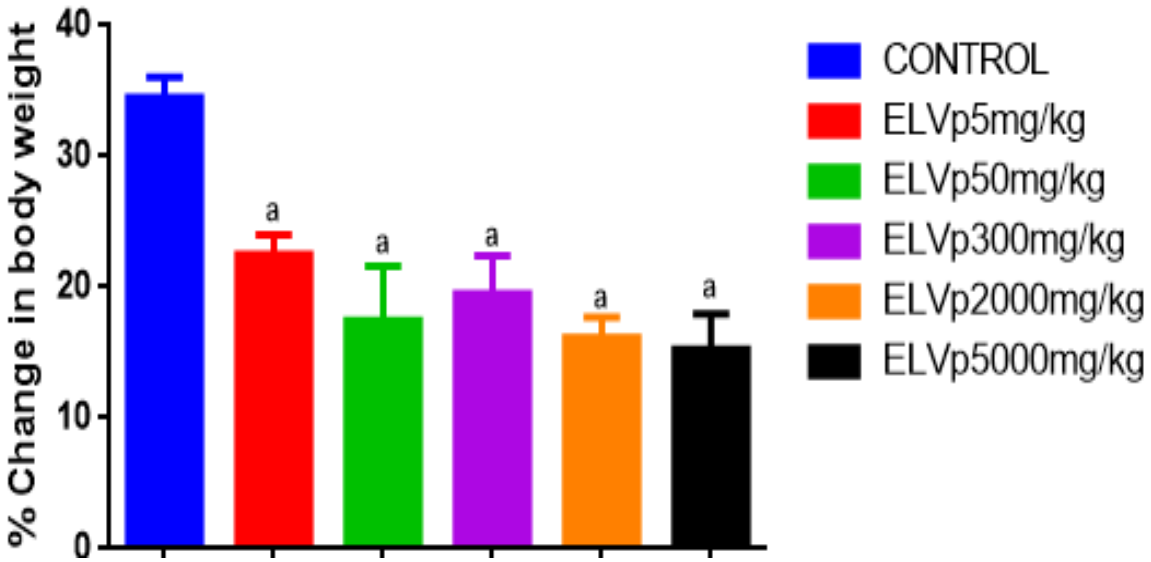

Figure 4.7: The effect of ELVp on percentage change in body weight of female wistar rats.

Where ‘a ’ represent significant difference when compared to control.

ELVp represent the ethanol leaf extract of *Vitellaria paradoxa*

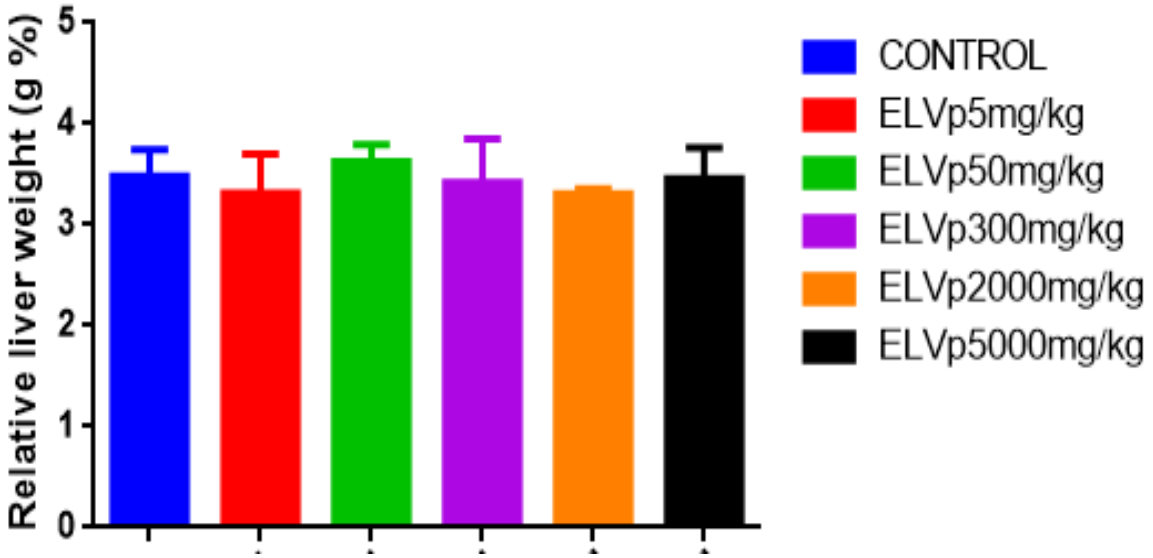

Figure 4.8: Effect of ELVp on relative liver weight of female wistar rats.

ELVp represent the ethanol leaf extract of *Vitellaria paradoxa*

4.4.3 Histological examination of rat liver treated with ELVp

The histological examination of the treated rat livers showed normal hepatocytes for control, no observable lesion in ELVp 5 mg/kg, no observable lesion in ELVp 50 mg/kg, no observable lesion in ELVp 300 mg/kg, mild periportal reaction and kupffer cell hyperplasia in ELVp 2000 mg/kg 5 and no observable lesion in ELVp 5000 mg/kg (Plate 4.1)

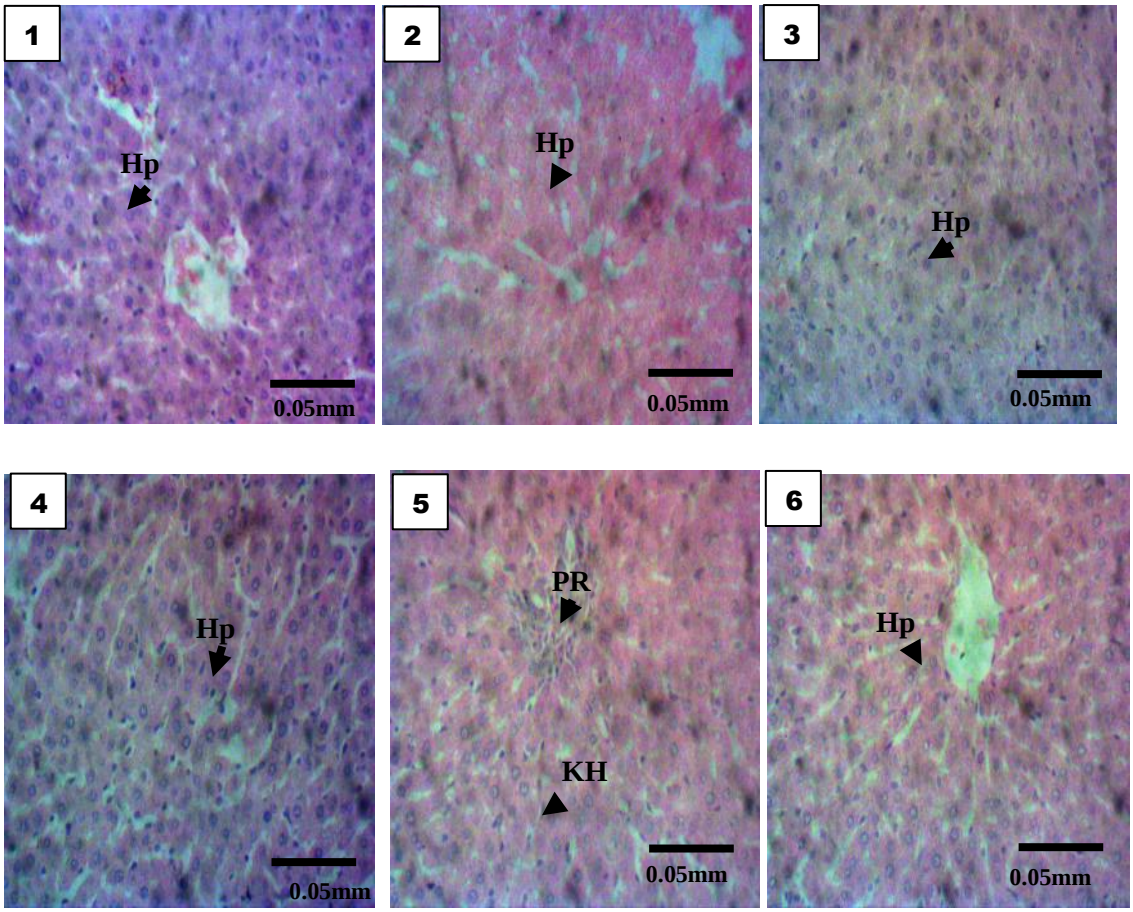

Plate 4.1: Photomicrograph of ELVp effect on the liver of Wistar rats

1: normal female rats administered distilled water with normal hepatocytes (Hp). 2: female rats administered ELVp (5 mg/kg) with normal hepatocytes (Hp). 3 female rats administered ELVp (50 mg/kg) with normal hepatocytes (Hp). 4 female rats administered ELVp (300 mg/kg) with normal hepatocytes (Hp). 5: female rats administered ELVp (2000 mg/kg) with mild periportal reaction (PR) and kupffer cell hyperplasia (KH). 6: female rats administered ELVp (5000 mg/kg) with normal hepatocytes (Hp) × 400.

4.5: **Effect of *Vitellaria paradoxa* hydroethanol leaf extract on sodium arsenite-induced toxicity in male wistar rats**

4.5.1: Effects of ELVp on sodium arsenite-induced change on % body weight and relative organs weight.

The percentage change in body weight (% ΔBW), relative liver weight (RLW) and relative kidney weight (RKW) of male wistar rats treated with vitamin E, ELVp, sodium arsenite (SA) and their combination are presented in Table 4.3.

Percentage change in body weight (%ΔBW): The percentage change in body weight (%ΔBW) of male Wistar rats was 47.93 ± 2.25 in control, 66.01 ± 8.62 in vitamin E (100 mg/kg), 54.97 ± 1.24 in ELVp (100 mg/kg), 55.62 ± 2.50 in ELVp (200 mg/kg), 42.54 ± 2.80 in SA (2.5 mg/kg), 46.53 ± 8.65 in combination of SA and vitamin E, 44.48 ±1.17 in SA and ELVp (100 mg/kg) and 29.34 ± 9.53 in SA and ELVp (200 mg/kg). The highest %ΔBW ($p<0.05$) was recorded in vitamin E (100 mg/kg), while the lowest was recorded in SA and ELVp (200 mg/kg). However, there was no significant difference in SA (2.5 mg/kg) when compared with control (Table 4.3).

Relative liver weight (RLW): The relative liver weight of male Wistar rats was 4.02 ± 0.19 in control, 4.99 ± 0.19 in vitamin E (100 mg/kg), 4.71 ± 0.24 in ELVp (100 mg/kg), 4.01 ± 0.04 in ELVp (200 mg/kg), 3.75 ± 0.12 in SA (2.5 mg/kg), 4.31 ± 0.10 in combination of SA and vitamin E, 4.09 ±0.17 in SA and ELVp (100 mg/kg) and 3.59 ± 0.13 in SA and ELVp (200 mg/kg). The highest RLW ($p<0.05$) was recorded in vitamin E (100 mg/kg), while the lowest was recorded in SA and ELVp (200 mg/kg) when compared to control. Also, Vitamin E and ELVp at 100 mg/kg increased significantly RLW when compared with SA ($p<0.05$) (Table 4.3).

Relative kidney weight (RKW): The relative kidney weight of male Wistar rats was 0.70 ± 0.02 in control, 0.87 ± 0.02 in vitamin E (100 mg/kg), 0.74 ± 0.02 in ELVp (100 mg/kg), 0.72 ± 0.04 in ELVp (200 mg/kg), 0.64 ± 0.00 in SA (2.5 mg/kg), 0.77 ± 0.03 in combination of SA and vitamin E, 0.67 ±0.01 in SA and ELVp (100 mg/kg) and 0.64 ± 0.00 in SA and ELVp (200 mg/kg). The highest RKW ($p<0.05$) was recorded in vitamin E (100

mg/kg), while overlapped indices was recorded for the the lowest in SA, and combination of SA and ELVp (200 mg/kg) when compared to control.

Significant ($p<0.05$) increased 35.9% in vitamin E, 15.6 % in ELVp (100 mg/kg), 12.5 % in ELVp (200 mg/kg), 20.3 in combination of SA and vitamin E, and 4.6 % in SA and ELVp (100 mg/kg) was observed when compared to SA (2.5 mg/kg) (Table 4.3).

Table 4.3: Effect of ELVp on sodium arsenite-induced change on % body weight and relative organs weight

Groups	ΔBW (%)	RLW	RKW
Control	47.93 ± 2.25	4.02 ± 0.19	0.70± 0.02
Vit E 100 mg/kg	66.01 ± 8.62 *,#	4.99 ± 0.19 *,#	0.87 ± 0.02*,#
ELVp 100 mg/kg	54.97 ± 1.24 *,#	4.71 ± 0.24 *,#	0.74 ± 0.02 #
ELVp 200 mg/kg	55.62 ± 2.50 *,#	4.01 ± 0.04	0.72 ± 0.04 #
SA 2.5 mg/kg	42.54 ± 2.80	3.75 ± 0.12	0.64 ± 0.00*
SA + Vit E	46.53 ± 8.65	4.31 ± 0.10 #	0.77 ± 0.03*,#
SA + ELVp 100 mg/kg	44.48 ± 1.17	4.09 ± 0.17	0.67 ± 0.01 #
SA + ELVp 200 mg/kg	29.34 ± 9.53 *	3.59 ± 0.13 *	0.64 ± 0.00 *

Values are mean of five animals ± Standard Deviation (S.D)

*significant at p< 0.05 when compared with control while #' significant at p< 0.05 when compared with sodium arsenite.

4.5.2: The hepato-remedative potential of ELVp on sodium arsenite-induced toxicity

The aspartate aminotransferase (AST), alanine aminotransferase (ALT) and alkaline phosphatase enzymes activities are presented in Figure 4.9.

Aspartate aminotransferase (AST): Mean AST activities in serum decreased from control value to vitamin E, ELVp (100 mg/kg) and ELVp (200 mg/kg). Also, mean AST activities decreased from 368.00 ± 5.29 IU in SA (2.5 mg/kg) value to 179.33 ± 2.66 IU in combination of SA + vitamin E, 274.00 ± 28.58 IU in SA+ ELVp (100 mg/kg), and 326.00 ± 9.45 IU in SA + ELVp (200 mg/kg) (Fig. 4.9).

Aspartate aminotransferase (AST) activity showed significant reduction ($p<0.05$) by 35.2 % from control (316.66 ± 15.67 IU) to vitamin E (205.33 ± 34.49 IU). While there was no significant differences recorded from control (316.66 ± 15.67 IU) to SA $_{2.5\ mg/kg}$ (368.00 ± 5.29 IU). However significant ($p<0.05$) reduction by 51.3% from SA $_{2.5\ mg/kg}$ (368.00 ± 5.29 IU) to combination of SA + Vitamin E (179.33 ± 2.66 IU) (Fig. 4.9).

Alanine aminotransferase (ALT): Mean ALT activities in serum decreased from control value to Vitamin E. While, mean ALT activities in serum increased from control value to SA (2.5 mg/kg).

Alanine aminotransferase (ALT) activity showed significant elevation ($p<0.05$) by 32.1 % from control (63.06 ± 3.01 IU) to SA $_{2.5\ mg/kg}$ (83.33 ± 1.27 IU). While there were no significant differences in values recorded for vitamin E, ELVp 100 mg/kg and ELVp 200 mg/kg when compared with control. ALT activity showed significant reduction ($p<0.05$) by 46.8% from SA $_{2.5\ mg/kg}$ (83.33 ± 1.27 IU) to SA+ Vitamin E (44.33 ± 1.53) and 17.5 % between SA $_{2.5\ mg/kg}$ (83.33 ± 1.27 IU) to SA + ELVp $_{100\ mg/kg}$ (68.73 ± 0.29) (Fig. 4.9).

Alkaline phosphatase (ALP): Mean ALP activities in serum decreased from control value to vitamin E and ELVp 100 mg/kg. While, mean ALP activities in serum increased from control values to SA (2.5 mg/kg).

Alkaline phosphatase (ALP) showed significant reduction ($p<0.05$) by 50.5 % from control (148.73 ± 15.86 IU) to vitamin E (73.60 ± 13.73 IU). While there were no significant

differences in values recorded for ELVp 100mg/kg and ELVp 200 mg/kgwhen compared with control.

Also ALP showed significant elevation ($p<0.05$) by 209.7 % from control (148.73 ± 15.86 IU) to SA $_{2.5\ mg/kg}$ (450.15 ± 40.10 IU). While, significant reduction ($p<0.05$) by 69.2 % from SA$_{2.5\ mg/kg}$ (450.15 ± 40.10 IU) to SA+ vitamin E (138.61 ± 17.81 IU); by 61.2 % from SA $_{2.5\ mg/kg}$ (450.15 ± 40.10 IU) to SA +ELVp $_{100\ mg/kg}$ (174.80 ± 1.06 IU) and by 56.1 % from SA $_{2.5\ mg/kg}$ (450.15 ± 40.10 IU) to SA + ELVp $_{200\ mg/kg}$ (197.49 ± 29.77 IU) (Fig. 4.9).

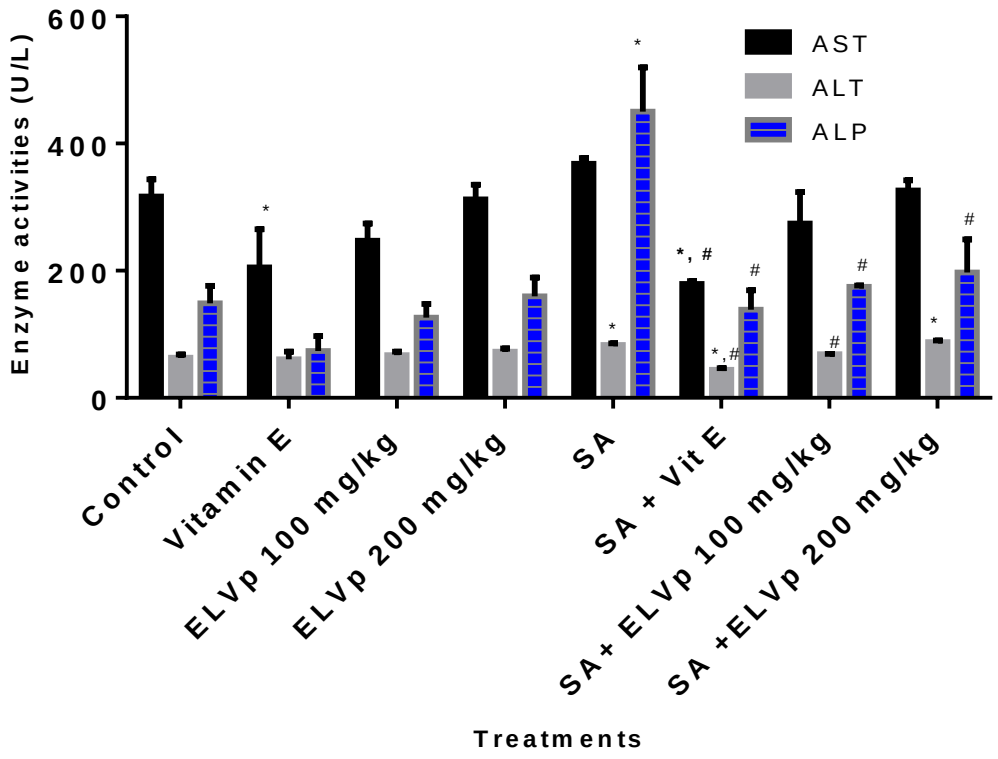

Figure 4.9: The results of the liver function markers in the treated and control animals

Values are stated as mean of five animals ± Standard Deviation (S.D)

*significant when compared with control at 5% level while #' significant when compared with sodium arsenite at 5% level.

Where SA represent sodium arsenite, ELVp represent the ethanol leaf extract of *Vitellaria paradoxa*

4.5.3 Liver histological examination

The histological examination of the treated rat livers showed normal hepatocytes for control, normal hepatocytes for vitamin E, Mild vascular congestion (arrow) and centrilobular cloudy swelling of hepatocytes for ELVp 100 (mg/kg), no observable lesion in ELVp (200 mg/kg), severe periportal inflammation with increase in connective tissue and fibroblast in the portal areas in SA (2.5 mg/kg), Mild periportal inflammation in SA +Vitamin E :, Mild periportal inflammation and mild vascular congestion in SA+ELVp (100 mg/kg) and mild periportal inflammation in SA+ELVp (200 mg/kg) (Plate 4.2).

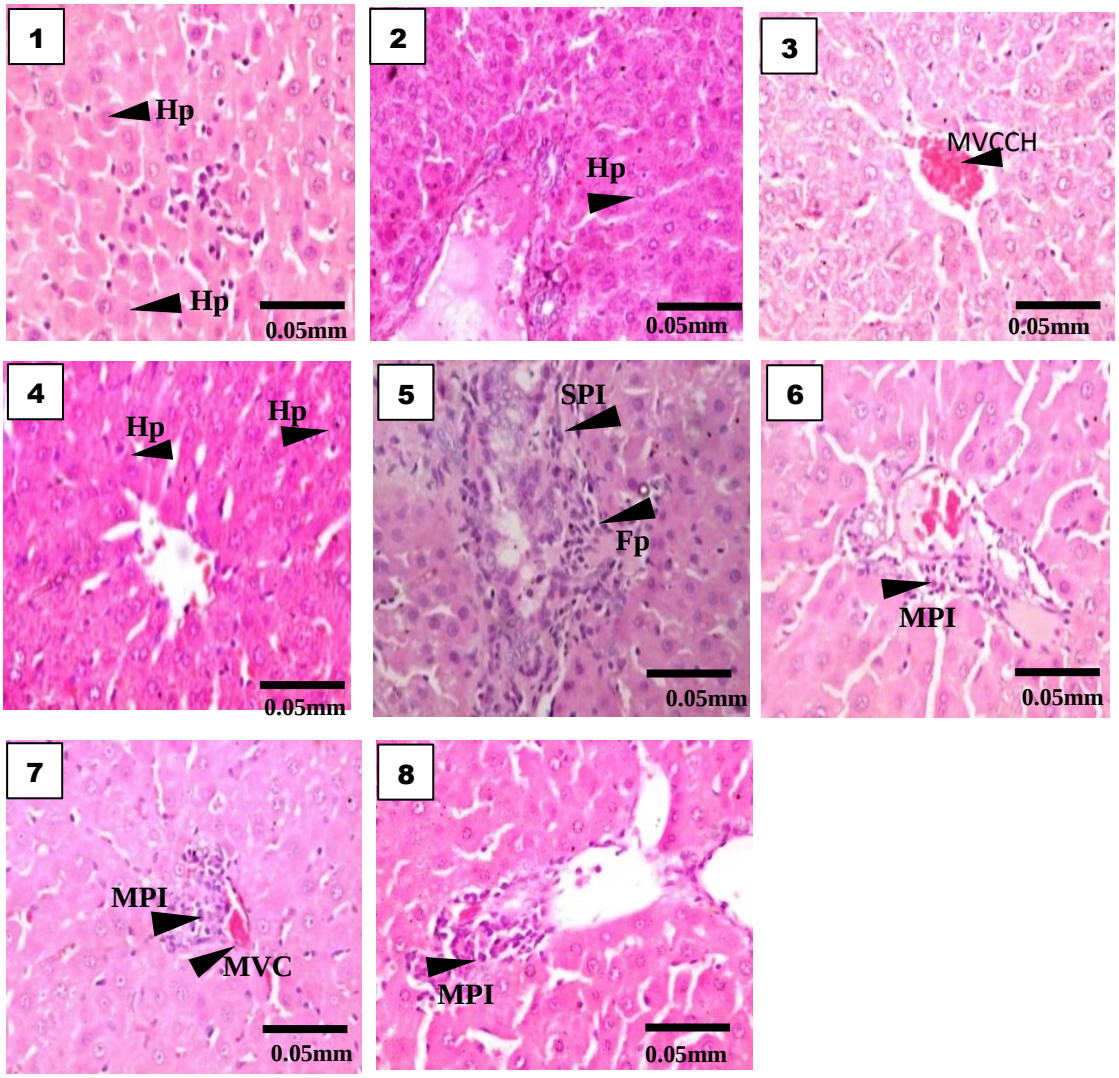

Plate 4. 2: Liver photomicrographs of rats administered ELVp and sodium arsenite (2.5 mg/kg.bw). Scale bar = 50µm. 1: Control with normal hepatocytes (Hp). 2: Vitamin E treated male Wistar rat with normal hepatocytes (Hp). 3: ELVp 100 mg/kg with mild vascular and centrilobular congestion of hepatocytes (MVCCH). 4: ELVp 200 mg/kg with normal hepatocytes (Hp). 5: SA with severe periportal inflammation (SPI) and increase in connective tissue with fibroblast in the portal areas (FP) 6: SA +Vit E with mild periportal inflammation (MPI). 7: SA+ELVp100 mg/kg with mild periportal inflammation (MPI) and mild vascular congestion (MVC). 8: SA+ELVp 200 mg/kg treated male Wistar rat displaying mild periportal inflammation (MPI) (× 400).

4.5.4: The nephro-remediative potential of ELVp on sodium arsenite induced toxicity

The urea and creatinine concentrations are presented in Figure 4.10 and 4.11 respectively.

Urea: Mean urea concentrations in serum decreased from control value to vitamin E, ELVp 100 mg/kg and ELVp 200 mg/kg. While, mean urea concentration in serum increased from control values to SA (2.5 mg/kg).

Urea concentration showed significant reduction ($p<0.05$) by 50.4 % from control (52.88 ± 3.25 mg/dL) to vitamin E (26.19 ± 3.67 mg/dL) and by 32.5 % from control (52.88 ± 3.25 mg/dL) to ELVp $_{100\ mg/kg}$ (35.72 ± 1.70 mg/dL).

Urea concentration showed significant elevation ($p<0.05$) by 42.0 % from control (52.88 ± 3.25 mg/dL) to SA $_{2.5\ mg/kg}$ (75.13 ± 0.64 mg/dL). While, significant reduction ($p<0.05$) by 61.9 % from $SA_{2.5\ mg/kg}$ (75.13 ± 0.64 mg/dL) to SA+ vitamin E (28.56 ± 3.18 mg/dL); by 55.1 % from $SA_{2.5\ mg/kg}$ (75.13 ± 0.64 mg/dL) to SA +ELVp $_{100\ mg/kg}$ (33.71 ± 5.23 mg/dL) and by 25.1 % from $SA_{2.5\ mg/kg}$ (75.13 ± 0.64 mg/dL) to SA + ELVp $_{200\ mg/kg}$ (56.21 ± 6.36 mg/dL) (Fig. 4.10)

Creatinine: Mean creatinine concentrations in serum decreased from control value to ELVp 100 mg/kg. While, mean urea concentration in serum increased from control values to SA (2.5 mg/kg).

Creatinine concentrations showed significant elevation ($p<0.05$) by 69.2 % from control (1.14 ± 0.08 mg/dL) to SA $_{2.5\ mg/kg}$ (1.93 ± 0.08 mg/dL). While, significant reduction ($p<0.05$) by 27.5 % from $SA_{2.5\ mg/kg}$ (1.93 ± 0.08 mg/dL) to SA+ vitamin E (1.40 ± 0.08 mg/dL); by 32.1 % from $SA_{2.5\ mg/kg}$ (1.93 ± 0.08 mg/dL) to SA +ELVp $_{100\ mg/kg}$ (1.31 ± 0.00 mg/dL) and by 40.9 % between $SA_{2.5\ mg/kg}$ (1.93 ± 0.08 mg/dL) and SA + ELVp $_{200\ mg/kg}$ (1.14 ± 0.17 mg/dL) (Fig. 4.11)

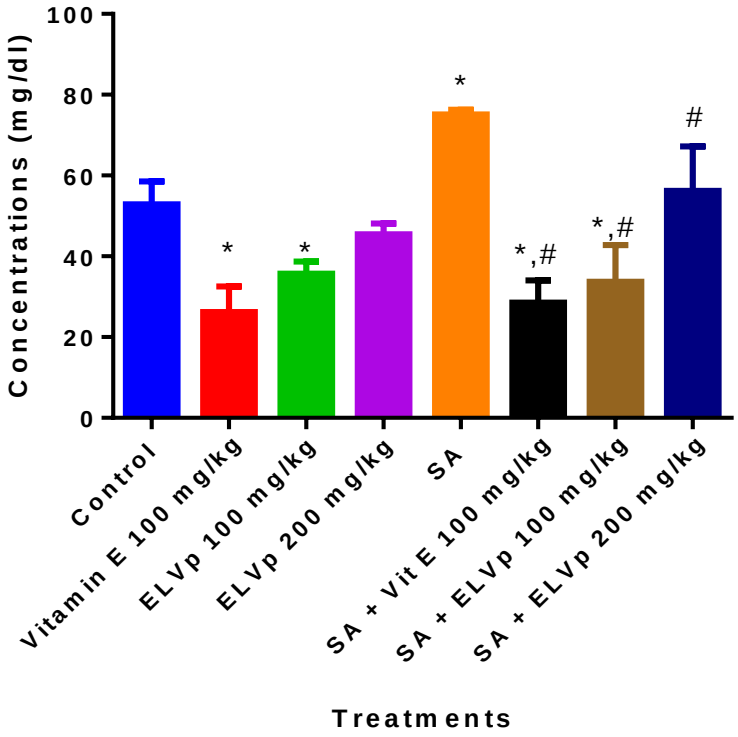

Figure 4.10: Effect of ELVp on the urea concentration of sodium arsenite –induced nephrotoxicity

Values are mean of five animals ± Standard Deviation (S.D)

*significant at 5% level in comparison with control while '#' significant at 5% level in comparison with sodium arsenite (positive control group)

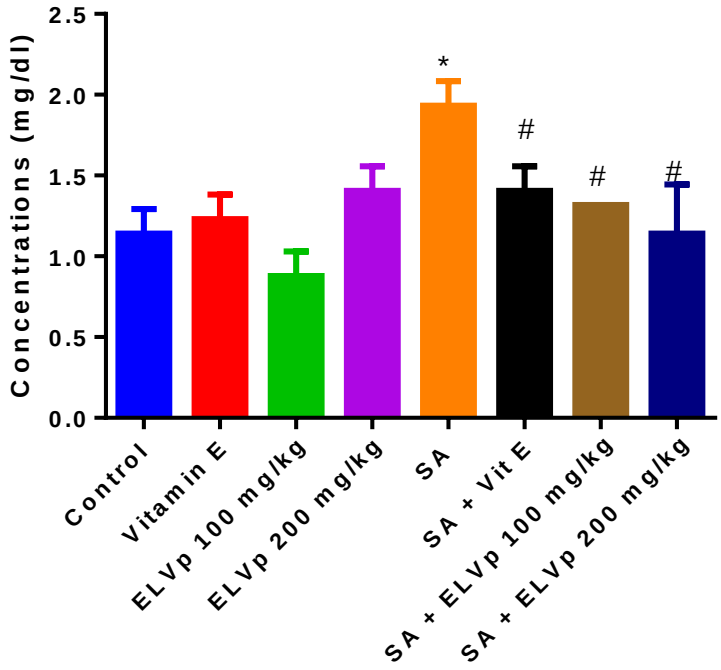

Figure 4.11: Effect of ELVp on the creatinine concentration of sodium aresenite – induced nephrotoxicity

Values are mean of five animals ± Standard Deviation (S.D)

*significant at p< 0.05 in comparison with control while '#' significant at p < 0.05 in comparison with sodium arsenite.

4.5.5 Kidney histological examination

The histological examination of the treated rat kidneys showed normal kidney cells for control, normal kidney cells for vitamin E, normal kidney cells for ELVp 100 (mg/kg), no observable lesion in ELVp (200 mg/kg), moderate glomerular capillary, interstitial congestion and peritubular inflammation in SA (2.5 mg/kg), vascular congestion, mild hemorrhagic lesion and slight peritubular inflammation in SA +Vitamin E :, moderate peritubular inflammation in SA+ELVp (100 mg/kg) and normal kidney cells in SA+ELVp (200 mg/kg) (Plate 4.3).

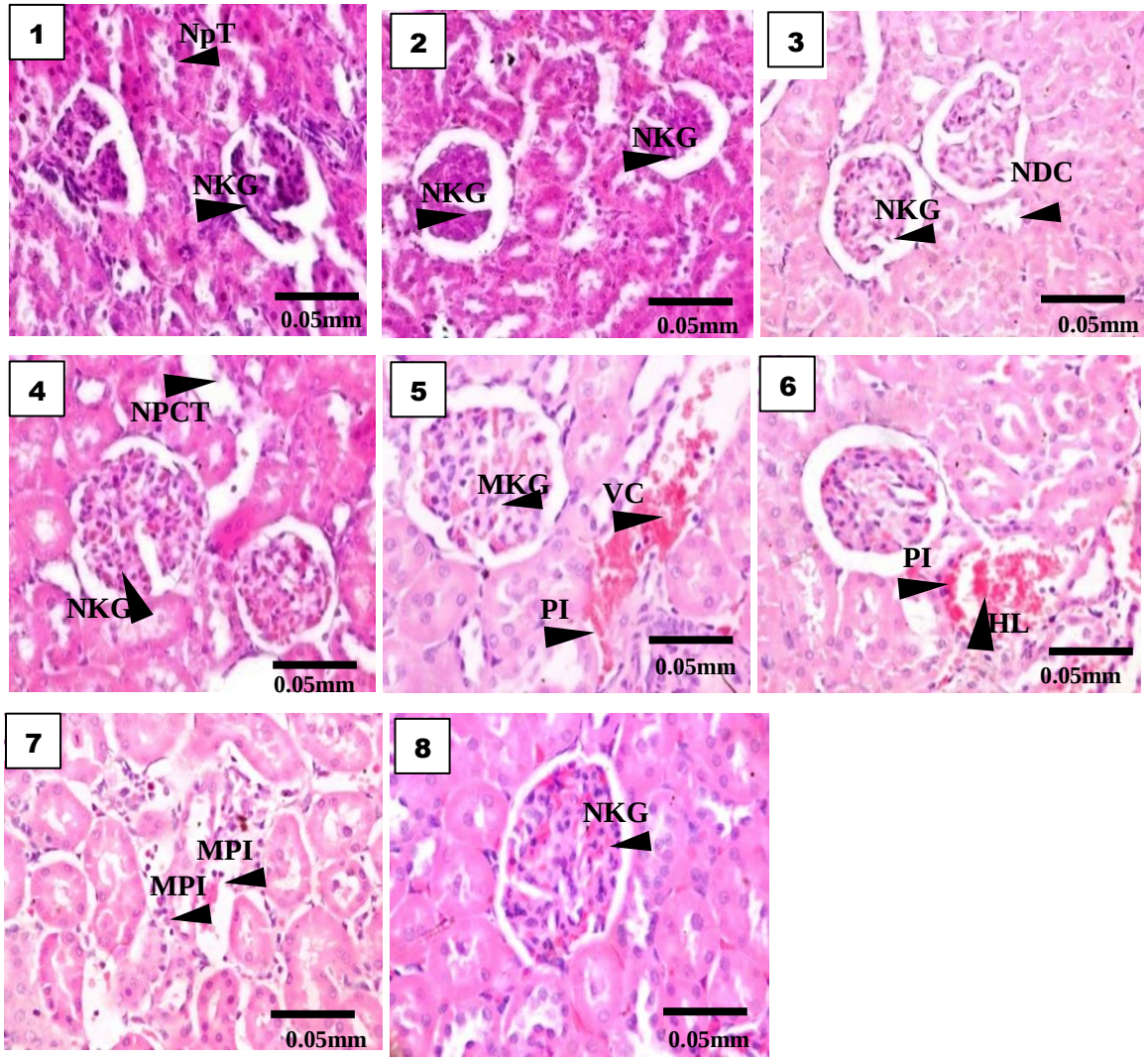

Plate 3: Kidney photomicrographs of rats administered ELVp, vitamin and sodium arsenite (2.5mg/kg.bw). Scale =0.050mm

1: Control rats displayed normal kidney glomerulus (NKG) and normal proximal tubular (NPT). 2 i: Vitamin E displayed normal kidney glomerulus (NKG). 3: ELVp 100 mg/kg displayed normal kidney glomerulus (NKG) and normal ductal convoluted tubules (NDCT). 4: ELVp 200 mg/kg displayed normal kidney glomerulus (NKG) and normal proximal convoluted tubules (NPCT). 5: SA (0.0625 mM) displayed moderate glomerular capillary (MGC), vascular congestion (VC) and peritubular inflammation (PI). 6: SA +Vit E displayed slight peritubular inflammation (PI) and mild hemorrhagic lesion (HL). 7: SA+ELVp100 mg/kg displayed moderate peritubular inflammation (MPI) and 8: SA+ELVp 200 mg/kg displayed normal kidney glomerulus (NKG) × 400.

4.5.6: Assessment of the remediative potential of ELVp on sodium arsenite-induced toxicity on haematological parameters

The red blood cells (RBC), haemoglobin (HGB), haematocrit ((HCT), platelet (PLT), lymphocyte (LYMP) and white blood cell (WBC) are presented in Table 4.4.

Red blood cells (RBC): The red blood cells (RBC) was decreased from control value to vitamin E, ELVp 100 mg/kg, ELVp 200 mg/kg, SA 2.5 mg/kg., combination of SA + vitamin E, and SA + ELVp 100 mg/kg.

Red blood cells levels showed Significant decreased ($p<0.05$) by 8.8 % from control (7.04±0.26) to vitamin E (6.42 ±0.25) and by 9.0 % from control (7.04±0.26) to SA $_{2.5\ mg/kg}$ (6.40 ±0.39). While significant elevation ($p<0.05$) by 13.9 % from SA $_{2.5\ mg/kg}$ (6.40 ±0.39) to SA + ELVp $_{200\ mg/kg}$ (7.29 ±0.36).

Haemoglobin (HGB): The haemoglobin was decreased from control value to vitamin E, ELVp 100 mg/kg, ELVp 200 mg/kg, SA 2.5 mg/kg., combination of SA + vitamin E, SA + ELVp 100 mg/kg and SA + ELVp 200 mg/kg.

Haemoglobin (HGB) levels showed significant decreased ($p<0.05$) by 10.3 % from control (152.0±6.00) to vitamin E (136.3 ±2.89); by 11.3 % control was (152.0 ± 6.00) to ELVp $_{100\ mg/kg}$ (134.7±3.51) and by 12.3 % between control (152.0±6.00) and SA $_{2.5\ mg/kg}$ (133.3 ±2.52). While significant elevation ($p<0.05$) by 12.3 % from SA $_{2.5\ mg/kg}$ (133.3 ±2.52) to SA + ELVp $_{200\ mg/kg}$ (149.7 ±1.53).

Haematocrit (HCT): the haematocrit was decreased from control value to vitamin E, ELVp 100 mg/kg, SA 2.5 mg/kg., combination of SA + vitamin E, SA + ELVp 100 mg/kg and SA + ELVp 200 mg/kg.

Haematocrit (HCT) levels showed significant decreased ($p<0.05$) by 23.0 % from control (48.08±0.91) to vitamin E (37.00 ±0.32); by 10.2% from control (48.08± 0.91) to ELVp $_{100\ mg/kg}$ (43.17±1.78); by 13.1 % from control (48.08±0.91) to SA $_{2.5\ mg/kg}$ (41.77 ±0.92); by 14.2 % from control (48.08 ±0.91) to SA + vitamin E (41.24 ±1.41); by 13.0 % from control (48.08 ±0.91) to SA + ELVp $_{100\ mg/kg}$ (41.79 ±1.56) and by 8.2 % between control (48.08 ±0.91) and SA + ELVp $_{200\ mg/kg}$ (44.16 ±1.44).

Platelet (PLT): The platelet count decreased from control value to vitamin E, ELVp 100 mg/kg, and increased for SA (2.5 mg/kg). However, platelet count decreased from SA (2.5 mg/kg) to combination of SA + vitamin E, SA + ELVp 100 mg/kg and SA + ELVp 200 mg/kg.

Platelet (PLT) levels showed significant elevation ($p<0.05$) by 17.2 % from control (629.3 ± 60.96) to SA $_{2.5\ mg/kg}$ (738.0 ± 51.88). While, significant reduction ($p<0.05$) by 13.9 % from $SA_{2.5\ mg/kg}$ (738.0 ± 51.88) to SA+ vitamin E (634.7 ± 25.58); and by 11.2 % from $SA_{2.5\ mg/kg}$ (738.0 ± 55.88) to SA + ELVp $_{200\ mg/kg}$ (655.0 ± 37.32) (Table 4.4).

Lymphocytes (LYMP): The lymphocytes count decreased from control value to vitamin E, SA + vitamin E, SA + ELVp 200 mg/kg and increased for ELVp 100 mg/kg, ELVp 200 mg/kg, SA (2.5 mg/kg) and SA + ELVp 100 mg/kg. However, platelet count decreased from SA (2.5 mg/kg) to combination of SA + vitamin E and SA + ELVp 200 mg/kg.

Lymphocytes (LYMP) shiwed significant elevation ($p<0.05$) by 9.2 % from control (81.50± 4.07) to ELVp $_{100\ mg/kg}$ (89.05 ± 0.51); by 9.6 % from control (81.50 ± 4.07) to ELVp $_{200\ mg/kg}$ (89.33± 1.82); by 10.5 % from control (81.50 ± 4.07) to SA $_{2.5\ mg/kg}$ (90.08 ± 4.23). While, significant reduction ($p<0.05$) by 16.1 % from $SA_{2.5\ mg/kg}$ (90.08 ± 4.23) to SA+ vitamin E (75.58 ± 2.97); and by 19.3 % from $SA_{2.5\ mg/kg}$ (90.08 ± 4.23) to SA + ELVp $_{200\ mg/kg}$ (72.74 ± 2.08) (Table 4.4).

Table 4.4: Remediative potential of ELVp on sodium arsenite induced toxicity on haematological parameters

GROUPS	RBC	HGB	HCT	PLT	LYMP	WBC
control	7.04 ± 0.26	152.0 ± 6.00	48.08 ± 0.91	629.3± 60.96	81.50 ± 4.07	4.97 ± 0.81
Vit E	6.42 ± 0.25 *	136.3 ± 2.89*	37.00 ± 0.32 *	560.7 ± 22.55	79.67 ± 4.19	6.93 ± 1.39
ELVp 100mg/kg	6.57 ± 0.07	134.7 ± 3.51 *	43.17 ± 1.78 *	683.0 ± 30.45	89.05 ± 0.51 *	6.60 ± 0.96
ELVP 200mg/kg	6.84 ± 0.20	150.0 ± 4.36	48.24 ± 0.91	566.7± 22.23	89.33 ± 1.82 *	5.60 ± 0.52
SA 2.5mg/kg	6.40± 0.39 *	133.3 ± 2.52*	41.77 ± 0.92 *	738.0 ± 51.88 *	90.08 ± 4.23 *	6.73± 0.78
SA + Vit E	6.00 ± 0.05 *	142.7 ± 5.69	41.24± 1.41 *	634.7 ± 25.58 #	75.58 ± 2.97 *,#	4.40 ± 0.26
SA+ ELVP 100mg/kg	6.84 ± 0.13	136.7 ± 6.35*	41.79 ± 1.56*	676.0 ± 65.28	90.73± 0.23 *	7.23 ± 1.96
SA+ ELVP 200mg/kg	7.29 ± 0.36 #	149.7 ± 1.53 #	44.16 ± 1.44 *	655.0 ± 37.32 #	72.74 ± 2.08 *,#	8.27± 1.05

Values are mean of five animal's ± Standard Deviation (S.D)

*significant at $p < 0.05$ in comparison with control while #' significant at $p < 0.05$ in comparison with sodium arsenite.

4.5.7: Effect of ELVP in sodium arsenite induced lipid peroxidation

The malondiaaldehyde (MDA) concentrations of liver and kidney organs are presented in Figure 4.12-4.13.

Liver: The mean malondiaaldehyde (MDA) concentration decreased from control value to vitamin E, ELVp 100 mg/kg and ELVp 200 mg/kg. While, mean MDA concentration increased from control values to SA (2.5 mg/kg). Furthermore, the mean MDA decreased from SA (2.5 mg/kg) to combination of SA+ vitamin E, SA +ELVp (100 mg/kg) and SA + ELVp (200 mg/kg).

Significant ($p<0.05$) reduction from control to vitamin E was 53.4 % (0.043 ± 0.006 µmole/gprotein) to (0.020 ± 0.003 µmole/gprotein) and control to ELVp 100 mg/kg was 39.5 % (0.043 ± 0.006 µmole/gprotein) to (0.026 ± 0.001 µmole/gprotein).

Significant ($p<0.05$) elevation from control to SA (2.5 mg/kg) was 55.8 % (0.043 ± 0.006 µmole/gprotein) to (0.067 ± 0.012 µmole/gprotein). While, significant ($p<0.05$) reduction from SA to SA+ vitamin E was 53.7 % (0.067 ± 0.012 µmole/gprotein) to (0.031 ± 0.008 µmole/gprotein), SA to SA +ELVp (100 mg/kg) was 26.8 % (0.067 ± 0.012 µmole/gprotein) to (0.049 ± 0.004 µmole/gprotein) and SA to SA + ELVp (200 mg/kg) was 38.8 % (0.067 ± 0.012 µmole/gprotein) to (0.041 ± 0.007 µmole/gprotein) (Fig. 4.12).

Kidney: The mean malondiaaldehyde (MDA) concentration increased from control values to SA (2.5 mg/kg). Furthermore, the mean MDA decreased from SA (2.5 mg/kg) to combination of SA+ vitamin E, SA +ELVp (100 mg/kg) and SA + ELVp (200 mg/kg).

Significant ($p<0.05$) elevation from control to SA (2.5 mg/kg) was 250 % (0.014 ± 0.005 µmole/gprotein) to (0.049 ± 0.006 µmole/gprotein). While, significant ($p<0.05$) reduction from SA to SA+ vitamin E was 71.4 % (0.049 ± 0.006 µmole/gprotein) to (0.014 ± 0.012 µmole/gprotein), SA to SA +ELVp (100 mg/kg) was 46.9 % (0.049 ± 0.006 µmole/gprotein) to (0.026 ± 0.008 µmole/gprotein) and SA to SA + ELVp (200 mg/kg) was 53.01 % (0.049 ± 0.006 µmole/gprotein) to (0.023 ± 0.002 µmole/gprotein) (Fig. 4.13).

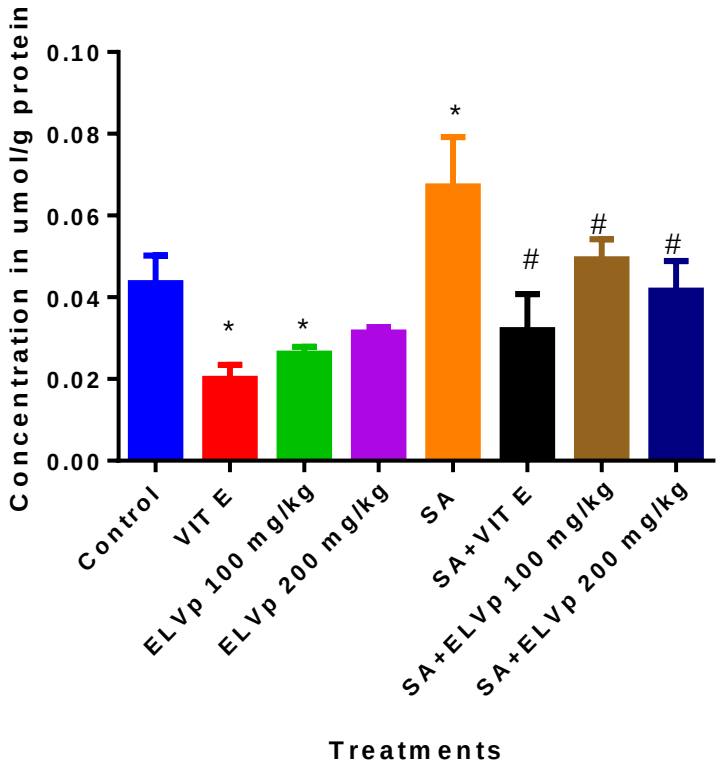

Figure 4.12: The remediative potential of ELVp agains sodium arsenite-induced liver lipid peroxidation.

Values are mean of five animal's ± Standard Deviation (S.D)

*significant at $p< 0.05$ in comparison with control while # significant at $p< 0.05$ in comparison with sodium arsenite.

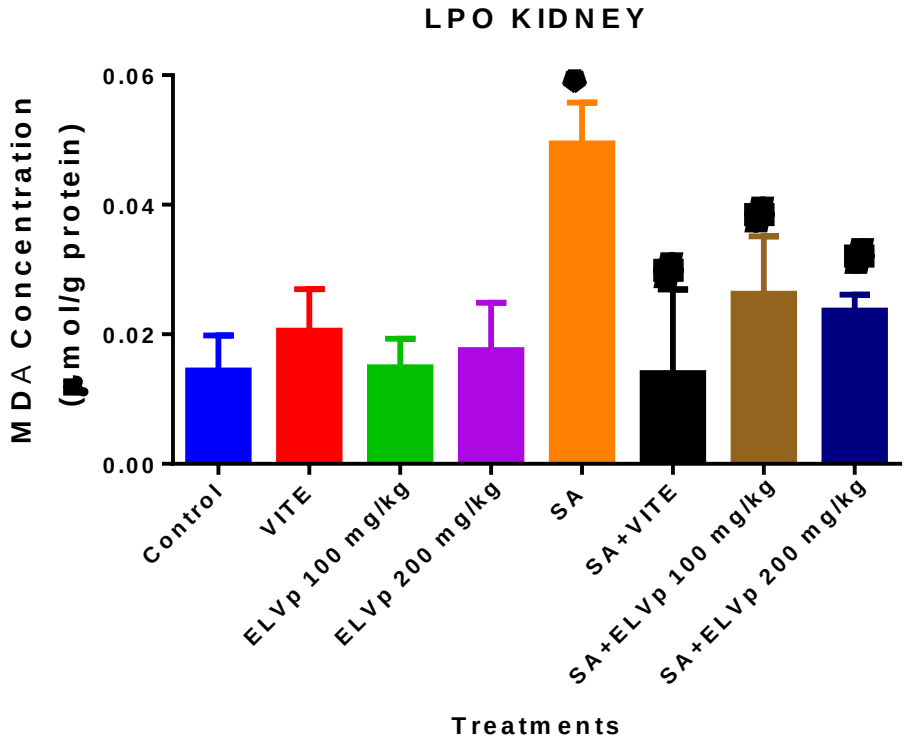

Figure 4.13: The remediative potential of ELVp against sodium arsenite- induced kidney lipid peroxidation.

Values are mean of five animal's ± Standard Deviation (S.D)

*significant at p< 0.05 when compared with control while # significant at p< 0.05 when compared with sodium arsenite.

4.5.8: Effect of ELVp on SA- induced clastogenicity

The frequency of polychromatic erythrocytes cells (mPCEs) are presented in Figure 4.14.

The mean frequency of polychromatic erythrocytes cells (mPCEs) increased from control values to SA (2.5 mg/kg). Furthermore, the mean mPCEs decreased from SA (2.5 mg/kg) to combination of SA+ vitamin E, SA +ELVp (100 mg/kg) and SA + ELVp (200 mg/kg).

Mean frequency of polychromatic erythrocytes cells (mPCEs) showed significant elevation ($p<0.05$) by 300 % from control (4.00 ± 0.81 nMPES/1000PCEs) to SA $_{2.5\ mg/kg}$ (16.00 ± 1.15 nMPES/1000PCEs). While, significant reduction ($p<0.05$) was by 45.9 % from $SA_{2.5\ mg/kg}$ (16.00 ± 1.15 nMPES/1000PCEs) to SA+ vitamin E (8.66 ± 1.76 nMPES/1000PCEs); by 37.5 % from $SA_{2.5\ mg/kg}$ (16.00 ± 1.15 nMPES/1000PCEs) to SA +ELVp $_{100\ mg/kg}$ (10.00 ± 1.41 nMPES/1000PCEs) and by 50 % from $SA_{2.5\ mg/kg}$ (16.00 ± 1.15 nMPES/1000PCEs) to SA + ELVp $_{200\ mg/kg}$ (8.00 ± 1.15 nMPES/1000PCEs) (Fig. 4.14).

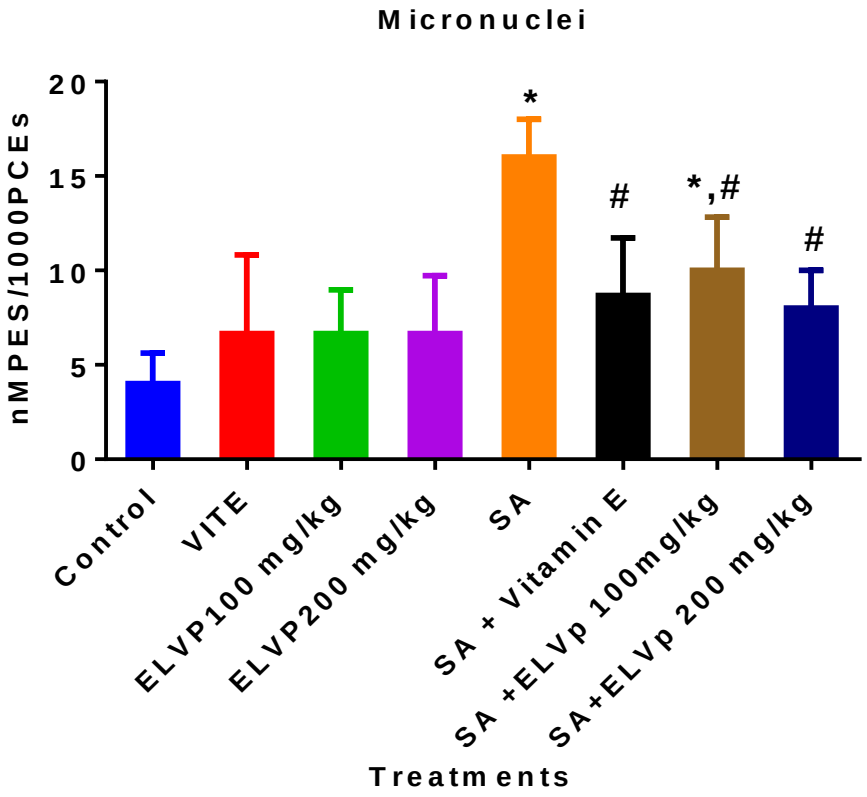

Figure 4.14: Remediative potential of ELVp on clastogenicity induced by sodium arsenite

Values are mean of five animal's ± Standard Deviation (S.D)

*significant at p< 0.05 when compared with control while # significant at p< 0.05 when compared with sodium arsenite.

4.5.9 Effect of ELVp on SA-induced inflammatory

The expression of NF-κB in liver and kidney organs are presented in Plate 4.4 - 4.5 and Figure 4.15-4.16.

Liver: The expression of NF-κB decreased from control values to vitamin E, ELVp (100 mg/kg) and ELVp (200 mg/kg).

Expression of NF-κB showed significant reduction ($p<0.05$) by 38.5 % from control (198.35 ± 6.00) to vitamin E (121.93± 6.00); 31.6 % from control (198.35 ± 6.00) to ELVp $_{100\ mg/kg}$ (135.58 ± 14.00) and 31.5 % between control (198.35 ± 6.00) and ELVp $_{200\ mg/kg}$ (135.87 ± 41.00) (Plate 4.4 and Fig. 4.15).

Kidney: The expression of NF-κB decreased from control values to vitamin E, ELVp (100 mg/kg) and ELVp (200 mg/kg). However, the expression of NF-κB increased from control values to SA (2.5 mg/kg). Furthermore, the expression of NF-κB decreased from SA (2.5 mg/kg) to combination of SA+ vitamin E.

Expression of NF-κB showed significant reduction ($p<0.05$) by 29.5 % from control (198.28 ± 2.00) to vitamin E (139.91± 6.00); 32 % from control (198.28 ± 2.00) to ELVp $_{100\ mg/kg}$ (135.00 ± 9.00) and 33.0 % from control (198.28 ± 2.00) to ELVp $_{200\ mg/kg}$ (132.81 ± 8.00) (Plate 4.4 and Figure 4.14). Also, showed significant elevation ($p<0.05$) by 13.8 % from control (198.28 ± 2.00) to SA $_{2.5\ mg/kg}$ (225.76 ± 21.00). While, showed significant reduction ($p<0.05$) by39.8 % from SA$_{2.5\ mg/kg}$ (225.76 ± 21.00) to SA+ vitamin E (135.84 ± 5.00) (Plate 4.5 and Fig. 4.16).

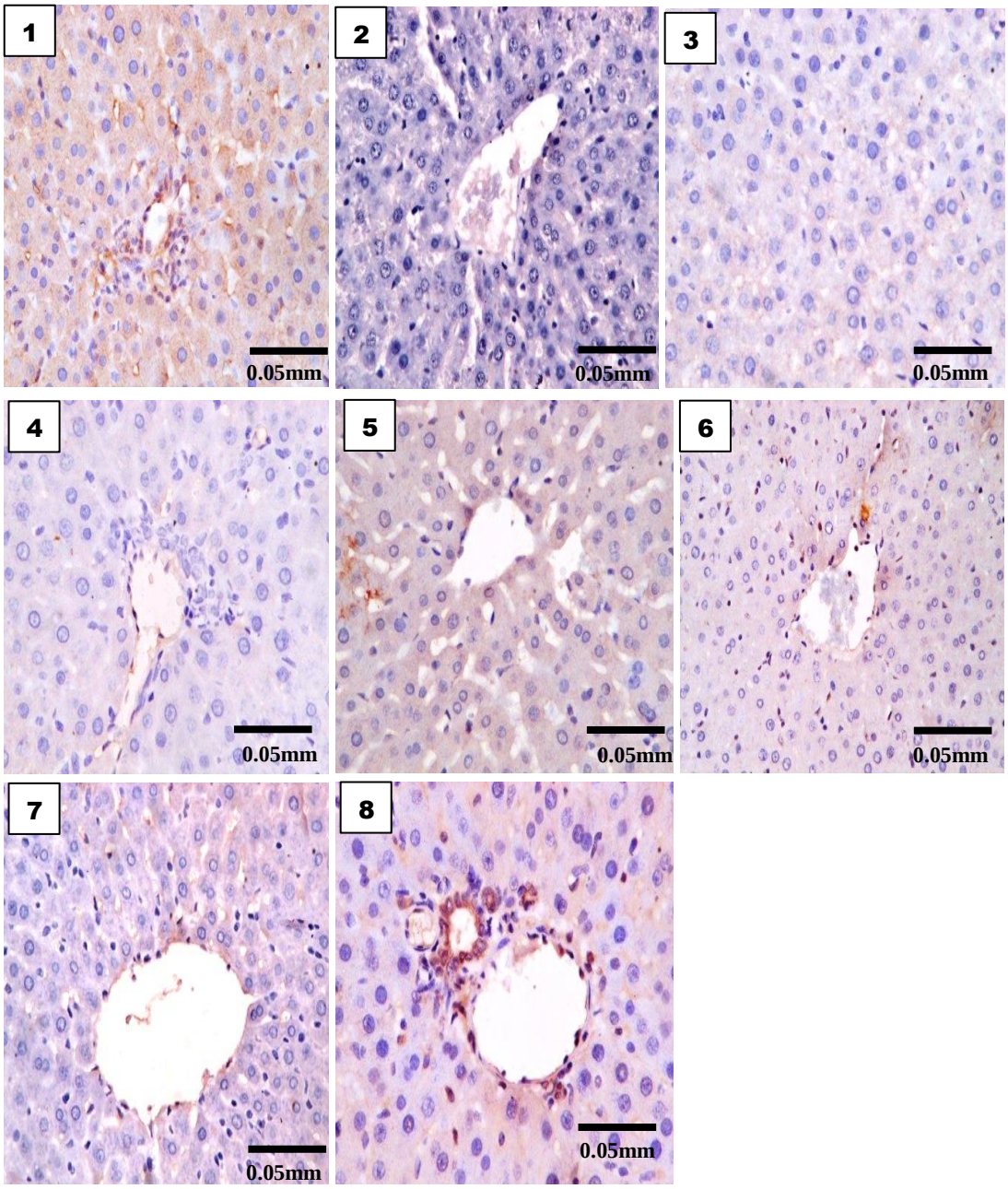

Plate 4.4: Photomicrograph of liver showing the expression of NF-kB.

1: Control. 2: Vitamin E (100 mg/kg). 3: ELVp 100 mg/kg. 4: ELVp 200 mg/kg. 5: SA (2.5 mg/kg). 6: SA +Vit E. 7: SA+ELVp100 mg/kg. 8: SA+ELVp 200 mg/kg.

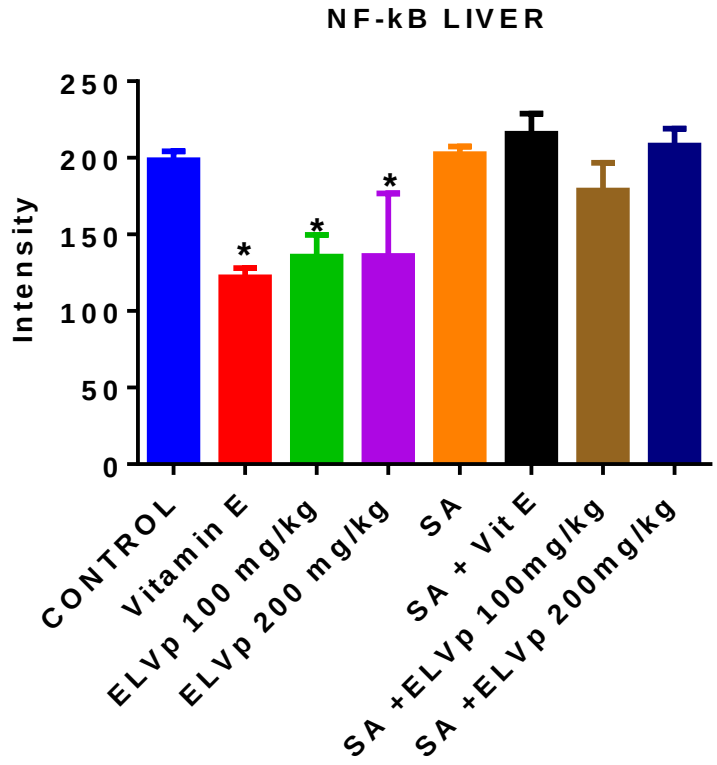

Figure 4. 15: Effect of vitamin E, ELVp or SA on NF-kB expression in liver

Where * represent significant difference in comparison with control.

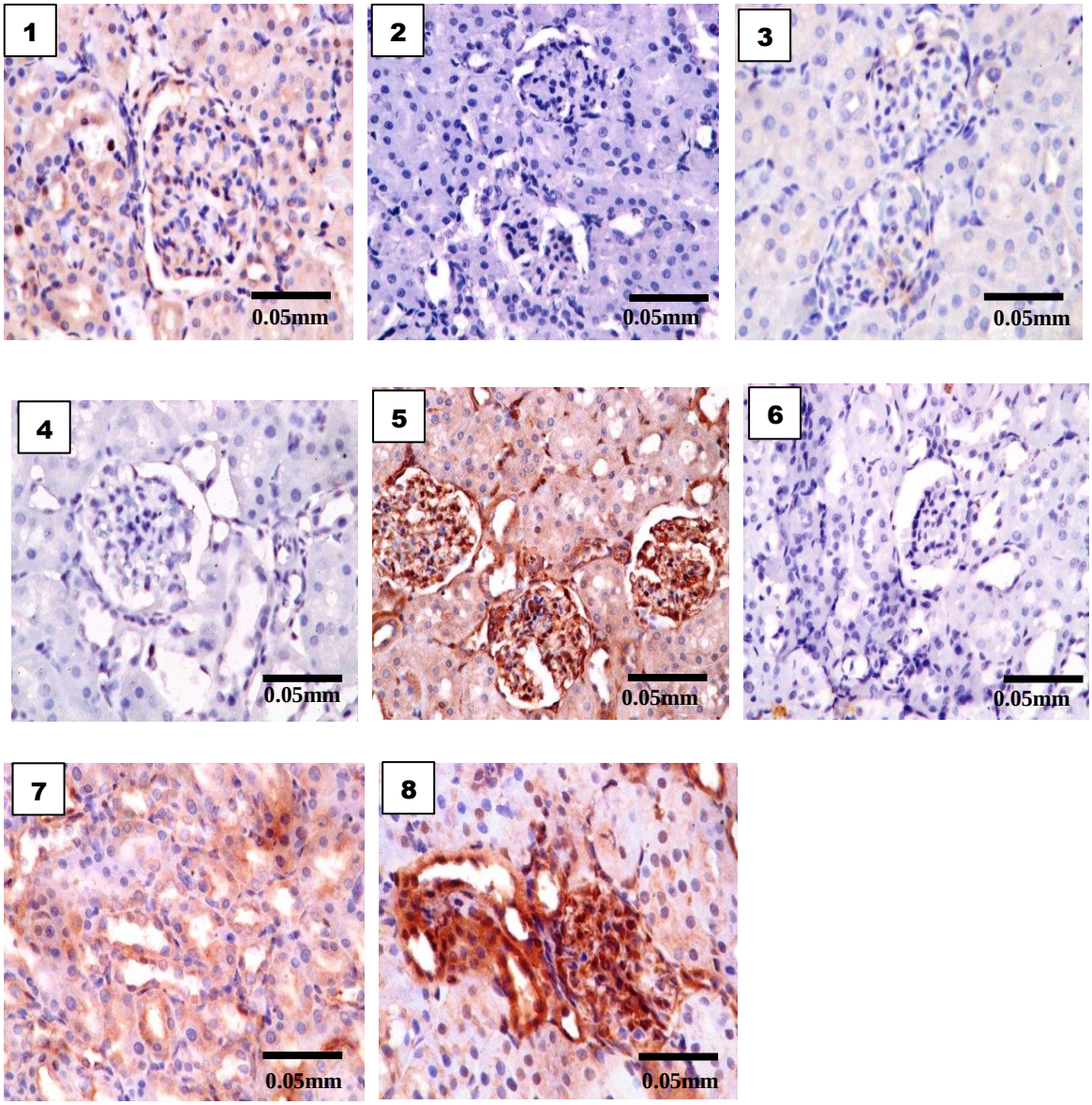

Plate 4.5: Photomicrograph of kidney showing the expression of NF- κB

1: Control. 2: Vitamin E. 3: ELVp 100 mg/kg. 4: ELVp 200 mg/kg. 5: SA (2.5 mg/kg). 6: SA +Vit E. 7: SA+ELVp100 mg/kg. 8: SA+ELVp 200 mg/kg.

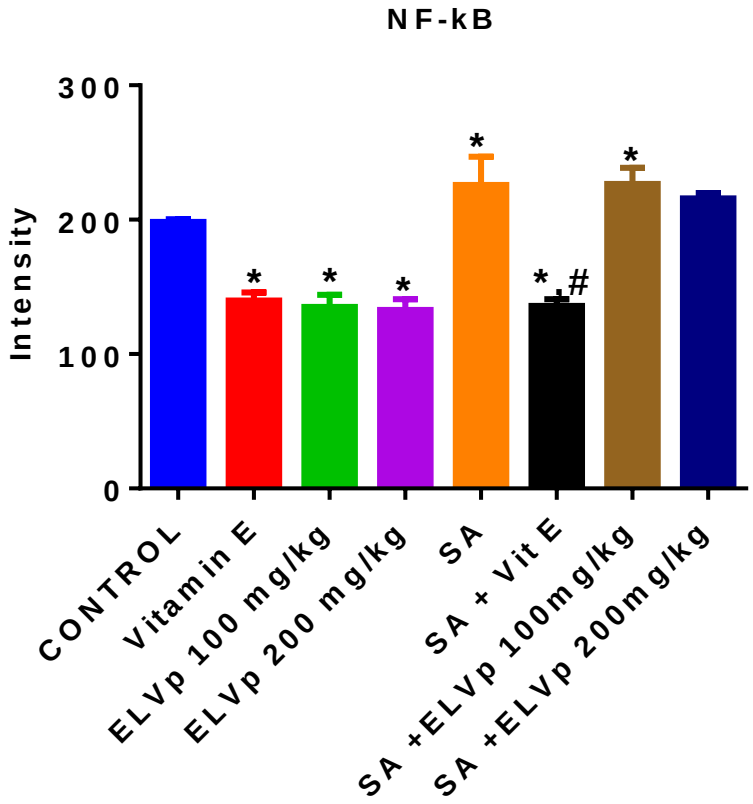

Figure 4.16: Effect of vitamin E, ELVp or SA treatment on NF-kB expression in kidney

Where * represent significant difference when compared to control and # when compared with sodium arsenite (SA)

4.5.10 Effect of ELVp on SA-induced apoptotic marker

P53 protein expression

The expression of p53 in liver and kidney organs are presented in Plate 4.6 - 4.7 and Figure 4.17-4.18.

Liver: The expression of p53 increased from control values to vitamin E, ELVp (100 mg/kg) and ELVp (200 mg/kg). Also, the expression of p53 increased from SA to cotreatment of SA +vitamin E, SA + ELVp 100 mg/kg and SA + ELVp 200 mg/kg.

The highest significant ($p<0.05$) increase from control was recorded in ELVp 100 mg/kg (212.67 ± 18.00). Although, there were no significant differences in values recorded from control to SA. However, showed significant increased ($p<0.05$) by 45.1 % from $SA_{2.5\ mg/kg}$ (144.89 ± 9.00) to SA + vitamin E (210.30 ± 20.00); 39.0 % from $SA_{2.5\ mg/kg}$ (144.89 ± 9.00) to SA + $ELVp_{\ 100\ mg/kg}$ (201.51 ± 11.00) and 43.6 % from $SA_{2.5\ mg/kg}$ (144.89± 9.00) to SA + $ELVp_{\ 200\ mg/kg}$ (208.13 ± 11.00) (Plate 4.6 and Fig. 4.17).

Kidney: The expression of p53 increased from control values to ELVp (100 mg/kg), ELVp (200 mg/kg), SA (2.5 mg/kg), SA+ vitamin E, SA + ELVp 100 mg/kg and SA + ELVp 200 mg/kg.

The highest significant ($p<0.05$) increased from control was recorded in ELVp 200 mg/kg (213.67 ± 11.00). (Plate 4.7 and Fig. 4.18).

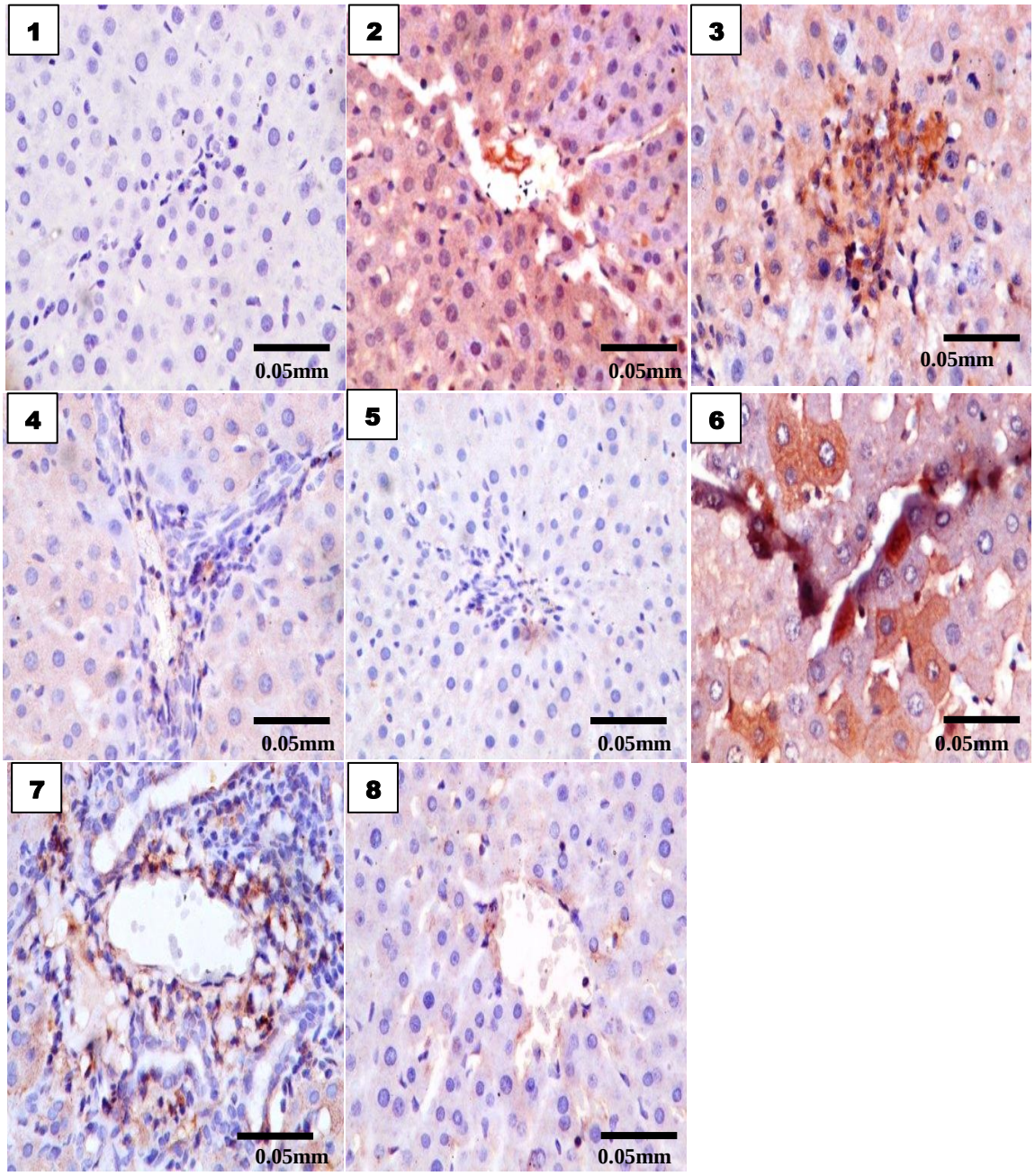

Plate 4. 6: Photomicrograph of liver showing the expression of p53 protein.

1:Control. 2: Vitamin E (100 mg/kg). 3: ELVp 100 mg/kg. 4: ELVp 200 mg/kg. 5: SA (2.5 mg/kg). 6: SA +Vit E. 7: SA+ELVp100 mg/kg. 8: SA+ELVp 200 mg/kg.

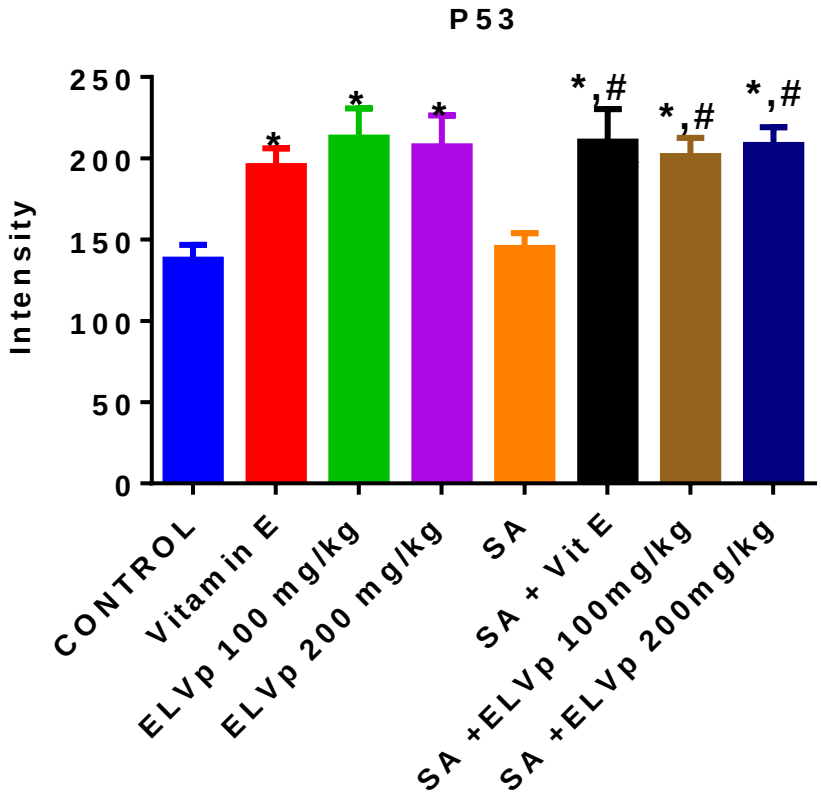

Figure 4.17: Effect of vitamin E, ELVp or SA treatment on p53 expression in liver

Where * represent significant difference in comparison to control and # when compared with sodium arsenite (SA)

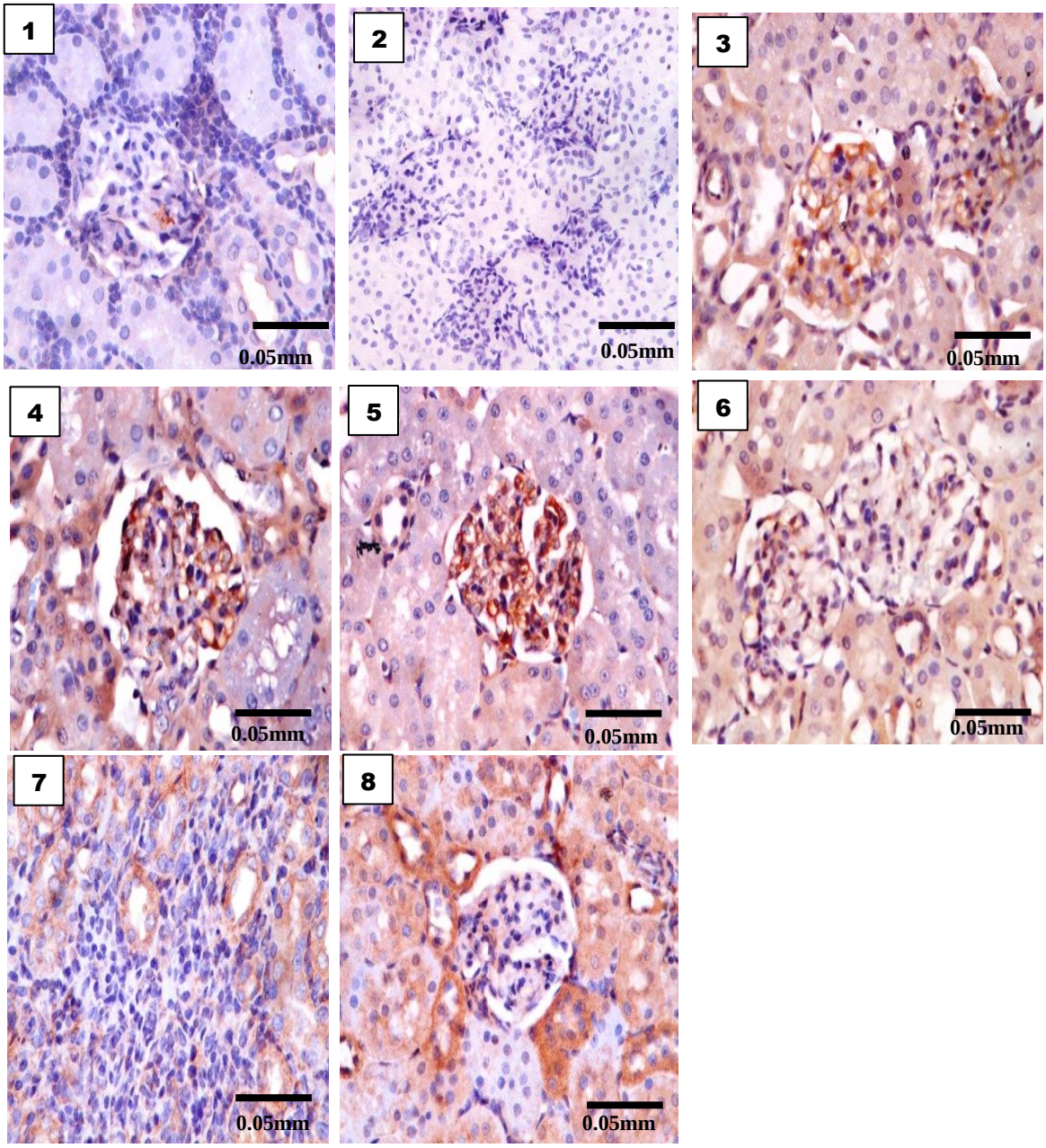

Plate 4.7: Photomicrograph of kidney showing the expression of p53.

1: Control. 2: Vitamin E (100 mg/kg). 3: ELVp 100 mg/kg. 4: ELVp 200 mg/kg. 5: SA (2.5 mg/kg). 6: SA +Vit E. 7: SA+ELVp100 mg/kg. 8: SA+ELVp 200 mg/kg.

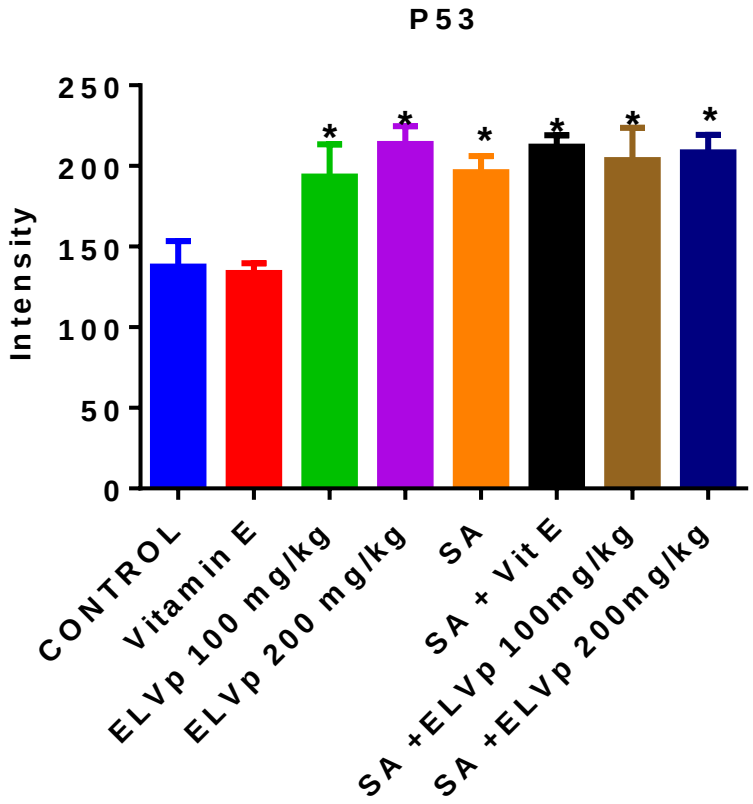

Figure 4.18: Effect of vitamin E, ELVp or SA treatment on p53 expression in kidney

Where * represent significant difference when compared to control

BCL-2 protein expression

The expression of BCL-2 in liver and kidney organs are presented in Plate 4.8 - 4.9 and Figure 4.19-4.20.

Liver: The expression of BCL-2 decreased from control values to vitamin E and ELVp (100 mg/kg). While the expression of BCL-2 increased from control values to SA and SA+ vitamin E. On the other hand, the expression of BCL-2 decreased from SA to cotreatment of SA + ELVp 100 mg/kg and SA + ELVp 200 mg/kg.

Expression of BCL-2 showed significant reduction ($p<0.05$) by 24.4 % from control (189.36 ± 3.00) to vitamin E (143.23± 6.00) and 28.2% from control (189.36 ± 3.00) to ELVp $_{100\ mg/kg}$ (135.98 ± 12.00) (Plate 4.8 and Figure 4.19). Also, showed significant elevation ($p<0.05$) by 14.2 % from control (189.36 ± 3.00) to SA $_{2.5\ mg/kg}$ (216.32 ± 8.00). While, showed significant reduction ($p<0.05$) by 43.3 % from $SA_{2.5\ mg/kg}$ (216.32 ± 8.00) to SA+ ELVp $_{100\ mg/kg}$ (122.61 ± 12.00) and 25.6 % from $SA_{2.5\ mg/kg}$ (216.32 ± 8.00) to SA+ ELVp $_{100\ mg/kg}$ (161.01 ± 8.00) (Plate 4.8 and Fig. 4.19).

Kidney: The expression of BCL-2 decreased from control values to vitamin E, ELVp (100 mg/kg) and ELVp 200 mg/kg. While the expression of BCL-2 increased from control values to SA. On the other hand, the expression of BCL-2 decreased from SA to cotreatment of SA+ vitamin E and SA + ELVp 100 mg/kg.

Expression of BCL-2 showed significant reduction ($p<0.05$) by 43.1 % from control (207.87 ± 32.00) to vitamin E (145.25± 12.00). Also, showed significant elevation ($p<0.05$) by 51 % from control (207.87 ± 32.00) to SA $_{2.5\ mg/kg}$ (218.61 ± 28.00). While, showed significant reduction ($p<0.05$) by 45.9 % from $SA_{2.5\ mg/kg}$ (218.61 ± 28.00) to SA+ vitamin E (118.11 ± 18.00) (Plate 4.9 and Fig. 4.20).

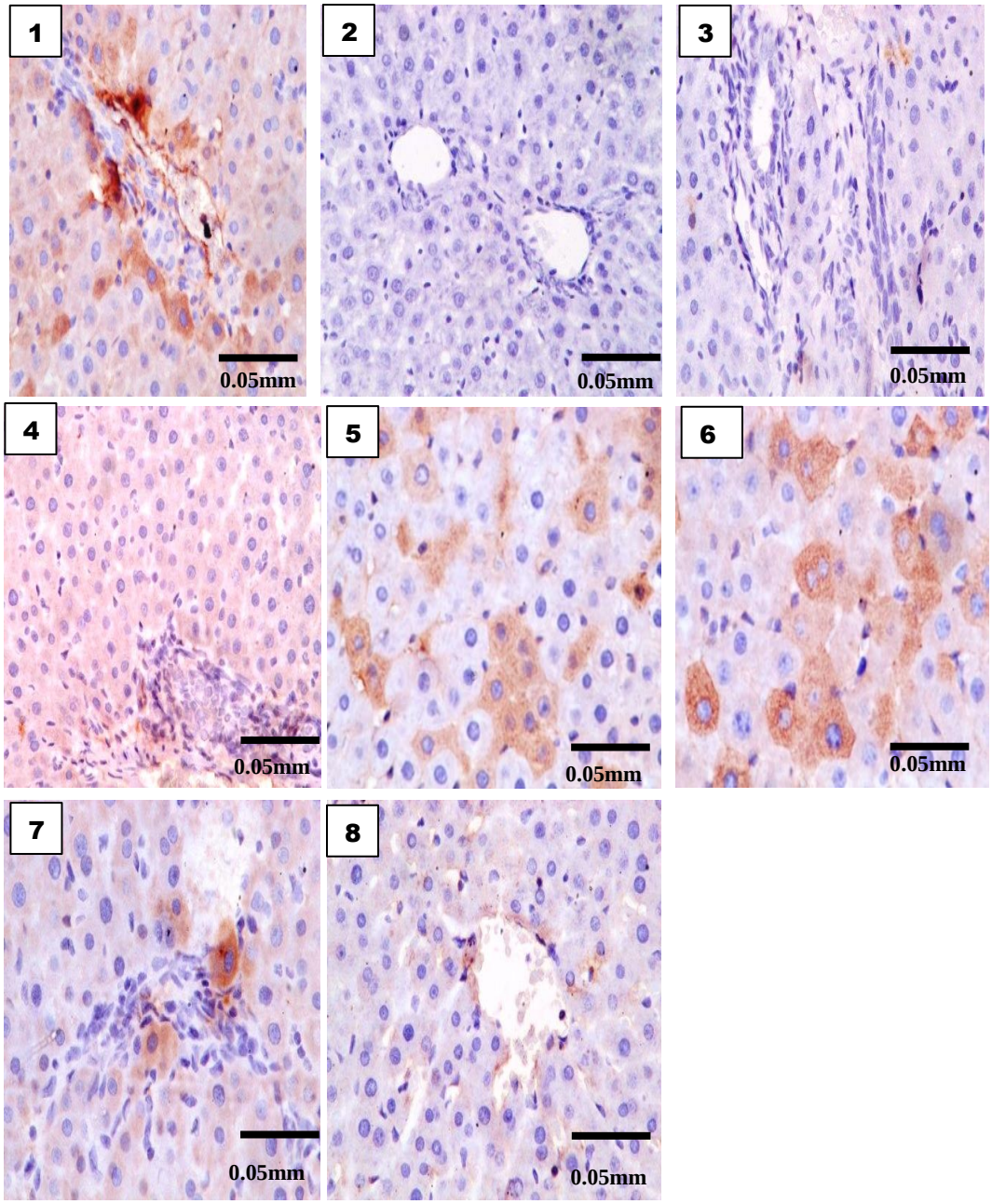

Plate 4.8: Photomicrograph of liver showing the expression of BCL-2 protein.

1: Control. 2:Vitamin E (100 mg/kg). 3: ELVp 100 mg/kg. 4: ELVp 200 mg/kg. 5: SA (2.5 mg/kg). 6: SA +Vit E. 7: SA+ELVp100 mg/kg. 8: SA+ELVp 200 mg/kg.

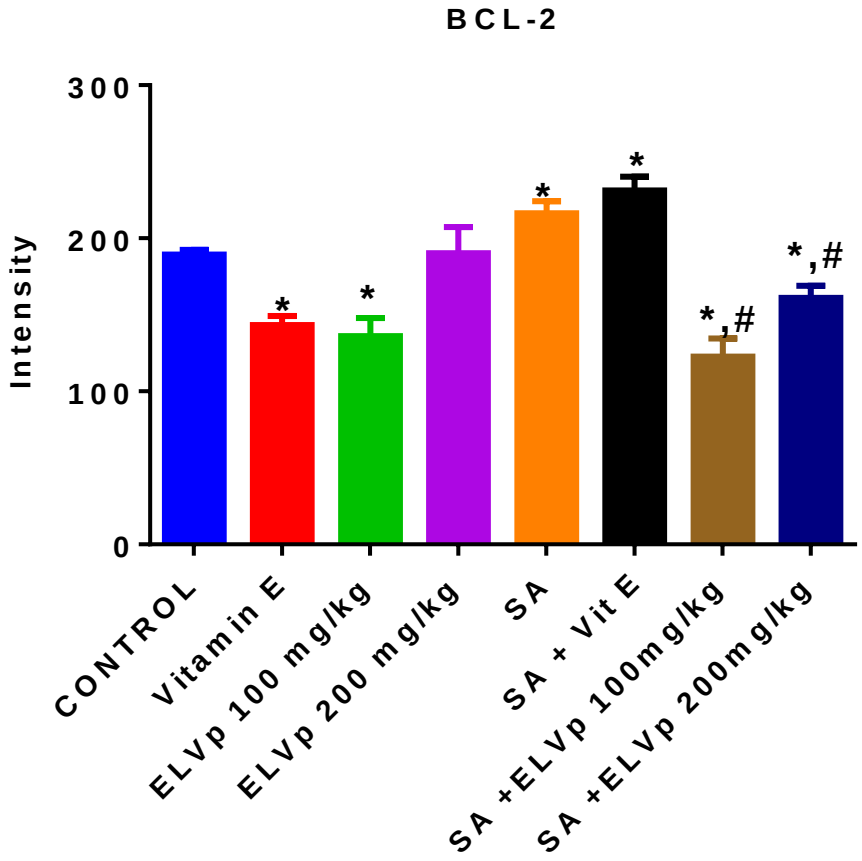

Figure 4.19: Effect of vitamin E, ELVp or SA treatment on BCL-2 expression in liver

Where * represent significant difference in comparison to control and # when compared with sodium arsenite (SA)

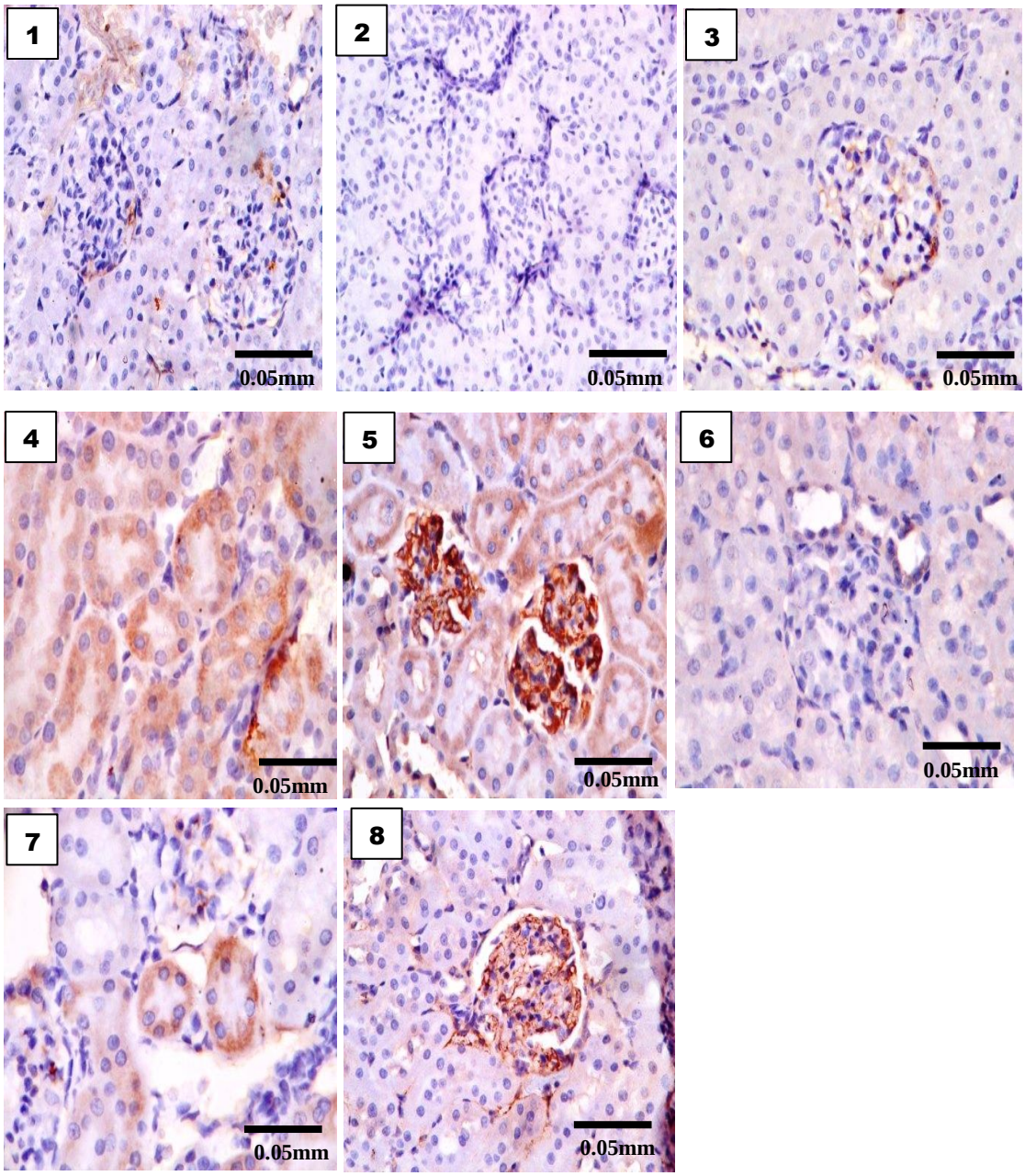

Plate 4.9: Photomicrograph of Kidney showing the expression of BCL-2 protein.

1: Control. 2: Vitamin E (100 mg/kg). 3: ELVp 100 mg/kg. 4: ELVp 200 mg/kg. 5: SA (2.5 mg/kg). 6: SA +Vit E. 7: SA+ELVp100 mg/kg. 8: SA+ELVp 200 mg/kg.

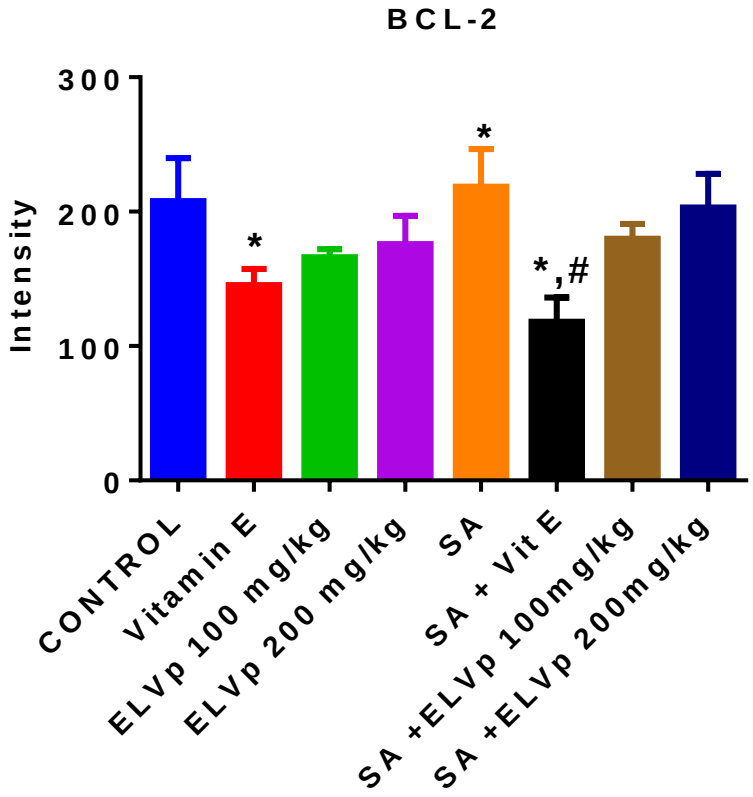

Figure 4.20: Effect of vitamin E, ELVp or SA treatment on BCL-2 expression in kidney

Where * represent significant difference when compared to control and # when compared with sodium arsenite (SA)

4.6 Qualitative phytochemicals, total flavonoid and phenol content of fraction of ELVp

The n-hexane, chloroform, ethyl acetate and ethanol fraction of the hydroethanol extract of V. paradoxa were used in this study. The ethyl acetate fraction had the highest number of phytochemical. While the n-hexane fraction had the lowest number of phytochemical. The phytochemical present in the ethyl acetate fraction include terpenoids, steroids, saponins, tannins, flavonoids, cardiac glycoside, anthraquinones and phenols (Table 4.5)

The total flavonoid and phenol contents of n-hexane, chloroform, ethyl acetate and ethanol fraction are presented in Figure 4.21-4.22.

The total flavonoid content (TFC): The total flavonoid content was not detected for n-hexane fraction. However, it was 1.46 ± 0.01 for chloroform fraction, 9.61 ±0.004 for ethyl acetate fraction and 3.41 ± 0.08 for ethanol fraction. The highest TFC ($p<0.05$) was recorded in ethyl acetate fraction (9.61 ± 0.004) (Fig. 4.21).

Total phenol content (TPC): The TPC was 246.4 ± 7.53 in ethyl acetate fraction and 147.6 ± 4.39 in ethanol fraction. The highest TPC ($p<0.05$) was recorded for ethyl acetate fraction (246.4 ±7.53). While TPC was absent in n-hexane and chloroform fraction (Fig. 4.22).

Table 4.5: The qualitative phytochemical of fractions of hydroethanol leaf extract of *Vitellaria paradoxa*.

PYTOCHEMICALS	N-HEXANE	CHLOROFORM	ETHYL ACETATE	ETHANOL
TERPENOIDS	+	+	+	+
STERIODS	+	++	++	+
SAPONINS	_	_	+	++
TANNINS	_	_	++	+
FLAVONOIDS	_	+	++	++
CARDIAC GLYCOSIDES	_	_	++	_
ANTHRAQUINONE	_	+	+	+
ALKALOIDS	_	+	+	++
PHENOLS	_	_	++	+

Where: - represent not detected, + represent present, ++ represent strongly present

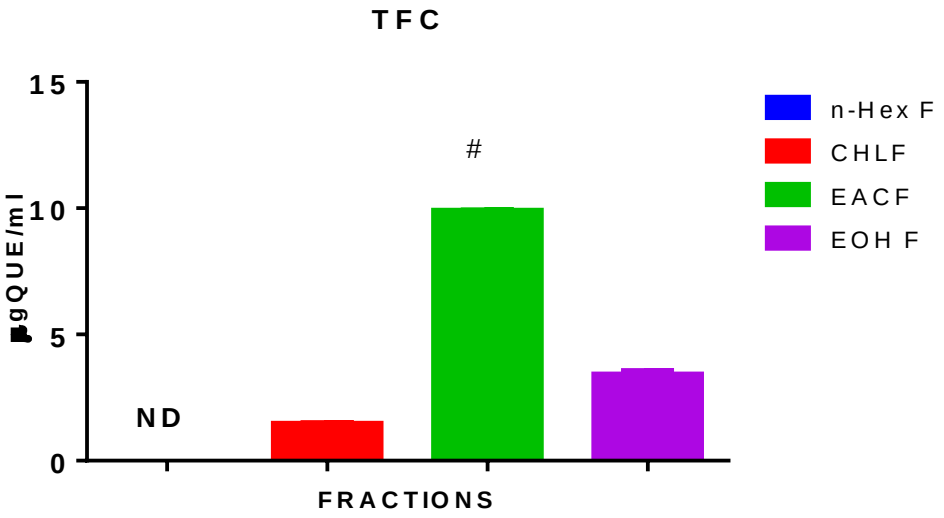

Figure 4.21: Total flavonoid content of the fractions in relation to quercetin.

Where "#" represent EACF significant in comparison to all fractions.

ND represent not detected

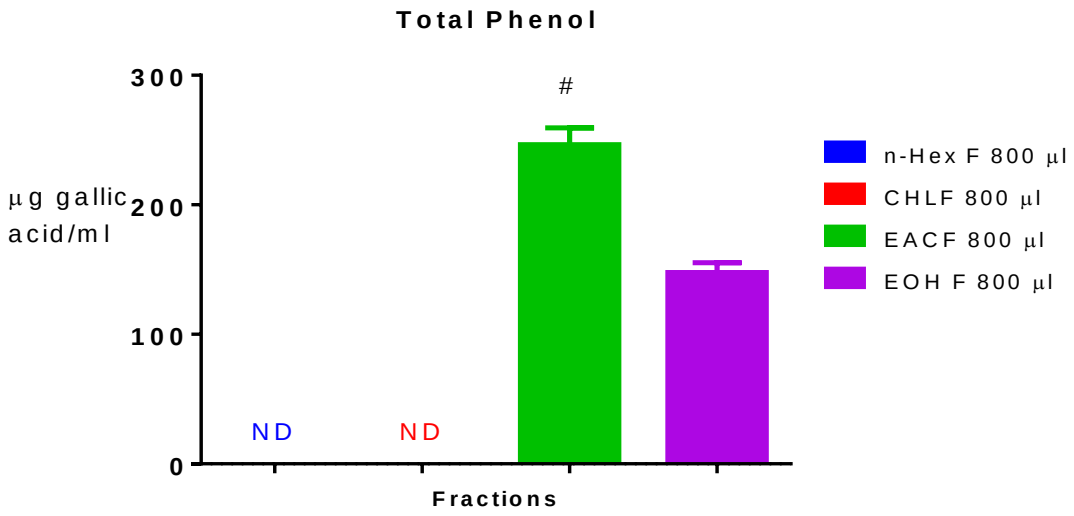

Figure 4.22: Total phenol content of the fractions in relation to gallic acid.

Where "#" represent EACF significant in comparison to all fractions

ND represent not detected

4.6.2 *In vitro* antioxidant content of fractions of ELVp

The reducing power and total scavenging ability of the n-hexane, chloroform, ethyl acetate and ethanol fractions of ELVp are presented in Figure 4.23 -4.24

Reducing power: All four fractions had lower ($p<0.05$) capacity to reduce iron (iii) to (ii) when compared with ascorbic acid the standard at 100 to 800 (µg/ml) (Figure 4.24). Among the fractions, ethyl acetate fraction had the greatest ability to reduce iron (III) across the concentration 200 to 800 µg/ml (Fig. 4.23).

Total antioxidant content (TAC): The TAC of ELVp fractions was 0.531 ± 0.03 µgAAE/mL in n-hexane fraction, 1.833 ± 0.01 µgAAE/mL in chloroform fraction, 3.254 ± 0.02 µgAAE/mL in ethyl acetate fraction and 2.357 ± 0.02 µgAAE/mL in ethanol fraction (Figure 4.25). Significant ($p<0.05$) increase in TAC activity was recorded in ethyl acetate fraction when compared to all other fractions (Fig. 4.24).

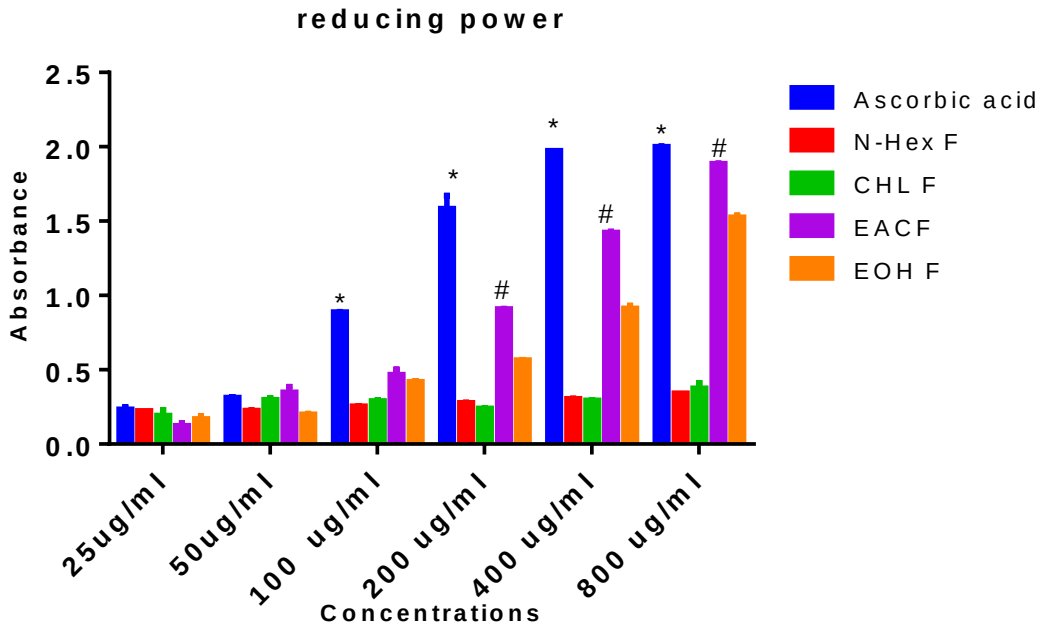

Figure 4. 23: Antioxidant potential of ELVp fractions to reduce iron (iii) to iron (ii). Where "*" represent ascorbic acid significant in comparison to the fractions while "#" represent EACF significant in comparison to all fractions.

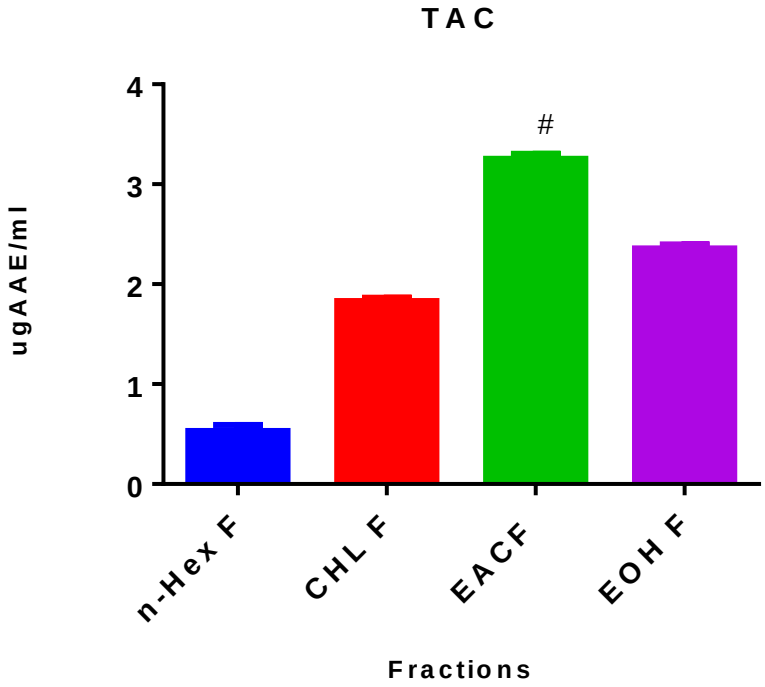

Figure 4. 24: Total antioxidant capacity of the fractions.

Where "*" represent ascorbic acid significant in comparison to the fractions while "#" represent EACF significant in comparison to all fractions.

4.7 Effect of sodium arsenite on survival rate and generation of reactive oxygen species of *Drosophila melanogaster*

4.7.1 Effects of SA on adult survival and offspring emergence of *D. melanogaster*

The survival rate and offspring emergence rate of *D. melanogaster* treated with sodium arsenite are presented in Figure 4.25-4.27.

Survival rate (SR): The survival rate of flies treated with SA (0, 0.0312, 0.0625 and 0.125 mM) at the end of 14 days was 77.67, 63.33, 34.33 and 0 respectively. Significant ($p<0.05$) reduction in fly survival was 100 % for SA (0.125 mM) and 65.7 % for SA (0.0625 mM) when compared to control 22.4 % (Fig. 4.25).

The surival rate of *D. melanogaster* decreased from control values to SA (0.0625 mM and 0.125 mM). Significant ($p<0.05$) reduction in life span upon exposure from control to SA 0.125 mM was 68.3 % (98.00 ± 1.00) to (31.00 ± 13.32) for a five days survival rate (Fig. 4.26).

Offsprings emergence: The rate of offsprings emergence decreased from control value to SA (0.0302 mM, 0.0625 mM and 0.125 mM). Also, offspring emergence showed significant ($p<0.05$) concentration dependent reduction by 41.3 % from control was (25.00 ± 3.48) to SA $_{0.0625\ mM}$ (14.67 ± 1.33) and by 56 % from control (25.00 ± 3.48) to SA $_{0.125\ mM}$ (11.00 ± 1.00) (Fig. 4.27).

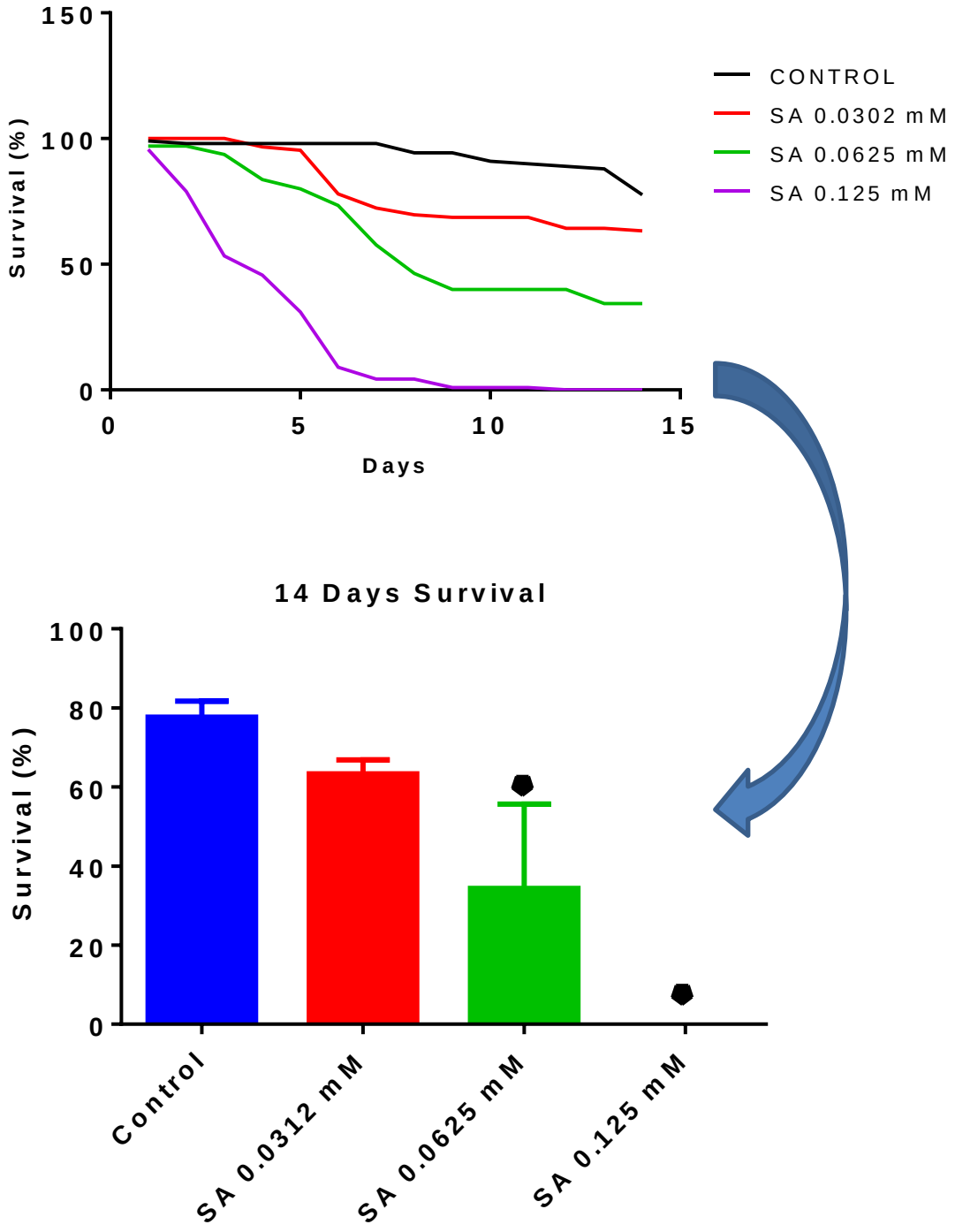

Figure 4.25: Effect of sodium arsenite (SA) on survival of *D. melanogaster* after 14 days.

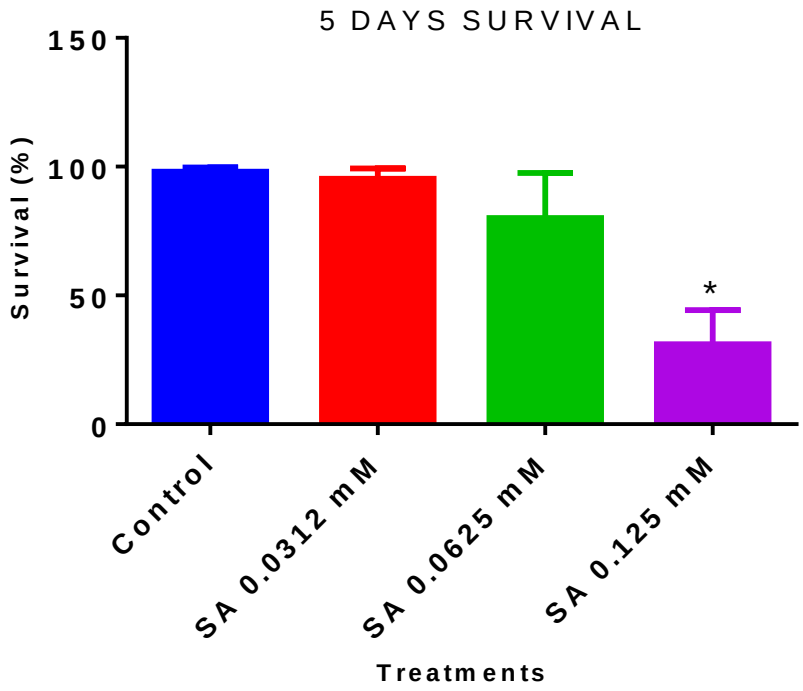

Figure 4.26: Dose effect of sodium arsenite on survival rate of *D. melanogaster*

Where * stand for significant difference in comparison to control.

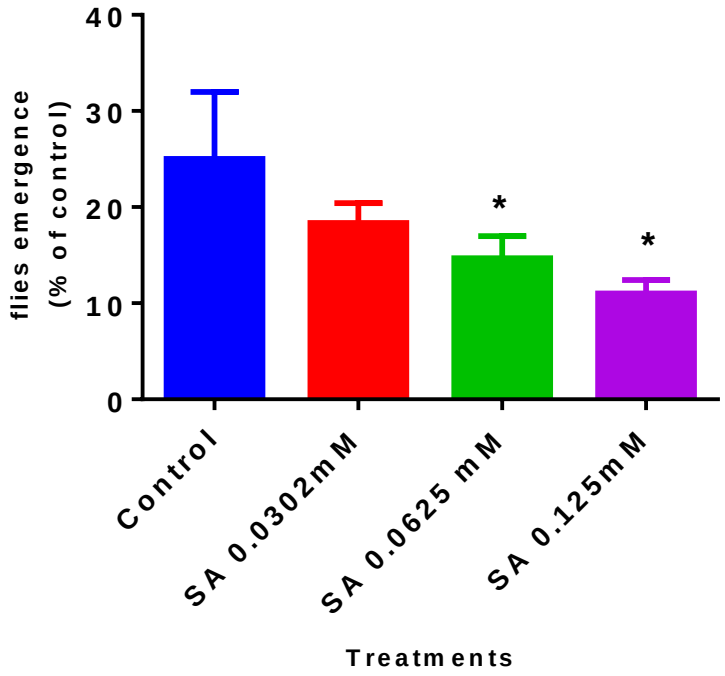

Figure 4. 27: Effect of sodium arsenite on *D. melanogaster* emergence rate

Where * stand for significant difference in comparison to control.

4.7.2 Elevation of NO and H_2O_2 levels by SA in *D. melanogaster*

The hydrogen peroxide (H_2O_2) and nitric oxide (NO) generated are presented in Figure 4.28-4.29.

Hydrogen peroxide (H_2O_2): The hydrogen peroxide levels of flies treated with SA (0.0312, 0.0625 and 0.125 mM) for 5 days increased. H_2O_2 levels showed significant elevation ($p<0.05$) by 11.9 % from control (0.617 ± 0.009) to SA $_{0.0302\ mM}$ (0.691 ± 0.015); 15 % from control (0.617 ± 0.009) to SA $_{0.0625\ mM}$ (0.710 ± 0.014) and 19.2 % from control (0.617 ± 0.009) to SA $_{0.125\ mM}$ (0.736 ± 0.018) (Fig. 4.28).

Nitric oxide (NO): The nitric oxides levels of *D. melanogaster* increased from control values to SA (0.0302 mM and 0.125 mM). Nitric oxide levels showed significant elevation ($p<0.05$) by 17 % from control (1.17 ± 0.03) to SA $_{0.0302\ mM}$ (1.37 ± 0.01) and 9 % from control (1.17 ± 0.03) to SA $_{0.125\ mM}$ (1.28 ± 0.03) for a five days treatment (Fig. 4.29).

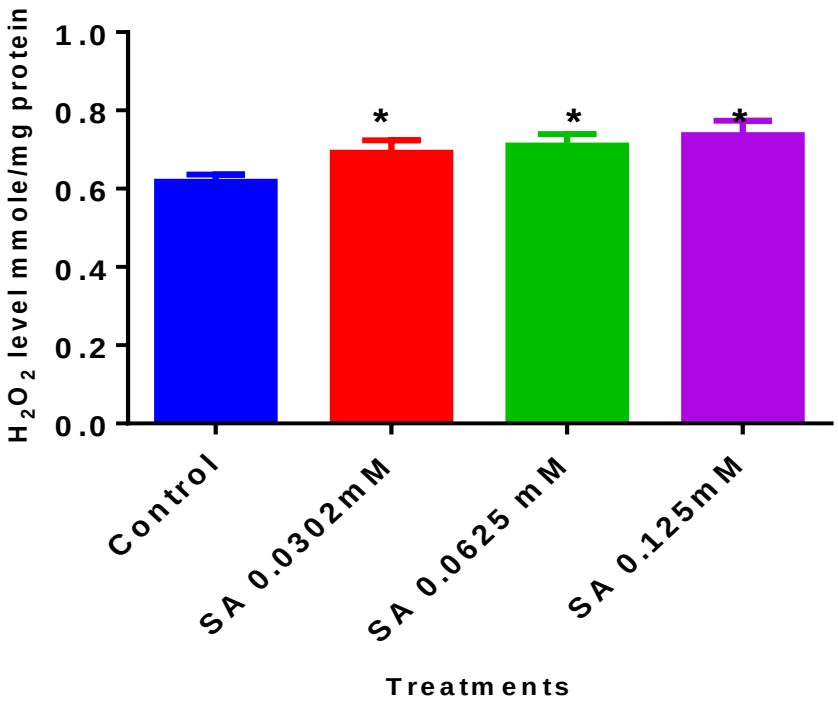

Figure 4.28: Effect of sodium arsenite (SA) on the levels of hydrogen peroxide generation of *D. melanogaster*

Where * stand for significant difference in comparison to control.

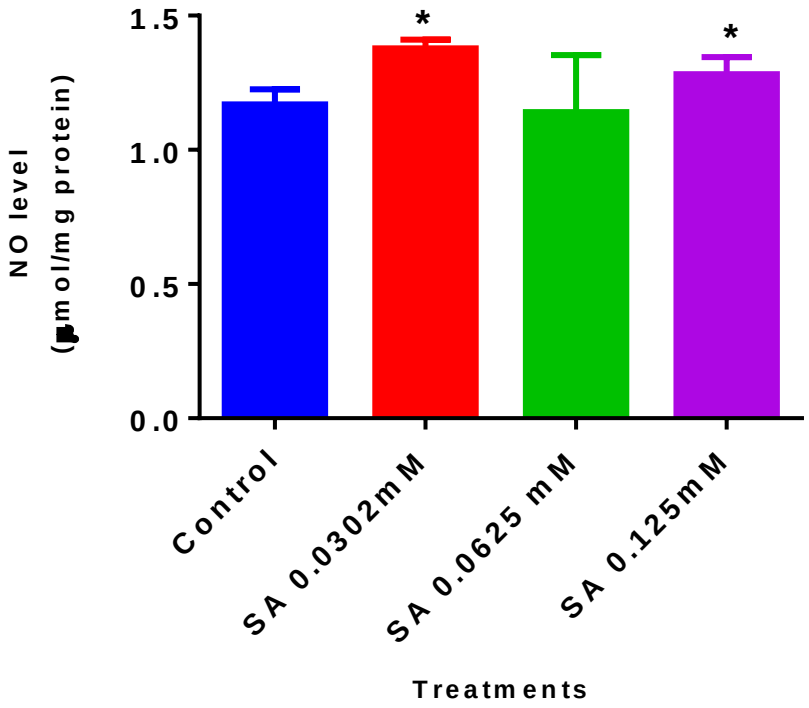

Figure 4.29: Effect of sodium arsenite on the level of nitric oxide generation using *D. melanogaster* model

Where * stand for significant difference in comparison to control.

4.7.3 Inhibition of catalase, GST activities and reduction of total thio and GSH contents by SA in *D. melanogaster*

The catalase, glutathione S-transferase activities, total thio and reduced glutathione levels are presented in Figure 4.30-4.33.

Catalase: The catalase activities of flies treated with SA (0.0312, 0.0625 and 0.125 mM) for 5 days decreased in a dose dependent manner. Catalase activitities showed significant reduction ($p<0.05$) by 30.9 % from control (2871.0 ± 314.1) to SA $_{0.0302\ mM}$ (1982.0 ± 240.6); 63.6 % from control (2871.0 ± 314.1) to SA $_{0.0625\ mM}$ (1044.0 ± 175.0) and 71.5 % from control (2871.0 ± 314.1) to SA $_{0.125\ mM}$ (818.1 ± 98.5) (Fig. 4.30).

Glutathione S- transferase (GST): The GST activities of *D. melanogaster* decreased from control values to SA (0.0302 mM, 0.0625 mM and 0.125 mM). GST activities showed significant reduction ($p<0.05$) by 76.89 % from control (0.554 ± 0.143) to SA $_{0.0625\ mM}$ (0.128 ± 0.031) and by 89.89 % from control (0.554 ± 0.143) to SA $_{0.125\ mM}$ (0.056 ± 0.018) for a five days treatment (Fig. 4.31).

Total thio (T-SH): The total thio levels of *D. melanogaster* decreased from control values to SA (0.0625 mM and 0.125 mM). T-SH levels showed significant reduction ($p<0.05$) by 15.65 % from control (152.70 ± 8.89) to SA $_{0.0625\ mM}$ (128.80 ± 5.40) and by 36.3% from control (152.70 ± 8.89) to SA $_{0.125\ mM}$ (97.22 ± 14.95) for a five days treatment (Fig. 4.32).

Glutathione (GSH): The GSh levels of *D. melanogaster* decreased from control values to SA (0.0302 mM, 0.0625 mM and 0.125 mM). GSH levels showed significant reduction ($p<0.05$) by 68.7 % from control (36.08 ± 1.85) to SA $_{0.0625\ mM}$ (11.29 ± 5.06) and by 71 % from control (36.08 ± 1.85) to SA $_{0.125\ mM}$ (10.46 ± 3.35) for a five days treatment (Fig. 4.33).

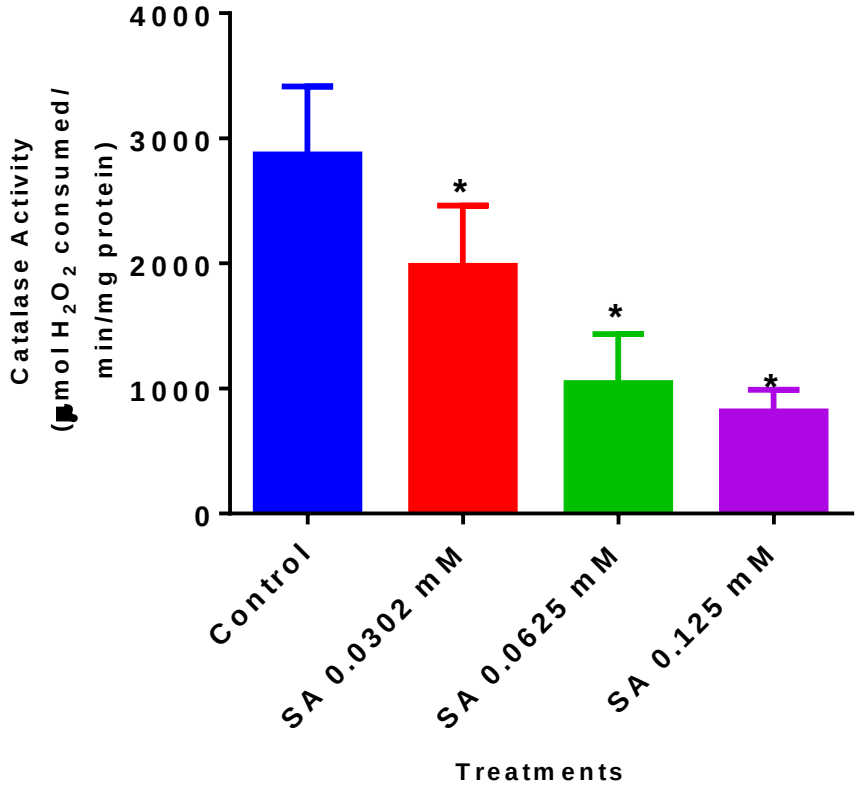

Figure 4.30: Sodium arsenite inhibits catalase activity of *D. melanogaster*.

Where * stand for significant difference in comparison to control.

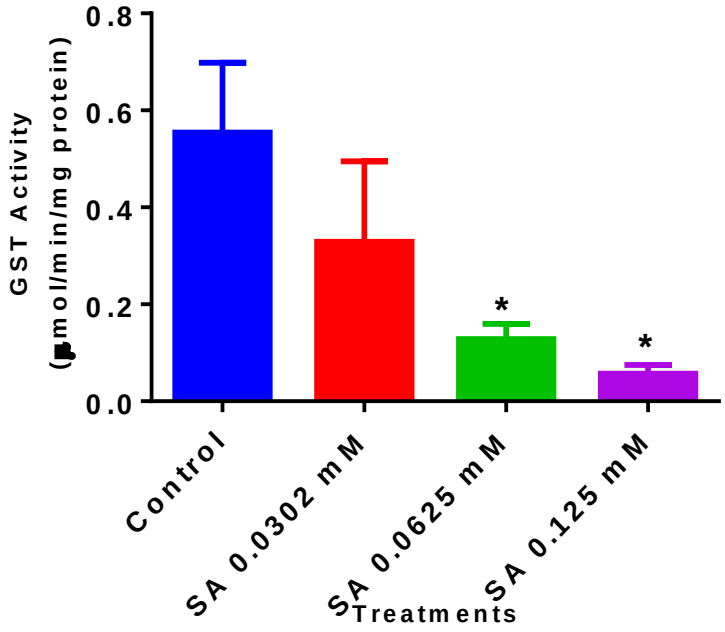

Figure 4.31: Sodium arsenite inhibites glutathione S- transferase (GST) activity in *Drosophila melanogaster* treated for five days.

Where * stand for significant difference in comparison to control.

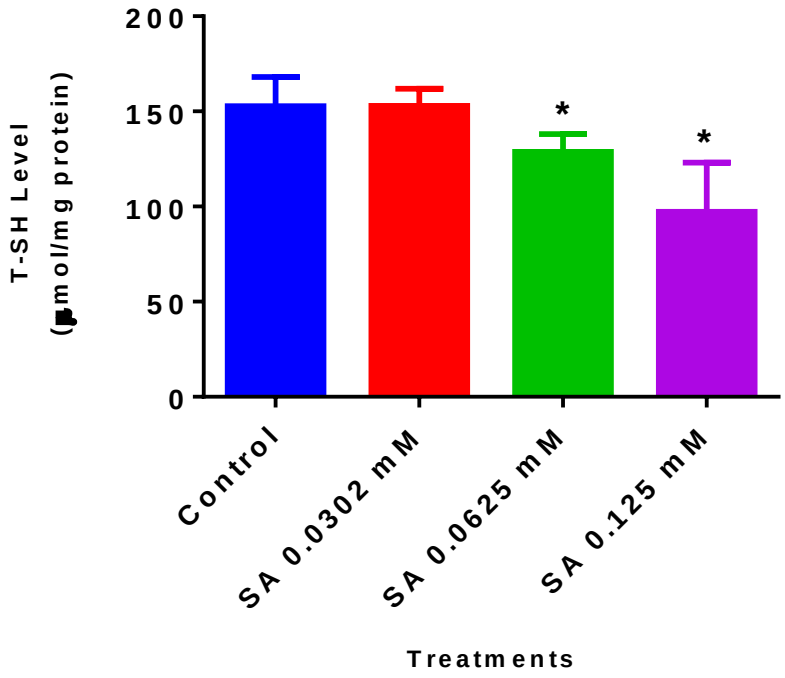

Figure 4.32: Sodium arsenite inhibit the level of total thio level in *D. melanogaster*.

Where * stand for significant difference in comparison to control.

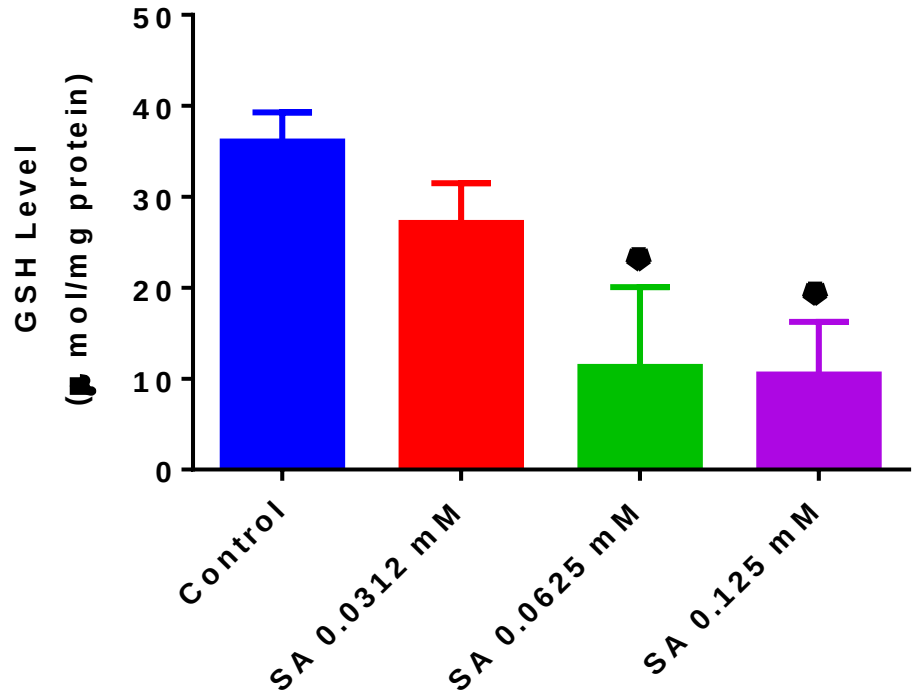

Figure 4.33: Sodium arsenite deplete glutathione content in *D. melanogaster* after treatment for five days

Where * stand for significant difference ($p < 0.05$) when compared to control.

4.7.4 Effect of SA on locomotive performance of *D. melanogaster*

The locomotive performance of the flies are presented in Figure 4.34.

Negative geotaxis: The locomotive performance of flies treated with SA (0.0312 and 0.125 mM) for 5 days decreased. There were no significant differences in the locomotor performance of all sodium arsenite (SA) treatments used when compared to control (Fig. 4.34).

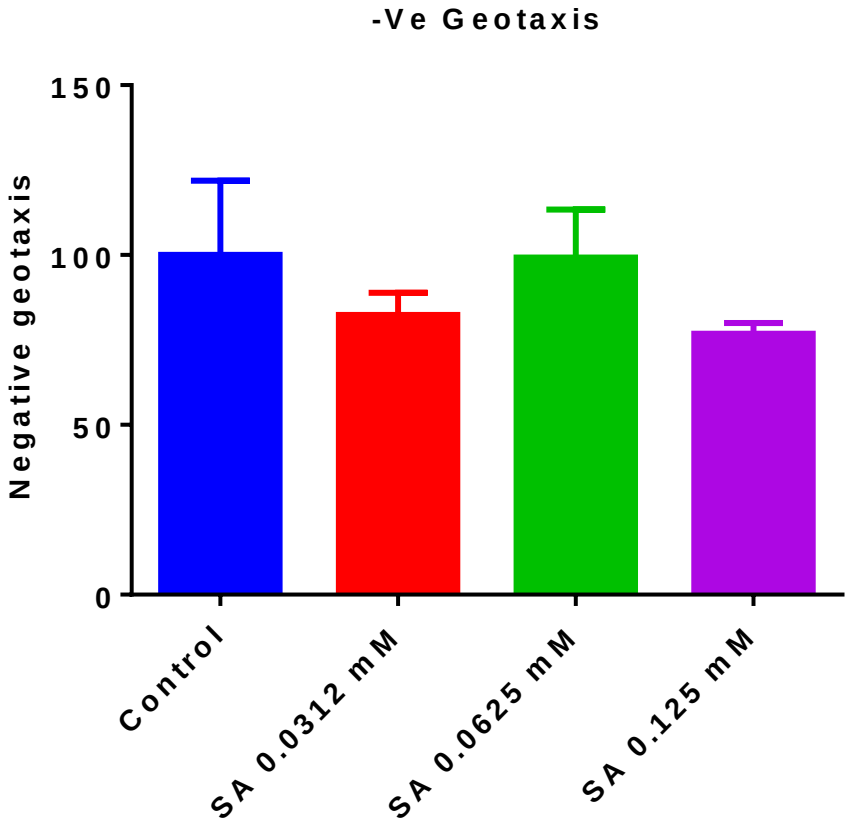

Figure 4. 34: Effect of sodium arsenite on locomotor performance of *D. melanogaster* after five days treatment.

4.8 Effects of fractions of *Vitellaria paradoxa* leaf extract on longevity and generation of reactive oxygen species of *Drosophila melanogaster*

The longevity rate, hydrogen peroxide, nitric oxides generations and total thios levels of *D. melanogaster* treated with various doses of chloroform (CHLF), ethyl acetate (EACF) and ethanol (EOHF) fractions of ELVp are presented in Figure 4.35-4.38.

Longevity: The life span of flies treated with EOHF 1 mg/10 g diet, CHLF 3 mg/10g diet, CHLF 1 mg/ 10 g diet, CHLF 2 mg/10g diet, EOHF 2 mg/10 g diet, EACF 2 mg/10 g diet and EOHF 3 mg/10g diet decreased from control value. The ethyl acetate fraction (EACF) at 3 mg/ 10 g diet prolonged the life span by 20% when compared with control. (Fig. 4.35).

Hydrogen peroxide (H_2O_2): The generation of hydrogen peroxides increased from control values to CHLF 1 mg/10 g/diet, CHLF 2 mg/10 g diet, CHLF 3 mg/10 diet, EACF 2 mg/10 g diet, EOHF 1 mg/10 g diet, EOHF 2 mg/10 g diet and EOHF 3 mg/10g diet. H_2O_2 generation showed significant increased ($p<0.05$) by 8.4 % from control (0.628± 0.015) to CHLF $_{1\ mg/10\ g\ diet}$ (0.681 ± 0.024); 8.1 % from control (0.628 ± 0.015) to EOHF $_{2\ mg/10\ g\ diet}$ (0.679 ± 0.019) and 14.6 % from control (0.628 ± 0.015) to EOHF $_{3\ mg/10\ g\ diet}$ (0.720 ± 0.015) for a five days treatment (Fig. 4.36).

Nitric oxide: The levels of nitric oxide generated decreased from control value to all treatment doses of the fractions. (Fig. 4.37).

Total thiol (T-SH): The levels of total thio increased from control value to CHLF 2 mg/10 g diet, CHLF 3 mg/10 g diet, EACF 1 mg/10 g diet, EACF 2 mg/10 g diet, EACF 3 mg/10 g diet, EOHF 1 mg/10 g diet and EOHF 3 mg/10 g diet. Total thiol levels showed significant increased ($p<0.05$) by 49.5 % from control (9.91 ± 1.37) to CHLF $_{2\ mg/10\ g\ diet}$ (14.82 ± 1.17) and by 38.6 % from control (9.91 ± 1.37) to EACF $_{1\ mg/10\ g\ diet}$ (13.74 ± 1.32) (Fig. 4.38).

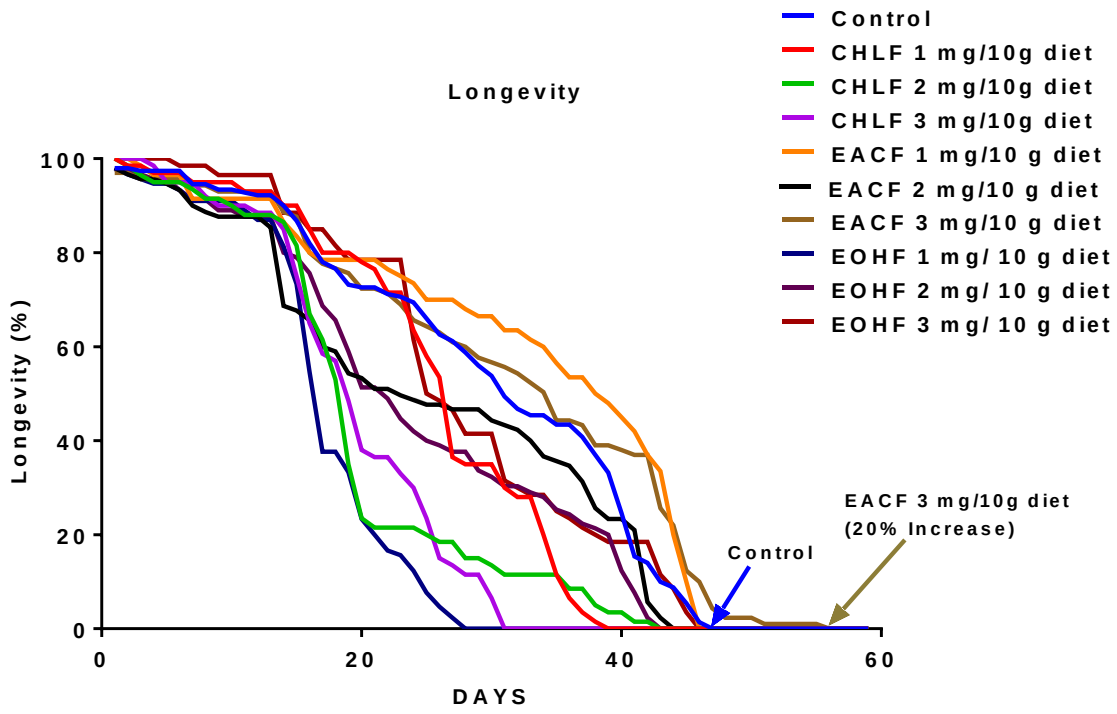

Figure 4.35: Longevity of *Drosophila melanogaster* treated with three concentration of *Vitellaria paradoxa* leaf fractions.

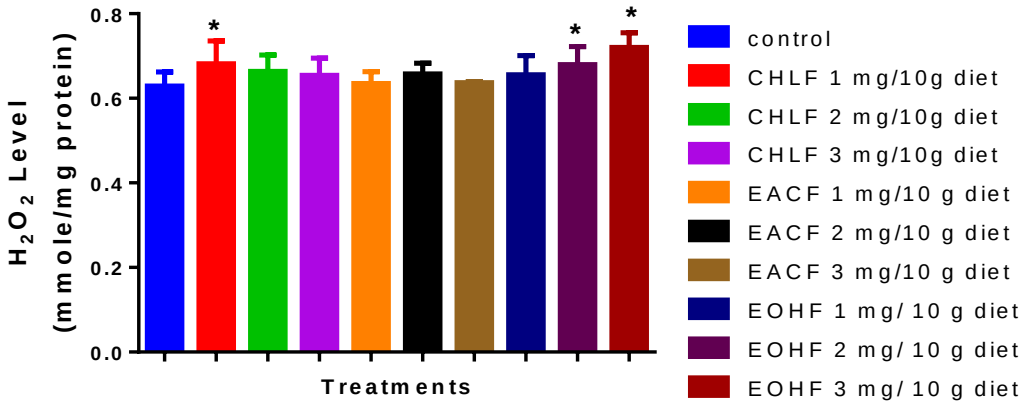

Figure 4.36: Hydrogen peroxide level of *D. melanogaste*r treated with *Vitellaria paradoxa* fractions for five days.

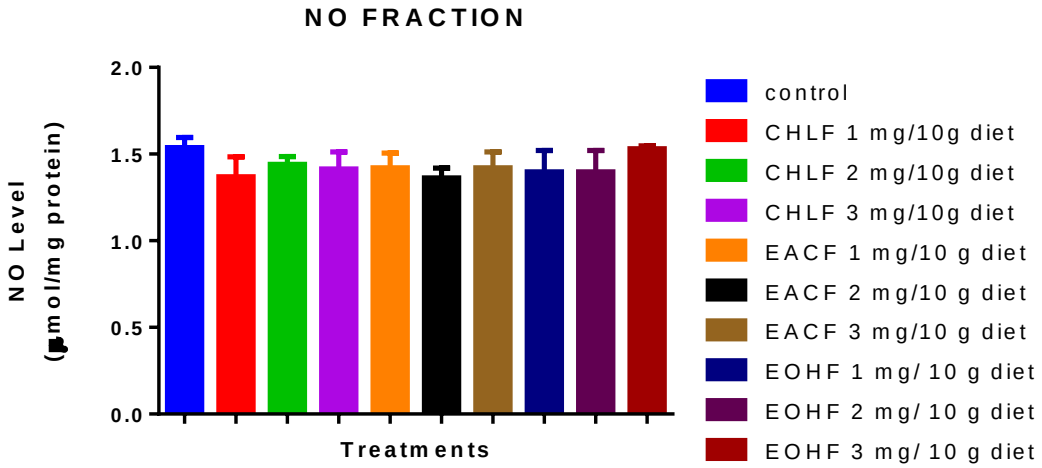

Figure 4.37: Nitric oxide level of *D. melanogaster* treated with *Vitellaria paradoxa* fractions for five days.

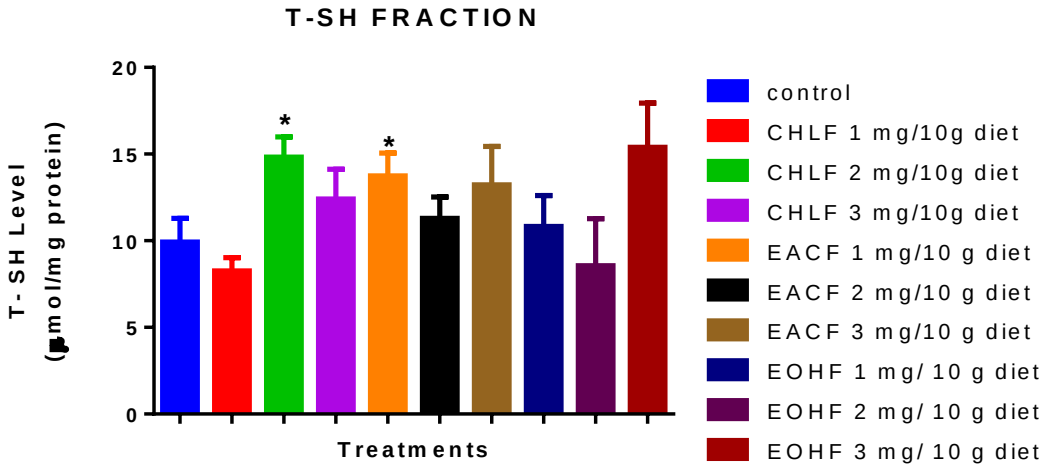

Figure 4.38: Effect of *Vitellaria paradoxa* fraction on *D. melanogaster* total thio content after five days treatment.

Where * stand for significant difference when compared to control

.

4.9 The cytoremediative potentials of ethyl acetate fraction of *Vitellaria paradoxa* leaf extract on sodium arsenite –induced toxicity in *Drosophila melanogaster*.

4.9.1 EACF reduced the elevation of H_2O_2 and NO levels indued by SA in *D. melanogaster*

The hydrogen peroxide (H_2O_2) and nitric oxide (NO) generated upon ethyl acetate (EACF) treatment of sodium arsenite (SA) induced toxicity in *D. melanogaster* are presented in Figure 4.39-4.40.

Hydrogen peroxide (H_2O_2): The mean hydrogen peroxide levels decreased from control value to EACF (1 and 3 mg/10 g diet). Also, mean H2O2 levels increased from control value to SA (0.0625 mM).

Hydrogen peroxide levels showed significant reduction ($p<0.05$) by from control (0.729± 0.023) to EACF $_{1\ mg/10g\ diet}$ (0.689 ± 0.007). While significant elevation ($p<0.5$) by 15.7 % from control (0.729 ± 0.023) to SA $_{0.0625\ mM}$ (0.844 ± 0.029). However, showed significant reduction ($p<0.5$) by 18.6 % from SA $_{0.0625\ mM}$ (0.844 ± 0.029) to SA+EACF $_{1\ mg/10\ g\ diet}$ (0.687 ± 0.021) (Fig. 4.39).

Nitric oxide (NO): The mean nitric oxide (NO) levels decreased from control value to EACF (1 and 3 mg/10 g diet). Also, mean nitric oxide levels increased from control value to SA (0.0625 mM).

Nitric oxide (NO) levels showed significant reduction ($p<0.05$) by 51.4 % from control (0.937 ± 0.017) to EACF $_{1\ mg/10g\ diet}$ (0.455 ± 0.072) and by 53.57 % from control (0.937 ± 0.017) to EACF $_{3\ mg/10g\ diet}$ (0.435 ± 0.090). While showed significant elevation by 26.36 % from control (0.937 ± 0.017) to SA $_{0.0625\ mM}$ (1.184 ± 0.022). However, showed significant reduction ($p<0.05$) by 13.26 % from SA $_{0.0625\ mM}$ (1.184 ± 0.022) to SA+EACF $_{1\ mg/10\ g\ diet}$ (1.027 ± 0.047) and by 23.7 % from SA $_{0.0625\ mM}$ (1.184 ± 0.022) to SA+EACF $_{3\ mg/10g\ diet}$ (0.903 ± 0.017) (Fig. 4.40).

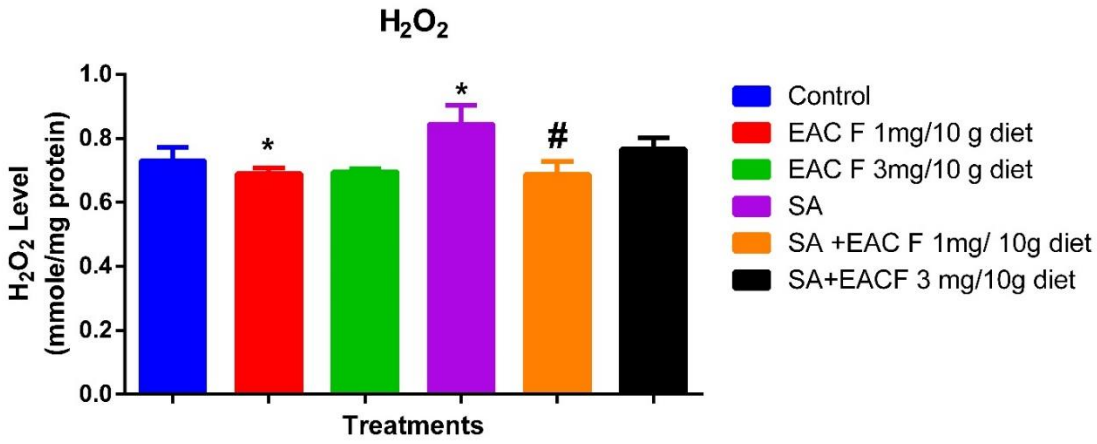

Figure 4.39: Effect of ethyl acetate fraction on sodium arsenite induced hydrogen peroxide elevation in *D. melanogaster*.

Where * represent significant difference ($p < 0.05$) when compared to control and # significant difference ($p < 0.05$) when compared to SA alone.

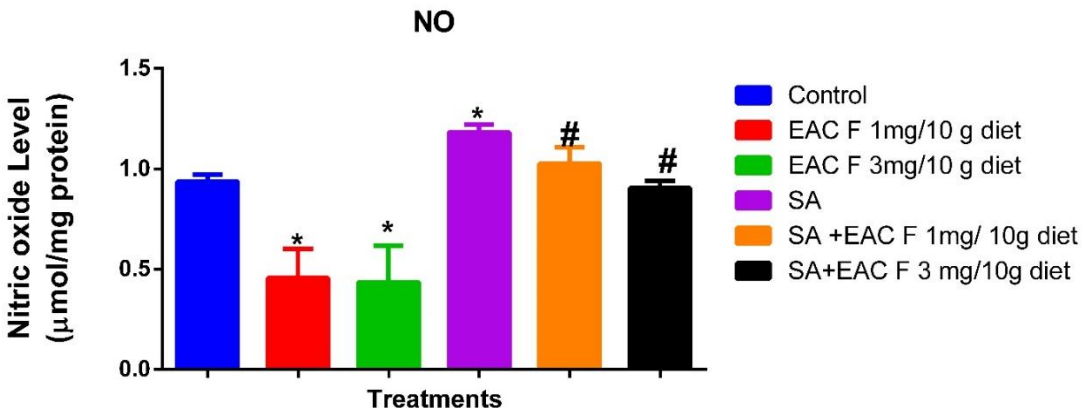

Figure 4.40: Ethyl acetate fraction of ELVp protected against sodium arsenite – induced elevation of nitric oxide in *D. melanogaster*.

Where * represent significant difference ($p < 0.05$) when compared to control and # significant difference ($p < 0.05$) when compared to SA alone.

4.9.2 EACF elevated SA-induced reduction of total thiol and GSH levels in *D. melanogaster*

The total thiol (T-SH) and glutathione (GSH) levels of ethyl acetate (EACF) treatment of sodium arsenite (SA) induced toxicity in *D. melanogaster* are presented in Figure 4.41-4.42.

Total thio (T-SH): The mean total thio levels increased from control value to EACF (1 and 3 mg/10 g diet). Also, mean total thio levels decreased from control value to EACF (3 mg/10 g diet) and SA (0.0625 mM).

Total thiol levels showed significant elevation ($p<0.05$) by 16.2 % from control (116.6 ± 6.61) to EACF $_{1\ mg/10g\ diet}$ (135.5 ± 4.10). While showed significant reduction ($p<0.05$) by 21.86 % from control (116.6 ± 6.61) to EACF $_{3\ mg/10\ g\ diet}$ (91.1 ± 3.98) and 39.3 % from control (116.6 ± 6.61) to SA $_{0.0625\ mM}$ (70.7 ± 0.70). However, showed significant elevation ($p<0.05$) by 47.2 % from SA $_{0.0625\ mM}$ (70.7 ± 0.70) to SA+EACF $_{1\ mg/10\ g\ diet}$ (104.1 ± 9.13) and 87.5 % from SA $_{0.0625\ mM}$ (70.7 ± 0.70) to SA+EACF $_{3\ mg/10\ g\ diet}$ (132.6 ± 3.97) (Fig. 4.41).

Reduced glutathione (GSH): The mean reduced glutathione (GSH) levels increased from control value to EACF (1 and 3 mg/10 g diet). Also, mean GSH levels decreased from control value to SA (0.0625 mM).

Reduced glutathione (GSH) levels showed significant reduction ($p<0.05$) by 83.8 % from control (1394.00 ± 99.39) to SA $_{0.0625\ mM}$ (225.40 ± 33.52). However, showed significant elevation ($p<0.05$) by 378 % from SA $_{0.0625\ mM}$ (225.40 ± 33.52) to SA+EACF $_{1\ mg/10\ g\ diet}$ (1078.00 ± 164.80) and 253.8 % from SA $_{0.0625\ mM}$ (225.40 ± 33.52) to SA+EACF $_{3\ mg/10g\ diet}$ (797.60 ± 90.08) (Fig. 4.42).

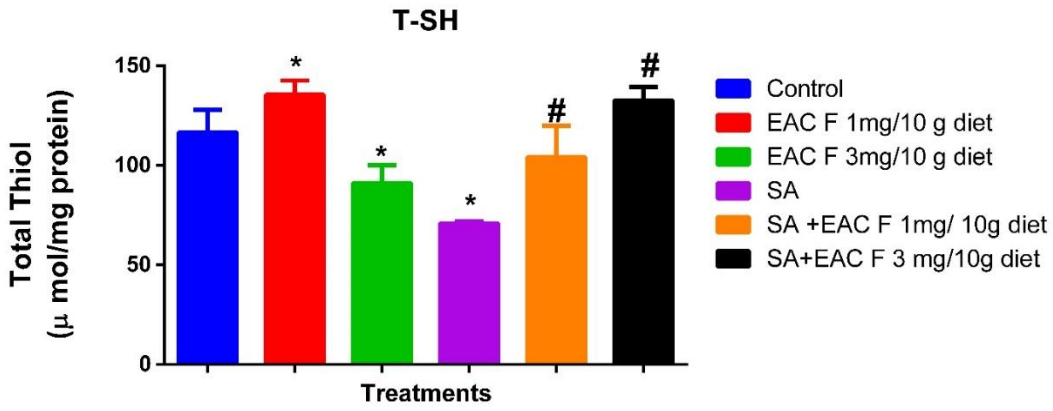

Figure 4.41: Effect of ethyl acetate fraction of *V. paradoxa* leaf on sodium arsenite induced reduction in total thio content.

Where * represent significant difference ($p < 0.05$) when compared to control and # significant difference ($p < 0.05$) when compared to SA alone.

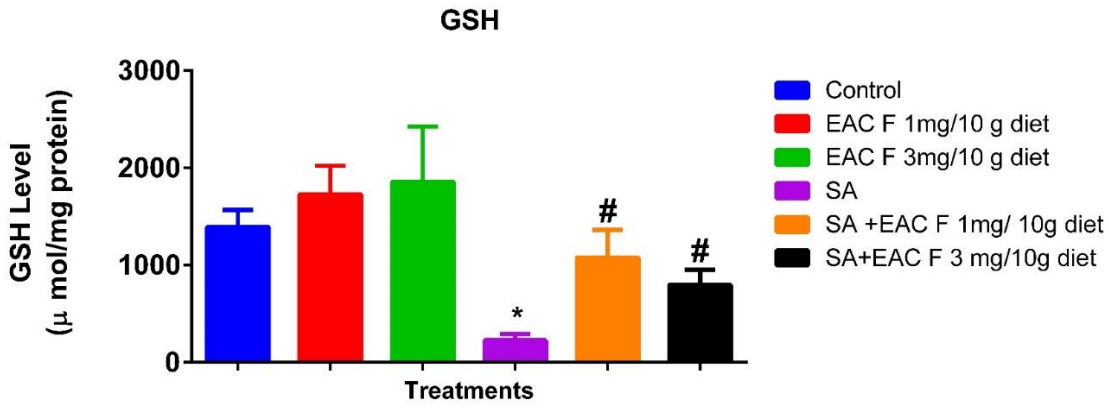

Figure 4.42: Effect of ethyl acecate fraction of *V. paradoxa* on sodium arsenite-induced reduction in reduced glutathione content.

Where * represent significant difference ($p < 0.05$) when compared to control and # significant difference ($p < 0.05$) when compared to SA alone.

4.9.3 EACF elevated SA-induced reduction of catalase and GST activities in *D. melanogaster*

The effects of EACF on SA-induced reduction of catalase and GST activities are presented in figure 4.43-4.44.

Catalase: The mean catalase activities increased from control value to EACF (3 mg/10 g diet). Also, mean catalase activities decreased from control value to SA (0.0625 mM).

Catalase activities showed significant reduction ($p<0.05$) by 44.14 % from control (4388.0 ± 395.2) to SA $_{0.0625\ mM}$ (2451.0 ± 518.4). However, showed significant elevation ($p<0.05$) by 57.8 % from SA $_{0.0625\ mM}$ (2451.0 ± 518.4) to SA+EACF $_{1\ mg/10\ g\ diet}$ (3868.0 ± 351.7) (Fig. 4.43).

Glutathione-S-transferase (GST): The mean glutathione-S-transferase (GST) activities increased from control value to EACF (3 mg/10 g diet). Also, mean GST activities decreased from control value to SA (0.0625 mM).

Glutathione-S-transferase (GST) activities showed significant reduction ($p<0.05$) by 70.4 % from control (1.403 ± 0.210) to SA $_{0.0625\ mM}$ (0.415 ± 0.081). However, showed significant elevation ($p<0.05$) by 156.3 % from SA $_{0.0625\ mM}$ (0.415 ± 0.081) to SA+EACF $_{1\ mg/10\ g\ diet}$ (1.064 ± 0.035) and 242.6 % from SA $_{0.0625\ mM}$ (0.415 ± 0.081) to SA+EACF $_{3\ mg/10g\ diet}$ (1.422 ± 0.103) (Fig. 4.44).

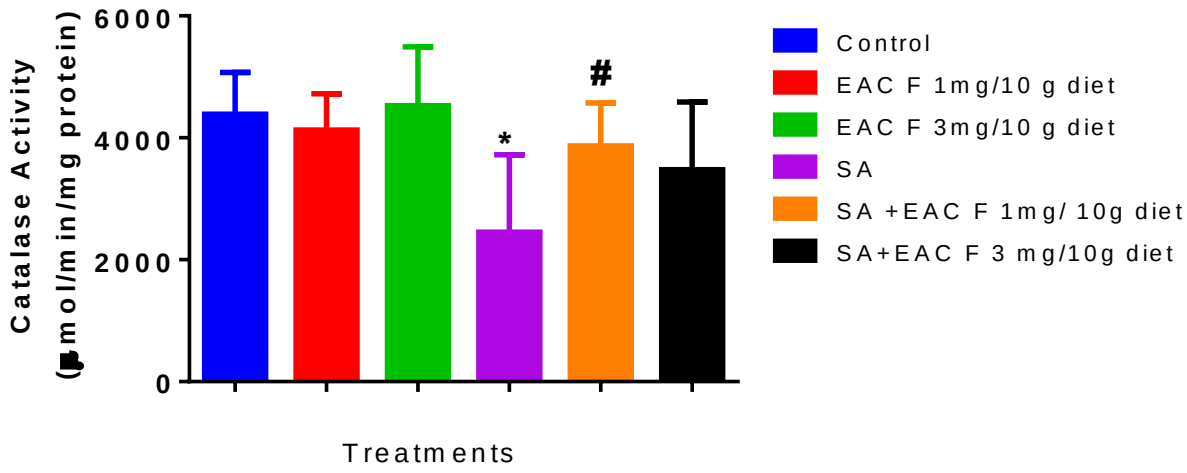

Figure 4.43: Effect of ethyl acetate fraction of *Vitellaria paradoxa* leaf on sodium arsenite reduced catalase activity in *D. melanogaster*.

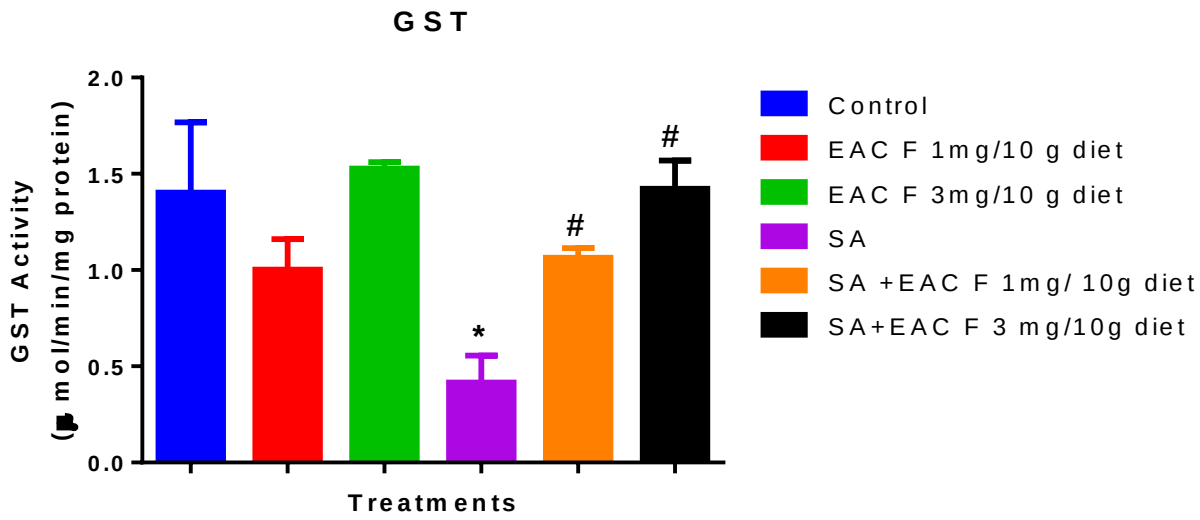

Figure 4.44: Ethyl acetate fraction of ELVp improves sodium arsenite- induced reduction in GST activity.

Where * represent significant difference ($p < 0.05$) when compared to control and # significant difference ($p < 0.05$) when compared to SA alone.

4.9.4 Effects of EACF and SA on offspring emergence, locomotive and acetylcholinesterase activities in *D. melanogaster*

The effects of EACF and SA in offspring emergence, locomotive performance and acetylcholinesterase activity are presented in Figure 4.45-4.47.

Offspring emergence: The mean offsprings emergence increased from control value to EACF (1 mg/10 g diet). Also, mean offsprings emergence decreased from control value to SA (0.0625 mM). However, co-administration of SA with EACF at (1 and 3 mg/10 g diet) increased the offspring emergence relative to SA (0.0625 mM).

Offsprings emergence showed significant reduction ($p<0.05$) by 70.2 % from control (92.95 ± 33.35) to SA $_{0.0625\ mM}$ (27.64 ± 12.47). However, showed significant elevation ($p<0.05$) by 178.2 % from SA (27.64 ± 12.47) to SA+EACF $_{3\ mg/10\ g\ diet}$ (76.92 ± 12.10) (Fig. 4.45).

Negative geotaxis: The mean locomotive performance increased from control value to EACF (1 and 3 mg/10 g diet). Also, mean locomotive performance increased from SA (0.0625mM) value to SA + EACF (3 mg/10 g diet).

Locomotive performance showed significant increased ($p<0.05$) by 25.7 % from control (103.20 ± 1.47) to EACF $_{1\ mg/10\ g\ diet}$ (129.80 ± 2.95) and 12.59% from control (103.20± 1.47) to EACF $_{3\ mg/10\ g\ diet}$ (116.20 ± 2.78). While there was no significant differences in values recorded for control and SA (0.0625 mM). However, showed significant elevation ($p<0.05$) by 20.5 % from SA $_{0.0625\ mM}$ (100.30 ± 2.95) to SA+EACF $_{3\ mg/10\ g\ diet}$ (120.90 ± 7.80) (Fig. 4.46).

Acetylcholinesterase activity: The mean acetylcholinesterase activities increased from control value to EACF (1 mg/10 g diet). Also, mean acetylcholinesterase activities decreased from control value to SA (0.0625 mM).

Acetylcholinesterase activities showed significant increased ($p<0.05$) in by 131.6 % from control (9.94 ± 0.59) to EACF $_{1\ mg/10\ g\ diet}$ (23.03 ± 0.89) and there was no significant differences in values recorded from control to EACF (3 mg/10 g diet). Also, showed significant reduction ($p<0.05$) by 60.3 % form control (9.94 ± 0.59) to SA $_{0.0625\ mM}$ (3.94 ± 1.73). However, showed significant elevation ($p<0.05$) by 377.6 % from SA $_{0.0625\ mM}$ (3.94 ± 1.73) to SA+EACF $_{1\ mg/10\ g\ diet}$ (18.82 ± 1.21) (Fig. 4.47).

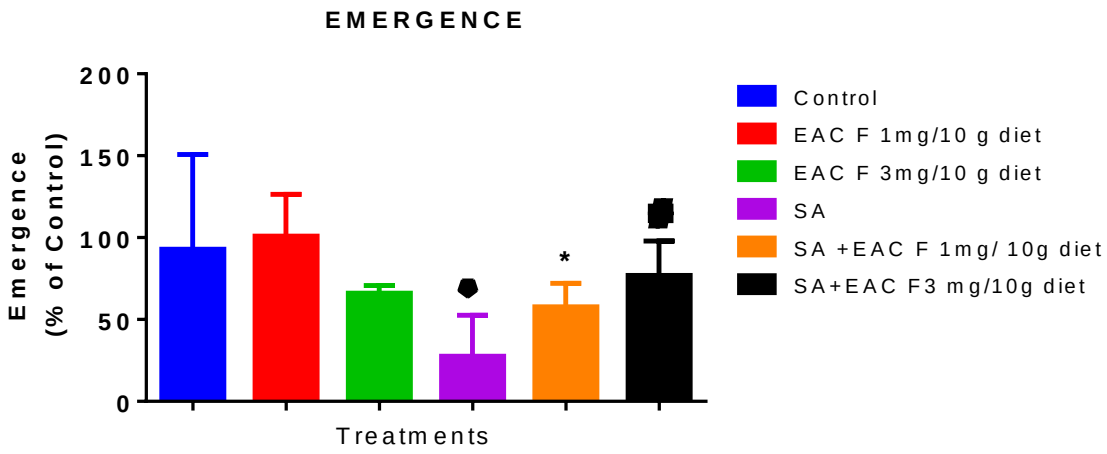

Figure 4.45: Percentage of offsprings emergence from treated flies with sodium arsenite and ethyl acetate fraction of *V. paradoxa* leaf extract.

Where * represent significant difference ($p < 0.05$) when compared to control and # significant difference ($p < 0.05$) when compared to SA alone.

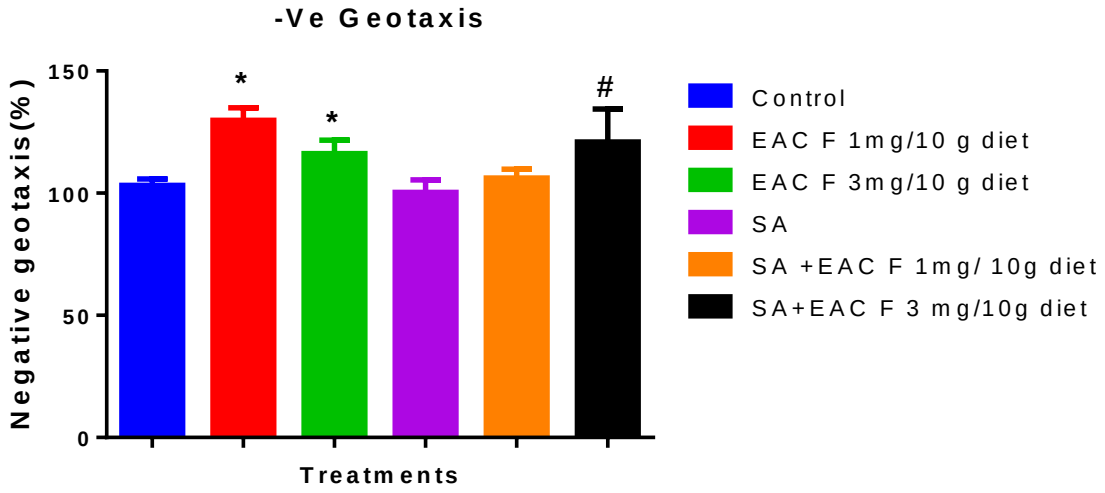

Figure 4.46: Negative geotaxis of *D. melanogaster* treated with sodium arsenite and ethyl acetate fraction of *V. paradoxa* leaf extract

Where * represent significant difference ($p < 0.05$) when compared to control and # significant difference ($p < 0.05$) when compared to SA alone.

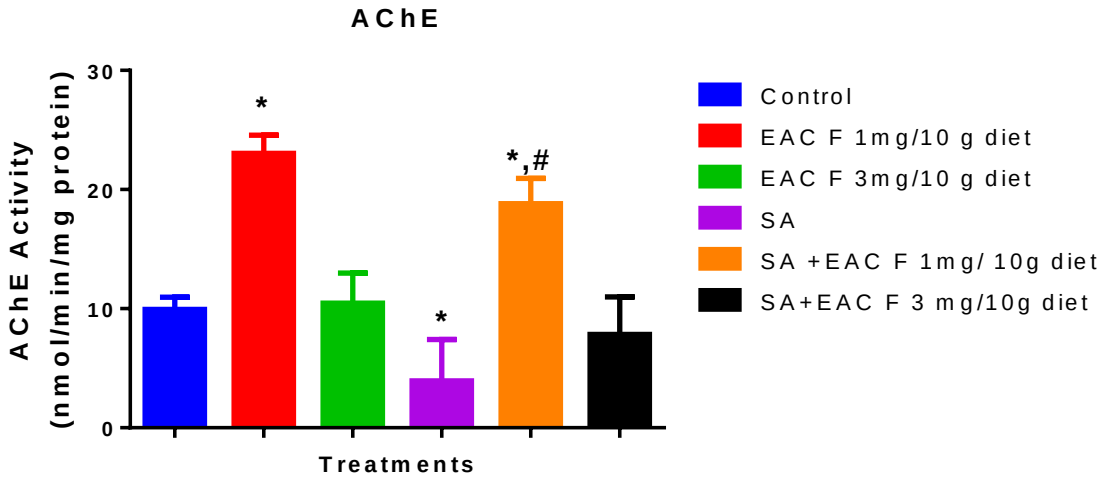

Figure 4.47: Effect of ethyl acetate fraction of *V. paradoxa* leaf on the activity of acetyl cholinesterase activity on *D. melanogaster* induced with sodium arsenite

Where * represent significant difference ($p < 0.05$) when compared to control and # significant difference ($p < 0.05$) when compared to SA alone.

4.9.5 Histological analysis of fat body cells of *D. melanogaster*

The histological examination of the treated D. melanogaster fat bodies showed normal fat bodies for control, normal fat bodies for EACF (1 mg/10 g diet), normal fat bodies for EACF (3 mg/10 g diet), atrophy of most region, degeneration and few layers of cells for SA (0.0625 mM), normal fat bodies for SA+EACF (1 mg/ 10g diet) and normal fat bodies for SA+EACF (3 mg/ 10 g diet) (Plate 4.10).

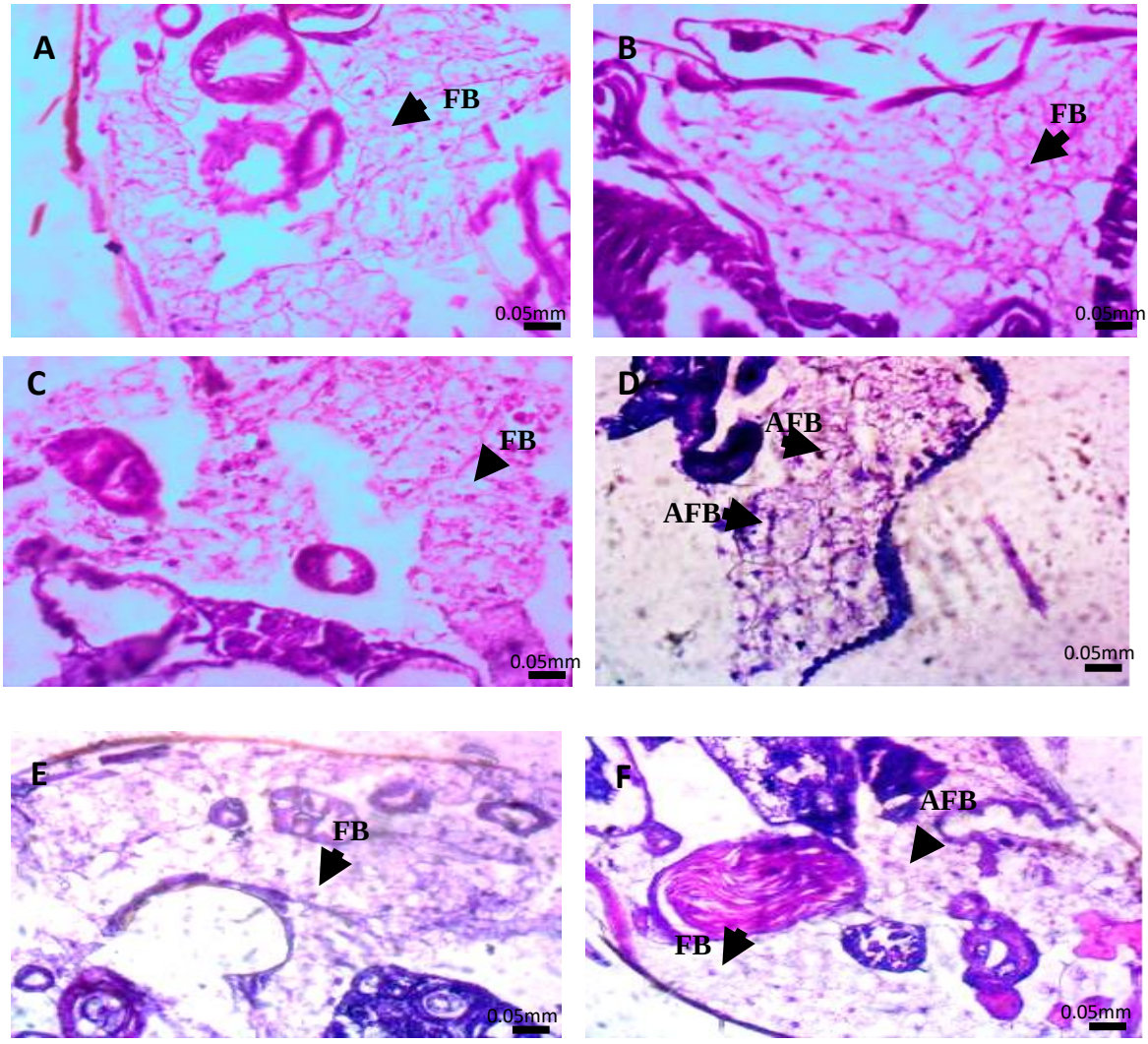

Plate 10: Pictomicrograph of *D. melanogaster* fat bodies following exposure to sodium arsenite and ethyl acetate fraction of *V. paradoxa* leaf extract.

A: Normal flies treated with 2% ethanol displayed normal fat bodies (FB). B: Flies treated with EACf (1/10 g diet) displayed norm EACf 1l f EACf 1t bodies (FB). C: Flies treated with EACf (3 mg/10 g diet) displayed normal fat bodies (FB). D: flies treated with SA (0.0625 mM) displayed atrophic fat bodies (AFB). E: Flies treated with SA+ EACf (1 mg/10 g diet) displayed normal fat bodies (FB). F: Flies treated with SA + EACf (3 mg /10 g diet) displayed sparing atrophic fat bodies (AFB) and normal fat bodies (FB) ×400.

4.10 Evaluation of cytotoxicity of fractions of *Vitellaria paradoxa* on three cancer cell line

4.10.1 Effect of fractions of ELVp on cytotoxicity of MCF-7 cells

The fractions were subjected to cytotoxity assessment and the results presented in Figure 4.48-4.50.

The MTT assay performed for 24hrs, 48 hrs and 72 hrs showed different cytotoxic effect of chloroform and ethyl acetate fractions (Figure 4.48-4.50). For the MCF-7 cells, the polar ethanol fraction at all doses and time duration, did not show effect on cell viability (Figure 4.48-4.50). While the chloroform or ethyl acetate fraction at 250, 500 and 1000 µg/mL exhibited a significant ($p<0.05$) reduction in the number of viable cells. In addition, an inverse relationship with MCF-7 cells viability decreasing with increase in concentration and period of exposure to the ethyl actate fraction compared with control (Fig. 4.48-4.50).

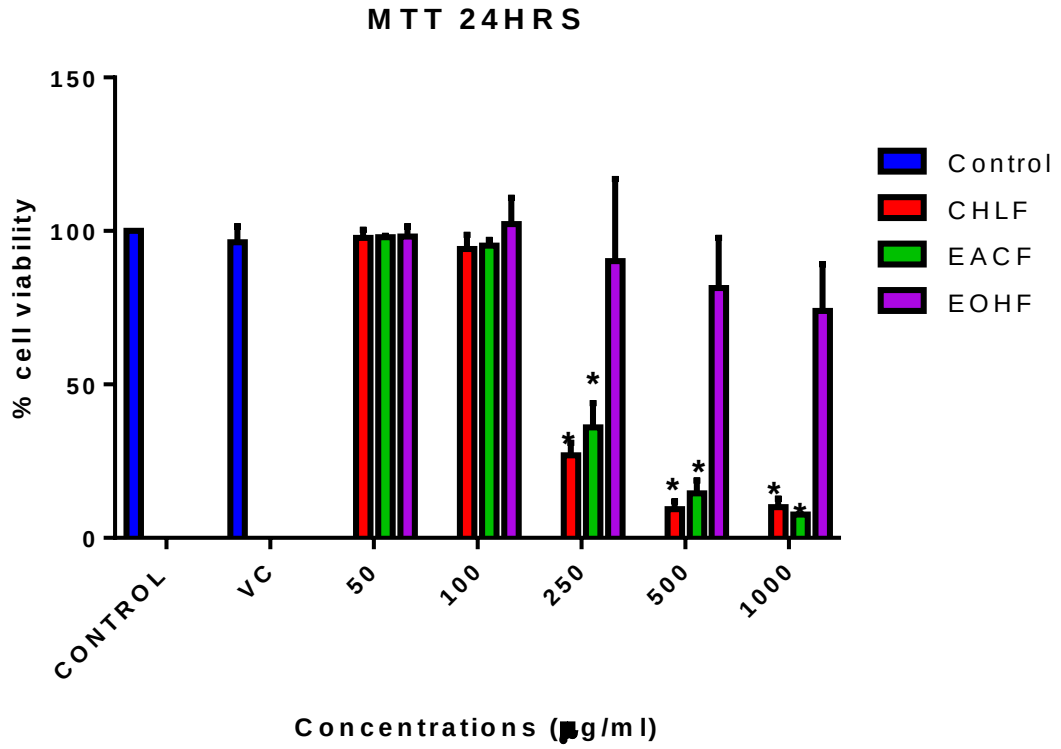

Figure 4. 48: Effect of fractions of *V.paradoxa* on MCF-7 cell viability after 24 hours treatment.

Where * is significant difference when compared with control.

VC is Vehicle control (0.1% DMSO)

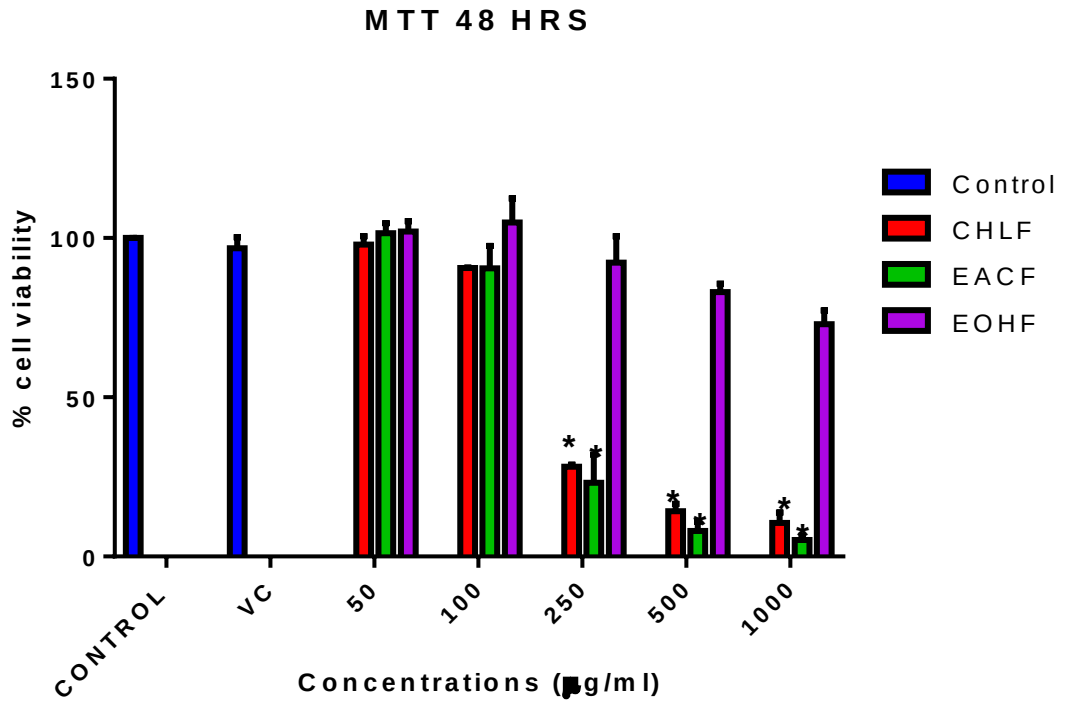

Figure 4.49: Effect of *V. paradoxa* fraction on MCF-7 cell viability after 48 hours of treatment.

Where * is significant difference when compared to control.

VC is Vehicle control (0.1% DMSO)

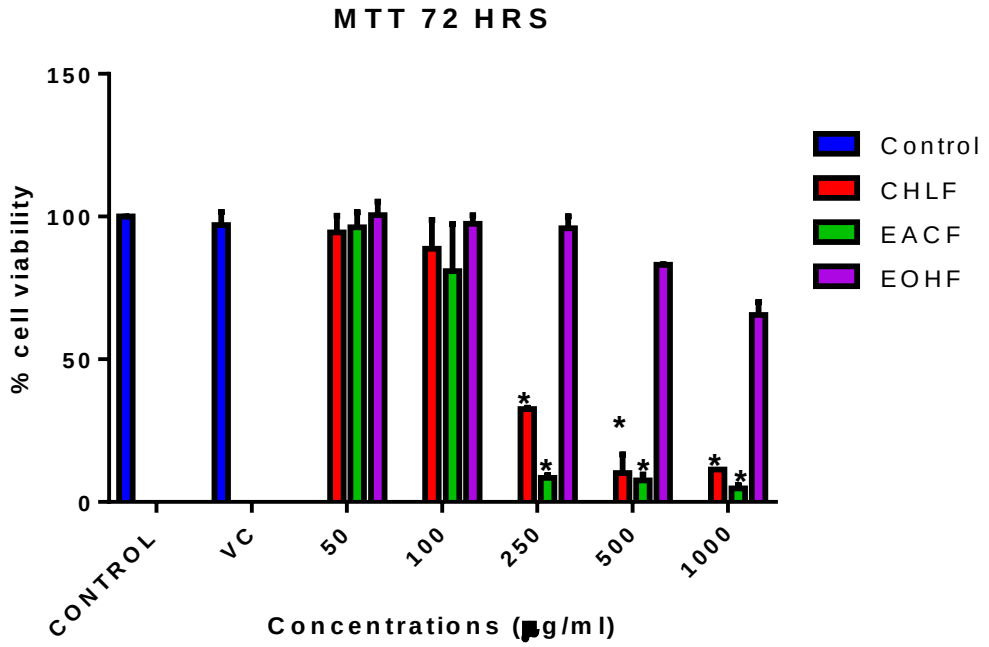

Figure 4.50: Effect of *V. paradoxa* fractions on MCF-7 cell viability after 72 hours of treatment.

Where * is significant difference when compared to control.

VC is Vehicle control (0.1% DMSO)

4.10.2 Cytotoxic activity of EACF in MCF-7, Hep G2 and A549 cells

The ethyl acetate fraction was suggested to screening using three cell lines to determine the cell line in which it is most cytotoxic. The cytotoxic activities of EACF in MCF-7, Hep G2 and A549 cells are presented in Figure 4.51 and 4.52.

MTT assay performed for 24 and 72 hrs showed different cytotoxic effects on MCF-7, Hep G2 and A549 cells (Fig. 4.51-4.52). For all three cell lines, the ethyl acetate fraction at 50-100 µg/ml did not show effect on cell viability. While ethyl acetate fraction exhibited a decrease of cell viability reaching 64% for MCF-7, 52% for Hep G2 and 63% for A549 at 250 µg/ml for 24 hrs and 92% for MCF-7, 25% for HepG2 and 76% for A549 cells at 250 µg/ml for 72 hrs (Fig. 4.51-4.52). The ethyl acetate fraction has more cytotoxic activity against MCF-7 cells when compared to Hep G2 and A549.

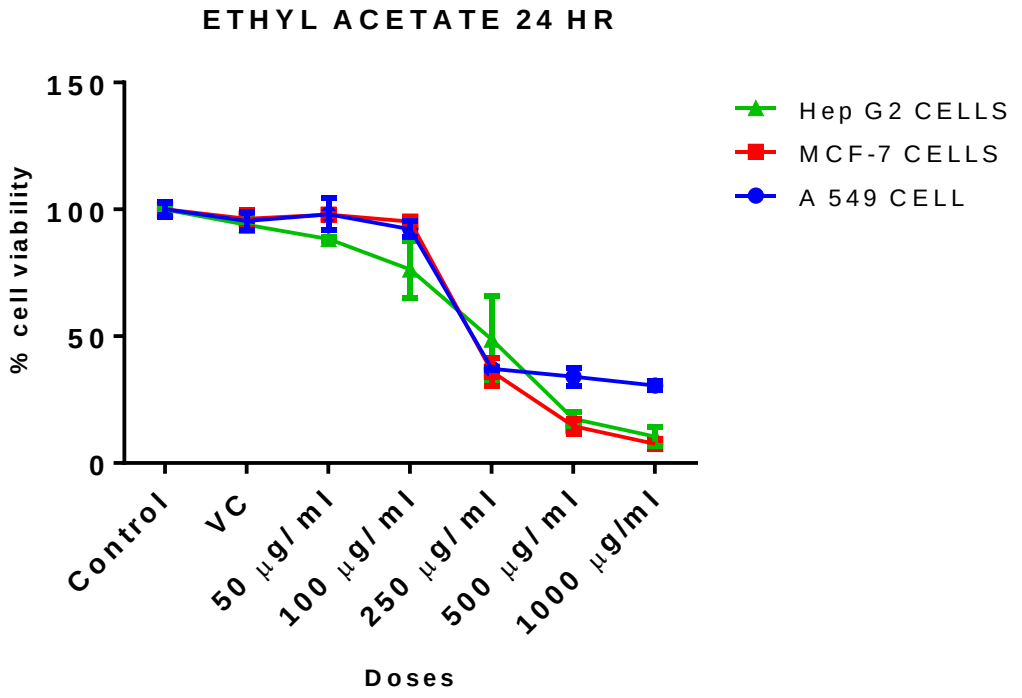

Figure 4.51: Cell viability of Hep G2, MCF-7 and A549 cells exposed to ethyl acetate fraction for 24 hours.

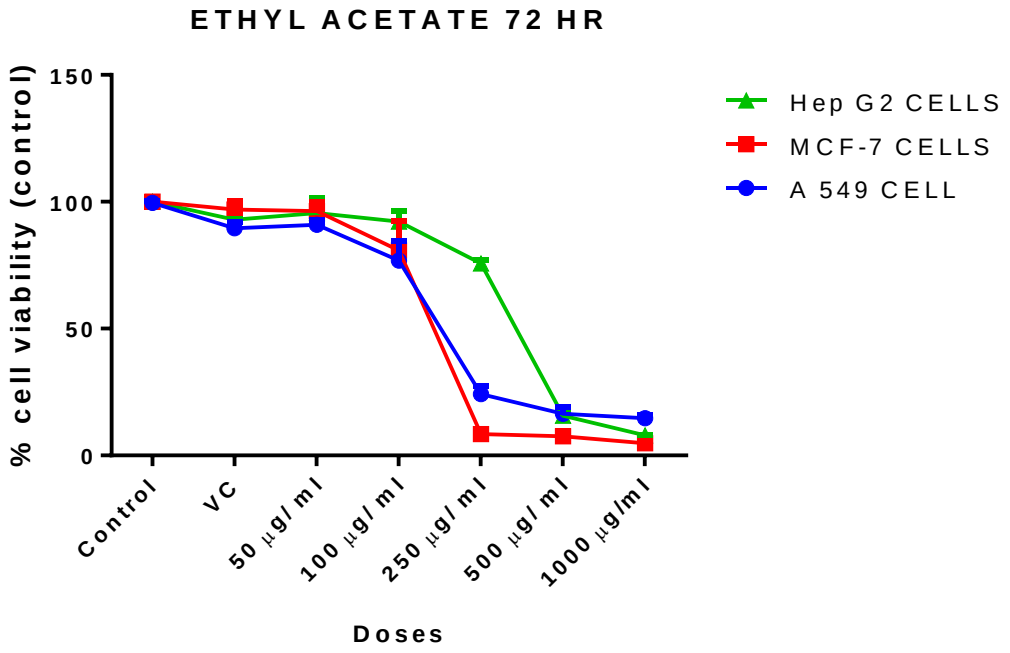

Figure 4.52: Cell viability of Hep G2, MCF-7 and A549 cells exposed to ethyl acetate fraction for 72 hours.

4.10.3 Anti-proliferative activities of EACF on MCF-7 cells

The ethyl acetate fraction was further suggested to antiproliferative activity and colony formation using MCF-7 cells. The antiroliferative activities and colony formation ability of ethyl acetate fraction treated MCF-7 cells are presented in Figure 4.53-4.56.

Antiproliferative activity: The ethyl acetate fraction (EACF) showed different cytotoxic effects at various dose range of IC_{50} and time duration. Cell viability showed significant reduction ($p<0.05$) by 19.3 % from control (100.00 ± 1.95) to EACF $_{1/2\ IC50}$ (80.63 ± 1.32); 33.1 % from control (100.00 ± 61.95) to $EACF_{IC50}$ (66.83 ± 4.08) and 64.9 % from control (100.00 ± 1.95) to $EACF_{DIC50}$ (35.07 ± 3.88) at 24 hrs (Figure 4.53). While showed significant reduction ($p<0.05$) of cell viability by 22.9 % from control (100.00 ± 0.96) to EACF $_{1/2\ IC50}$ (77.10 ± 5.42); 77.7 % from control (100.00 ± 0.96) to EACF $_{IC50}$ (22.30 ± 1.63) and 90.9 % from control (100.00 ± 0.96) to EACF $_{DIC50}$ (9.07 ± 1.09) at 48 hrs (Fig. 4.54).

Cell viability (trypan blue): Cell viability showed significant reduction ($p<0.05$) by 20.5 % from control (99.97 ± 0.72) to EACF $_{1/2\ IC50}$ (79.45 ± 0.00) and 78.2 % from control (99.97 ± 0.72) to EACF $_{IC50}$ (21.76 ± 4.10) at 24 hrs (Fig. 4.55).

Colony formation: Colony formation ability showed significant reduction ($p<0.05$) of MCF-7 cell by 22.6 % from control (100.00 ± 2.46) to vehicle control (77.34 ± 5.41) and 84.5 % from control (100.00 ± 2.46) to EACF $_{IC50}$ (15.44± 4.19) at 24 hrs (Fig. 4.56).

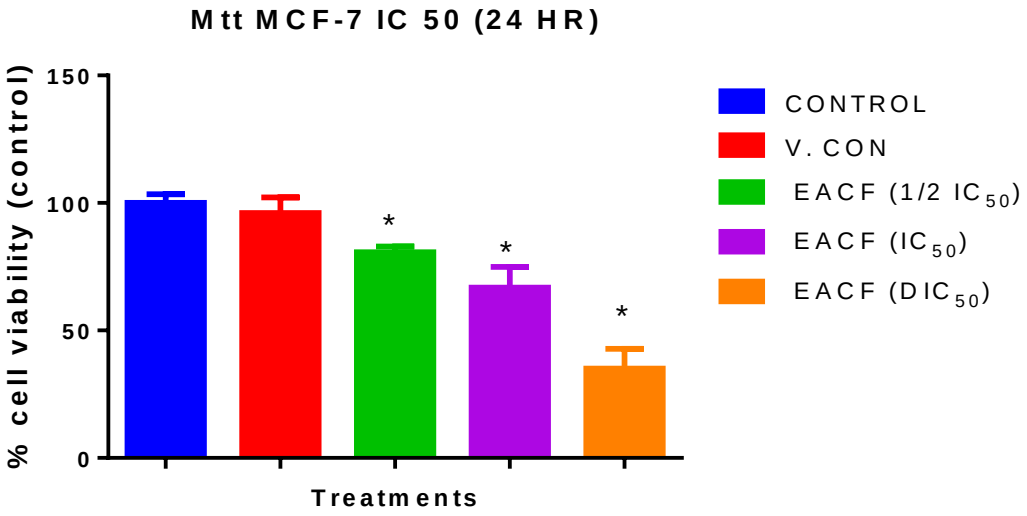

Figure 4.53: Cell viability of MCF-7 cells after 24 hours treatment with various IC_{50} range of doses.

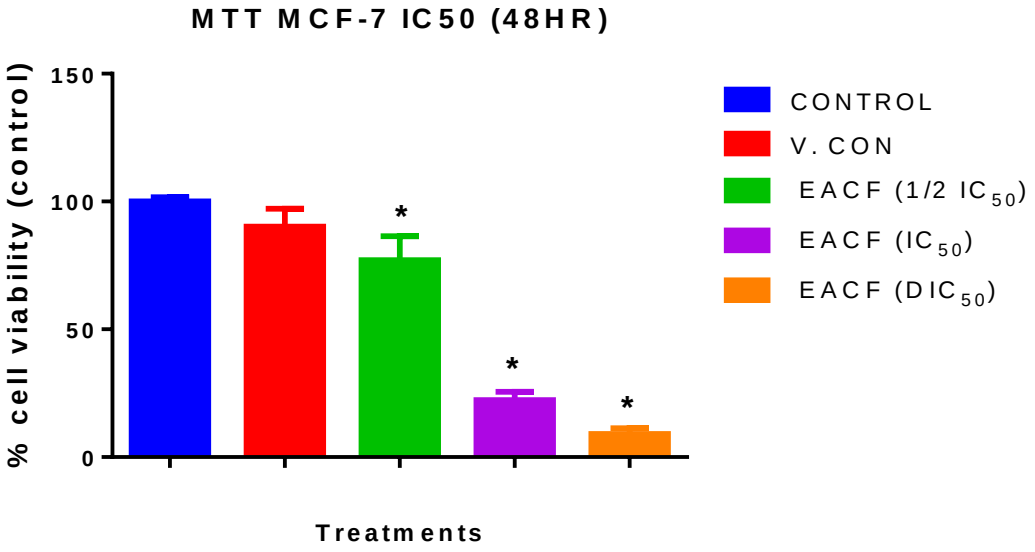

Figure 4. 54: Cell viability of MCF-7 after 48 hours treatment with various IC_{50} range of doses.

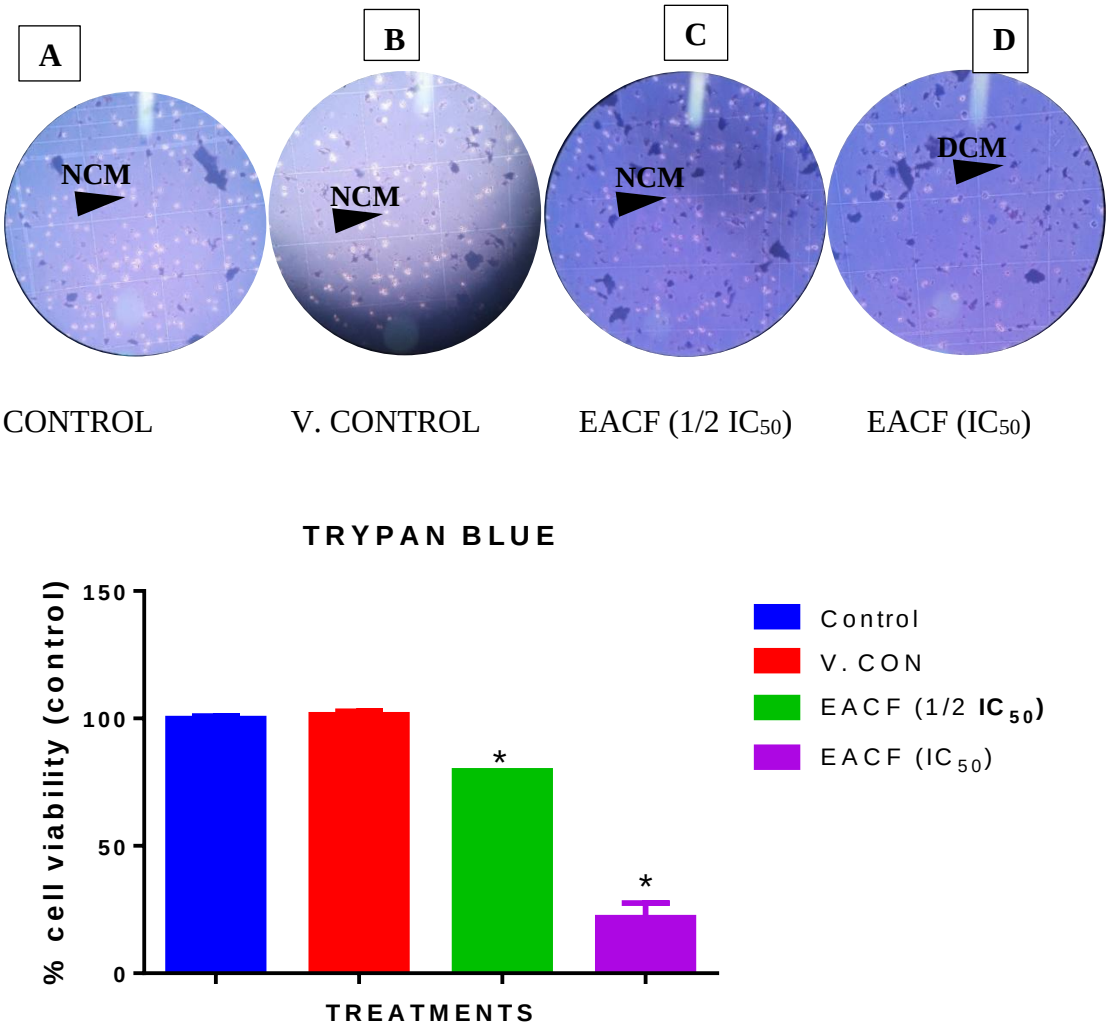

Figure 4.55: Cytotoxic effect of ethyl acetate fraction of *V. paradoxa* on MCF-7 cells at 48 hours

A: Control cells with normal cell membrane (NCM). B: Vehicle control cells with normal cell membrane. C: EACF ½ IC_{50} treated cells (Some normal cell membrane. D: EACF (IC_{50}) treated cells with damaged cell membrane.

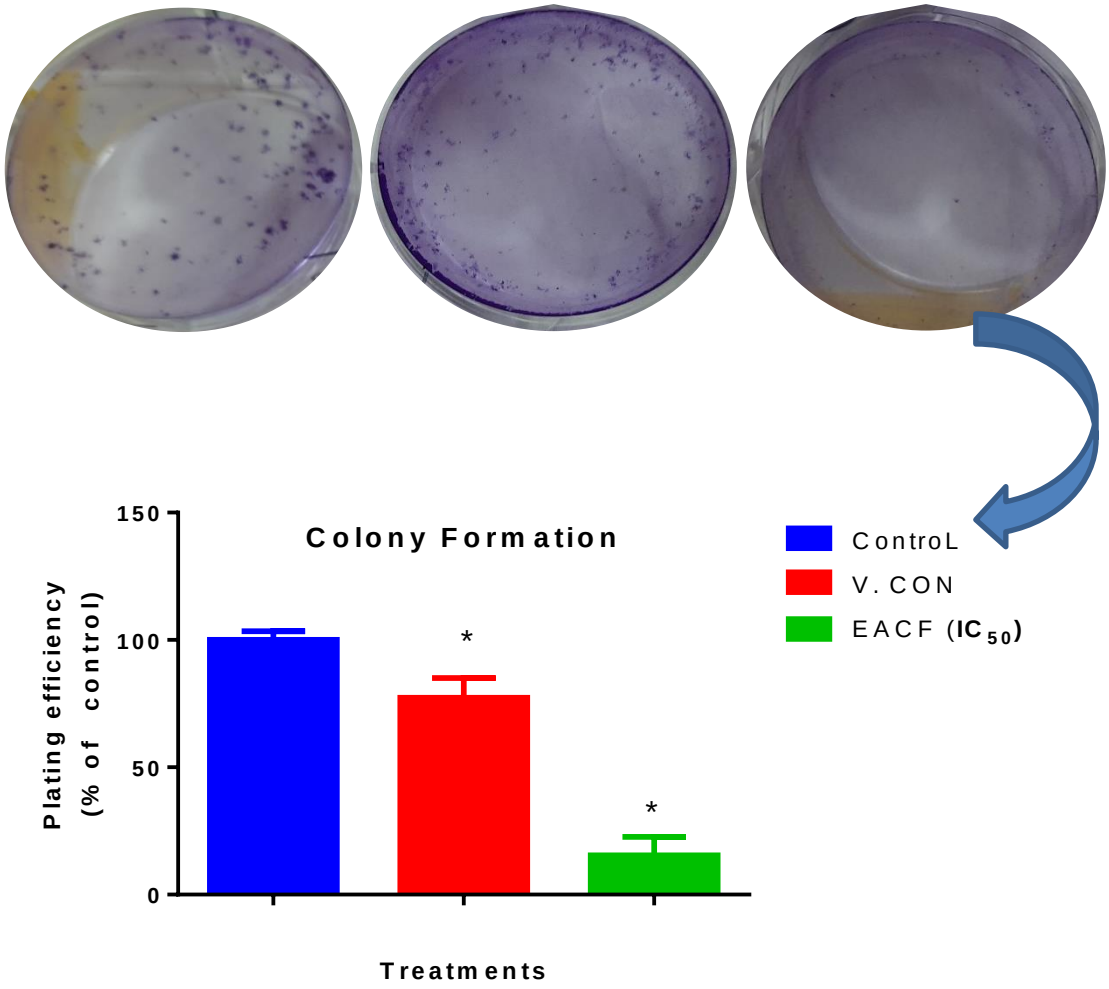

Figure 4.56: Effect of 24 hours treatment with fractions of *V. paradoxa* on MCF-7 colony formation

Where * is significant difference when compared to control.

4.10.4 EACF reduced ROS production in MCF-7 cells

The effect of EACF in ROS production in MCF-7 cells is presented in Figure 4.57.

Reactive oxygen species (ROS) production: The ethyl acetate fraction (EACF) decreased the percentage of ROS produced different at all dose range of IC_{50}. ROS production showed significant increased ($p<0.05$) by 11.9 % from control (100.00 ± 7.21) to vehicle control $_{(V. CON)}$ (111.90 ± 3.19). While showed significant reduction ($p<0.05$) by 46.16 % from control (100.00 ± 7.21) to EACF $_{IC50}$ (53.84 ± 0.92) and 57.81 % from control (100.00 ± 721) to EACF $_{DIC50}$ (42.19 ± 1.30) (Fig. 4.57).

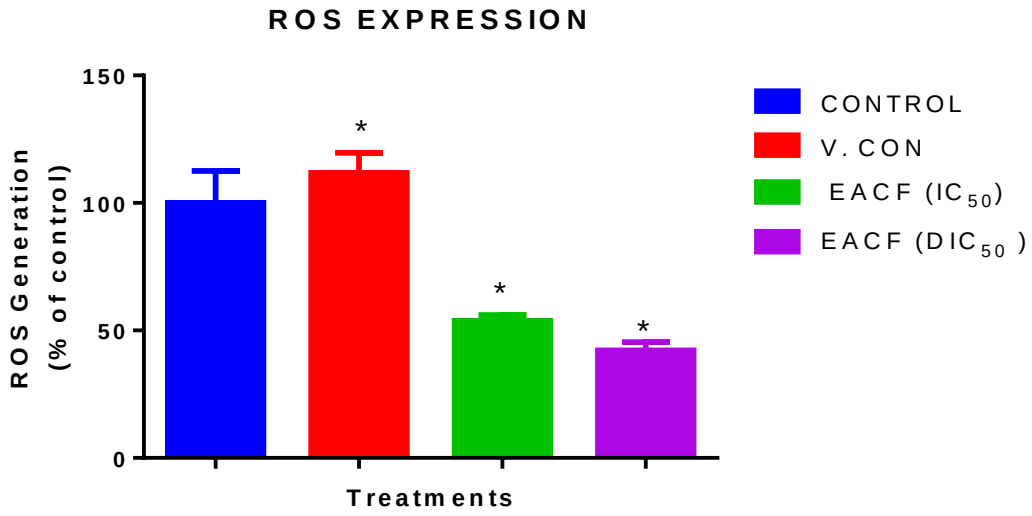

Figure 4.57. Effect of ethyl acetate fraction of *V. paradoxa* leaf on ROS generation after six (6) hours treatment.

Where * represent significant difference when compared to control.

.

4.10.5 Effects of EACF on cell cycle phases of MCF-7 cells

The effects on the cell cycle phases of MCF-7 cells after treatment with EACF for 24, 48, and 72 hrs respectively are shown in Figure 4.58-4.60.

Sub G0: There were no significant differences in values recorded for control and vehicle control at the various time duration. While treatment with EACF increased the values recorded from control. Sub G0 value showed significant elevation ($p<0.05$) by 191 % from control (3.975 ± 0.425) to EACF $_{IC50}$ (11.570 ± 0.410) at 24 hrs; 78.6 % from control (14.82 ± 1.46) to EACF $_{IC50}$ (26.48 ± 2.11) at 48 hrs and 231.2 % from control (19.83 ± 1.33) to EACF $_{IC50}$ (65.69 ± 0.33) at 72 hrs (Fig. 4.58-60).

G0/G1: There were decrease in values recorded for control and vehicle control at the various time duration. While treatment with EACF increased the values recorded from control. G0/G1 phase value showed significant elevation ($p<0.05$) by13 % from control (77.78 ± 2.25) to EACF $_{IC50}$ (81.24 ± 2.34) at 24 hrs; 16.1 % from V. control (71.87 ± 0.87) to EACF $_{IC50}$ (83.49 ± 0.07) at 48 hrs and 17.1 % from control (65.21 ± 0.82) to EACF $_{IC50}$ (76.39 ± 1.91) at 72 hrs (Fig. 4.58-60).

S: There were increase in values recorded for control and vehicle control at the various time duration. While treatment with EACF decreased the values recorded from control. S phase value showed significant reduction ($p<0.05$) by 23.7 % from control (20.285 ± 1.975) to EACF $_{IC50}$ (15.470 ± 1.150) at 24 hrs; 38.3 % from V. control (23.52 ± 0.44) to EACF $_{IC50}$ (14.49 ± 0.13) at 48 hrs and 32.1 % from control (34.79 ± 0.82) to EACF $_{IC50}$ (23.61 ± 1.91) at 72 hrs (Fig. 4.58-60).

G2/M: There were no significant differences in values recorded for control, vehicle control, and EACF (IC_{50}) at 24 hrs. While treatment with EACF decreased the values recorded from control at 48 hrs. G2/M phase value showed significant reduction ($p<0.05$) by 56 % from V. control (4.610 ± 0.430) to EACF $_{IC50}$ (2.025 ± 0.065) at 48 hrs. (Fig. 4.58-60).

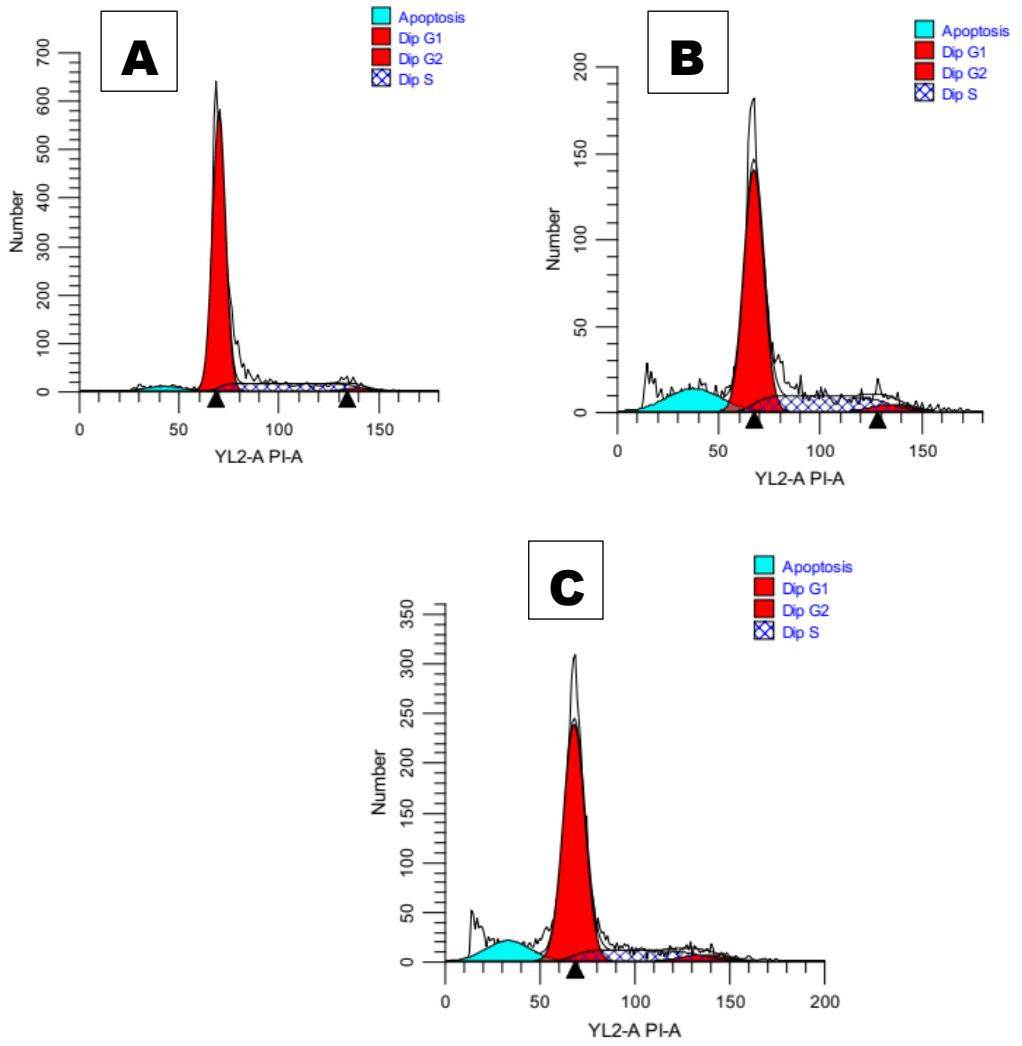

Fig 4.58A: Flow cytometry analysis of MCF-7 cells after 24 hr treatment with EACF

Where A is control, B is vehicle control and C is EACF at IC_{50} dose

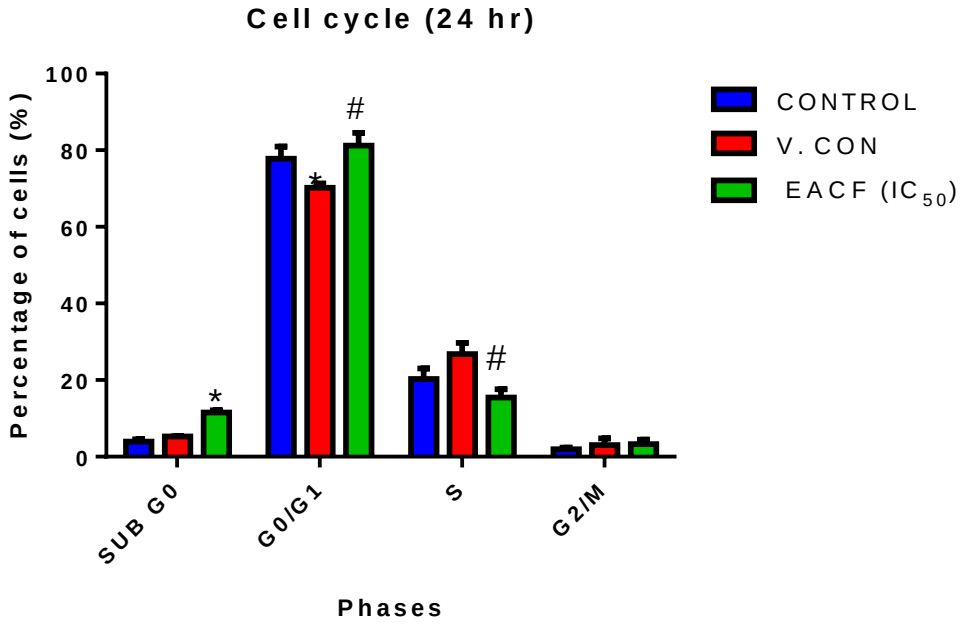

Fig 4.58B: Cell cycle phase after 24 hours treatment with EACF of *V. paradoxa*

Where * represent significant difference when compared to control and # when compared with vehicle control (V. CON)

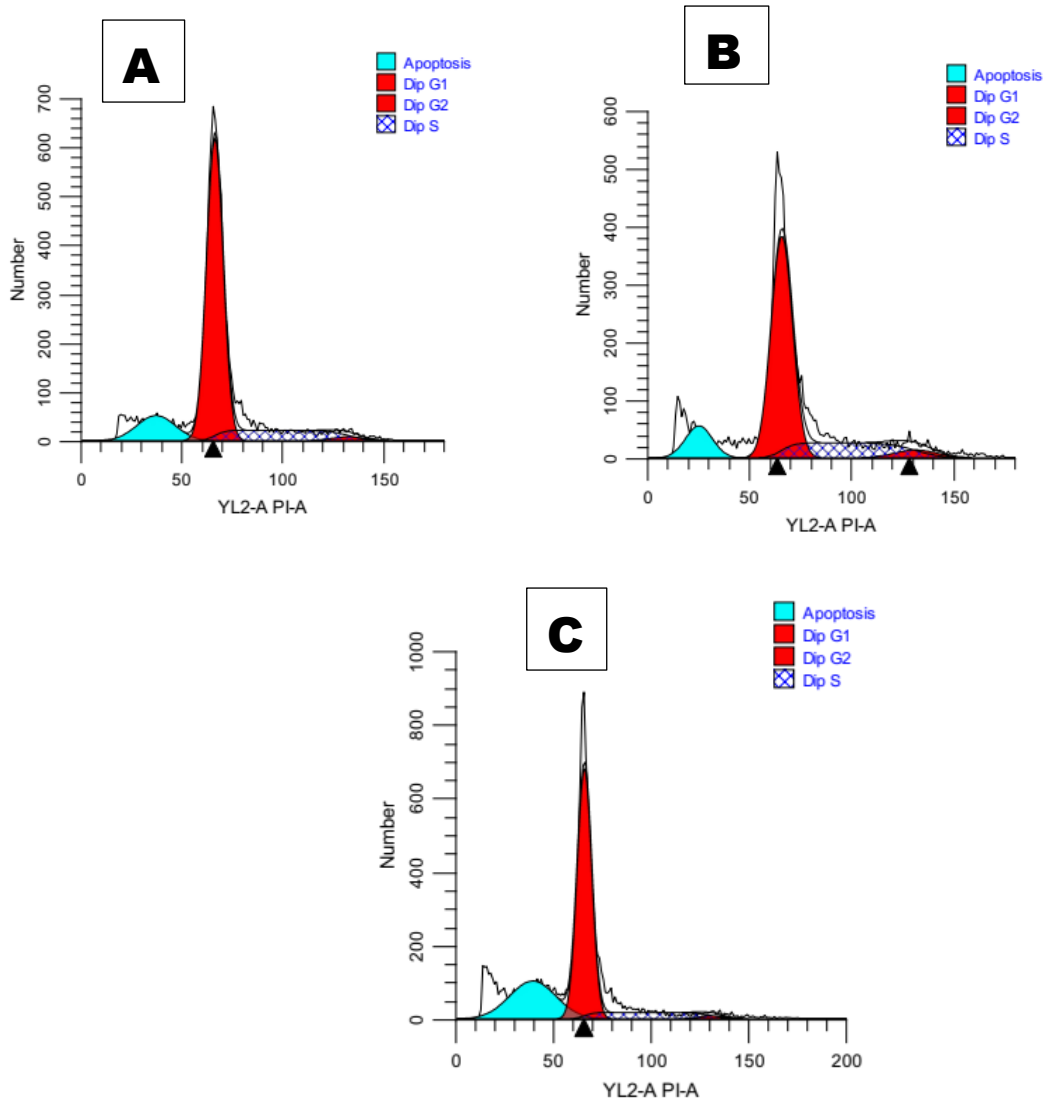

Fig 4.59A: Flow cytometry analysis of MCF-7 cells after 48 hr treatment with EACF

Where A is control, B is vehicle control and C is EACF at IC_{50} dose

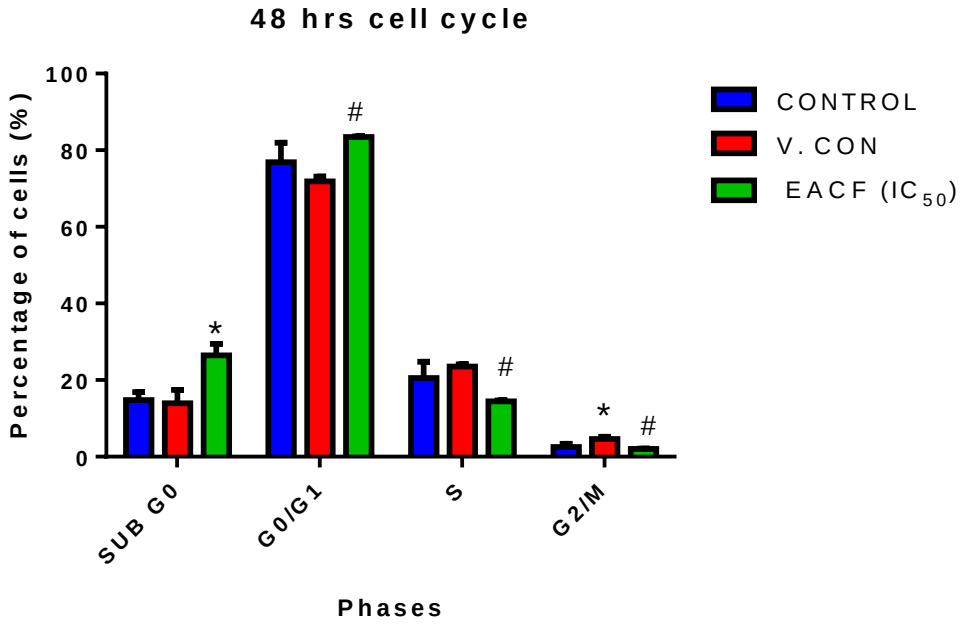

Fig 4.59B: Cellcycle phases after 48 hours treatment with fractions of *V. paradoxa*.

Where * represent significant difference when compared to control and # when compared with vehicle control (V. CON)

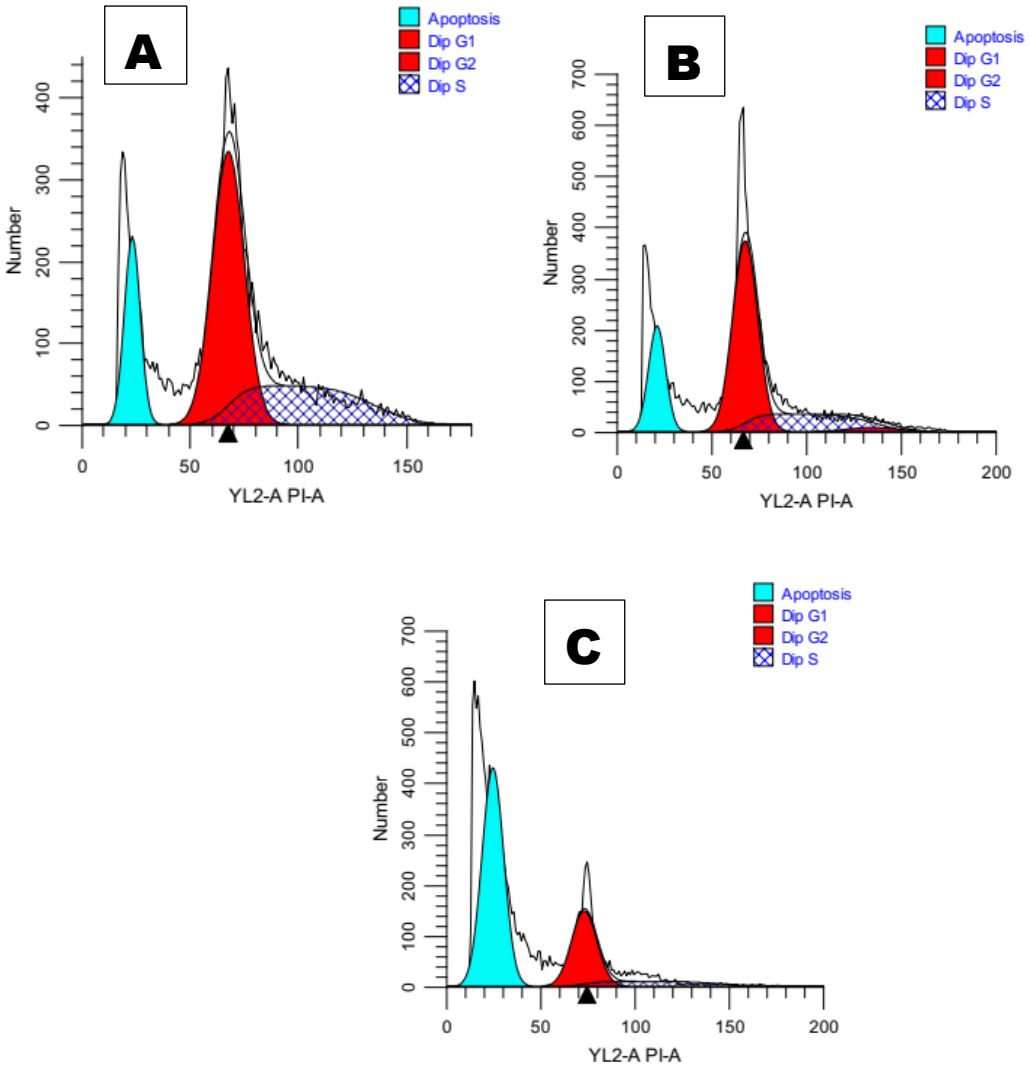

Fig 4.61A: Flow cytometry analysis of MCF-7 cells after 72 hr treatment with EACF

Where A is control, B is vehicle control and C is EACF at IC_{50} dose

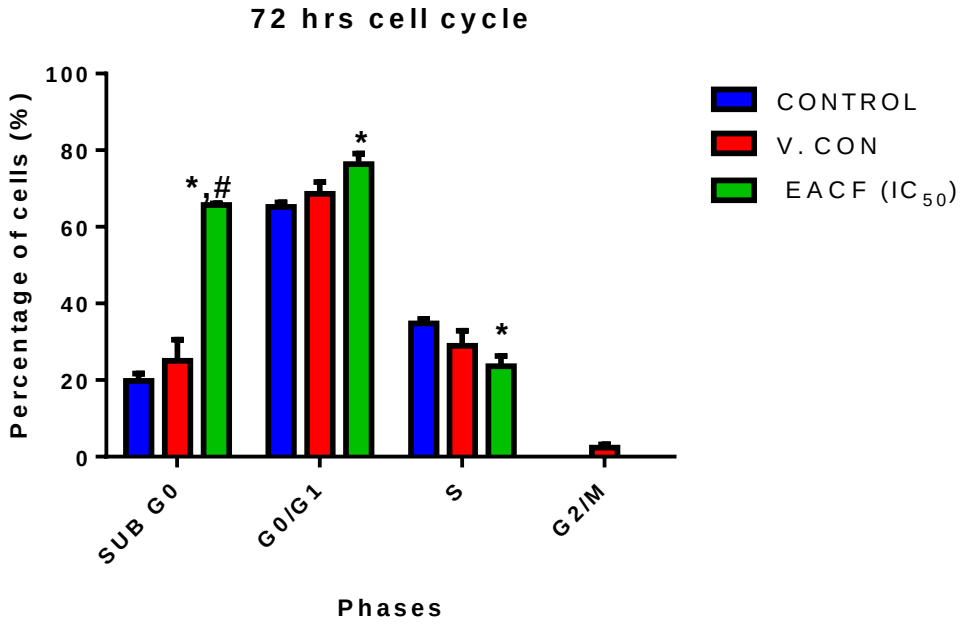

Fig 4.61B: Flow cytometry analysis of cell cycle phases after 72 hours treatment with EACF of *V. paradoxa*.

Where * represent significant difference when compared to control and # when compared with vehicle control (V. CON)

4.10.6 Effects of EACF on protein expression of cleaved caspase 3 and pro-caspase 3

The effects of EACF on the expression of cleaved caspase 3 and pro-caspase 3 protein are presented in figure 4.61-4.63.

Pro- caspase 3: There were no significant differences in values recorded for control and vehicle control. While expression of pro-caspase 3 showed significant reduction ($p<0.05$) by40.6 % from control (1.000 ± 0.000) to EACF $_{IC50}$ (0.594 ± 0.011) (Fig. 4.62).

Cleaved caspase 3: The mean expression of cleaved caspase 3 decreased from control value to vehicle control and increased from control to EACF (IC_{50}) (Fig. 4.63).

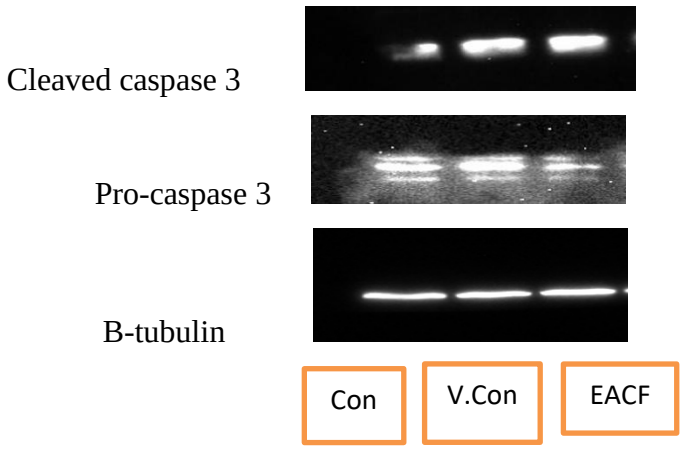

Figure 4.61: Cleaved caspase 3 and pro-caspase 3 protein expression after 24 hr treatment

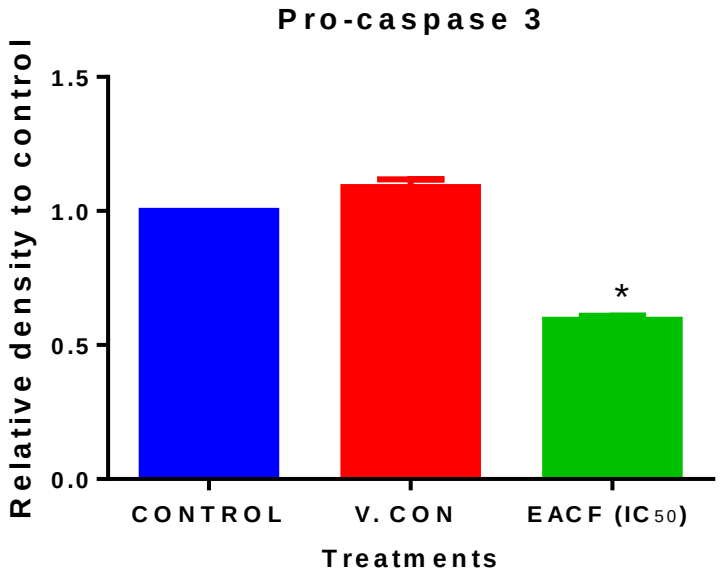

Figure 4.62: Pro-caspase 3 protein activity in MCF-7 cells treated for 24 hrs

Where * represent significant difference when compared to control

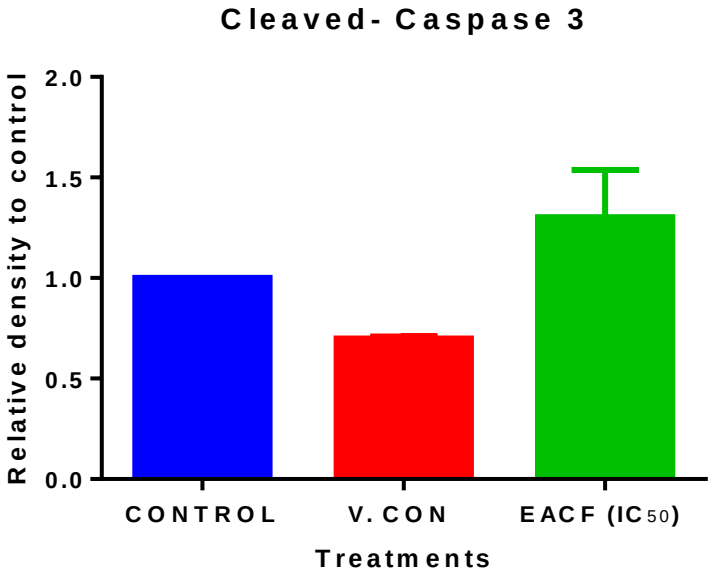

Figure 4.63: Cleaved caspase 3 protein activity in MCF-7 cells treated for 24 hrs

4.10.7: Analysis of active compounds present in EACF using GC-MS

The active compounds present in EACF was analysed using GC-MS. It was observed to have 12 peak representing 12 active compounds (Figure 4.64, Table 4.6). The compounds present include hexadecanoic acid, methyl ester;; Hexadecanoic acid, ethyl ester; 9,12-octadecadienoic acid (z,z); 11-octadecenoic acid, methy ester; phytol; Methyl stearate; Linoelaidic acid; Ethyl oleate; Octadecanoic, ethyl ester; Bis (2-ethylhexyl) phythalate; 1,4-benzenedicarboxylic acid, bis(2-ethylhexyl) ester; Squalene.

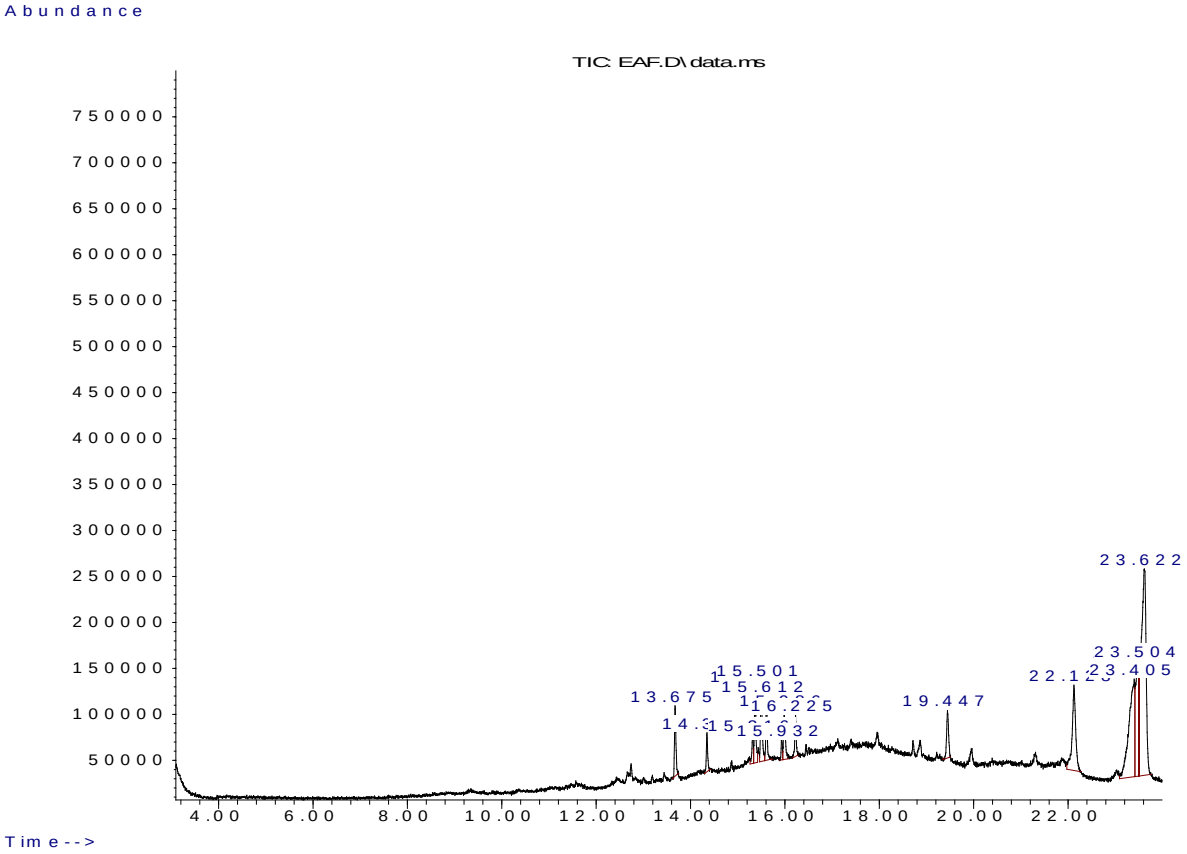

Figure 4. 64: Analysis of ethyl acetate fraction of *V. paradoxa* ethanol leaves extract using GC/MS

Table 4.6: Chemical compound detected from GC/MS analysis of ethyl acetate fraction of *V. paradoxa*

S/N	Retension time	Compound name	Molecular formular	Molecular weight	Peak area
1	13.673	Hexadecanoic acid, methyl ester	$C_{17}H_{34}O_2$	270.45	3.25
2	14.349	Hexadecanoic acid, ethyl ester	$C_{18}H_{36}O_2$	284.48	1.70
3	15.316	9,12-octadecadienoic acid (z,z)	$C_{18}H_{32}O_2$	280.45	1.33
4	15.368	11-octadecenoic acid, methy ester	$C_{19}H_{36}O_2$	296.5	3.87
5	15.501	phytol	$C_{20}H_{40}O$	128.17	4.38
6	15.611	Methyl stearate	$C_{19}H_{36}O_2$	298.51	3.00
7	15.930	Linoelaidic acid	$C_{18}H_{32}O_2$	280.45	0.78
8	15.987	Ethyl oleate	$C_{20}H_{38}O_2$	310.51	2.85
9	16.225	Octadecanoic, ethyl ester	$C_{20}H_{38}O_2$	312.5	1.92
10	19.449	Bis (2-ethylhexyl) phythalate	$C_{24}H_{36}O_4$	390.6	2.93
11	22.130	1,4-benzenedicarboxylic acid, bis(2-ethylhexyl) ester	$C_{24}H_{38}O_4$	390.6	9.76
12	23.406	Squalene	$C_{30}H_{50}$	410.7	17.93

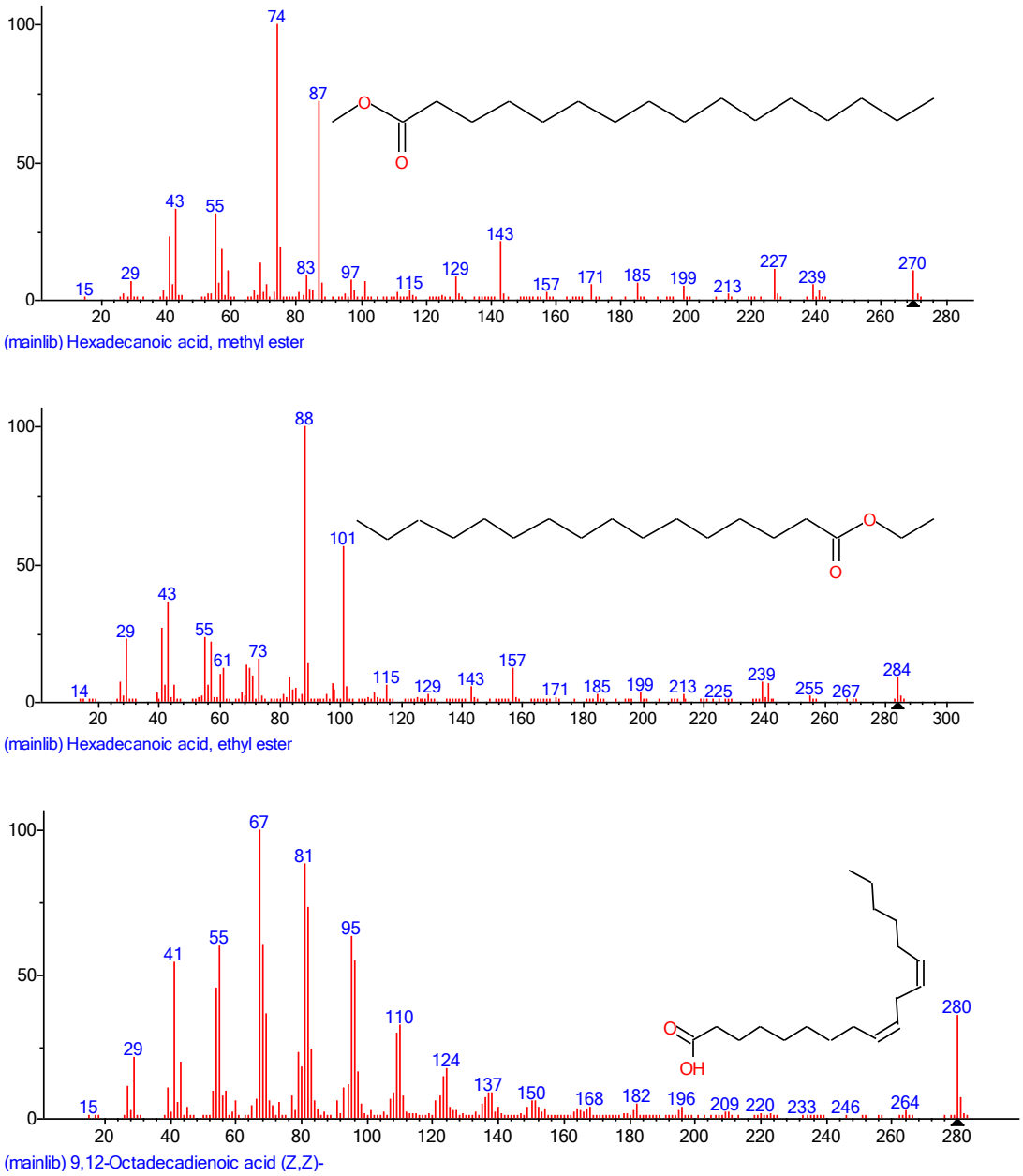

Fig. 4. 65A: Chemical structures of compouds present in ethyl acetate fraction of *Vitellaria paradoxa* leaf

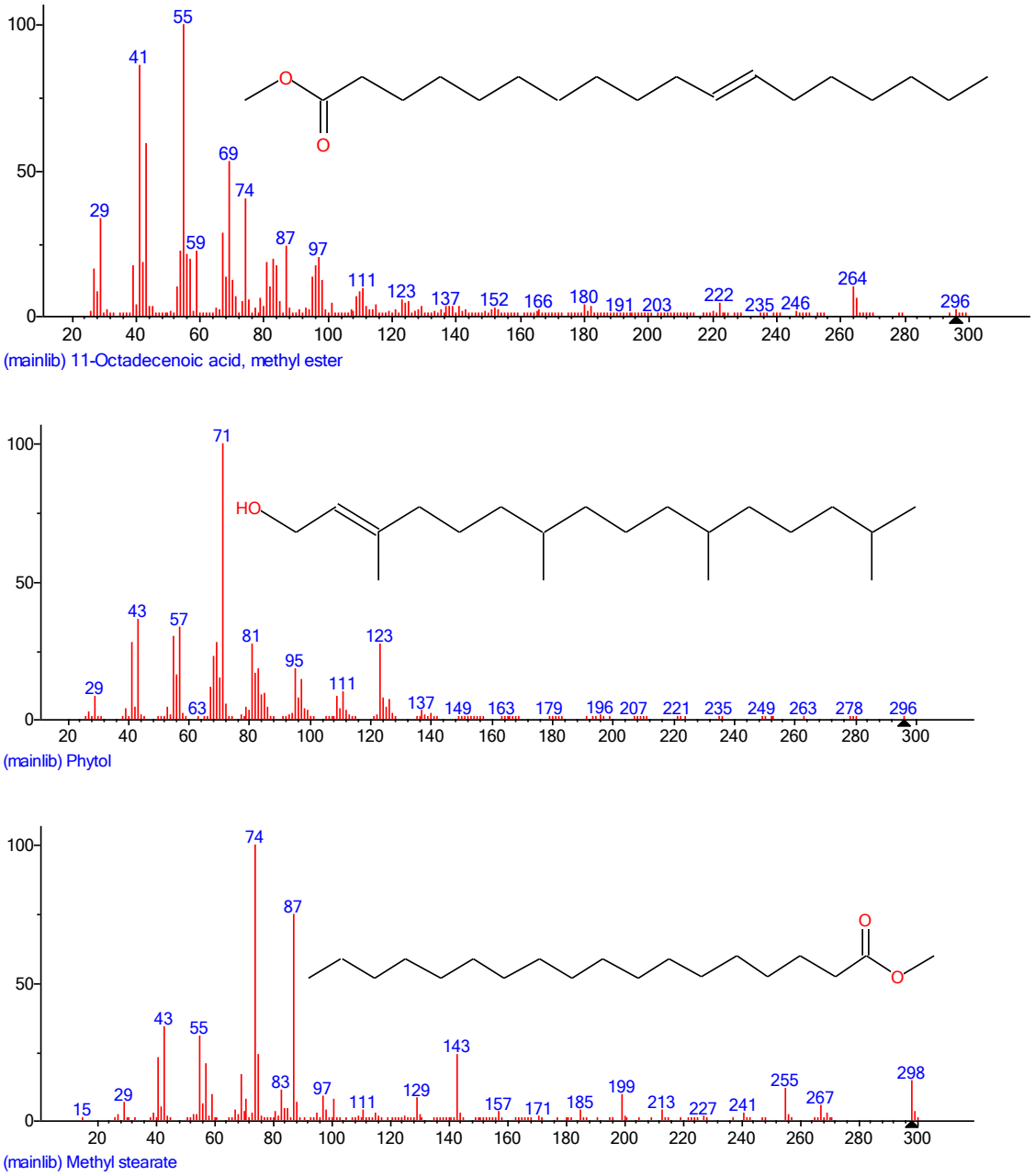

Fig. 4. 65B: Chemical structures of the compouds present in ethyl acetate fraction of *Vitellaria paradoxa* leaf

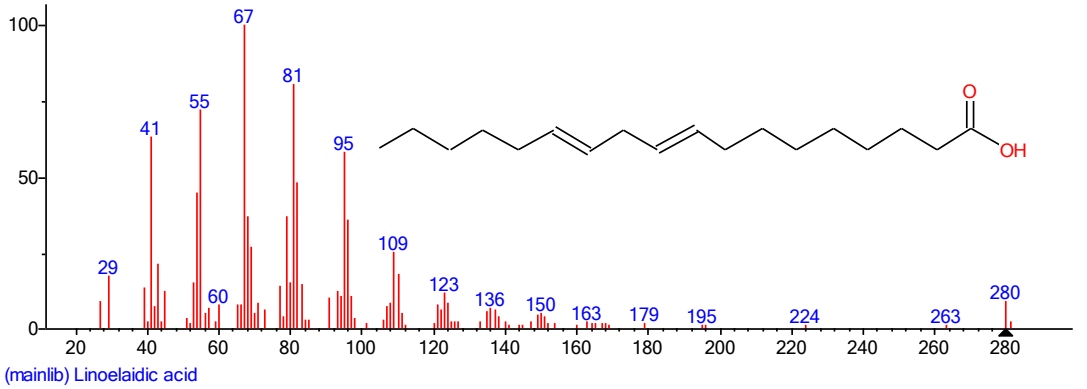

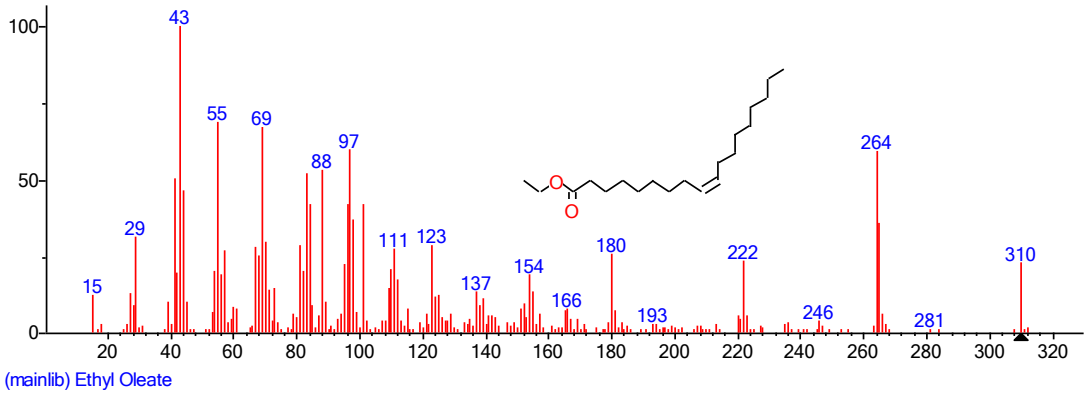

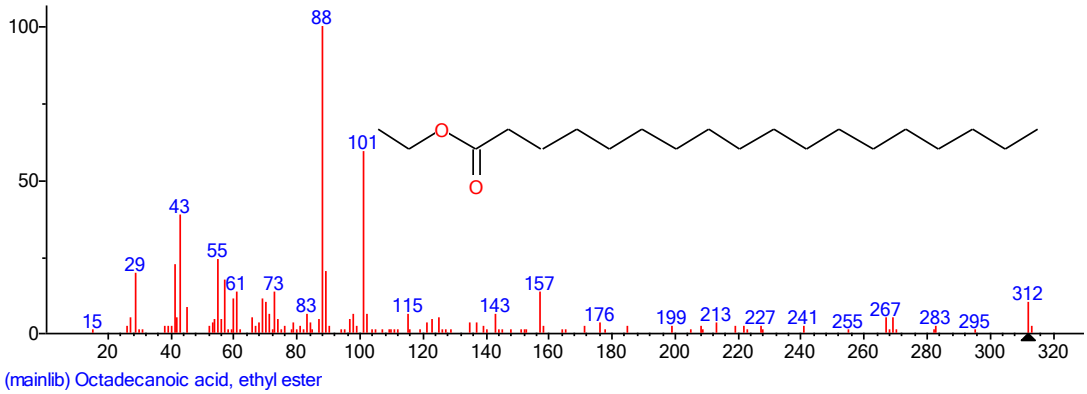

Fig 4. 65C: Chemical structures of the compouds present in ethyl acetate fraction of *Vitellaria paradoxa* leaf

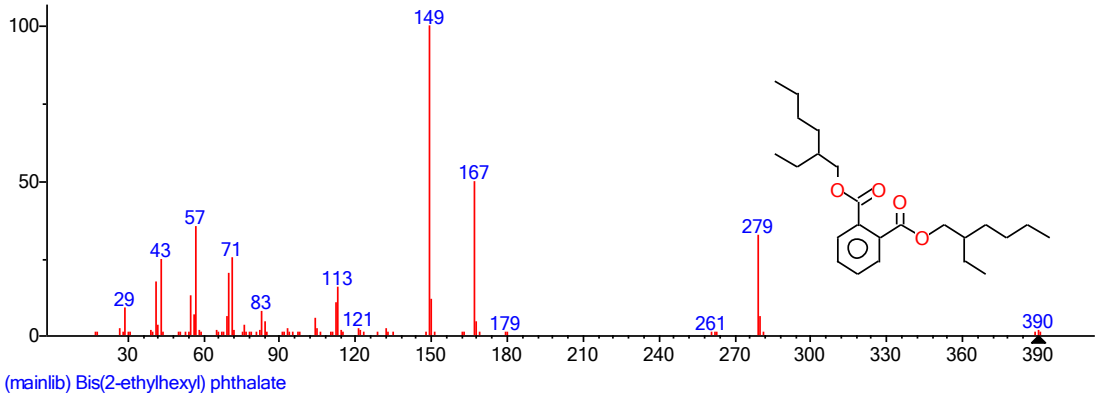

(mainlib) Bis(2-ethylhexyl) phthalate

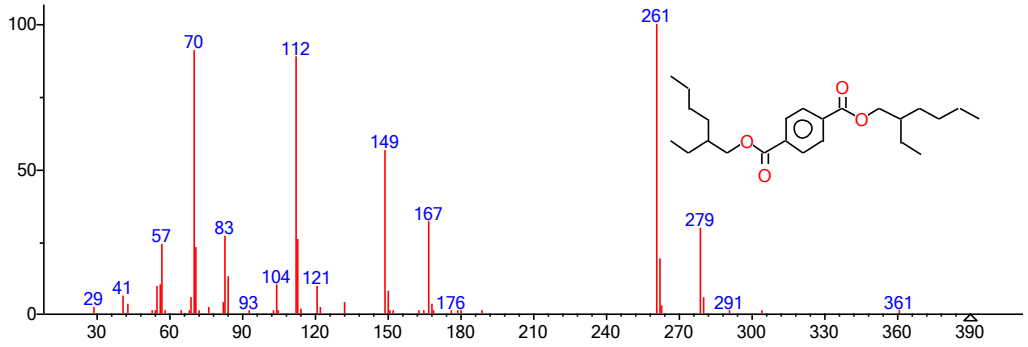

(mainlib) 1,4-Benzenedicarboxylic acid, bis(2-ethylhexyl) ester

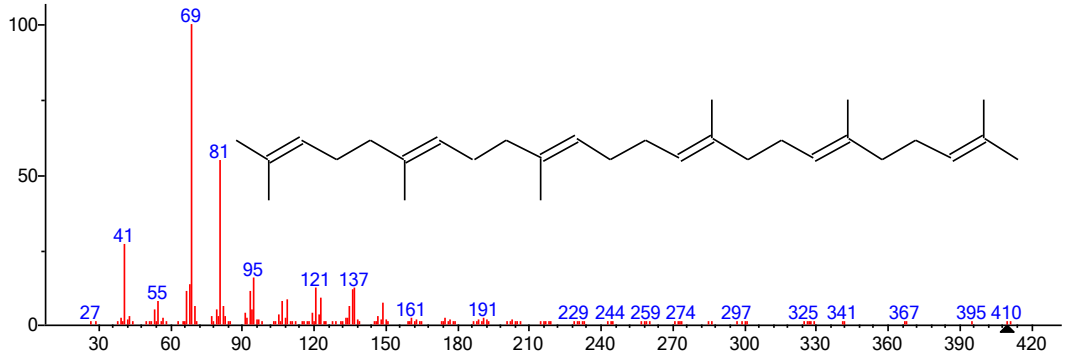

(mainlib) Squalene

Fig 4. 65 D: Chemical structures of the compouds present in ethyl acetate fraction of *Vitellaria paradoxa* leaf

CHAPTER FIVE
DISCUSSION

Cancer is a leading cause of death globally (Sung, 2021), and the increased incidence and mortality rate in low and middle income countries has been linked to environmental exposures to industrial and agricultural chemicals (Anetor, 2016: Ganapathy *et al*., 2019). Exposures to anthropogenic sources of arsenic has been implicated in the induction of organ/ tissue toxicity through the generation of reactive oxygen species, inhibition of thiol-containing enzymes and the induction of DNA damage that leads to chromosomal aberration (Del Razo *et al*., 2002). Major sources of exposures include contaminated drinking water and industrial emissions (Biswas *et al*., 2019). The search for medicinal plant which possess natural phytochemicals with protective antioxidant and anti-inflammatory properties that might mitigate the toxic effect of arsenic and by extension the menace of cancer is still ongoing.

Vitellaria paradoxa also called shea butter tree characteristic of the Savannah region and belonging to the Sapotaceae family have been reported to possess antioxidant (Odunola *et al*., 2019) and anti-inflammatory properties. Therefore, this study is an intergrated effort to investigate the cytoremediative potentials of *Vitellaria paradoxa* against sodium arsenic-induced toxicity in Wistar rats and fruit fly (*Drosophila melanogaster*) as well as its anti-proliferative action on breast cancer cells.

Results herein indicated that hydroethanol leaf extract of *Vitellaria padoxa* (ELVp) possess several phytochemicals and anti-oxidant potentials through the modulation of liver and kidney biomarkers and reduction of reactive oxygen species generated by arsenic. Interestingly, ethanol extract and ethyl acetate fraction of *Vitellaria paradoxa* leaf elevated the expression of P53, cleaved caspase 3 and reduced BCL-2 and procaspase 3 apoptotic proteins in models used for this study

5.1 Phytochemical and antioxidant profile of *Vitellaria paradoxa*

Data presented herein, indicated that the ethyl acetate fraction of *V. paradoxa* leaf possess the highest amount of bioactive compounds known as phytochemicals. Among the identified compounds present in the ethyl acetate fraction using GC-MS are; squalene, phytol and 9,12-octadecadienoic acid(z,z). Squalene have been reported to possess antibacterial, antioxidant, antitumour, cancer preventive, immunostimulant and lipoxygenase inhibitor properties (Kavitha *et al*., 2015). While, phytol classified as diterpene has cancer preventive, anti- inflammatory and anti-microbial (Tyagi and Agarwal, 2017) properties. Also, 9,12-octadecadienoic acid(z,z) has anti-inflammatory, antihistamic, hepatoprotective, hypocholesterolemic and antiarthritic properties (Kavitha *et al*., 2015; Tyagi and Agarwal 2017).

Furthermore, in this study the ethyl acetate fraction (EACF) possessed the highest amount of flavonoid and phenols. Flavonoid and phenols plays a major role as antioxidant and serves as scavengers of reactive oxygen species (Oboh *et al*., 2016). Hence, they may act as influencers and modulators of several cellular processes involving signalling and apoptosis. The polyphenolic substance (flavonoids) present in *V. paradoxa* leaf extract (ELVp) and ethyl acetate fraction (EACF) acts as hydrophilic antioxidant, photoreceptors as well as UV light filters (Pawlowska *et al*., 2019). Thus the ability of ELVp and EACF to reduce phosphomolybdenium (VI) to (V) and the presence of reductant in both extract of ELVp and fraction of EACF caused the loss of an electron by Fe^{3+}. Note worthy, reducing power of both samples is concentration dependent. Hence, the higher the concentration the more the reducing power. This is in line with Olugbami *et al*., (2015) and Lin *et al*., (2014). As against our result, Sahreen *et al*., (2017) observed that ethyl acetate fraction of *Carissa opaca* had the least reducing power capacicity while Jamkhande *et al*., (2013) showed the butanol fraction which was followed by the ethyl acetate fraction had the greatest reducing power. Therefore, the ability of ELVp and EACF to terminate chain reactions produced by radical by converting them to stable product may show that the phenols and polyphenols present in both samples are good electron donor. This might be because phenolic and flavonoid are able to donate their hydrogen group.

5.2 Safety assessment indices of *Vitellaria paradoxa*

The use of SOS chromotest have been used in testing genotoxicity because *E. coli* PQ37 bacterial system is sensitive and dependable. It makes use of an intricate regulatory system activated by substances that result to damage of DNA inducing a repair pathway, also known as SOS response, (Quillardet *et al*., 1982; Chaabane *et al*., 2012). From previous work, a compound is graded as non-genotoxic if the SOSIF is less than and equal to1.5, inconclusive if it is between 1.5- 2.0 and genotoxic if it exceed 2.0 (Fabiana *et al*., 2017). Therefore, the low SOSIF value of both extracts may indicates the non- genotoxic nature of *V. paradoxa* and this suggest that exposure to ELVp and ESVp may not cause DNA lesions that would prevent DNA synthesis (Chaabane *et al*., 2012). However, at the first concentration 800 µg/ml for both ELVP and ESVp extracts was inconclusive with SOSIF value of 1.5 and 1.6 respectively relative to the positive control 4-Nitroquinoline-1-oxide with value of 4.1.

In addition, acute toxicity test is a measure for determining the safety assessment of various drugs and extracts. In this study, the LD_{50} evaluation showed that the ingestion of ELVp even at the highest dose of 5000 mg/kg did not induced mortality on the rats. Therefore, the lack of mortality recorded in this study may suggest that ELVp is safe at 5000 mg/kg. This assumption is supported by Mainasara *et al*., (2016) and Fodouop *et al*., (2017) observations that showed the lethal dose to be greater than 5000 mg/kg in rats and 12000 mg/kg in mice respectively. However, the histological occurrence of inflammatory hepatocytes cells at 2000 mg/kg may indicate that exposure at high dose may induce toxicity that results in inflammation without leading to mortality. Hence this lead to the choice of 100 and 200 mg/kg for the toxicity testing.

5.3 Body weight, organo somatic and haematological indices

Body weight and organo somatic indices such as relative liver weight (RLW) and relative kidney weight (RKW) have been applied as screening biomarkers for impacts of environmental toxicant (Tchounwou *et al* 2012). In this study there was significant increase

in body and relative liver weights for vitamin E and ELVp group. The increase in body and relative weight may imply that it is beneficial to well being of rats. While, no changes was observed on both parameters for SA only treatment. Contrary to the result, Odunola *et al*., (2011) and Akin-Idowu *et al*., (2015) showed that when sodium arsenite alone is administered, relative liver weight increased in rodents. The difference between the present study and the report of Odunola *et al* (2011) and Akin-Idowu *et al* (2015) may be related to the differences in exposure time. The kidney is a fundamental site for excretion (Wang *et al*., 2018) hence making it one of the most favoured organ for arsenic toxicity (Rana *et al*., 2018). Treatment with SA orally for two weeks significantly decreased the relative kidney weight. The decrease in RKW recorded in SA group may be an indication of renal hypertrophy resulting form the toxic effect of arsenic. Sarker *et al*., (2013) observed that treatment with sodium arsenite decreased the relative kidney weight of rats. From the present study, co-treatment of SA+ ELVp (100 mg/kg) increased the relative liver and kidney weights of male Wistar rats. This findings may imply that it has a positive impact on the rats' well being.

Also, there was a siginificant reduction in RBC, HGB and HCT in SA treated rats. This could be because arsenic inhibites aminolevulinic acid dehydratase (ALAD) activity an enzyme key in heme synthesis pathway (Gupta and Flora, 2005). This results in a substantial increase in uninary porphyrins, uniquely characterized by a greater increase in uroporphyrin levels (Woods and Fowler., 1977). This assumption is supported by established knowledge indicating that is ALAD is inhibited by arsenic during heme synthesis (Woods and Fowler., 1977; Aguilar-Gonzalez *et al*., 1999; Mondal et al., 2016; Goudarzi *et al*., 2018 and Ola-Davis and Akinrinde, 2016). However upon, co-treatment with ELVp mostly at 200 mg/kg, there was significant increased in production of RBC and HGB, thus suggesting the erythropoietin-like properties of *V. paradoxa* leaf.

The exposure of animals to foregin toxic substances may result in an inflammatory reaction. Some indices for inflammation include: platelet, lymphocyte and white blood cell count. Rats exposed to SA significantly increased the platelet, lymphocytes and WBC. Elsewhere, Kim *et al*., 2020 reported that induction of arsenic resulted in morphological changes of platelets leading to increased platelet reactivity and ultimately contributing to thrombosis.

Thrombocytosis is described as a condition resulting from too many platelets in the blood. According to Appleby *et al*., 2017, thrombocytosis may be an inflammatory indices and a presenting sign for solid tumours and heamatological conditions. However, co-treatment with ELVp (200 mg/kg) reduced the levels of platelet and lymphocyte by 11.2 % and 19.3 % respectively when compared with SA (2.5 mg/kg) and this may indicate that *V. paradoxa* leaf has the potential to reduced inflammation resulting from arsenic ingestion in rats.

5.4 Modulation of liver and kidney biomarkers

The presence of several soluble enzymes like alanine aminotransferase (ALT), aspartate aminotransferase (AST) and alkaline phosphatase (ALP) in serum are considered as pointers for damaged liver (Dilruba *et al*., 2017). Specifically, ALT is an intracellular enzyme highly concentrated in the liver, which aid in the metabolism of aminoacids by transferring the amino group of alanine to α-oxoglutarate leading to the production of pyruvate. While AST is the enzyme necessary for the transference of amino group from aspartate to α-oxoglutarate leading to the production of oxaloacetate and glutamate.

The liver is a key organ involve in the methylation of arsenic (Choudhury *et al*., 2016). In this study, it was observed that SA induces ALT and ALP enzymes activities significantly ($p<0.05$) by a fold of 1 and 3 respectively compared to control. This findings corroborate previous reports in which SA have been shown to induced the activities of liver enzymes in serum (Gbadegesin *et al*., 2014; Gholamine, *et al*., 2019). Nevertheless, treatment of SA + ELVp at 100 mg/kg reduced the AST, ALT and ALP enzymes activities on a fold of 1.3, 1.3, and 2.6 when compared with SA alone group. This suggest the protective property of ELVp on the liver. Previously, Fodouop *et al*., (2017) revealed that leaf of *V. paradoxa* aqueous extracted with water has liver protective properties against bacterial infection caused by *Salmonella typhinum*. Similaly Ojo *et al*., (2006) revealed the protective nature of the leaf against paracetamol hepato-toxicity. Worthy of note is vitamin E a lipophilic antioxidant, it lower the ALP enzyme activity when compared to SA 6 folds however when compared to control 2 fold. This support the fact that stress arising from redox and antioxidant in-balance are primary indicators for liver damage however with the help of

antioxidant enzymes and compound such damage are prevented (Adetutu *et al*., 2013). The pathological alteration such as periportal inflammation, vascular congestion and fibroblast observed in SA 2.5 mg/kg, SA + vitamin E, SA + ELVp 100 mg/kg and SA + ELVp 200 mg/kg compared with control (distilled water) may have profound effect on the integrity of the liver. This may have enhanced the leakage of the liver function enzymes to the blood resulting in the increased ALT and ALP enzymes observed with SA.

Urea and creatinine are indices use for determining the funtionallity of kidney. The 1.7 and 1.4 fold significant increased in creatinine and urea respectively observed for SA compared with control suggest a damage in the kidney. This may also corroborates studies that have implicated SA as nephrotoxic (Adil *et al*., 2015; Sankar *et al*., 2016). However, ELVp extract at both concentrations ameliorated the nephron-toxic effect of SA. This indicates the protective potential of ELVp against SA-induced nephrotoxicity. The pathological examination of the kidney showed intestinal congestion and moderate peritubular inflammation for SA when compared to control with normal glomerulus. However the alterations observed for SA was reversed when it was co-treated with ELVp 200 mg/kg. This may indicate the nephron-protective potentials of ELVp against sodium arsenite.

5.5 Effect on ROS and antioxidant pathways

One of the most important feature of arsenic as a class 1 human carcinogen is the generation of reactive oxygen species (ROS). The oxidation of arsenic results in the production of hydrogen peroxide (H_2O_2) which can be catabolised by Fenton reaction producing the highly reactive hydroxyl radical (Jomova *et al*., 2011) and the oxidation of its secondary metabolite dimethylarsine leading to the formation of dimethylarsenic radical and superoxide anion. Del Razo *et al* (2002) reported that the ingestion of arsenic result in organelle pertubtion which lead to the uncoupling of the electron transport chain and the generation of reactive species such as OH- and H_2O_2. These events result in the complexation of arsenic with glutathione (As-GSH complex), loss of thiol status, oxidation of cellular constituents and cell injury (Del Razo *et al*., 2002). Bearing the aforementioned in mind, this study showed that exposure to SA significantly increased hydrogen peroxide levels as treatment doses increased. Hydrogen peroxide is among the main ROS causing oxidation in the presence of metals. Specifically H_2O_2 is produced via the dismutasion of

$O2^{\cdot -}$ by superoxide dismutase leading to production of hydroxyl radical OH- (Lee *et al*. 2004; Farina *et al*., 2013). On the contrary, in this study SA co-administration with EAcF at 1 mg/ 10 g diet reduced significantly the generation of H_2O_2 by 18.6 %. This observation is in line with antioxidant properties observed in *Vitellaria paradoxa* leafs earlier in the study.

Catalase is the enzyme that deplete H_2O_2 to water and molecular oxygen hence preventing the formation of hydroxyl radical from H_2O_2. While GST catalyses the conjugation of glutathione to electrophile. In this study, the significant inhibition of catalase and GST activities by sodium arsenite observed follows the outcome of Turk *et al*. (2019). Glutathione S-transferase is a phase 2 enzyme that funtions in organismal survival in response to oxidative stress (Abolaji *et al*. 2015). Thus, the observation that SA inhibited GST activity implies increased ROS generation partly demonstrated here by the accumulation of hydrogen peroxide due to the inhibition of catalase activity. Although, co-admistration of SA with EAcF had no significance for catalase activity however the activity of GST in co-administered treatment group was elevated significantly.

Data presented herein, indicated that the total thiol level and GSH content in flies exposed to SA for 5 days was significantly reduced by 39.3% and 83.8 % respectively when compared to control. This observation may be because arsenic compounds interact with thiol-containing proteins and enzymes thereby altering their native structure as reported by Sunderman (1984). A very important observation herein and worthy of note is that when SA was co-treated with EAcF 1 and 3 (mg/10g diet) respectively the levels of T-SH and GSH significantly increased. It has been reported that T-SH comprises of GSH and other thiol-compounds in the tissue. And both T-SH and GSH are important antioxidant in biological system which prevent damages caused by ROS (Farombi *et al*., 2018). Hence the amelioration of EAcF against SA induced depletion of T-SH and GSH confirms is anti-oxidative potential. Elsewhere, Sharma et al. (2018), reported that treatment of arsenic induced Swiss albino mice with vitamin E and coenzyme Q_{10} significantly increased the T-SH levels.

Although ROS/RNS play an important part in a range of biological activities however elevated intracellular ROS resulting from environmental toxicant like SA induced oxidative

damage to cellular macromolecule in the biological system (Abolaji *et al*., 2014). Furthermore, arsenic toxicity causes increased peroxidation of tissue lipid, a core aspect of oxidative damage (Bhattacharya and Haldar, 2012). Hence, the increased levels of MDA observed for SA treated group in both organs suggest increase in free radical generation in the treated rats. Earlier work of researchers have revealed that treatment with SA induces peroxidation of lipid in liver, testes, kidney and brain (Odunola *et al*., 2013; Adegoke *et al*., 2015). Additionally, the protection of cellular macromolecules like proteins, lipids, nucleic acids from insults of free radicals is promoted by antioxidant enzymes (Abolaji *et al*. 2017). Thus, in this study, cotreatment of SA with vitamin E or ELVp significantly reduced MDA level. This may corroborate the antioxidant property of *V. paradoxa* leaf extract as shown in the *in vitro* study.

Importantly, nitric oxide is involved in several physiological processes in signalling, inflammation and immune function. However, when it accumulates in tissues, it is regarded as a pro-inflammatory biomarker associated with increased oxidative stress (Bashandy *et al*. 2015). The observation that SA increased nitric oxide level is consistent with earlier study of Mehrzadi *et al*. (2018). Also, in this study the increased levels of NO produced by SA was significantly reduced by treatment with EAcF. This is in line with Bera *et al*., (2010) research were L- ascorbate protect rats hepatocytes against sodium arsenite induced NO elevation hence preventing disorders involving excessive cell damage. Research have shown that arsenic damaged is involved in the activating the signalling pathway involving NF-κB whose place in inflammatory reaction is essential (Liu *et al*., 2017). From our result, in the liver, there was no difference in the expression of NF-κB for SA only. However, for the kidney organ it was significantly increased expressed. This may be as a result of the kidney involvement in excretion of arsenic metabolite which are said to be more toxic than the parent compound. This is inline with previous study by Prabu and Muthumani, (2012) were SA increased NF-κB expression. Treatment with vitamin E and ELVp reduced NF-κB expression for both organs, when compared to control. However, the no changes observed upon co-treatment with SA may be that these concentration of ELVp were not high enough to provide anti-inflammatory.

Some studies have highlighted that inflammation are revelevent biological factors that interact with external stimuli and neurophysiological mechanism that triggers movement disoders (Ignacio *et al*., 2019). Acetylcholinesterase is an enzyme that converts acetylcholine to choline and acetate by hydrolysis. It partake in cholinergic neurotramission and control of locomotion activities (Akinyemi *et al*. 2018). The observed decrease in AChE activity in SA treated flies could lead to motor deficits. Earlier report by Abolaji *et al*., (2018) shows that the inhibition of AChE activity could have impeding effect on locomotive activity. Thus suggesting that sodium arsenite caused locomotor deficit in the flies. On the contrary, in this study SA co-administration with EAcF at 1 mg/ 10 g diet increased significantly the activity of AChE. This may have resulted in the increased in locomotive activity observed for the flies when SA was co-treated with EACF at 3 mg/ 10 g diet.

5.6 Survival and fat body histopathological indices

In this study, exposure of flies to SA (0.0625 and 0.125 mM) for 14 days caused significant mortality, this observation could be attributed to accumulation of SA above threshold concentrations with increased exposure time. Similar report was documented by Arnold *et al*. (2014) who displayed increased cytotoxicity of the urothelium of rats and mice in response to increased concentrations of SA. Similarly, Morakinyo *et al,* (2010) recorded the promiscuity of SA in reproductive toxicity. In their study, SA caused diminution of sperm parameters including sperm count and motility accompanied with increased abnormal morphology. This justifies the observation of reduced emergence of offsprings following exposure to SA. Also, Polak *et al*. (2002) observed significant death from embryo to adult *D. melanogaster* following exposure to SA.

On the other hand, in this study, EAcF fraction 1 and 3 mg/10 g diet prolong life span of *D. melanogaster*. Previous studies have shown that phytochemicals such as resveratrol, and curcumin improves life span of *D. melanogaster* (Abolaji *et al*., 2018; Abolaji *et al*., 2020). Also, the present findings showed that co-treatment of SA with EAcF respectively increased the emergence of *D. melanogaster* flies when compared to SA treatment alone. This is in line with previuous study were co-exposure of MPTP and resveratrol improved the

emergence of flies when compared to MPTP (Abolaji *et al*., 2018). It is therefore possible that the antioxidant properties of *V. paradoxa* help in improving reproduction in *D. melanogaster*. However this should be confirmed by researching on reduction in *D. melanogaster* from the point of copulation to emergence.

In the present study, SA induced atrophy of most region and degeneration cells of fat bodies of *D. melanogaster*. Earlier it was stated that the fat body of *D. melanogaster* functions as the liver. Also several studies with rats have shown the toxicity of liver by arsenic compounds (Odunola *et al*., 2011). However treatment with EAcF at both dose showed normal fat bodies. This implies the protective effect of *V.paradoxa* on *D. melanogaster* fatty bodies. Furthermore, co-treatment of SA with EAcF remarkably diminished the atrophy and degeneration of cells induced by SA which collaborate is remediative potential against sodium arsenite induced toxicity in drosophila.

5.7 Effect on clastogenic and proliferative mechanism

The micronucleus test is used in identifying double strands break in DNA and mitotic interference which are indications of carcinogenesis (Samelo *et al*., 2020). Hence, the cytoremediative potential of ELVp on sodium arsenite-induced clastogenicity in rat bone marrow cells was investigated. Treatment with SA resulted in significant increase of mPCEs when compared with control. This is consistent with earlier work from our laboratory which showed induction of mPCEs by sodium arsenite (Odunola *et al*., 2007, Gbadegesin *et al*., 2014). However, upon co-adminsitration with ELVp the frequency of mPCEs was significantly reduced. This improvement may be as a result of the phenols and polyphenols present in ELVp which have the ablity to donate is hydrogen ion hence preventing sequential oxidation reactions.

The first step in the quest for new anticancer drugs is cytotoxicity evaluation. Here, cytotoxicity activity of three fraction of *V. paradoxa* ethanol leaves extract were determined using MTT. The chloroform (CHLF) and ethyl acetate fraction (EACF) significantly reduced cell viability of MCF-7 cells in a concentration manner. However, the ethyl acetate fraction was more cytotoxic as the duration of treatment increased. Hence, EACF fraction

was used in screening A549, MCF-7 and HepG2. This cell lines was chosen for the present study, because lungs, breast and liver cancer remains the leading cause of cancer death (Sung *et al*., 2021). The present study showed that the ethyl acetate fraction (EACF) significantly induced cytotoxicity to A549, MCF-7 and Hep G2 in a concentration and time dependent manner. However, it was most active in MCF-7, thus MCF-7 cell lines were used for further *in vitro* antiproliferative assays. The result observed for the MTT assay was consistent with Al-Zharani *et al*., (2019) who found that the greatest cytotoxic effect against MCF-7 and MDA-MB 231 cells was displayed by chloroform and ethyl acetate fraction of Rhazya stricta fruit extract. In addition, the cytotoxicity of triterpenoid of stem bark of *Vitellaria paradoxa* against breast cancer cell line have been reported by Eyong *et al*., (2018).

Apart from using MTT to determine cytotoxicity, colony formation assay has high sensitivity in determining anti-proliferative activity. The inhibition observed for colony formation confirms the anti-proliferative activity of EACF in MCF-7 cells because the eradication of the capacity for unlimited proliferation is required for the prevention of tumours (Franken *et al*., 2006).

Also, cancer cells exhibits elevated oxidative stress which aggregate cell proliferation as a result of metabolic and signalling aberration. Therefore one approach in cancer therapy is the use of antioxidant which scavenge reactive species, impairs oxidative stress and inhibit cell growth. Hence, the determination of ROS generation of MCF-7 cell by DCFDA. Interestingly, various dose of EACF reduced the amount of ROS generated significantly. This confirms the antioxidantive potential of the ethyl acetate fraction. This is in line with Teoh *et al*., (2013) research which showed the ethyl acetate fraction to exhibit good antioxidant and antiproliferative effect out of all fractions of methanol extract of Gynura procumbens. This may suggest that ethyl acetate fraction of ELVp induced is antiproliferative activity independent of ROS. In contrast to our result, Anatole *et al*., (2013) reported the ethyl acetate fraction of Garcina epunctata to induce apoptosis through the generation of ROS in human promyleocytic cells (HL60).

5.8 Cell cycle and apoptotic pathway

In the present study, most cells of MCF-7 was at sub G0 peak after treatment with ethyl acetate fraction of *Vitellaria paradoxa* leaf. This result suggest that ethyl acetate fraction induced cell death in MCF-7 cells. Also, treatment of MCF-7 with ethyl acetate fraction at 72 hrs drastically reduced the G2/M population and increased G0/G1 population. This may indicate that ethyl acetate fraction of *V.paradoxa* leaf arrest cells in the G0/G1 phase by inducing cells to go from the G2/M phase to the sub G0 phase.

During a cell cycle there are checkpoints that help in arresting damaged cells thereby inducing an occasion for repair or activating programmed cell death in situations of irreversibility of cellular damaged which is accompanying with increased sub G0 peak considered as apoptotic cells (Hussin *et al*., 2018; Otitoju *et al*., 2019). Simillarly Anatole *et al*., (2013) have shown that the ethyl acetate fraction of *G. epunctata* treatment significantly arrested HL-60 cells at the G0/G1 phase.

Furthermore, p53 a protein involve in regulatory process of apoptosis and cell cycle when triggered by was assessed. The present study showed that p53 expression in kidney was significantly increased for SA treated rats. Also, upon administration ELVp there was increase in p53 expression in both organs. This may be because ROS is involve in initiating the intrinsic process of apoptosis. The reduction in BCL-2 observed for co-treated group for both organs support that ELVp may carry out is remediative property against arsenic by inducing apoptosis. Apoptosis, is a vital physiological process necessary for homeostasis and development of an organism. Apoptosis is mainly regulated by caspases which are grouped into initiator and executor caspases (Elmore, 2007). In the present study the executor caspase 3 was assessed in his un-activated from i.e pro-caspase 3 and cleaved form i.e after activation. The result showed that treatment of MCF-7 with EACF drastically reduced the activity of pro-caspase 3 and increased cleaved caspase 3 suggesting that apoptosis might play a role in its antiproliferative activity.

CHAPTER SIX

SUMMARY AND CONCLUSION

6.1 Summary

Exposure to arsenic is one of the predisposing factors of cancer. However, the search for drugs which have the ability to target cancer cells without inducing damage to normal cells is still ongoing. This study, investigated the cytoremediative potentials of *Vitellaria paradoxa* against arseni- induced toxicity in Wistar rats and *Drosophila melanogaster* along with its antiproliferative action on MCF-7 cells.

In this study, the profile for the *in vitro* antioxidant and genotoxic potentials of the hydroethanol extracts of *V. paradoxa* leaves and seed were assessed. The effects of the hydroethanol leaves extract of *V. paradoxa* (ELVp) on liver, kidney, haematological indices, clastogenic marker, and expression of inflammatory and apoptotic proteins were investigated in sodium arsenite-treated rats. Oxidative stress markers such as hydrogen peroxide and nitric oxide levels, catase and glutathione-S-transferase activities, total thiol and reduced glutathione (GSH) levels as well as life span elongation by ethyl acetate fraction of ELVp was determined in sodium arsenite-treated *Drosophila melanogaster*. Finally, the antiproliferative mechanism of the ethyl acetate fraction of ELVp was determined in MCF-7 cells.

The hydroethanol leaves extract of *Vitellaria paradoxa* possessed important phytochemical and antioxidant properties. The lethal dose of ELVp is greater than 5000 mg/kg however higher doses may induce inflammatory response. In line with the antioxidant properties, treatment of ELVp markedly ameliorated hepatotoxicity, nephrotoxicity, clastogenity induced by sodium arsenite in rats. The ethyl acetate fraction (EACF) prolong life span of D. melanogaster, it ameliorated SA- induced elevtion of NO and H_2O_2 levels, reduction of contents of T-SH and GSH and inhibition of catalase and GST activities. The ethyl aetate

fraction of ELVp was more cytotoxic against MCF-7 cells, it significantly reduced ROS generation and induced antiproliferative activity.

6.2 Conclusion

Exposure to environmental toxicants such as arsenic has a high implication in carncinogenesis. The epidemiology of cancer is associated with mechanism involving ROS generation, uncontrolled proliferation of damaged cells, lack of cell cycle arrest and evasion of apoptosis. This study provided evidence that hydro ethanol extract (ELVp) and ethyl acetate fraction (EACF) of the leaves of *Vitellaria paradoxa* leaves possess high antioxidant and antiproliferative porperties. The occurance of liver function enzymes and kidney function biomarkers in the serum is an indication of liver and kidney toxicity by arsenic. For the first time in this study, ELVp protected liver and kidney from arsenic damage by induction of P53 and inhibiton of BCL-2 proteins. Also, the induction of ROS/RNS by arsenic based on increased hydrogen peroxide and nitric oxide levels and reduction in antioxidant biomarkers were remediated by EACF through the augmentation of the antioxidant enzyme's system leading to the protection and extension of life span of the *Drosophila melanogaster*.

The antiproliferative activity recorded in MCF-7 cells is an indication of the antioxidant activity of *Vitellaria parvdoxa* leaf which resulted in the reduction of ROS generation and arrest of MCF-7 cells at the G0/G1 phase of the cell cycle. These activities might be because phytol and squalene are present in the ethyl acetate fraction.

6.3 Recommendation

It is recommended that further scientific research be carried out on the use of *Vitellaria paradoxa* leaves on the treatment of cancer focusing on other mechanistic pathways using a higher model. Also the bioactive compounds present in *V. paradoxa* leafs can be formulated into drugs for the treatment of cancer by pharmaceutical companies.

6.4 Contributions to Knowledge

1. This study is probably the first empirical evidence of *Vitellaria paradoxa* leaf eliciting it hepato-protective and nephron-protective activities against arsenic induced toxicities via the upregulation of P53 and inhibition of BCL-2 proteins.
2. The study is probably the first report on the ability of ethyl acetate fraction of *Vitellaria paradoxa* ethanol leaf extract to augment the antioxidant enzymes system of *D. melanogaster* from sodium arsenite-induced oxidative stress due to the presence of high antioxidant properties in *Vitellaria paradoxa* leaf.
3. The antiprolioferative activity of the ethyl acetate fraction is independent of ROS and through the arrest of DNA damage at G0/G1 phase of cell cycle in MCF-7 cells.

REFERENCES

Abolaji, A. O., Adedara, A. O., Adie, M. A., Vicente-Crespo, M. and Farombi, E. O. 2018. Resveratrol prolongs lifespa n and improves 1-methyl-4-phenyl-1,2,3,6-tetrahydropyridine-induced oxidative damage and behavioural deficits in Drosophila melanogaster. *Biochemical and biophysical research communications*, 503.2: 1042–1048.

Abolaji, A. O., Fasae, K. D., Iwezor, C. E., Aschner, M., and Farombi, E. O. 2020. Curcumin attenuates copper-induced oxidative stress and neurotoxicity in *Drosophila melanogaster*. *Toxicology reports* 7: 261–268.

Abolaji, A. O., Kamdem, J. P., Lugokenski, T. H., Farombi, E. O., Souza, D. O., da Silva Loreto, É. L., and Rocha, J. 2015. Ovotoxicants 4-vinylcyclohexene 1,2-monoepoxide and 4-vinylcyclohexene diepoxide disrupt redox status and modify different electrophile sensitive target enzymes and genes in Drosophila melanogaster. *Redox biology* 5: 328–339.

Abolaji, A. O., Kamdem, J. P., Lugokenski, T. H., Nascimento, T. K., Waczuk, E. P., Farombi, E. O., Loreto, É. L. and Rocha, J. B. 2014. Involvement of oxidative stress in 4-vinylcyclohexene-induced toxicity in Drosophila melanogaster. *Free radical biology and medicine* 71: 99–108.

Abolaji, A.O., Babalola, O.V., Adegoke, A.K. and Farombi, E.O. 2017. Hesperidin, a citrus bioflavonoid, alleviates trichloroethylene-induced oxidative stress in Drosophila melanogaster. *Environmental Toxicology and Pharmacology* 55: 202-207

Abolaji, A.O., Kamdem, J.P., Farombi, E.O. and Rocha, J.B.T. 2013. Drosophila melanogaster as a promising model organism in toxicological studies: A Mini review. *Archieve of Basic and Applied Medicine* 1: 33-38.

Abu-Darwish, M. S. and Efferth, T. 2018. Medicinal Plants from Near East for Cancer Therapy. *Frontiers in pharmacology* 9: 56.

Acehan, D., Jiang, X., Morgan, D. G., Heuser, J. E., Wang, X. and Akey, C. W. 2002. Three-dimensional structure of the apoptosome: implications for assembly, procaspase-9 binding, and activation. *Molecular cell* 9.2: 423–432.

Adegoke, A. M., Gbadegesin, M. A., and Odunola, O. A. 2017. Methanol Extract of *Adansonia digitata* Leaf Protects Against Sodium Arsenite-induced Toxicities in Male Wistar Rats. *Pharmacognosy research* 9.1: 7–11.

Adegoke, A.M., Gbadegesin, M.A., Otitoju, A.P. and Odunola, O.A. 2015. Hepatotoxicity and genotoxicity of sodium arsenite and cyclophosphamide in rats: protective effect of aqueous extract of Adansonaia digitata L. Fruit pulp. *British Journal of Medicine and medical research* 8.11: 963-974.

Adetutu, A., Owoade, O.A. and Oyekunle, O.S. 2013. Comparative effects of some medicinal plants on sodium arsenite - induced clastogenicity. *International Jornal of Pharma and Bio Sciences* 4.2: 777-783.

Adil, M., Kandhare, A. D., Visnagri, A. and Bodhankar, S. L. 2015. Naringin ameliorates sodium arsenite-induced renal and hepatic toxicity in rats: decisive role of KIM-1, Caspase-3, TGF-β, and TNF-α. *Renal failure* 37.8: 1396–1407.

Agarwal, M. L., Agarwal, A., Taylor, W. R. and Stark, G. R. 1995. p53 controls both the G2/M and the G1 cell cycle checkpoints and mediates reversible growth arrest in human fibroblasts. *Proceedings of the National Academy of Sciences of the United States of America*, *92*.18: 8493–8497.

Aguilar-González, M. G., Hernández, A., López, M. L., Mendoza-Figueroa, T. and Albores, A. 1999. Arsenite alters heme synthesis in long-term cultures of adult rat hepatocytes. Toxicological sciences: an official journal of the Society of Toxicology, 49(2), 281–289.

Ahluwalia, A., Jones, M.K., Matysiak-Budnik, T. and Tarnawski, A.S. 2014**.** VEGF and colon cancer growth beyond angiogenesis: does VEGF directly mediate

colon cancer growth via a non-angiogenic mechanism? *Curr Pharm Des*. 20.7: 1041-4.

Ahmed, R.N., Sani, A. and Igunnugbemi, O. O. 2009. Antifungal Profiles of Extracts of Vitellaria paradoxa (Shea-Butter) Bark. *Ethnobotanical Leaflets* 13: 679-88.

Akhter, S., Halim, A. Sohel, S.I. Serker, S.K. Chowdhury, M.H.S. and Sonet, **S.S.** 2008. A review of the use of non timber forest products in beauty care in Bangladesh. *J. Forest. Res*. 19: 72-78.

Akin-idowu, P.E., Odunola, O.A., Gbadegesin, M.A., Aduloju, A.O., Owumi, S.A. and Adegoke, A.M. 2015**.** Hepatoprotective effect of Amaranthus hypochondriacus seed extract on sodium arsenite – induced toxicity in male wistar rats. *Journal of Medicinal plants research* 9.26: 731-740.

Akinyemi, A. J., Oboh, G., Ogunsuyi, O., Abolaji, A. O. and Udofia, A. 2018. Curcumin-supplemented diets improve antioxidant enzymes and alter acetylcholinesterase genes expression level in Drosophila melanogaster model. *Metabolic brain disease* 33.2: 369–375.

Al-Zharani, M., Nasr, F.A., Abutaha, N., Alqahtani, A.S., Noman, O.M., Mubarak, M. and Wadaan, M.A. 2019. Apoptotic Induction and Anti-Migratory Effects of *Rhazya Stricta* Fruit Extracts on a Human Breast Cancer Cell Line. *Molecules* 24.21: 3968.

American Cancer Society. 2018. Global Cancer Facts & Figures 4th Edition. Atlanta: American Cancer Society;

American Cancer Society. 2019. Cancer Fact and Figure - (www. Cancer.org> research> cancer. Accessed November 30, 2019, 10.50 AM).

Anatole, C. P., Guru, S. K., Bathelemy, N., Jeanne, N., Bhushan, S., Murayama, T. and Saxena, A. K. 2013. Ethyl acetate fraction of Garcina epunctata induces apoptosis in human promyelocytic cells (HL-60) through the ROS generation and G0/G1 cell cycle arrest: a bioassay-guided approach. *Environmental toxicology and pharmacology* 36.3: 865–874.

Andrew, A. S., Burgess, J. L., Meza, M. M., Demidenko, E., Waugh, M. G., Hamilton, J. W., and Karagas, M. R. 2006. Arsenic exposure is associated with decreased DNA repair in vitro and in individuals exposed to drinking water arsenic. *Environmental health perspectives* 114.8: 1193–1198.

Anetor, G. O. 2016. Waste dumps in local communities in developing countries and hidden danger to health. *Perspectives in public health* 136.4: 245–251.

Anwar, N. and Qureshi, I. Z. 2019. *In vitro* application of sodium arsenite to mice testicular and epididymal organ cultures induces oxidative, biochemical, hormonal, and genotoxic stress. *Toxicology and industrial health 35*.10: 660–669.

Appleby, N., and Angelov, D. 2017. Clinical and laboratory assessment of a patient with thrombocytosis. *British journal of hospital medicine* (London, England: 2005), 78(10), 558–564.

Arnold, L.L., Suzuki, S., Yokohira, M., Kakiuchi-Kiyota, S., Pennington, K.l. and Cohen, S.M. 2014**.** Time course of Urothelial change in rats and mice orally administered arsenite. *Toxicological Pathology* 42.5: 855-962.

Ashkenazi, A., Fairbrother, W. J., Leverson, J. D. and Souers, A. J. 2017. From basic apoptosis discoveries to advanced selective BCL-2 family inhibitors. *Nature reviews. Drug discovery 16*.4: 273–284.

Ayankunle, A., Kolawole, O.T., Adesokan, A.A. and Akiibinu, M.O. 2012. Antibacterial Activity and Sub-chronic Toxicity Studies of Vitellaria paradoxa Stem Bark Extract. Journal of Pharmacology and Toxicology 7: 298-304.

Azam, S. M., Sarker, T. C. and Naz, S. 2016. Factors affecting the soil arsenic bioavailability, accumulation in rice and risk to human health: a review. *Toxicology mechanisms and methods 26*.8: 565–579.

Barbieri, R., Coppo, E., Marchese, A., Daglia, M., Sobarzo-Sánchez, E., Nabavi, S. F. and Nabavi, S. M. 2017. Phytochemicals for human disease: An update on

plant-derived compounds antibacterial activity. *Microbiological research 196*: 44–68.

Bashandy, S.A.E., El-Awdan, S.A, Ebaid, H. and Alhazza, I.M. 2015. Antioxidant potential of Spirulina platensis mitigates oxidative stress and reprotoxicity induced by sodium arsenite in male rats. *Oxidative Medicine and Cellular Longevity*, 2016, 7174351.

Basu, A.K. 2018. DNA damage, mutagenesis and cancer. *Int J Mol Sci* 19. 4: 970.

Bera, A. K., Rana, T., Das, S., Bandyopadhyay, S., Bhattacharya, D., Pan, D., De, S. and Das, S. K. 2010. L-Ascorbate protects rat hepatocytes against sodium arsenite--induced cytotoxicity and oxidative damage. *Human & experimental toxicology 29*.2: 103–111.

Bhattacharya, S. 2017. Medicinal plants and natural products in amelioration of arsenic toxicity: a short review. *Pharmaceutical biology 55*.1: 349–354.

Bhattacharya, S. and Haldar, P.K. 2012. Trichosanthes dioica fruit ameliorates experimentally induced arsenic toxicity in male albino rats through the alleviation of oxidative stress. *Biol Trace Elem Res*. 148.2: 232-41**.**

Biau, J., Chautard, E., Court, F., Pereira, B., Verrelle, P., Devun, F., De Koning, L., and Dutreix, M. 2016. Global Conservation of Protein Status between Cell Lines and Xenografts. *Translational oncology* 9.4: 313–321.

Biswas, A., Swain, S., Chowdhury, N.R., Joardar, M., Das, A., Mukherjee, M. and Roychowdhury, T. 2019. Arsenic contamination in Kolkata metropolitan city: perspective of transportation of agricultural products from arsenic – endemic areas. Environ Sci Pollut Res Int. 26,22: 22929-22944.

Bjørklund, G., Aaseth, J., Chirumbolo, S., Urbina, M. A., and Uddin, R. 2018. Effects of arsenic toxicity beyond epigenetic modifications. *Environmental geochemistry and health* 40.3: 955–965.

Borner, C. 2003. The Bcl-2 protein family: sensors and checkpoints for life-or-death decisions. *Molecular immunology 39*.11: 615–647.

Brand, A. H. and Perrimon, N. 1993. Targeted gene expression as a means of altering cell fates and generating dominant phenotypes. *Development (Cambridge, England)*, 118.2: 401–415.

Brand-Williams, W., Cuvelier, M.E. and Berset, C. 1995. Use of a free radical method to evaluate antioxidant activity. LWT—*Food Sci. Technol*. 28: 25–30.

Brucken, U., Schmidt, M., Pressler, S., Janseen, T., Thombiano, A. and Zizka, G. 2008. *Vitellaria paradoxa*, a West African Plant: A Photoguide. Senkenberg Research Institute, Germany.

Bryant, P. J., and Schmidt, O. 1990. The genetic control of cell proliferation in Drosophila imaginal discs. *Journal of cell science. Supplement* 13: 169–189.

Chaabane, F., Boubaker, J., Loussaif, A., Neffati, A., Kilani- jaziri, S., Ghedira, K. and Chekir-Ghedira, L. 2012. Antioxidant, genotoxic and antigenotoxic activities of daphne gnidium leaf extract. *BMC Complementary and Alternative Medicine* 12: 153.

Chatterjee, D., Katewa, S. D., Qi, Y., Jackson, S. A., Kapahi, P. and Jasper, H. 2014. Control of metabolic adaptation to fasting by dILP6-induced insulin signaling in Drosophila oenocytes. *Proceedings of the National Academy of Sciences of the United States of America*, *111*.50: 17959–17964.

Chen, S.J., Yan, X.J. and Chen, Z. 2013. Arsenic in Tissues, Organs, and Cells. In: Kretsinger R.H., Uversky V.N., Permyakov E.A. (eds) Encyclopedia of Metalloproteins. Springer, New York, NY. https://doi.org/10.1007/978-1-4614-1533-6_491

Chen, W., Yang, J., Chen, J., and Bruch, J. 2006. Exposures to silica mixed dust and cohort mortality study in tin mines: exposure-response analysis and risk

assessment of lung cancer. *American journal of industrial medicine* 49.2: 67–76.

Chen, X., Chen, J., Gan, S., Guan, H., Zhou, Y., Ouyang, Q. and Shi, J. 2013. DNA damage strength modulates a bimodal switch of p53 dynamics for cell-fate control. *BMC biology 11*: 73.

Chien, S., Reiter, L. T., Bier, E. and Gribskov, M. 2002. Homophila: human disease gene cognates in Drosophila. *Nucleic acids research 30*.1: 149–151.

Chiocchetti, G. M., Domene, A., Kühl, A. A., Zúñiga, M., Vélez, D., Devesa, V. and Monedero, V. 2019**.** In vivo evaluation of the effect of arsenite on the intestinal epithelium and associated microbiota in mice. Arch Toxicol. 93.8: 2127-2139.

Chiocchetti, G. M., Domene, A., Kühl, A. A., Zúñiga, M., Vélez, D., Devesa, V. and Monedero, V. 2019**.** In vivo evaluation of the effect of arsenite on the intestinal epithelium and associated microbiota in mice. Arch Toxicol. 93.8: 2127-2139.

Choudhury, S., Ghosh, S., Mukherjee, S., Gupta, P., Bhattacharya, S., Adhikary, A. and Chattopadhyay, S. 2016. Pomegranate protects against arsenic-induced p53-dependent ROS-mediated inflammation and apoptosis in liver cells. *The Journal of nutritional biochemistry 38*: 25–40.

Claiborne, A. 1985. Catalase activity. In: Greenwald, R.A., Ed., CRC Handbook of Methods for Oxygen Radical Research, CRC Press, Boca Raton, 283-284.

Cohen, S. M., Ohnishi, T., Arnold, L. L. and Le, X. C. 2007. Arsenic-induced bladder cancer in an animal model. *Toxicology and applied pharmacology* 222.3: 258–263.

Cominetti, M. R., Altei, W. F., and Selistre-de-Araujo, H. S. 2019. Metastasis inhibition in breast cancer by targeting cancer cell extravasation. *Breast cancer (Dove Medical Press) 11*: 165–178.

Costa, M. 2019. Review of arsenic toxicity, speciation and polyadenylation of canonical histones. *Toxicology and applied pharmacology* 375: 1–4.

Coulibaly, F.A., Nonvide, F.K., Yaye, G.Y. and Djaman JA. 2014**.** Evaluation of the antidiabetic activity of the extracts of *Vitellaria paradoxa* in oryctolaguscumculus rabbits. *The Experiment International Of Science And Technology* 24.3: 1673- 1682.

Cragg, G. M. and Pezzuto, J. M. 2016. Natural Products as a Vital Source for the Discovery of Cancer Chemotherapeutic and Chemopreventive Agents. *Medical principles and practice : international journal of the Kuwait University, Health Science Centre* 25*. Suppl 2*: 41–59.

Das, S., Upadhaya, P. and Giri, S. 2016. Arsenic and smokeless tobacco induce genotoxicity, sperm abnormality as well as oxidative stress in mice in vivo. *Genes and environment: the official journal of the Japanese Environmental Mutagen Society 38*: 4.

de Sá Junior, P. L., Câmara, D., Porcacchia, A. S., Fonseca, P., Jorge, S. D., Araldi, R. P. and Ferreira, A. K. 2017. The Roles of ROS in Cancer Heterogeneity and Therapy. *Oxidative medicine and cellular longevity* 2467940.

Deepa Parvathi Va, Akshaya Amritha Sa, and Solomon FD Paul 2009. Wonder animal model for genetic studies - drosophila melanogaster –its life cycle and breeding methods – a review *Sri Ramachandra Journal of Medicine* 2: 33-38

Del Razo, L. M., Garcia-Vargas, G. G., Garcia-Salcedo, J., Sanmiguel, M. F., Rivera, M., Hernandez, M. C., & Cebrian, M. E. 2002. Arsenic levels in cooked food and assessment of adult dietary intake of arsenic in the Region Lagunera, Mexico. Food and chemical toxicology : an *international journal published for the British Industrial Biological Research Association*, 40(10), 1423–1431.

Demerec, M. and Kaufman, P. 1996. Drosophila Guide: Introduction to the genetics and cytology of Drosophila melanogaster. Cold Spring Harbor Laboratory; 4-8.

Desai, A. G., Qazi, G. N., Ganju, R. K., El-Tamer, M., Singh, J., Saxena, A. K., Bedi, Y. S., Taneja, S. C. and Bhat, H. K. 2008. Medicinal plants and cancer chemoprevention. *Current drug metabolism* 9.7: 581–591.

Dilruba, S., Hasibuzzaman, M.M., Rahman, M., Mohanto, N.C., Aktar, S., Rahman, A., Hossain, M.I., Noman, A.S.M., Nikkon, F., Saud, Z.A. and Hossain, k. 2017. Ameliorating effects of Raphanus sativus leaves on sodium arsenite-induced perturbation of blod indiced in Swiss albino mice. *Asian Pacific Journal of Tropical Biomedicine* 7.10: 915-920**.**

Donnez, J., Binda, M. M., Donnez, O. and Dolmans, M. M. 2016. Oxidative stress in the pelvic cavity and its role in the pathogenesis of endometriosis. *Fertility and sterility 106*.5: 1011–1017.

Egbinola, C. N. and Amanambu, A. C. 2014. Groundwater contamination in Ibadan, South-West Nigeria. *SpringerPlus*, *3*: 448.

Ellman, G.L. 1959. Tissue sulfhydryl groups. *Arch. Biochem. Biophys*. 82: 70-77.

Ellman, G.L., Courtney, K.D., Andres, V. and Feathers-Stone, R.M. 1961. A new and rapid colorimetric determination of acetylcholinesterase activity. *Biochem. Pharmacol*. 7: 182-189.

El-Mahmood, A. M, Doughari, J. H. and Ladan, N. 2008. Antimicrobial screening of stem bark extracts of Vitellaria paradoxa against some enteric pathogenic microorganisms. *African Journal of Pharmacy and Pharmacology* 2.5: 089-094.

Elmore, S. 2007. Apoptosis: a review of programmed cell death. *Toxicologic pathology* 35.4: 495–516.

Engeland, K. 2018. Cell cycle arrest through indirect transcriptional repression by p53: I have a DREAM. *Cell death and differentiation* 25.1: 114–132.

Eyong, K.O., **Bairy, G., Eno, A.A., Taube, J., Hull, K.G., Folefoc, G.N., Foyet, H.S. and Romo, D.** 2018. Triterpenoids from stem bark of Vitellaria paradoxa (Sapotaceae) and derived esters exhibits cytotoxicity against a breast cancer cell line. *Med Chem Res* 27: 268-277.

Fabiana, F., Maribel, G., Marioly, V.T., Carlos, F.M. M. and Ángel, S. 2017. Toxic Evaluation of Cymbopogon citratus Chemical Fractions in E. coli. *Cosmetic* 4: 20.

Faita, F., Cori, L., Bianchi, F. and Andreassi, M. G. 2013. Arsenic-induced genotoxicity and genetic susceptibility to arsenic-related pathologies. *International journal of environmental research and public health* 10.4: 1527–1546.

Famewo, E. B., Clarke, A. M. and Afolayan, A. J. 2016. Identification of bacterial contaminants in polyherbal medicines used for the treatment of tuberculosis in Amatole District of the Eastern Cape Province, South Africa, using rapid 16S rRNA technique. *Journal of health, population and nutrition 35*.1: 27.

Farina, M., Avila, D. S., da Rocha, J. B. and Aschner, M. 2013. Metals, oxidative stress and neurodegeneration: a focus on iron, manganese and mercury. *Neurochemistry international*, *62*:5: 575–594.

Farombi, E.O., Abolaji, A.O., Farombi, T.H., Oropo, A.S., Owoje, O.A. and Awunah, M. T. 2018. Garcinia kola seed biflavonoid fraction (kolaviron), increases longevity and attenuates rotenone-induced toxicity in Drosophila melanogaster. *Pesticide Biochemistry and Physiology* 145: 39-45.

Feany, M.B. and Bender, W.W. 2000. A Drosophila model of parkinson's disease. *Nature* 404: 394-398.

Ferlay, J., Shin, H. R., Bray, F., Forman, D., Mathers, C. and Parkin, D.M. 2010. Estimates of worldwide burden of cancer in 2008: GLOBOCAN 2008. *Int. J. Cancer* 127: 2893-2917.

Ferry, M.P., Gessain, M. and Geeain, R. 1974. Vegetative Propagation of Shea, Kola and Pentadesma. Cocoa research institute, Ghana Annual Report (1987/88): 98-100.

Fodouop, S.P.C., Tala, S.D. Keilah, L.P. Kodjio, N. Yemele, M.D. Nwabo, A.h.k. Njikah, B. Tchoumboue, J. and Gatsing. D. 2017**.** BMC Complementary and Alternative Medicine. 17: 160

Foe, V.E. Odeli, G.M. and Edgar, B.A. 1993. Mitosis and Morphogenesis in the Drosophila embryo. In The Development of Drosophila melanogaster (Vol. I) (Arias, M.B.a.A.M., ed.), pp. 149–300, Cold Spring Harbor Laboratory Press

Foyet, H.S., Tsala, D.E. Bodo, J.C.Z.E. Carine, A.N. Heroyne, L.T. and Oben. E.K. 2015**.** Anti-inflammatory and anti-arthritic activity of a methanol extract from *Vitellaria paradoxa* stem back. *Pharmacognosy Res*. 7.4: 367.

Franken, N.A.P., Rodermond, H.M., Stap, J., Haveman, J. and Bree, C.V. 2006. Clonogenic assays of cells in vitro. *Nature protocol* 1.5: 2315-239.

Ganapathy, S., Liu, J., Xiong, R., Yu, T., Makriyannis, A. and Chen, C. 2019**.** Chronic low dose arsenic exposure preferentially pertubs mitotic phase of the cell cycle. Genes cancer. 10.1-2: 39-51

Gbadegesin, M.A., Adegoke, A.M., Ewere, E. G. and Odunola, O.A. 2014. Hepatatoprotective and anticlastogenic effects of ethanol extract of Irvingia gabonensis (IG) leaves in sodium arsenite induced toxicity in male wistar rats. *Niger. J. Physiol. Sci.* 29: 029-036.

Gbadegesin, M.A., Odunola, O.A., Akinwumi, K.A. and Osifeso, O.O. 2009. Comparative hepatotoxicity and clastogenicity of sodium arsenite and three petroleum products in experimental Swiss Albino mice: the modulatory effect of Aloe vera gel. *Food Chem Toxicol* 47.10: 2454-2457.

Genthe, B., Kapwata, T., Le Roux, W., Chamier, J. and Wright, C. Y. 2018. The reach of human health risks associated with metals/metalloids in water and

vegetables along a contaminated river catchment: South Africa and Mozambique. *Chemosphere 199*, 1–9.

Gholamine, B., Houshmand, G., Hosseinzadeh, A., Kalantar, M., Mehrzadi, S. and Goudarzi, M. 2019. Gallic acid ameliorated sodium arsenite-induced renal and hepatic toxicity in rats. *Drug Chem Toxicol*. 25: 1-12.

Gholamine, B., Houshmand, G., Hosseinzadeh, A., Kalantar, M., Mehrzadi, S. and Goudarzi, M. 2019. Gallic acid ameliorated sodium arsenite-induced renal and hepatic toxicity in rats. *Drug Chem Toxicol*. 25: 1-12.

Gillet, J.P., Varma, S. and Gottesman, M. M. 2013. The clinical relevance of cancer cell lines. *J Natl Cancer Inst*. 105.7: 452–458.

Goldar, S., Khaniani, M. S., Derakhshan, S. M., and Baradaran, B. 2015. Molecular mechanisms of apoptosis and roles in cancer development and treatment. *Asian Pacific journal of cancer prevention: APJCP*, *16*.6: 2129–2144.

Gonzalez, C. 2013. Drosophila melanogaster: a model and a tool to investigate malignancy and identify new therapeutics. *Nature reviews. Cancer* 13.3: 172–183.

Goodspeed, A., Heiser, L. M., Gray, J. W. and Costello, J. C. 2016. Tumor-Derived Cell Lines as Molecular Models of Cancer Pharmacogenomics. *Molecular cancer research: MCR, 14*.1: 3–13.

Goudarzi, M., Fatemi, I., Siahpoosh, A., Sezavar, S.H., Mansouri, E. and Mehrzadi, S. 2018. Protective Effect of Ellagic Acid Against Sodium Arsenite-Induced Cardio- and Hematotoxicity in Rats. *Cardiovasc Toxicol.* 18.4: 337-345.

Green L.C., Wagner D.A., Glogowski J., Skipper P.L., Wishnok J.S. and Tannenbaum S.R. 1982. Analysis of nitrate, nitrite and (^{15}N) nitrate in biological fluids. Anal. Biochem. 126:131–138.

Greenwell, M. and Rahman, P. K. 2015. Medicinal Plants: Their Use in Anticancer Treatment. *International journal of pharmaceutical sciences and research, 6*.10: 4103–4112.

Gupta, R. and Flora, S.J. 2005. Protective value of Aloe vera against some toxic effects of arsenic in rats. *Phytother Res*. 19: 23-28.

Gutiérrez, J. B. and Salsamendi, A. L. 2001. Fundamientos de ciência toxicológica. *Diaz de Santos, Madrid,* p. 155–177.

Gwali, S., Okullo, J. B. L., Eilu, G., Nakabonge, G., Nyeko, P. and Vuzi, P. 2011. Folk classification of Shea butter tree (Vitellaria paradoxa subsp. nilotica) ethno-varieties in Uganda. *Ethnobot. Res. Appl.* 9: 243- 256.

Habig, W.H. and Jakoby, W.B. 1981. Assays for differentiation of glutathione-S-transferase *Methods Enzymol*. 77: 398-405.

Hall, J. B., Aebischer, D. P., Tomlison, H.F., Osei-Amaning, E. and Hindle, J.R. 1996. Vitellaria paradoxa: a monograph. School of Agricultural and Forest Sciences, University of Wales, Bangor

Harquin, S. F., Acha, E. A., Eyong, K. O., Oana, C. and Monica, H. L. 2015. Effect of the methanolic extract of *Vitellaria paradoxa* stem bark against scopolamine –induced cognitive dysfunction and oxidative stress in the rat hippocampus. *Cellular and molecular neurobiology* pp1-11

Hassen, S., Ali, N. and Chowdhury, P. 2012. Molecular signaling mechanisms of apoptosis in hereditary non-polyposis colorectal cancer. *World journal of gastrointestinal pathophysiology*, *3*.3: 71–79.

Hata, A. N., Engelman, J. A., and Faber, A. C. 2015. The BCL2 Family: Key Mediators of the Apoptotic Response to Targeted Anticancer Therapeutics. *Cancer discovery 5*.5: 475–487.

He, Y. C., He, L., Khoshaba, R., Lu, F. G., Cai, C., Zhou, F. L., Liao, D. F. and Cao, D. 2019. Curcumin Nicotinate Selectively Induces Cancer Cell Apoptosis

and Cycle Arrest through a P53-Mediated Mechanism. *Molecules (Basel, Switzerland)*, *24*.22: 4179.

Heddle, J.A, Sudharsan R.A.and Krepinsky A.B 1981. The micronucleus assay II: In vitro. Topics in environmental physiology and medicine. Short term tests for chemical carcinogens. H.F. Stich and R. H.C. San. Eds. Springer-Verlag, New York, Heidelberg, Berlin

Henry A. N., Chithra V. and Nair N. C. 1983. Vitellaria vs. Butyrospermum (Sapotaceae). Taxon, 32: 282-286

Herranz, H. and Cohen, S. M. 2017. Drosophila as a Model to Study the Link between Metabolism and Cancer. *Journal of developmental biology 5*.4: 15.

Hientz, K., Mohr, A., Bhakta-Guha, D., and Efferth, T. 2017. The role of p53 in cancer drug resistance and targeted chemotherapy. *Oncotarget*, 8.5: 8921–8946.

Hong, T.D., Linigton, S. and Ellis, R.H. 1996. Seed Storage Behavior: A Compendium Handbook for Genebanks. IPGRI, Rome, pp: 656.

https://monographs.iarc.who.int/wp-content/uploads/2018/06/mono100C-6. Accessed 1 June 2019

https://www.iccp-portal.org/system/files/plans/NCCP_Final%20%5B1%5D accessed January 2021

Hughes M. F. 2002. Arsenic toxicity and potential mechanisms of action. *Toxicology letters 133*.1: 1–16.

Hussin, Y., Aziz, M., Che Rahim, N. F., Yeap, S. K., Mohamad, N. E., Masarudin, M. J., Nordin, N., Abd Rahman, N., Yong, C. Y., Akhtar, M. N., Zamrus, S., and Alitheen, N. B. (2018). DK1 Induces Apoptosis via Mitochondria-Dependent Signaling Pathway in Human Colon Carcinoma Cell Lines In Vitro. *International Ojournal of molecular sciences* 19.4: 1151.

Ignácio, Z. M., da Silva, R. S., Plissari, M. E., Quevedo, J., and Réus, G. Z. 2019. Physical Exercise and Neuroinflammation in Major Depressive Disorder. Molecular neurobiology, 56(12), 8323–8335.

Iwu, M. 1993. *Handbook of African Medicinal Plants*. Boca Raton, FL: CRC Press;

Jamkhande, P.G., Patiil, P.H. and Tidke, P.S. 2013. In vitro antioxidant activity of Butea monosperma flowers fractions. *International Journal of Drug Development and Research* 5.3: 245-255.

Jedy-Agba, E., Curado, M. P., Ogunbiyi, O., Oga, E., Fabowale, T., Igbinoba, F., Osubor, G., Otu, T., Kumai, H., Koechlin, A., Osinubi, P., Dakum, P., Blattner, W. and Adebamowo, C. A. 2012. Cancer incidence in Nigeria: a report from population-based cancer registries. *Cancer epidemiology 36*.5: e271–e278.

Jin, Z., and El-Deiry, W. S. 2005. Overview of cell death signaling pathways. *Cancer biology & therapy* 4.2: 139–163.

Joker, D. 2000. Vitellaria paradoxa Gaertn. F. Danida Forest Seed Centre, Seed Leaflet No.50,

Jollow, D. J., Mitchell, J. R., Zampaglione, N. and Gillette, J. R. 1974. Bromobenzene-induced liver necrosis. Protective role of glutathione and evidence for 3,4-bromobenzene oxide as the hepatotoxic metabolite. *Pharmacology*, *11*(3), 151–169.

Jomova, K., Jenisova, Z., Feszterova, M., Baros, S., Liska, J., Hudecova, D., Rhodes, C. J., and Valko, M. 2011. Arsenic: toxicity, oxidative stress and human disease. *Journal of applied toxicology 31*.2: 95–107.

Kalra A, Yetiskul E, Wehrle CJ, Tuma F. 2021. Ohysiology, Liver. In: Statpearls. Treasure Island (FL): Statpearls Publishing.

Kamalabadi-Farahani1, M., Najafabadi, M. R. H. and Jabbarpour, Z. 2019. Apoptotic Resistance of Metastatic Tumor Cells in Triple Negative Breast Cancer: Roles of Death Receptor-5. *Asian Pac J Cancer Prev*, 20.6: 1743-1748.

Katt, M. E., Placone, A. L., Wong, A. D., Xu, Z. S., and Searson, P. C. 2016. *In Vitro* Tumor Models: Advantages, Disadvantages, Variables, and Selecting the Right Platform. *Frontiers in bioengineering and biotechnology 4*: 12.

Kavitha, S., Lincy, M.L.P., Kala, S.M.J., Mohan, V.R. and Maruthupandian, A. 2015. GC-MS analysis of ethanol extract of stem of Nothapodytes nimmoniana (Graham). *World Jornal of Pharmaceutical Sciences***:** 3.6: 1145-1150.

Kerr, J. F., Wyllie, A. H. and Currie, A. R. 1972. Apoptosis: a basic biological phenomenon with wide-ranging implications in tissue kinetics. *British journal of cancer 26*.4: 239–257.

Kim, D., Jeond, S. and Lee, C. 2003. Antioxidant capacity of phenolic phytochemicals from various cultivars of plums. *Food Chemistry* 81: 321-326.

Kim, K., Shin, E. K., Chung, J. H., & Lim, K. M. 2020. Arsenic induces platelet shape change through altering focal adhesion kinase-mediated actin dynamics, contributing to increased platelet reactivity. *Toxicology and applied pharmacology*, 391, 114912.

Kooti, W., Servatyari, K., Behzadifar, M., Asadi-Samani, M., Sadeghi, F., Nouri, B. and Zare Marzouni, H. 2017. Effective Medicinal Plant in Cancer Treatment, Part 2: Review Study. *Journal of evidence-based complementary & alternative medicine 22*.4: 982–995.

Lagoa, R., Marques-da-Silva, D., Diniz, M., Daglia, M. and Bishayee, A. 2020. Molecular mechanisms linking environmental toxicants to cancer development: Significance for protective interventions with polyphenols. *Seminars in cancer biology*, S1044-579X(20)30035-3.

Lee, J., Koo, N. and Min, D.B., 2004**.** Reactive oxygen species, arging, and antioxidant nutraceuticals. *Comprehensive Reviews in Food Science and Food Safety* 3.1: 21-33.

Li, B., Li, X., Zhu, B., Zhang, X., Wang, Y., Xu, Y., Wang, H., Hou, Y., Zheng, Q., and Sun, G. 2013. Sodium arsenite induced reactive oxygen species generation, nuclear factor (erythroid-2 related) factor 2 activation, heme oxygenase-1 expression, and glutathione elevation in Chang human hepatocytes. *Environmental toxicology*, *28*(7), 401–410.

Lichota, A., and Gwozdzinski, K. 2018. Anticancer Activity of Natural Compounds from Plant and Marine Environment. *International journal of molecular sciences 19*.11: 3533.

Lin, E., Li, C. and Chou, H. 2014. Evaluation of the antioxidant and antiradical activities of perilla seed, leaf and stalk extracts. *Journal of Medicinal Plants Research* 8.2: 109-115.

Liskova, A., Stefanicka, P., Samec, M., Smejkal, K., Zubor, P., Bielik, T., Biskupska-Bodova, K., Kwon, T. K., Danko, J., Büsselberg, D., Adamek, M., Rodrigo, L., Kruzliak, P., Shleikin, A. and Kubatka, P. 2020. Dietary phytochemicals as the potential protectors against carcinogenesis and their role in cancer chemoprevention. *Clinical and experimental medicine* 20.2: 173–190.

Liu, T., Zhang, L., Joo, D. and Sun, S. C. 2017. NF-κB signaling in inflammation. *Signal transduction and targeted therapy 2*: 17023–.

Lowry, H.O., Rosebrough, N.J., Farr, A.L. and Randall, R.J. 1951. Protein measurement with the folin phenol reagent. *J.Biol. Chem*. 193: 265-275.

Mahomoodally M. F. 2013. Traditional medicines in Africa: an appraisal of ten potent african medicinal plants. *Evidence-based complementary and alternative medicine: eCAM*, *2013*, 617459.

Mainasara, A. S., Oduola, T., Musa, U., Mshelia, A. S., Muhammed, A. O. and Ajayi, A. S. 2016. Hepatotoxicity Assessment in Wistar Rats Exposed to Vitellaria paradoxa Stem Bark Extract. *European Journal of Medicinal Plants* 13.3: 1-9.

Mallogo, R.J., 1989. Burkinofaso: Importance to bee keeping of the butter tree, *Butryrospernum paradoxum*, Lucust bean tree and *Parkia biglobosa*. Revue Francaise Apiculture 482: 72-74.

Maranz, S. and Wiesman, Z. 2003. Evidence for indigenous selection and distribution of the shea tree, Vitellaria paradoxa. *J. Biogeogr*. 30: 1505-1516.

Mathew, M.S., Vinod, K., Jayaram, P.S., Jayasree, R.S. and Joseph, K. 2019. Improved Bioavailability of Curcumin in Gliadin-Protected Gold Quantum Cluster for Targeted Delivery. ACS Omega . 4: 14169−14178.

Medina-Pizzali, M., Robles, P., Mendoza, M. and Torres, C. 2018. Ingesta de arsénico: el impacto en la alimentación y la salud humana [Arsenic Intake: Impact in Human Nutrition and Health]. *Revista peruana de medicina experimental y salud publica 35*.1: 93–102.

Mehrzadi, S., Fatemi, I., Malayeri, A. R., Khodadadi, A., Mohammadi, F., Mansouri, E., Rashno, M. and Goudarzi, M. 2018. Ellagic acid mitigates sodium arsenite-induced renal and hepatic toxicity in male Wistar rats. *Pharmacological reports* 70.4: 712–719.

Miklos, G. L. and Rubin, G. M. 1996. The role of the genome project in determining gene function: insights from model organisms. *Cell 86*.4: 521–529.

Mills, C. C., Kolb, E. A. and Sampson, V. B. 2017. Recent Advances of Cell-Cycle Inhibitor Therapies for Pediatric Cancer. *Cancer research 77*.23: 6489–6498.

Moirangthem, A., Bondhopadhyay, B., Mukherjee, M., Bandyopadhyay, A., Mukherjee, N., Konar, K., Bhattacharya, S. and Basu, A. 2016. Simultaneous knockdown of uPA and MMP9 can reduce breast cancer

progression by increasing cell-cell adhesion and modulating EMT genes. *Scientific reports*, *6*: 21903.

Mondal, P. and Chattopadhyay, A. 2020. Environmental exposure of arsenic and fluoride and their combined toxicity: A recent update. *Journal of applied toxicology* 40.5: 552–566.

Mondal, R., Biswas, S., Chatterjee, A., Mishra, R., Mukhopadhyay, A., Bhadra, R. K., & Mukhopadhyay, P. K. 2016. Protection against arsenic-induced hematological and hepatic anomalies by supplementation of vitamin C and vitamin E in adult male rats. Journal of basic and clinical physiology and pharmacology, 27(6), 643–652.

Morakinyo, A.O., Achema, P.U. and Adegoke, O.A. 2010. Effect of Zingiber officinale (ginger) on sodium arsenite –induced reproductive toxicity in male rats. *Afr. J. Biomed. RES*. 13: 39-45.

Mosmann, T. 1983. Rapid colorimetric assay for cellular growth and survival: application to proliferation and cytotoxicity assays. *J Immunol Methods* 65: 55-63.

Naujokas, M. F., Anderson, B., Ahsan, H., Aposhian, H. V., Graziano, J. H., Thompson, C. and Suk, W. A. 2013. The broad scope of health effects from chronic arsenic exposure: update on a worldwide public health problem. *Environmental health perspectives 121*.3: 295–302.

Ndukwe, I. G., Amupitan, J. O., Isah, Y. and Adegoke, K. S. 2007. Phytochemical and antimicrobial screening of the crude extracts from the root, stem bark and leaves of Vitellaria paradoxa (GAERTN. F). *African Journal of Biotechnology* 6.16: 1905-1909,

Neena Gopinathan Panicker , Sameera Omar Mohammed Saeed Balhamar, Shaima Akhlaq, Mohammed Mansour Qureshi , Tania Shamim Rizvi , Ahmed Al-Harrasi , Javid Hussain and Farah Mustafa 2019. Identification and Characterization of the Caspase-Mediated Apoptotic Activity of Teucrium

mascatense and an Isolated Compound in Human Cancer Cells. *Molecules* 24: 977.

Nemery, B., and Banza Lubaba Nkulu, C. 2018. Assessing exposure to metals using biomonitoring: Achievements and challenges experienced through surveys in low- and middle-income countries. *Toxicology letters* 298: 13–18.

Newman, D. J. and Cragg, G. M. 2016. Natural products as sources of new drugs from 1981 to 2014. *J. Nat. Prod*. 79. 3: 629-661.

Noble, R.W. and Gibson, Q.H. 1970. The reaction of ferrous horseradish peroxidase with hydrogen peroxide. *J Biol Chem*. 245.9: 2409-2413.

Nyarko, G., Mahunu, G.K., Chimsah, F.A., Yidana, J.A., Abubakari, A.H., Abagale, F.K., Quainoo, A., and Poudyal, M. 2012. Leaf and fruit characteristics of Shea (Vitellaria paradoxa) in Northern Ghana. *Res. Plant Biol*. 2.3:38-45.

Oboh, G., Odubanjo, V. O., Bello, F., Ademosun, A. O., Oyeleye, S. I., Nwanna, E. E. and Ademiluyi, A. O. 2016. Aqueous extracts of avocado pear (Persea americana Mill.) leaves and seeds exhibit anti-cholinesterases and antioxidant activities in vitro. *Journal of basic and clinical physiology and pharmacology* 27.2: 131–140.

Odebiyi, A. and Sofowora, A.E. 1978. Phytochemical Screening of Nigeria Medicinal Plants (Part III) *Lodydia* 41: 234-246

Odunola O.A., Uka. E., Akinwumi, K,A., Gbadegesin. M.A., Osifeso, O.O. and Ibegbu, M.D. 2008. Exposure of laboratory mice to domestic cooking gas: Implication for toxicity. *Int J Environ Res Public Health* 5.3: 172-176.

Odunola, O. A., Muhammad, A., Farooq, A.D., Dalvandi, K., Rasheed, H., Choudhary, M.I. and Erukainure, O.L. 2013**.** Comparative assessment of redox sensitive biomarkers due to acacia honey and sodium arsenite administration invivo. *Mediterr J Nutr Metab*. 6.2: 119-126.

Odunola, **O.A., Akinwumi**, **KA., Ogunbiyi**, **B. and Tugbobo, O.** 2007**.** Interaction and enhancement of the toxic effects of sodium arsenite and lead acetate in wistar rats. *African Journal of Biomedical Research* 10: 59 – 65.

Odunola, O.A., Kazeem, A.K. and Ibegbu, D .M. 2011. The influence of Garlic and Spondias mombin on sodium arsenite induced clastogenicity and hepatotoxicity in rats. *The Pacific J of Sci. and Tech.* 12.2: 401-409.

Odunola, O.A., Oyibo, A., Gbadegesin, M.A. and Owumi, S.E. 2019. Assessment of in vitro antioxidant and genotoxicity in E.coli of ethanol extract of *Vitellaria paradoxa* (Gaertn.F). *Achives of Basic and Applied Medicine* 7: 13-20

Ogunbiyi, J.O., Stefan, D.C. and Rebbeck, T.R. 2016. African Organization for Research and Training in Cancer: position and vision for cancer research on the African continent. *Infect Agents Cancer* 11, 63.

Ohshima, H., Tazawa, H., Sylla, B. S. and Sawa, T. 2005. Prevention of human cancer by modulation of chronic inflammatory processes. *Mutation research*, 591.1-2: 110–122.

Ojo, O.O., Nadro, M.S. and Tella, I.O. 2006. Protection of rats by extracts of some common Nigeria trees against acetaminophen – induced hepatotoxicity. *African Journal of Biotechnology*. 5: 755-760.

Okullo, J.B.L., Hall, J.B. and Obua, J. 2004. Leafing, flowering and fruiting of Vitellaria paradoxa subsp. nilotica in savanna parklands in Uganda. *Agroforest. Syst*. 60.1: 77-91.

Ola-Davis, O. E. and Akinrinde, A.S. 2016**.** Acute sodium arsenite –induced haematological and biochemical changes in rats: protective effect of ethanol extract of Ageratum conyzoides, *Pharmacognosy Res*. 8.1: 26-30.

Olaleye, O.O., Adetunji, C. O. and Kolawole, O .M. 2015. Identification of Phytochemical Constituents of the Methanolic extract of Vitellaria paradoxa

Responsible for Antimicrobial Activity against Selected Pathogenic Organisms

Oliveira, P. A., Colaço, A., Chaves, R., Guedes-Pinto, H., De-La-Cruz P., L. F., and Lopes, C. 2007. Chemical carcinogenesis. *Anais Da Academia Brasileira de Ciências 79*.4: 593–616.

Olugbami J.O., Gbadegesin, M.A. and. Odunola, O.A. 2015. *In vitro* free radical scavenging and antioxidant properties of ethanol extract of *Terminalia glaucescens*. *Phcog Res* 7: 49-56.

Ong, C., Yung, L. Y., Cai, Y., Bay, B. H., and Baeg, G. H. 2015. Drosophila melanogaster as a model organism to study nanotoxicity. *Nanotoxicology 9*.3: 396–403.

Opferman, J. T., and Kothari, A. 2018. Anti-apoptotic BCL-2 family members in development. *Cell death and differentiation 25*.1: 37–45.

Organization for Economic Cooperation and Development. 2008. Repeated dose oral toxicity test method. In: OECD Guidelines for testing of chemicals, N° 423, Paris, France

Otitoju, A. P., Longdet, I.Y., Alemika, T. E., Adegoke, A.M., and Gota, V.P. (2019). Cytotoxic activity of *Boswellia dalzielii* (Hutch) stem bark extract against head and neck squamous cell carcinoma of the tongue (AW8507 cell line). *Journal of Pharmacy and Bioresources* 16.2: 187-194.

Ouyang, L., Shi, Z., Zhao, S., Wang, F. T., Zhou, T. T., Liu, B., and Bao, J. K. 2012. Programmed cell death pathways in cancer: a review of apoptosis, autophagy and programmed necrosis. *Cell proliferation, 45*.6: 487–498.

Oyaizu, M. 1986. Studies on products of browning reactions: antioxidant activities of products of browning reaction prepared from glucosamine. *J. Nutrit*. 44: 307–315.

Oyibo, A.. Gbadegesin, M. A. and Odunola. O. A. 2021. Ethanol extract of *Vitellaria paradoxa* (Gaertn, F) leaves protects against sodium arsenite-induced toxicity in male wistar rats. *Toxicology Reports* 8: 774-784.

Pawlowska, E., Szczepanska, J., Koskela, A., Kaarniranta, K. and Blasiak, J. 2019. Dietary Polyphenols in Age-Related Macular Degeneration: Protection against Oxidative Stress and Beyond. *Oxid Med Cell Longev*. 2019:9682318.

Pfeffer, C. M. and Singh, A. 2018. Apoptosis: A Target for Anticancer Therapy. *International journal of molecular sciences 19*.2: 448.

Pflaum, J., Schlosser, S., and Müller, M. 2014. p53 Family and Cellular Stress Responses in Cancer. *Frontiers in oncology 4*: 285.

Phi, L., Sari, I. N., Yang, Y. G., Lee, S. H., Jun, N., Kim, K. S., Lee, Y. K., and Kwon, H. Y. 2018. Cancer Stem Cells (CSCs) in Drug Resistance and their Therapeutic Implications in Cancer Treatment. *Stem cells international* 5416923.

Pistritto, G., Trisciuoglio, D., Ceci, C., Garufi, A. and D'Orazi, G. 2016. Apoptosis as anticancer mechanism: function and dysfunction of its modulators and targeted therapeutic strategies. *Aging 8*.4: 603–619.

Plati, J., Bucur, O. and Khosravi-Far, R. 2011. Apoptotic cell signaling in cancer progression and therapy. *Integrative biology: quantitative biosciences from nano to macro*, *3*.4: 279–296.

Poirier, M. C. 2012. Chemical induced DNA damage and human cancer risk. *Discov Med*. 14 (77): 283-288.

Polak, M., Opoka, R. and Cartwright, I. L. 2002. Response of fluctuating asymmetry to arsenic toxicity: support for the developmental selection hypothesis. *Environmental pollution (Barking, Essex : 1987)*, *118*.1: 19–28.

Potter, C. J., Turenchalk, G. S. and Xu, T. 2000. Drosophila in cancer research. An expanding role. *Trends in genetics* 16.1: 33–39.

Prabu, S. M. and Muthumani, M. 2012. Silibinin ameliorates arsenic induced nephrotoxicity by abrogation of oxidative stress, inflammation and apoptosis in rats. *Molecular biology reports 39*.12: 11201–11216.

Prieto, P., Pineda, M., and Aguilar, M. 1999. Spectrophotometric quantitation of antioxidant capacity through the formation of a phosphomolybdenum complex: specific application to the determination of vitamin E. *Anal. Biochem.* 269: 337–341.

Quillardet, Huisman, D'ari and Hofnung. 1982. SOS-Chromotest, a direct assay for induction of an SOS function in Escherichia cole K-12 to measure genotoxicity. *Proc. Nat. Acad. Sci*. 79: 5971-5975.

Ramos-Vara, J. A., and Miller, M. A. 2014. When tissue antigens and antibodies get along: revisiting the technical aspects of immunohistochemistry--the red, brown, and blue technique. *Veterinary pathology* 51.1: 42–87.

Rana, M. N., Tangpong, J., and Rahman, M. M. 2018. Toxicodynamics of Lead, Cadmium, Mercury and Arsenic- induced kidney toxicity and treatment strategy: A mini review. *Toxicology reports 5*: 704–713.

Reitman, S. and Frankel, S. 1957. Colourimetric method for the determination of serum transaminases. *Am. J. Clin. Pathol.* 28: 56-61.

Roy, J. S., Chatterjee, D., Das, N., and Giri, A. K. 2018. Substantial Evidences Indicate That Inorganic Arsenic Is a Genotoxic Carcinogen: a Review. *Toxicological research 34*.4: 311–324.

Sahreen, S., Khan, M.R. and Khan, R.A. 2017. Evaluation of antioxidant profile of various solvent extracts of Carissa opaca leaves: an edible plant. *Chemistry Central Journal* 11: 83.

Samelo, R. R., da Cunha de Medeiros, P., de Carvalho Cavalcante, D. N., Aranha, M., Duarte, F. A., de Castro, Í. B., Ribeiro, D. A. and Perobelli, J. E. 2020. Low concentrations of sodium arsenite induce hepatotoxicity in prepubertal male rats. *Environmental toxicology 35*.5: 553–560.

Sankar, P., Telang, A.G., Kalaivanan, R., Karunakaran, V., Suresh, S., and Kesavan, M. 2016. Oral nanoparticulate curcumin combating arsenic-induced oxidative damage in kidney and brain of rats. *Toxicol Ind Health* 32.3: 410-421.

Sankpal, U. T., Pius, H., Khan, M., Shukoor, M. I., Maliakal, P., Lee, C. M., Abdelrahim, M., Connelly, S. F. and Basha, R. 2012. Environmental factors in causing human cancers: emphasis on tumorigenesis. *Tumour biology: the journal of the International Society for Oncodevelopmental Biology and Medicine 33*.5: 1265–1274.

Sarker, R.S.J., Ahsan, N. and Akhand, A.A. 2013**.** Sodium arsenite induced systemic organ damage in various blood parameter in mice. *Dhaka University J.Pharm.Sci*. 11.2: 169-172

Schmid, W. 1975.The micronucleus test. *Mutat Res*. 31.1: 9-15.

Serene, A., Millogo, R. J., Guinko, S. and Nacro, M. 2008. Propriétés thérapeutiques des plantes à tanins du Burkina Faso. *Pharmacopée et Médecine Traditionnelle Africaine* 15.1: 41-49.

Shahid, M., Pourrut, B., Dumat, C., Nadeem, M., Aslam, M. and Pinelli, E. 2014. Heavy-metal-induced reactive oxygen species: phytotoxicity and physicochemical changes in plants. *Rev Environ Contam Toxicol*. 232: 1-44.

Sharma, A., Kshetrimayum, C., Sadhu, H. G., & Kumar, S. 2018. Arsenic-induced oxidative stress, cholinesterase activity in the brain of Swiss albino mice, and its amelioration by antioxidants Vitamin E and Coenzyme Q10. *Environmental science and pollution research international,* 25(24), 23946–23953.

Soladoye, M.O., Orhiere, S.S. and Ibimode, B.M. 1989**.** Ethanobotanical Study of two Indigenous Multipurpose Plants in the Guinea Savanna of Kwara State - Vitellaria paradoxa and Parkia biglobosa. Biennial Conference of Ecological Society of Nigeria, 14 August, 1989, Forestry Research Institute, Ibadan. p.13

Sunderman, F.W. 1984**.** Jr Recent advances in metal carcinogenesis. *Annals of Clinical and Laboratory Sci*ence 14.2: 93-122.

Sung, H., Ferlay, J., Siegel, R. L., Laversanne, M., Soerjomataram, I., Jemal, A., and Bray, F. 2021. Global Cancer Statistics 2020: GLOBOCAN Estimates of Incidence and Mortality Worldwide for 36 Cancers in 185 Countries. CA: a *cancer journal for clinicians*, 71(3), 209–249.

Susan, A., Rajendran, K., Sathyasivam, K. and Krishnan, U. M. 2019. An overview of plant-based interventions to ameliorate arsenic toxicity. *Biomedicine & pharmacotherapy = Biomedecine & pharmacotherapie 109*: 838–852.

Sylla, B. S. and Wild, C. P. 2012. A million africans a year dying from cancer by 2030: what can cancer research and control offer to the continent? *International journal of cancer 130*.2: 245–250.

Tagne, R. S., Telefo, B. P., Nyemb, J. N., Yemele, D. M., Njina, S.N., Goka, S.M.C., Lienou, L.L., Kamdje, A.H.N., M oundipa, P. F. and Farooq, A.D. 2014. Anticancer and antioxidant activities of methanol extracts and fractions of some Cameroonian medicinal plants. *Asian Pac J Trop Med* 7.1: 442-447.

Tamori, Y. 2019. The Initial Stage of Tumorigenesis in Drosophila Epithelial Tissues. *Advances in experimental medicine and biology 1167*: 87–103.

Tchounwou, P. B., Yedjou, C. G., Patlolla, A. K., and Sutton, D. J. 2012. Heavy metal toxicity and the environment. *Experientia supplementum* (2012), 101, 133–164.

Teoh, W. Y., Sim, K. S., Moses Richardson, J. S., Abdul Wahab, N. and Hoe, S. Z. 2013. Antioxidant Capacity, Cytotoxicity, and Acute Oral Toxicity of Gynura bicolor. *Evidence-based complementary and alternative medicine: eCAM, 2013*, 958407.

Tokar, E.J., Qu, W., Liu, J., Liu, W., Webber, M.M., Phang, J.M. and Waalkes, M.P. 2010. Arsenic-specific stem cell selection during malignant transformation. *J. Nat. Cancer Inst*. 102: 638–649.

Tolwinski, N.S. 2017. Introduction: Drosophila- A model system for developmental biology. *J. Dev.Biol*. 5: 9.

Tomita, T. 2017. Apoptosis of pancreatic β-cells in Type 1 diabetes. *Bosnian journal of basic medical sciences* 17.3: 183–193.

Torre, L.A., Siegel, R.L., Ward, E. M. and Jemal, A. 2016. Global cancer incidence and mortality rates and trends- An update. *Cancer Epidemiol. Biomarkers Prev*. 25.1: 16-27.

Trosko, J. E. 2001. Commentary: is the concept of "tumor promotion" a useful paradigm? *Mol Carcinog* 30: 131– 137.

Turk, E., Kandemir, F. M., Yildirim, S., Caglayan, C., Kucukler, S. and Kuzu, M. 2019. Protective Effect of Hesperidin on Sodium Arsenite-Induced Nephrotoxicity and Hepatotoxicity in Rats. *Biological trace element research* 189.1: 95–108.

Tyagi, T. and Agarwal, M. 2017**.** Phytochemical screening and GC-MS analysis of bioactive constituents in the ethanolic extract of Pistia stratiotes L. and Eichhornia crassipes (Mart.) solms. *Journal of Pharmacognosy and Phytochemistry* 6.1: 195-206.

Ugese, F.D., Baiyeri, K.P. and Mbah, B.N. 2008. Nutritional composition of shea (*Vitellaria paradoxa*) fruit pulp across its major distribution zones in Nigeria. *Fruits* 63: 163– 169.

Ugur, B., Chen, K. and Bellen, H. J. 2016. Drosophila tools and assays for the study of human diseases. *Disease models & mechanisms* 9.3: 235–244.

Vande Walle, L., Lamkanfi, M. and Vandenabeele, P. 2008. The mitochondrial serine protease HtrA2/Omi: an overview. *Cell death and differentiation 15*.3: 453–460.

Vasudevan, D. and Ryoo, H. D. 2016. Detection of Cell Death in Drosophila Tissues. *Methods in molecular biology (Clifton, N.J.)* 1419: 131–144.

Vining, L.C. 1992. Secondary metabolisms evolution and biochemical diversity: A review. *Gene* 115: 135-140.

Visconti, R., Della Monica, R. and Grieco, D. 2016. Cell cycle checkpoint in cancer: a therapeutically targetable double-edged sword. *Journal of experimental & clinical cancer research: CR, 35*.1: 153.

Von Maydell, H. 1990. Butyrospermum parkii (G. Don) Kotschy 202-207. Trees and Shrubs of the Sahel: Their Characte- ristics and Uses. English Text Revised J. Brase. Eschborn: Deutsche Gesellschaft fur Technische Zusammenarbeit (GTZ).

Wang, Y., Zhao, H., Guo, M., Shao, Y., Liu, J., Jiang, G. and Xing, M. 2018. Arsenite renal apoptotic effects in chickens co-aggravated by oxidative stress and inflammatory response. *Metallomics: integrated biometal science 10*.12: 1805–1813.

Wein, A. J., Kavoussi, L. R., Novick, A. C., Partin, A.W. and Peters C.A. 2007. The kidney and how they work. National Kidney and Urologic Diseases Information Clearinghouse (NKUDIC) Campbell-Walsh Urology. 9TH Ed. Saunders vol 1: p 24.

Winsor L.1994. Tissue processing.In woods A and Elis R eds. Laboratory histopathology. New York: Churchil Livingstone, 4.2.1-4.2.39.

Wolff, S.P. 1994. Ferrous ion oxidation in presence of ferric ion indicator xylenol orange for measurement of hydroperoxides. *Methods Enzymol*. 233: 182-189.

Woods, J.S. And Fowler, B.A.1977. Effect of chronic arsenic exposure on hematopoietic function in adult mammalian liver. *Environ Health Perspect*. 19: 209-213

World Health Organization. Global Health Observatory. Geneva: World Health Organization; 2018. who.int/gho/database/en/. Accessed June 21, 2018.

Wu, S., Zhu, W., Thompson, P. and Hannun, Y. A. 2018. Evaluating intrinsic and non-intrinsic cancer risk factors. *Nature communications* 9.1: 3490.

Xu, H., Wang, X. and Wang, W. 2018. Monomethylarsonous acid: Induction of DNA damage and oxidative stress in mouse natural killer cells at environmentally-relevant concentrations. *Mutation research. Genetic toxicology and environmental mutagenesis 832-833*: 1–6.

Xulu, K. R. and Hosie, M. J. 2017. HAART induces cell death in a cervical cancer cell line, HCS-2: A Scanning Electron Microscopy study. *Journal of microscopy and ultrastructure 5*.1: 39–48.

Yemoa, A.L., Gbenou, J.D., Johnson, R.C., Djego, J.G., Zinsou, C., Moudachirou, M., Quetin Leclercq. J., Bigot, A. and Portaels, F. 2008. Identification et étude phytochimique des plantes utilisées dans le traitement traditionnel de l'ulcère de Burili au Benin. *Ethnopharmacologia* 42: 51-53.

Yuan, S. and Akey, C. W. 2013. Apoptosome structure, assembly, and procaspase activation. *Structure (London, England: 1993), 21*.4: 501–515.

Yuxin H, Jin L, Bin L, Ruirui W, Gang W, Chunwei L, Huihui W, Jingbo P, and Yuanyuan X. 2020. The role of reactive oxygen species in arsenic toxicity. *Biomolecules* 10 (2):240

Zhishen, J., Mengcheng, T and Jianming, W. 1999. The determination of flavonoid contents in mulberry and their scavenging effects on superoxide radicals. *Food Chemistry* 64: 555-559.

APPENDICES

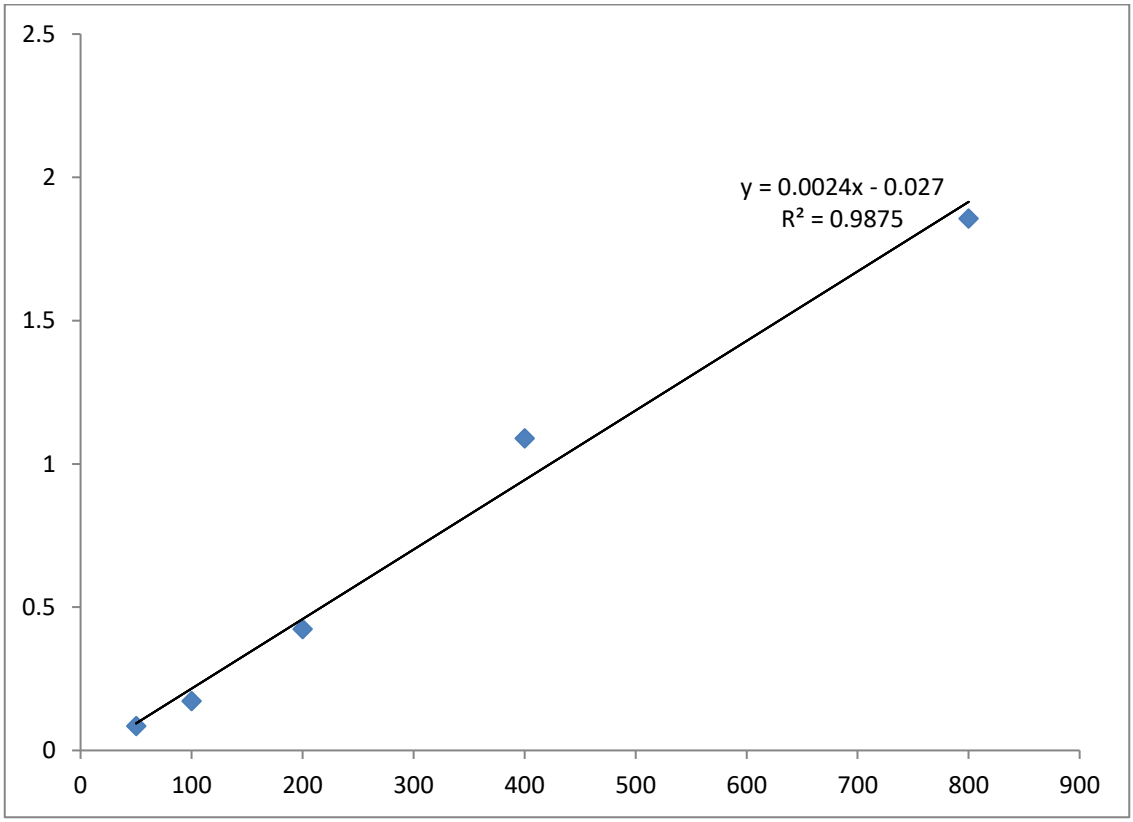

Appendix 1: Standard curve of total antioxidant capacity using ascorbic acid.

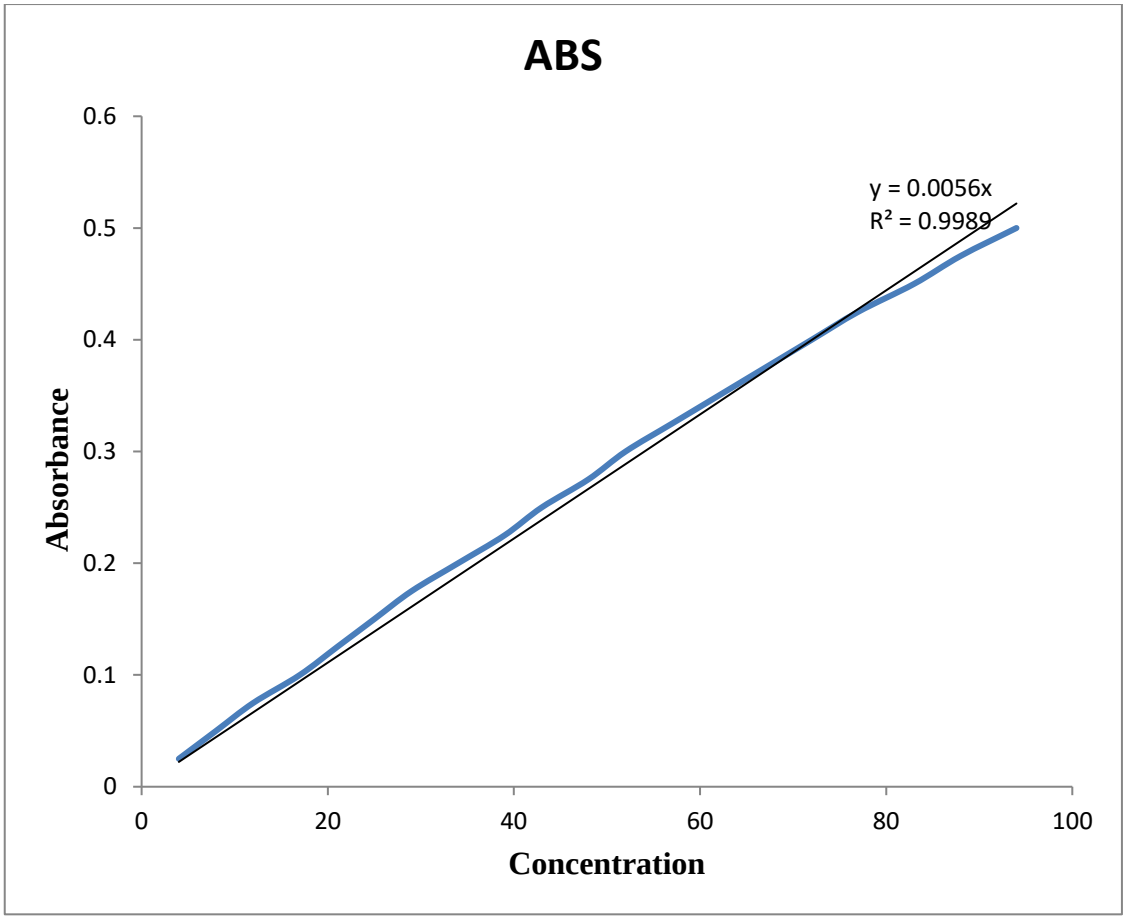

Appendix 2: Standard ALT curve

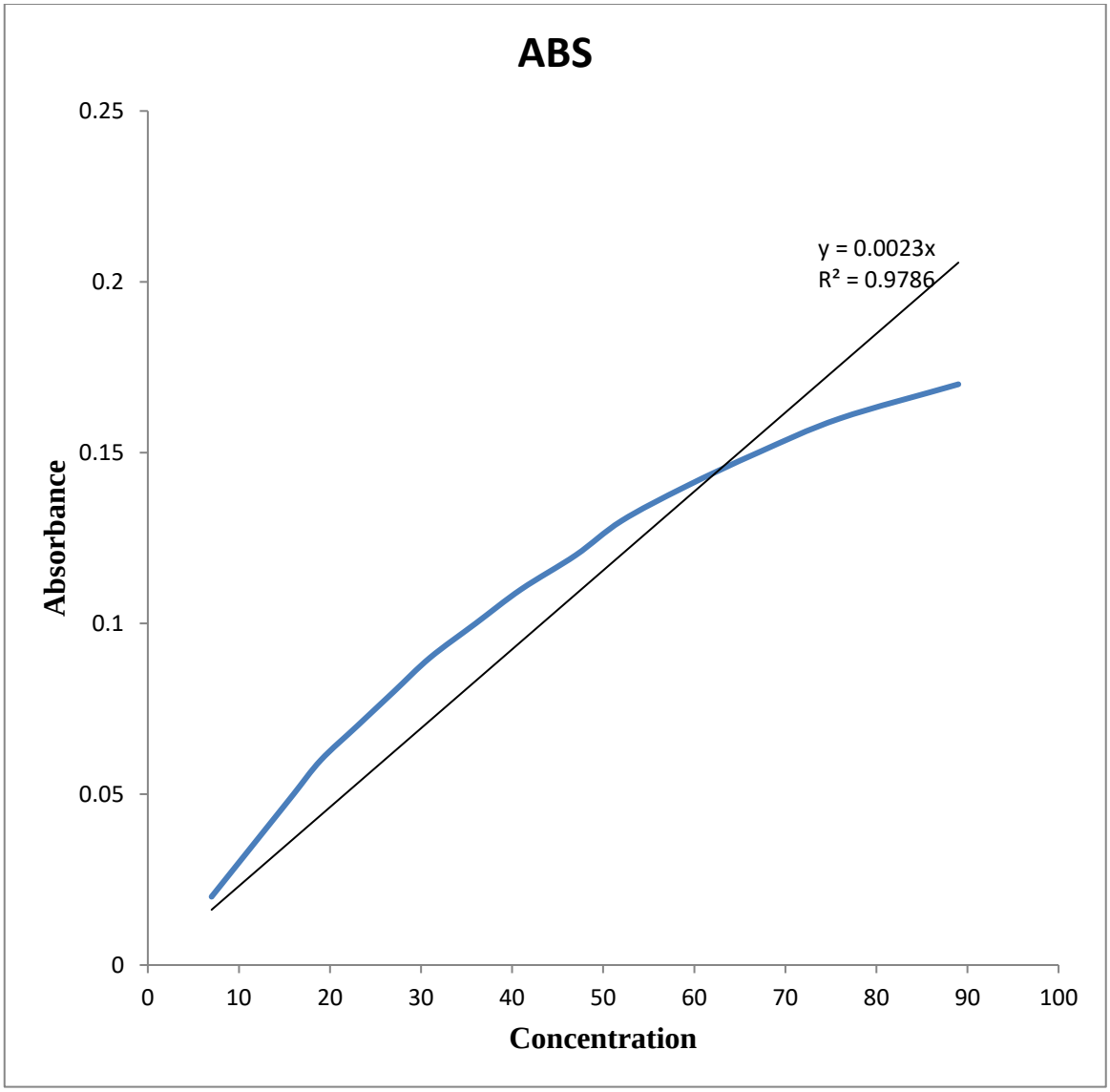

Appendix 3: Standard curve of AST

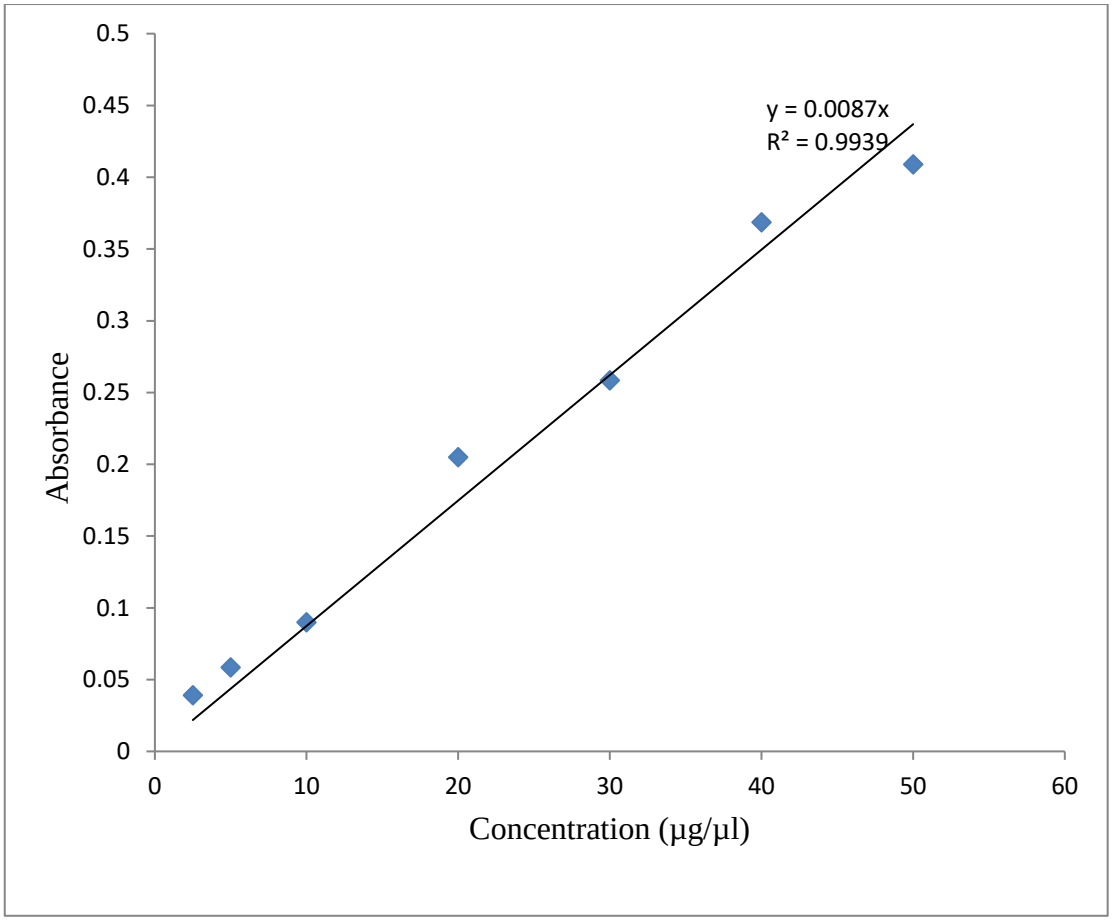

Appendix 4: Standard BSA curve by Lowry method

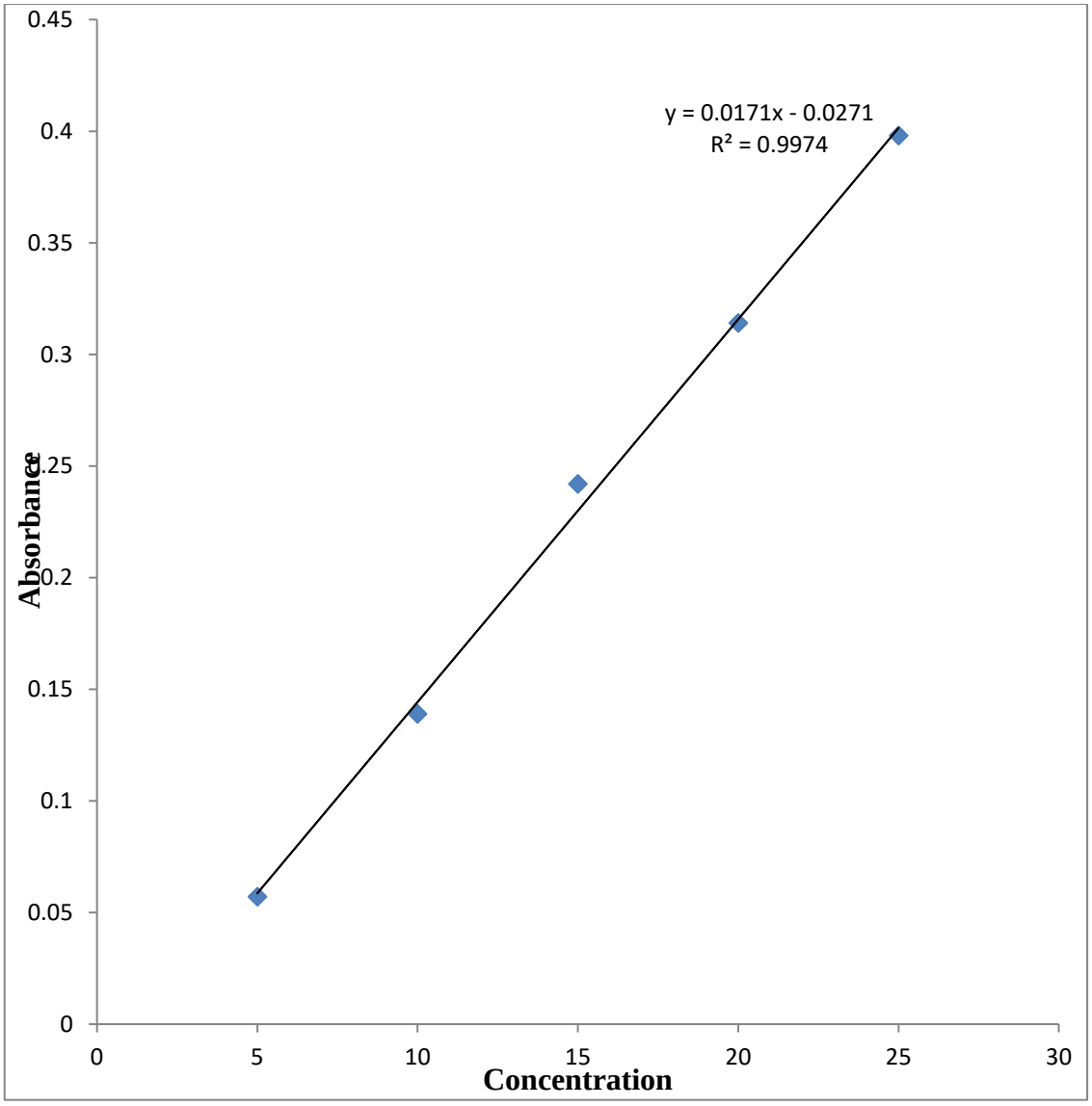

Appendix 5: Standard curve for total thiol

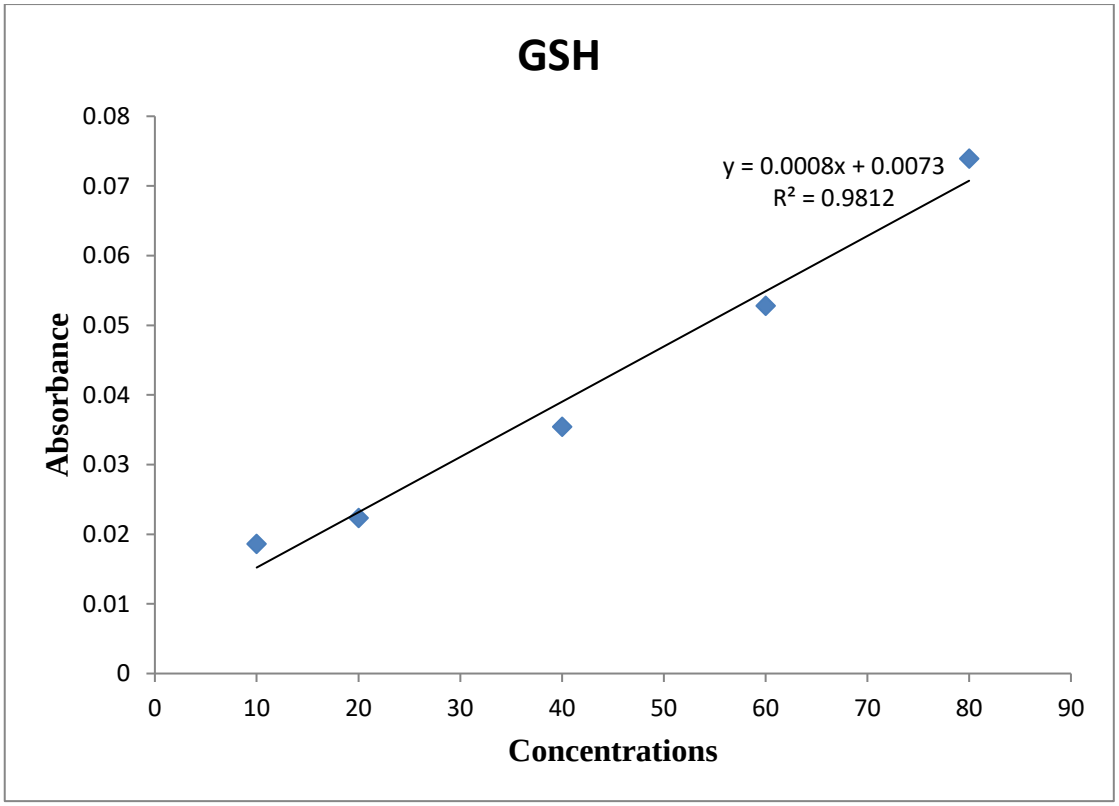

Appendix 6: Standard curve for Glutathione concentration

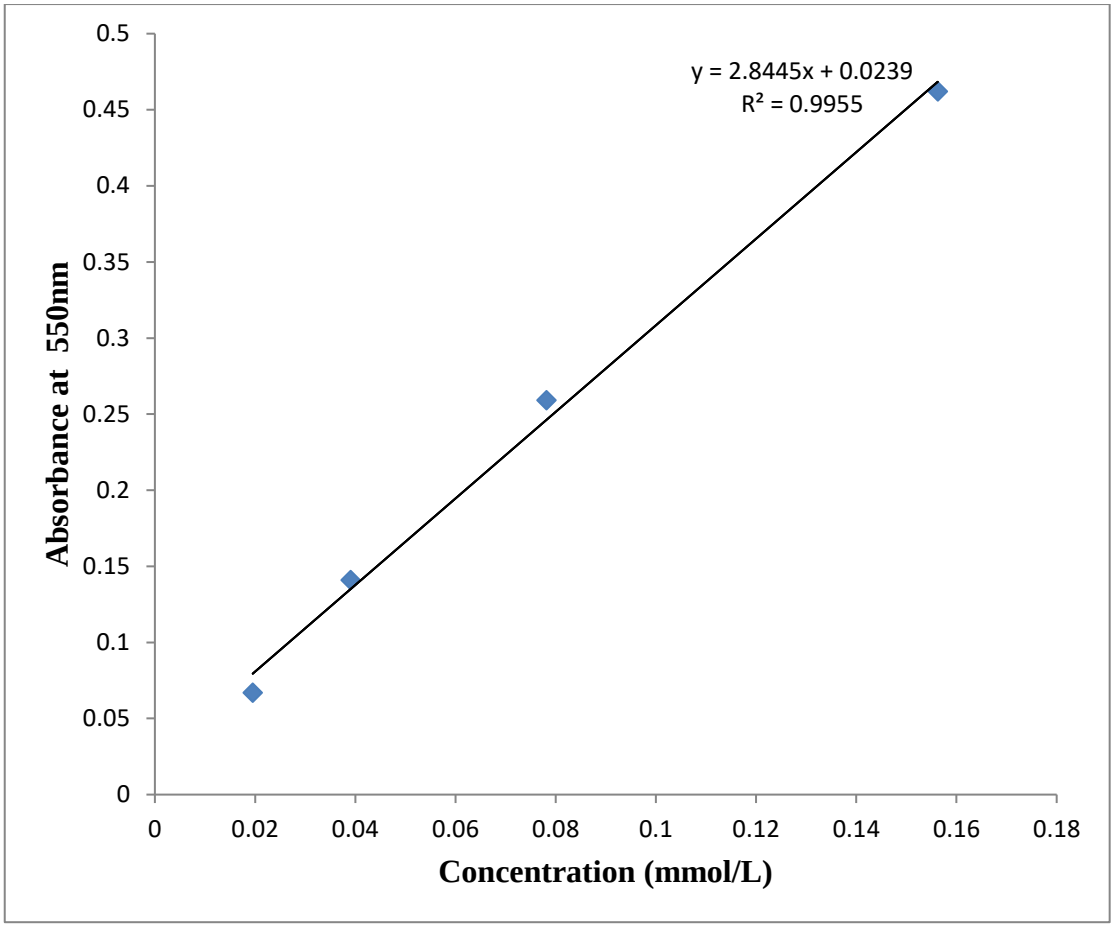

Appendix 7: Standard curve of Nitrite concentration

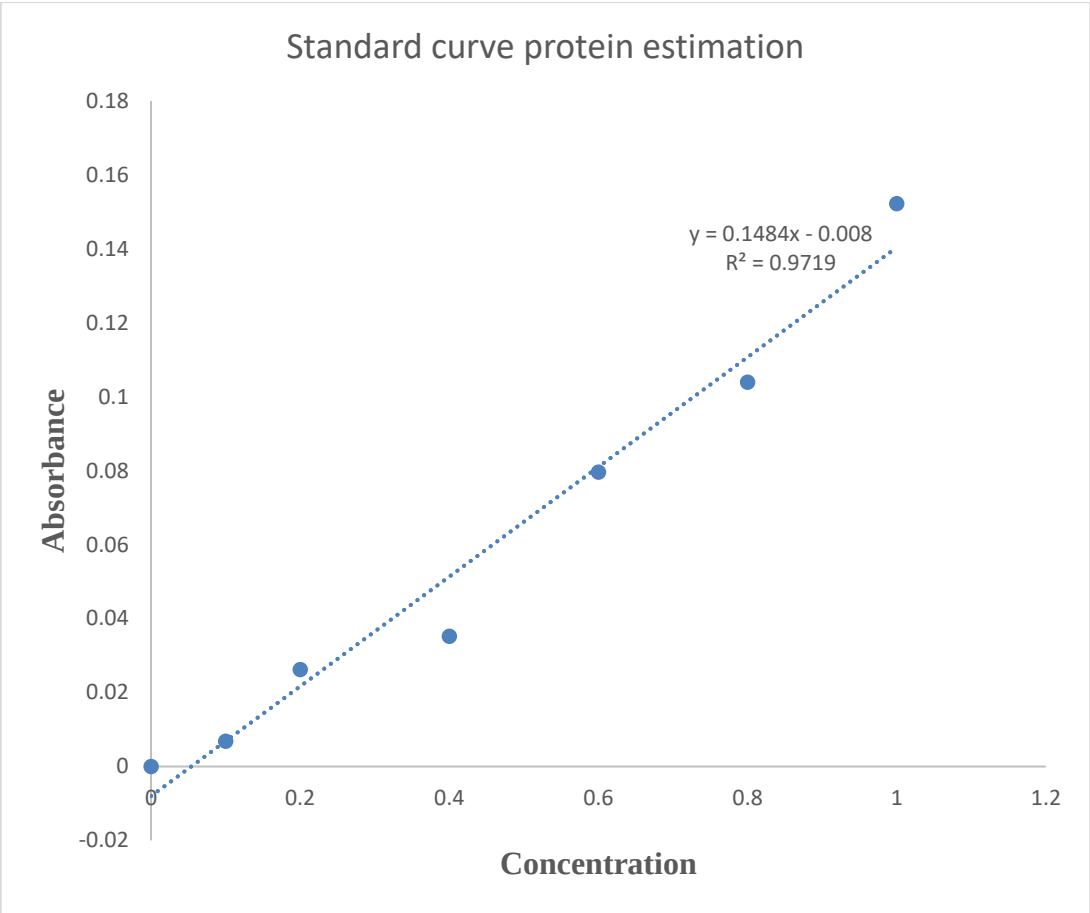

Appendix 8: Standard protein curve by Barford method